1-1-1978

Quasi-elastic light scattering study of the polyelectrolyte Na-copoly(ethyl acrylate-acrylic acid).

Stephanie Louisa Wunder
University of Massachusetts Amherst

QUASI-ELASTIC LIGHT SCATTERING STUDY OF THE POLYELECTROLYTE NA-COPOLY (ETHYL ACRYLATE-ACRYLIC ACID)

A Dissertation Presented

By

STEPHANIE LOUISA WUNDER

Submitted to the Graduate School of the
University of Massachusetts in partial fulfillment
of the requirements for the degree of

DOCTOR OF PHILOSOPHY

May 1978

Polymer Science and Engineering

PCM-74-19341 A01

and

AFOSR Grant 76-2183

QUASI-ELASTIC LIGHT SCATTERING STUDY OF THE POLYELECTROLYTE NA-COPOLY (ETHYL ACRYLATE-ACRYLIC ACID)

A Dissertation Presented

By

STEPHANIE LOUISA WUNDER

Approved as to style and content by:

Dr. Frank E. Karasz, Chairperson of Committee

Dr. Norman C. Ford, Cochairperson

Dr. Richard S. Stein, Member

Dr. Isaac Sanchez, Member

Dr. William MacKnight, Department Head
Polymer Science and Engineering

DEDICATION

To my mother and father.

ACKNOWLEDGMENTS

This work was suggested by Dr. Frank E. Karasz and Dr. Norman C. Ford, and carried out under their supervision. I would like to thank them for their assistance. I would also like to express my gratitude to the Department of Polymer Science and Engineering for financial support during my graduate study, which was made available through grants PCM-74-19341 A01 and AFOSR Grant 76-2183. I also wish to express my appreciation to the two other members of my thesis committee, Dr. Richard S. Stein and Dr. Isaac Sanchez, not only for their availability and support, but also for the contact I had with them in their capacity as teachers. I can attribute much that I learned in the field of polymer science to their interesting and stimulating lectures. Lastly, I would like to thank all the unfortunate individuals who came into contact with me during the writing of my dissertation for putting up with my foul moods during this undertaking.

ABSTRACT

Quasi-Elastic Light Scattering Study of the Polyelectrolyte
Na-copoly (ethyl acrylate-acrylic acid)

(May, 1978)

Stephanie Louisa Wunder, B.A., Barnard College
M.S., Ph.D., University of Massachusetts

Directed by: Professors Frank E. Karasz
Norman C. Ford

The translational diffusion constants of fractions of the polyelectrolyte Na-copoly (ethyl acrylate-acrylic acid) have been measured both in aqueous salt solutions as a function of ionic strength and in an organic theta solvent, 2 Heptanone. Since the samples were polydisperse, a method was developed to obtain the z-average diffusion constant. It was found that the polydispersity index of the fractions in a theta solvent could be related to the fractional increase in D_z over D_{eff}^{∞}, which was the diffusion constant obtained at very long sample times.

The results were analyzed within the framework of the two parameter theory of polymer solutions. The values of b in the relation $D = K_D M^{-b}$ were obtained from double logarithmic plots of the diffusion data and were found to agree within experimental error with the values calculated from $3b = a + 1$. The proportionality factor P_o relating the radius of gyration obtained from light scattering and the hydrodynamic radius from diffusion constant measurements was found to be about 25% larger than any theoretical predictions. Experimental values

of P decreased with decreasing ionic strength until the lowest ionic strengths as predicted theoretically, but then increased at the lowest ionic strength. The parameter β_o decreased with decreasing ionic strength at low ionic strengths and increased with decreasing ionic strength at high ionic strengths. This behavior could be explained by the effects of the ionic atmosphere on the motion of the macroions and by the effects of excluded volume. Unperturbed dimensions of the polymer were found to be obtainable using diffusion data plotted in a manner identical to that of the corresponding Stockmayer-Fixman intrinsic viscosity plots. The correction factors to the frictional coefficient obtained from the concentration dependence of the diffusion constant were found to be in reasonable agreement with a theory of Pyun and Fixman.

The copolymer Na-copoly (ethyl acrylate-acrylic acid) has both hydrophobic and hydrophylic groups along the chain and has been observed by other methods to undergo a conformational transition as a function of ionic strength from a compact to an extended random coil. The diffusion data obtained support this theory. The hydrodynamic radius in the organic theta solvent 2 Heptanone was 1.3 times larger than that in the aqueous theta solvent 1.2 N NaCl. The transition was observed as a change in slope of the diffusion constant plotted as a function of ionic strength.

TABLE OF CONTENTS

Chapter		Page
I.	INTRODUCTION	1
II.	QUASI-ELASTIC LIGHT SCATTERING THEORY	4
	Introduction	4
	Intensity Fluctuation Spectroscopy	6
	Introduction	6
	Scattered electric field	10
	Optical mixing techniques	15
	Polydispersity	20
	References	27
III.	DILUTE SOLUTION THEORY	29
	Two Parameter Theory	29
	Introduction	29
	Expansion factors	34
	Second virial coefficient	38
	Application to polyions	39
	Nonequilibrium Properties	45
	Concentration Dependence of Diffusion Constant	60
	Introduction	60
	Theories of k_f	62
	Heterogeneity Corrections	73
	Literature Survey for Polyions	78
	General	78
	Na-copoly (ethyl acrylate-acrylic acid)	85
	References	92
IV.	CONFORMATIONAL TRANSITIONS	98
	Literature Survey	98
	Na-copoly (ethyl acrylate-acrylic acid)	99
	References	112
V.	EXPERIMENTAL METHODS	114
	Apparatus	114
	Sample Characterization	123
	Polymerization and preparation	123
	Polydispersity index	124
	Intrinsic viscosity and viscosity average molecular weights	125

Chapter

Page

Solvent viscosity 129
Molecular weight from light scattering 137
Sample polydispersity 138
Light scattering studies 138
Diffusion Constant Measurements 139
Sample preparation 139
Sample cleaning 145
Cleaning procedures, still 145
Sample filtration 151
References 153

VI. RESULTS AND DISCUSSION 155

Conclusions 244
Suggestions for Further Work 246
References 248

APPENDICES 249

Appendix 3.1 250
Appendix 3.2 252
Appendix 6.1 255

LIST OF FIGURES

Figure		Page
2.1	Geometrical picture of the light scattering process where k = the incident light wave vector, k_s = the scattered wave vector, and θ = the scattering angle	7
2.2	Example showing two scattering particles in the incident light beam of angular frequency ω_o	17
3.1	Behavior of K(A) for small values of A, taken from Pyun and Fixman	67
3.2	Theoretical curves for "conjugate pairs" of $\Psi(\bar{z})$ and $\alpha_s(z)$, where the curves are identified by the abbreviated symbols listed in Table 3.1	80
3.3	Viscosity constant Φ/Φ_o versus α_η for several polyelectrolytes	84
3.4	Double logarithmic plots of the second virial coefficient versus ionic strength from Tan for several polyelectrolytes	87
3.5	Plots of α_s^2 versus $C_2^{-2/3}$ for fractions of Na-copoly (ethyl acrylate-acrylic acid), from Tan	89
4.1	(a) Radius of gyration versus ionic strength for fractions of Na-copoly (ethyl acrylate-acrylic acid), from Tan (b) The expansion factor, α_s^2, versus $C_s^{-2/3}$ for three fractions of Na-copoly (ethyl acrylate-acrylic acid), from Tan	101
4.2	(a) Intrinsic viscosity versus ionic strength for fractions of Na-copoly (ethyl acrylate-acrylic acid), from Tan (b) Intrinsic viscosity versus $C_s^{-1/2}$ for four fractions of Na-copoly (ethyl acrylate-acrylic acid), from Tan	103
4.3	Conformations of polyelectrolytes in different solvents, from Tan	107

Figure

Page

4.4 Relative fluorescence intensity of TNS in aqueous solutions of Na-copoly (ethyl acrylate-acrylic acid) + NaCl versus log C_s, from Tan 110

5.1 Block diagram of the light scattering apparatus from Olson 116

5.2 U.V. Calibration Curve. Absorbence at 220 nm versus concentration of unfractionated Na-copoly (ethyl acrylate-acrylic acid) 131

5.3 (a-d) Intrinsic viscosity plots of $(\ln\eta_r)/c$ or $(\ln\eta_r-1)/c$ versus concentration of Na-copoly (ethyl acrylate-acrylic acid) in 0.1 N NaCl for four polymer fractions, PC-80 F8, PC-80 FD, PC-80 F9, and PC-80 F1 133

5.4 Diagram of the glass water still and filtration apparatus, taken from Olson 147

6.1 (a-e) Plots of diffusion constant versus concentration of Na-copoly (ethyl acrylate-acrylic acid) for ionic strengths between 0.5 N NaCl and 1.2 N NaCl. Graphs a to e are for the five fractions PC-80 F8, PC-80 FD, PC-80 F9, PC-80 F4, and PC-80 F1 157

6.2 Plots of diffusion constant versus polymer concentration for two fractions of Na-copoly (ethyl acrylate-acrylic acid) in 2 Heptanone 163

6.3 (a-e) Plots of $1+2M_\nu A_2C/D$ versus polymer concentration for five fractions of Na-copoly (ethyl acrylate-acrylic acid) in ionic strength solutions from 0.5 N NaCl to 1.2 N NaCl. Graphs a to e are for fractions PC-80 F8, PC-80 FD, PC-80 F9, PC-80 F4, and PC-80 F1 165

6.4 Plots of diffusion constants for PC-80 F1 in 1.2 N NaCl as a function of $\Gamma\tau_{max}$ for several polymer concentrations 172

6.5 Percentage increase in diffusion constant as a function of the polydispersity index M_w/M_n for fractions of Na-copoly (ethyl acrylate-acrylic acid) in 1.2 N NaCl . . 175

6.6 Plots of P corrected for polydispersity effects as a function of ionic strength for fractions PC-80 F8, PC-80 FD, PC-80 F4, and PC-80 F1 of Na-copoly (ethyl acrylate-acrylic acid) 180

Figure

		Page
6.7	Plot of Flory viscosity "constant" Φ corrected for polydispersity effects as a function of ionic strength for fractions PC-80 F8, PC-80 FD, PC-80 F4, and PC-80 F1 of Na-copoly (ethyl acrylate-acrylic acid)	185
6.8	Plot of P_o calculated from $P_o = P_{APPQP}(\varepsilon)$ as a function of ionic strength for fractions PC-80 F8, PC-80 FD, PC-80 F4, and PC-80 F1 of Na-copoly (ethyl acrylate-acrylic acid)	188
6.9	Plot of Φ_o calculated from $\Phi_o = \Phi_{APPQ\Phi}(\varepsilon)$ as a function of ionic strength for fractions PC-80 F8, PC-80 FD, PC-80 F4, and PC-80 F1 of Na-copoly (ethyl acrylate-acrylic acid)	190
6.10	Plot of β corrected for polydispersity effects as a function of ionic strength for fractions PC-80 F8, PC-80 FD, PC-80 F4, and PC-80 F1 of Na-copoly (ethyl acrylate-acrylic acid)	193
6.11	Plot of β calculated from $\beta = 2.78\ \alpha_\eta/\alpha_f$ as a function of ionic strength for fractions PC-80 F8, PC-80 FD, PC-80 F4, and PC-80 F1 of Na-copoly (ethyl acrylate-acrylic acid)	195
6.12	Plot of β_o calculated from $\beta_o = \Phi_o^{1/3} P_o^{-1}$ as a function of ionic strength for fractions PC-80 F8, PC-80 FD, PC-80 F4, and PC-80 F1 of Na-copoly (ethyl acrylate-acrylic acid)	197
6.13	Double logarithmic plots of D_{z_o} versus M_D for fractions of Na-copoly (ethyl acrylate-acrylic acid) in aqueous salt solutions and 2 Heptanone	202
6.14	Plots of $1/D_{z_o} M_D^{1/2}$ versus $M_D^{1/2}$ for the fractionated samples of Na-copoly (ethyl acrylate-acrylic acid) in the designated ionic strength solutions	208
6.15	Plots of $1/D_{z_o}{}^2 M_D$ versus $D_{z_o}{}^3 M_D{}^3$ for the fractionated samples of Na-copoly (ethyl acrylate-acrylic acid) in the designated ionic strength solutions	210
6.16	Plots of the expansion factors α_f and $\alpha_\eta{}^3$ as a function of the excluded volume parameter z for fractions PC-80 F8, PC-80 FD, PC-80 F4 and PC-80 F1 of Na-copoly (ethyl acrylate-acrylic acid)	215

Figure

		Page
6.17	The correction factor to the frictional coefficient, k_f^c, versus ionic strength for fractions PC-80 F8, PC-80 FD, PC-80 F4, and PC-80 F1 of Na-copoly (ethyl acrylate-acrylic acid)	218
6.18	Plot of k_f^c versus $M_\eta^{1/2}(\alpha_\eta - \alpha_\eta^{-1})$ for fractions PC-80 F8, PC-80 FD, PC-80 F4, and PC-80 F1 of Na-copoly (ethyl acrylate-acrylic acid)	222
6.19	The correction factor to the frictional coefficient when polymer concentration expressed as a volume fraction, k_f^Φ, as a function of ionic strength for fractions PC-80 F8, PC-80 FD, PC-80 F4, and PC-80 F1 of Na-copoly (ethyl acrylate-acrylic acid)	226
6.20	Plot of $k_f^c - (k_f^c)\theta$ versus $M_\nu A_2$ for fractions PC-80 F8, PC-80 FD, PC-80 F4, and PC-80 F1 of Na-copoly (ethyl acrylate-acrylic acid), to test linear relationship predicted by Pyun and Fixman	228
6.21	Plot of $k_f^c - (k_f^c)\theta$ versus $M_\nu A_2$ for fractions PC-80 F8, PC-80 FD, PC-80 F4, and PC-80 F1 of Na-copoly (ethyl acrylate-acrylic acid)	231
6.22	Correction factor to the frictional coefficient at the theta point, $(k_f^c)_\theta$, versus $M_\eta^{1/2}$ for fractions of Na-copoly (ethyl acrylate-acrylic acid)	233
6.23	Plots of D_{z_o} as a function of ionic strength for fractions PC-80 F8, PC-80 FD, PC-80 F4, and PC-80 F1 of Na-copoly (ethyl acrylate-acrylic acid)	236
6.24	Plots of hydrodynamic radius R_H as a function of ionic strength for fractions PC-80 F8, PC-80 FD, PC-80 F4, and PC-80 F1 of Na-copoly (ethyl acrylate-acrylic acid)	238
6.25	Plots of the logarithm of the hydrodynamic radius, R_H(Å) versus ionic strength for fractions PC-80 F8, PC-80 FD, PC-80 F4, and PC-80 F1 of Na-copoly (ethyl acrylate-acrylic acid)	241
6.26	The expansion factors α_f and α_η^3 versus lnz for fractions PC-80 F8, PC-80 FD, PC-80 F4, and PC-80 F1 of Na-copoly (ethyl acrylate-acrylic acid) where lnz is proportional to ln I	243

LIST OF TABLES

Table		Page
3.1	Conjugate Pairs of $\alpha_s(z)$ and $\Psi(\bar{z})$	37
3.2	The Effect of Ionic Strength on α_s	43
3.3	Second Virial Coefficients, $A_2 \times 10^4$ (mol·cm^3/g^2), for Na-copoly (ethyl acrylate-acrylic acid) in NaCl Solutions, from Tan (14)	91
5.1	Values of f(A) Calculated as a Function of Aperture and Pinhole Size	118
5.2	Molecular Weight $\times 10^{-5}$ and Polydispersity Index, M_W/M_n	126
5.3	The Mark-Houwink Constants K_η and a in $[\eta] = K_\eta M_w^{-a}$ for Na-copoly (ethyl acrylate-acrylic acid) in Various Media	127
5.4	a and δ Values in the Relationship, $\langle s^2 \rangle = KM_w^{\nu}$, for Na-copoly (ethyl acrylate-acrylic acid), in Various Media	140
5.5	K and ν Values in the Relationship, $\langle s^2 \rangle = KM_w^{\nu}$, for Na-copoly (ethyl acrylate-acrylic acid) in Various Media	141
5.6	Limiting Concentrations, C_m, for Na-copoly (ethyl acrylate-acrylic acid) in Various Media	144
6.1	Values of D_{z_o} and k_f^c for Na-copoly (ethyl acrylate-acrylic acid) Fractions	179
6.2	Comparison of Values of b Obtained Experimentally from $D_{z_o} = K_D M_D^{-b}$ and From the Relation 3b' = a + 1	204
6.3	Comparison of Experimental Values of k_f^c with Predictions of Yamakawa, and Pyun and Fixman	220

CHAPTER I

INTRODUCTION

The technique of Intensity Fluctuation Spectroscopy has in recent years been added to the methods from which information about macromolecules can be obtained. It has been used to obtain the translational and rotational diffusion constants of macromolecules as well as the flexing modes of larger macromolecules. In the present study, the translational diffusion constants of a polyelectrolyte, Na-copoly (ethyl acrylate-acrylic acid) in the presence of added salt have been measured. This copolymer, which has both hydrophobic and hydrophylic groups along the chain, has been observed by other methods to undergo a conformational transition as a function of ionic strength from a compact to an extended random coil.

The purpose of this study is twofold. One is to access the limits and advantages of the technique of laser light scattering as a tool in the study of polymers. Of particular concern will be the problems introduced by the effects of polydispersity. Since polymers are always polydisperse to a greater or lesser degree, the ease with which a suitable average diffusion constant is obtained and its interpretability are of paramount importance to the extension of the technique as a routine analytic tool for polymers. In addition, in order to compare results of diffusion constant measurements with other techniques measuring size parameters of polymers, such as intrinsic viscosity and light scattering, an attempt will be made to see how well the two

parameter theory of polymer solutions predicts the interrelation between these measureable quantities.

The other purpose of this thesis is the study of polyelectrolytes using laser Rayleigh scattering. In particular, it was hoped that the diffusion studies would show more conclusively than from previous work the presence of a transition in Na-copoly (ethyl acrylate-acrylic acid). Unfortunately, it turned out that the problems of polydispersity were not worked out sufficiently to allow for unambiguous interpretation of the data, at least in terms of transition behavior. However, the analysis of the data still sheds light on the extension of the two parameter theory of polymer solutions to polyelectrolytes. In particular, theories predicting the correction factor to the frictional coefficient will be compared with those obtained here experimentally. Also, the theoretical expressions relating radii of gyration to hydrodynamic radii will be compared with those obtained experimentally for polyelectrolytes and contrasted with experimental observations found in the literature on nonionic polymers.

Chapter II contains an introduction to the theory of quasi-elastric light scattering which is necessary to understand the problems arising from the interpretation of the diffusion data. Also included is a summary of the methods presently available to handle the effects of polydispersity.

Chapter III contains background information on the two parameter theory of polymer solutions. It is covered in some detail because the concepts and especially the terminology are not easily available in textbook form, and are needed to understand the theories with which the

experimental results will be subsequently compared. The sections on nonequilibrium properties and the concentration dependence of the diffusion constant contain these pertinent theories. Since the theories are usually derived for monodisperse systems, Chapter III also contains a section on how the theories must be corrected for heterogeneity effects.

Chapter IV contains information on conformational transitions which have been observed in other polyelectrolyte systems as well as the methods which have been used to observe the transition in Na-copoly (ethyl acrylate-acrylic acid).

Chapter V describes the experimental methods used for the experiments. Chapter VI presents the results of the present study beginning with the important description of the data reduction and ending with the conclusions drawn from the data analysis.

C H A P T E R I I

QUASI-ELASTIC LIGHT SCATTERING

Introduction

The impingement of the electric field of light on matter induces an oscillating polarization of the electrons in the molecules. When these translational and rotational degrees of freedom of the molecules are excited, the molecules serve as secondary sources of light by reradiating it. From the analysis of the intensity, angular distribution and frequency shifts of this scattered light, it is possible to obtain information about the size, shape, molecular interactions and dynamics of the scattering material.

The theory of Rayleigh scattering, presented in 1871 (7), was originally derived for dilute gases, which were considered as assemblies of noninteracting particles sufficiently small compared to the wavelength of light to be regarded as point-dipole oscillators. The application of this theory to condensed phases predicted intensities of scattering which were at least an order of magnitude larger than those experimentally observed. The decrease in intensity was due to the destructive interference between waves scattered from different molecules. To circumvent this difficulty, Smoluchowski (2) (1908) and Einstein (3) (1910) considered the liquid to be a continuous medium in which thermal fluctuations give rise to local homogeneities and thereby to fluctuations in the local dielectric constant. Debye (4,5) attributed the

latter to density and concentration fluctuations. The fluctuation theory of light scattering was synthesized with the developments of Rayleigh's molecular theory of independent optically anisotropic scatterers by Debye and Zimm and coworkers (6). It led to the use of measurements of the total intensities of scattered light as a method of studying molecular weights, sizes, shapes, and second virial coefficients of macromolecules in solution.

Concurrent with this development was the treatment of local density fluctuations as thermally excited sound waves by Brillouin (7) (1914). By retaining the time behavior of the thermal phonons, Brillouin (8) (1922) and Mandel'shtam (9) (1926) independently reported the first consideration of the spectrum of light scattered from a condensed medium. They predicted a doublet in the frequency distribution of the scattered light. Experimental measurements of the Brillouin-Mandel'shtam components by Gross (10)(1930) indicated the presence of a central or Rayleigh line whose peak maximum was unshifted. Landau and Placzek (11) (1934) gave a theoretical explanation of the Rayleigh line using non-propagating local temperature fluctuations.

The frequency distribution of Rayleigh scattered light from dilute macromolecular solutions was obtained independently by Pecora (12) (1964) and Debye (13) (1965), who found that the spectrum had a Lorentzian shape and a half-width which was proportional to the diffusion constant of the molecules in solution. However, these frequency shifts, which are in the range $10\text{-}10^7$ Hz and appear as a broadening of the exciting frequency, are too small to be measured using conventional light sources and detector techniques. Two developments were neces-

sary before the measurements could be made.

One was the advent of the laser, which could provide a coherent beam with an extremely narrow spectral width and with power per wavelength interval greatly in excess of any conventional source. The other was the development of a nonlinear detection technique known as optical mixing (or beating) spectroscopy or intensity fluctuation spectroscopy by Cummins et al. (14) (1964) and Ford and Benedek (15) (1965). In this method, the scattered light is mixed at a detector, usually a photomultiplier tube, with a portion of the unscattered beam (heterodyne) or with itself (homodyne or self-beat) in order to shift the spectrum to audio or radio frequencies. The output of the photomultiplier is then analyzed in the time domain by real time autocorrelation techniques or in the frequency domain using a spectrum analyzer.

Intensity Fluctuation Spectroscopy

Introduction. In an intensity fluctuation spectroscopy experiment, shown in Figure 2.1, light from a laser illuminates a sample and is scattered into a detector placed at an angle with respect to the transmitted beam. The intersection between the incident beam and the scattered beam defines the scattering volume. Since the vector sum of the electric fields of the macromolecules in the scattering volume is changing with time due to Brownian motion, a detector of the scattered light, usually a photomultiplier which is sensitive to the square of the electric field impinging on it, will perceive a randomly fluctuating light intensity whose evolution in time will reflect the motions of the molecules.

Figure 2.1

Geometrical picture of the light scattering process where k = the incident light wave vector, k_s = the scattered wave vector, and θ = the scattering angle.

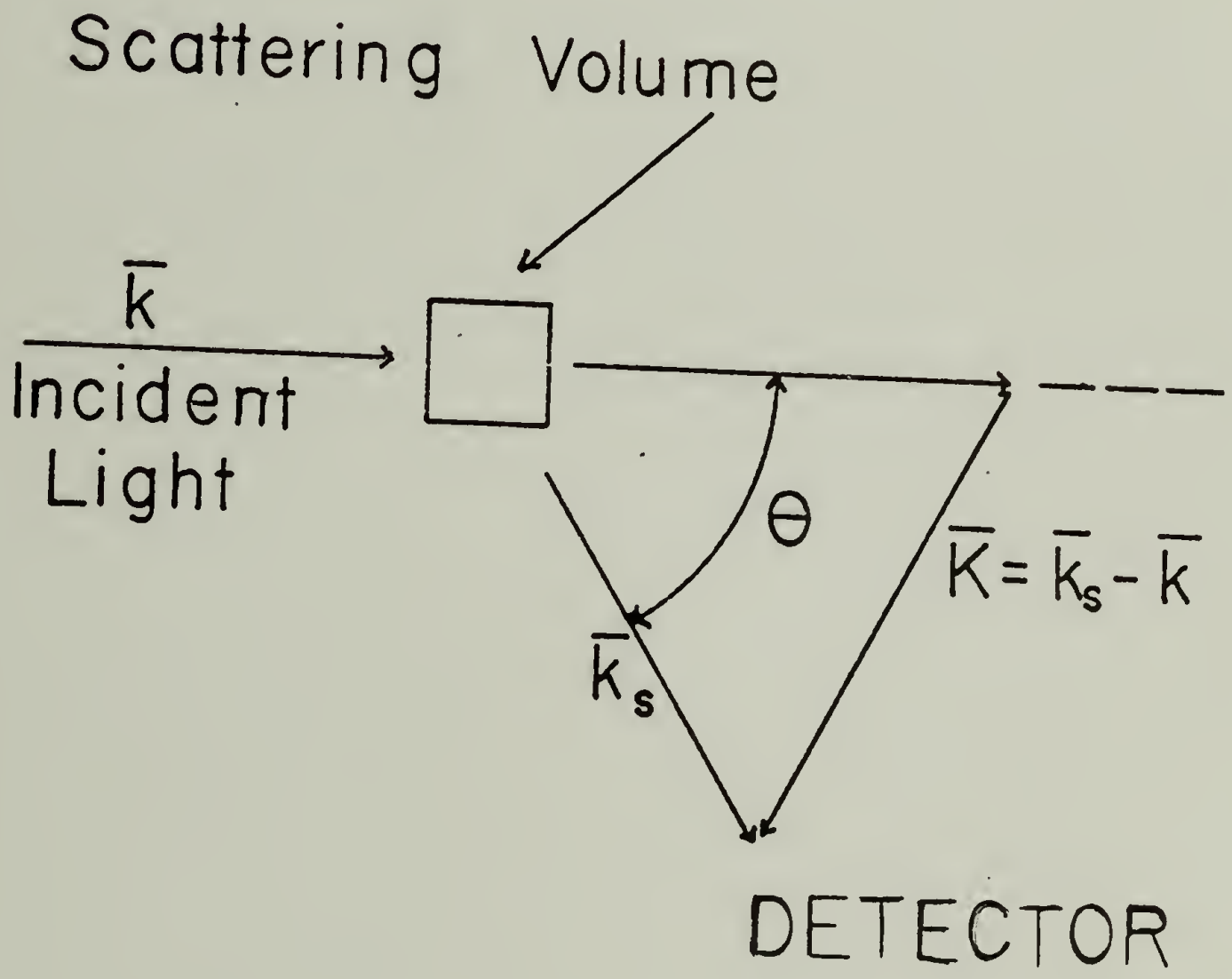

A physical picture of the origin of these intensity fluctuations can also be obtained by analogy with Bragg scattering (16). The randomly located macromolecules in solution can be regarded as a Fourier superposition of many crystalline arrays. The diffraction pattern arising from the scattering of monochromatic light by such an array consists of a superposition of many randomly placed maxima and minima, which will fluctuate with time. The fluctuations of the scattered light are detected by a photomultiplier having a photosensitive area roughly equal to the distance of one diffraction maximum. Thus the average time it takes for a diffraction minimum to replace a maximum at the detection point will be of the order of the time it takes a macromolecule to diffuse one wavelength of light (17).

Since the number of macromolecules in the scattering volume is quite large, it is of course impossible to follow the individual motions of each molecule. It thus becomes necessary to find statistical quantities which contain equivalent information. One such average quantity is the mean intensity of the scattered light. The time evolution of the total scattered electric field can be obtained, on the other hand, by two complementary methods which yield different but related average quantities.

The more convenient method, both from the computational and experimental viewpoints, is to measure the time autocorrelation function (or the intensity-intensity autocorrelation function) of the scattered light,

$$G^{(2)}(\tau) = \frac{1}{2T}\int_{-T}^{T} I(t)I(t+\tau)dt = \overline{I(t)I(t+\tau)} \qquad (2.1)$$

It is a measure of the similarity between the intensity at the photodetector at time t, $I(t)$ and that at time $t + \tau$, $I(t + \tau)$. It should be stressed that the signal received at the photomultiplier is essentially a randomly fluctuating light intensity. Thus the time dependence of $I(t)$ will resemble a noise pattern. Nevertheless, when τ is very small compared to times typifying the fluctuations in I, $I(t + \tau)$ will be very close to $I(t)$. As τ increases, it is more likely that the value of $I(t + \tau)$ will be different from that at $I(t)$. It is for this reason that the concept of correlation between $I(t)$ and $I(t + \tau)$ arises, a measure of which is given by the autocorrelation function, $G^{(2)}(\tau)$. It can be shown that the value of $G^{(2)}(\tau)$ is largest at $\tau = 0$. In addition, as $\tau \to \infty$, $I(t)$ and $I(t + \tau)$ are completely uncorrelated so that $G^{(2)}(\tau)$ approaches $\langle I \rangle^2$ or in other words just the square of the average intensity. Thus the autocorrelation function decays from a maximum to the equilibrium value of the total intensity. It is this characteristic time for the decay which is related to the time scale of motions of molecules in solution. In the special circumstances of independent, non-interacting particles, to be discussed later, the autocorrelation function decays like a single exponential whose time constant is related to the diffusion constant of macromolecules in solution. Thus

$$G^{(2)}(\tau) \sim e^{-2\Gamma\tau} \qquad (2.2)a$$

$$\Gamma = DK^2 \qquad (2.2)b$$

where K is the scattering vector.

On the other hand, if a frequency analysis is made of fluctua-

tions in the detector photocurrent, an average quantity called the power spectrum of the scattered light is obtained. Physically, this is explained as being due to the Brownian motion of the molecules which cause the scattered light to be Doppler-shifted from the incident frequency. In the case of independent non-interacting particles, the power spectrum is a Lorentzian whose half width at half height is related to the diffusion constant of the molecules in solution. Thus

$$I(\bar{K},\omega) \sim \frac{2\Gamma}{(\omega - \omega_0)^2 + (2\Gamma)^2} \qquad (2.3)$$

It should be stressed that these two methods are physically equivalent, since the power spectrum and the autocorrelation function form a Fourier-transform pair. In addition, the autocorrelation function or the power spectrum can be obtained whether the intensity fluctuations are studied using homodyne (self-beat) or heterodyne techniques. In the present experiments, the self-beat spectrum of the scattered light was measured using a real time autocorrelator.

In subsequent sections, a mathematical treatment will be presented to demonstrate explicitly how information on the time scale of motions of macromolecules is transmitted in the scattered electric field and how the technique of optical mixing spectroscopy, which is essential in order to make the information measurable, preserves the information on the time dependence. In addition, the effects of polydispersity and particle interaction will be considered.

Scattered electric field. (18,19,20,21) As shown in Figure 2.1, incident

light from a laser, assumed to be a uniform monochromatic plane polarized wave of wavelength λ_o passes through an isotropic solution of refractive index n and has the form

$$\bar{E}_i(\bar{r},t) = \bar{n}_i E_0 \exp[i(\bar{k}_i \cdot \bar{r} - \omega_o t)] \tag{2.4}$$

where ω_o is the angular frequency, $\bar{n}_i$ is the polarization, E_o is the amplitude, $\bar{r}$ is the position vector, and $\bar{k}_i$ is the wave vector given by

$$\bar{k}_i = \frac{2\pi n}{\lambda_o} .$$

This plane wave polarizes the medium according to the relation

$$\bar{P}(\bar{r},t) = \alpha(\bar{r},t)\bar{E}_i(\bar{r},t) \tag{2.5}$$

where $\alpha(\bar{r},t)$ is the local polarizability. Thermal fluctuations cause $\alpha(\bar{r},t)$ to vary locally, so that

$$\alpha(\bar{r},t) = \alpha_o + \delta\alpha(\bar{r},t) \tag{2.6}$$

where α_o is the time averaged polarizability and $\delta\alpha(\bar{r},t)$ is the local fluctuation in it. Substitution of Equation (2.6) into Equation (2.5) gives

$$\bar{P}(\bar{r},t) = \alpha_o\bar{E}_i(\bar{r},t) + \delta\alpha(\bar{r},t)\bar{E}_i(\bar{r},t) \tag{2.7a}$$

$$= \langle\bar{P}(\bar{r},t)\rangle + \delta\bar{P}(\bar{r},t) \tag{2.7b}$$

The latter term is a fluctuating polarization vector and it is this fluctuation of local polarization which causes scattering, or reradiation of the incident light. From classical electromagnetic theory,

the component of the scattered electric field at a large distance R from the scattering volume, is given by

$$E_s(\bar{R},t) = \frac{1}{c^2}\int_V \frac{1}{|\bar{R}-\bar{r}|}\hat{k}_s \times [\hat{k}_s \times \frac{d^2\delta P(\bar{r},t_R)}{dt^2}]\, dV \qquad (2.8)$$

where V is the scattering volume, c is the velocity of light in a vacuum, t_R is the retarded time, and $\hat{k}_s = (\bar{R}-\bar{r})/|\bar{R}-\bar{r}|$ is a unit vector in the direction of the scattered light. This equation is simplified as follows. Equation (2.7) is substituted into Equation (2.8) and the assumption is made that the magnitude of the first two time derivatives of $\delta\alpha(\bar{r},t)$ is negligible compared to ω_o. Then, using the relation that the dielectric constant, $\varepsilon = 4\pi\alpha + 1$ or $\delta\varepsilon = 4\pi\delta\alpha$, and representing the fluctuations in the local dielectric constant by a Fourier decomposition,

$$\delta\varepsilon(\bar{r},t) \sim \int \delta\varepsilon(\bar{K},t)\exp[i\bar{K}\cdot\bar{r}]d^3K \qquad (2.9)$$

leads to

$$\bar{E}_s(\bar{R},t) = (\frac{\omega_o}{c})^2 \frac{1}{4\pi R}\frac{1}{(2\pi)^{3/2}}\, \bar{k}_s \times (\bar{k}_s \times \bar{E}_i)\exp[i(\bar{k}_s\cdot\bar{R}-\omega_o t)]$$

$$\times \int \delta\varepsilon(\bar{K},t)\left\{\int_V \exp[i(\bar{k}_i - \bar{k}_s + \bar{K})\cdot\bar{r}dV\right\} d^3K \qquad (2.10)$$

The expression in brackets is a three dimensional Dirac delta function $\delta[\bar{K}-(\bar{k}_i-\bar{k}_s)]$ which has the property of being zero except when $\bar{K} = \bar{k}_i - \bar{k}_s$. Thus Equation (2.10) reduces to

$$\bar{E}_s(\bar{R},t) = (\frac{\omega_o}{c})^2 \frac{(2\pi)^{3/2}}{4\pi R} \bar{k}_s \times (\bar{k}_s \times \bar{E}_i)\delta\varepsilon(\bar{K},t)\exp[i(\bar{k}_s \cdot \bar{R} - \omega_o t)] \quad (2.11)$$

The physical significance of this result is that the scattering which is observed is due only to the component of the dielectric constant fluctuation whose wave vector is equal to the difference between the incident and scattered wave vectors. Thus, observing the scattering at an angle θ determines the particular wave vector, $\bar{K}$, which is observed. It can be shown that

$$|\bar{K}| = 2k \sin\frac{\theta}{2} = \frac{2\pi}{\lambda_o}\sin\frac{\theta}{2} \quad (2.12)$$

where the assumption has been made that $|\bar{k}_i| = |\bar{k}_s|$, since $\Delta\bar{K}/\bar{K} \sim 10^{-12}$, and the subscripts have been dropped. In addition, it can be seen from Equation (2.11) that information concerning the fluctuations of the dielectric constant is contained in the scattered electric field. If these dielectric fluctuations are considered as arising from local fluctuations in concentration, and using $\varepsilon = n^2$, then

$$\delta\varepsilon(\bar{K},t) = 2n\frac{dn}{dc}\delta c(\bar{K},t) \quad (2.13)$$

Thus

$$\bar{E}_s(\bar{R},t) = (\frac{k_s}{n})^2 \frac{2\pi}{2\pi R}^{3/2} \bar{k}_s \times (\bar{k}_s \times \bar{E}_i)\exp[i(\bar{k}_s \cdot \bar{R} - \omega_o t)]2n\frac{dn}{dc}\delta c(\bar{K},t) \quad (2.14)$$

where the relation $\frac{k_s}{n} = \frac{\omega_o}{c}$ has been used.

Since the Doppler shifts in frequency due to the Brownian motion of the particles are very small, amounting to only a few thousand hertz or less as compared with the incident light frequency of about 5×10^{14} hertz, they cannot be measured using conventional detection (e.g., Fabry-Perot interferometers) techniques. This can be demonstrated most clearly in the frequency domain by calculating the frequency spectrum of the scattered light. Taking the Fourier transform of Equation (2.14) yields

$$\bar{E}_s(\bar{R},\omega) = \int_{-\infty}^{\infty} \bar{E}_s(\bar{R},\omega)e^{i\omega t}dt = A \int_{-\infty}^{\infty} \delta c(\bar{K},t)e^{i(\omega - \omega_o)t}dt \qquad (2.15)$$

where the constant A will be left unspecified. The electric field itself is not directly measurable; instead what is measured is the spectral power density $S(K,\omega)$ which is proportional to $|\bar{E}(\bar{R},\omega)|^2$ and given by

$$S(\bar{K},\omega) = A' \left| \int_{-\infty}^{\infty} \delta c(\bar{K},t)e^{i(\omega - \omega_o)t}dt \right|^2 \qquad (2.16)$$

where A' is another constant.

In order to evaluate $S(\bar{K},\omega)$, a form for $\delta c(\bar{K},t)$ must be found. A simplified approach to this problem is to assume that the concentration fluctuation obeys Fick's second law of diffusion,

$$\frac{\partial}{\partial t} \delta c(\bar{r},t) = D\nabla^2 \delta c(\bar{r},t) \qquad (2.17)$$

where D is the translational diffusion coefficient. The solution to this simple differential equation is

$$\delta c(\bar{K},t) = \delta c(\bar{K},o)e^{-DK^2t} \tag{2.18}$$

where $\delta c(\bar{K},o)$ is the amplitude of the fluctuation at time zero. Substitution of Equation (2.18) into (2.16) and evaluation of the integral yields

$$S(\bar{K},\omega) = A'' \frac{\Gamma}{(\omega - \omega_o)^2 + \Gamma^2} \tag{2.19}$$

where $\Gamma = DK^2$ and A" is another constant. Using approximate values for ω and K and typical values of D for macromolecules ($\sim 10^{-7}$ cm^2/sec) it can be seen that the width of this Lorentzian spectrum will be only a few hundred hertz centered around an incident frequency of 10^{14} hertz. It thus becomes necessary to use optical mixing techniques which result in centering the Lorentzian around zero frequency, in order to allow resolution of this narrow line width.

Optical mixing techniques. (16,18,19,20) A simplified example of the principle of optical mixing is illustrated in Figure 2.2 for a self-beat system. In the case of 2 molecules which suffer frequency shifts of $\delta\omega_1$ and $\delta\omega_2$, where δ is used to indicate that these shifts are small compared to the incident frequency ω_o, the intensity at the detector, which is just the square of the total scattered electric field, is given by

$$I\alpha|\ E_1 + E_2|^2 = E_o^2[\cos(\omega_o + \delta\omega_1)t + \cos(\omega_o + \delta\omega_2)t]^2 \tag{2.20}$$

Using trigonometric identities and the fact that photomultiplier tubes

Figure 2.2

Example showing two scattering particles in the incident light beam of angular frequency ω_0. The Brownian motion of the particles causes the light scattered into the detector to be Doppler shifted by an amount $\delta\omega_1$, $\delta\omega_2$. Taken from Olson (20).

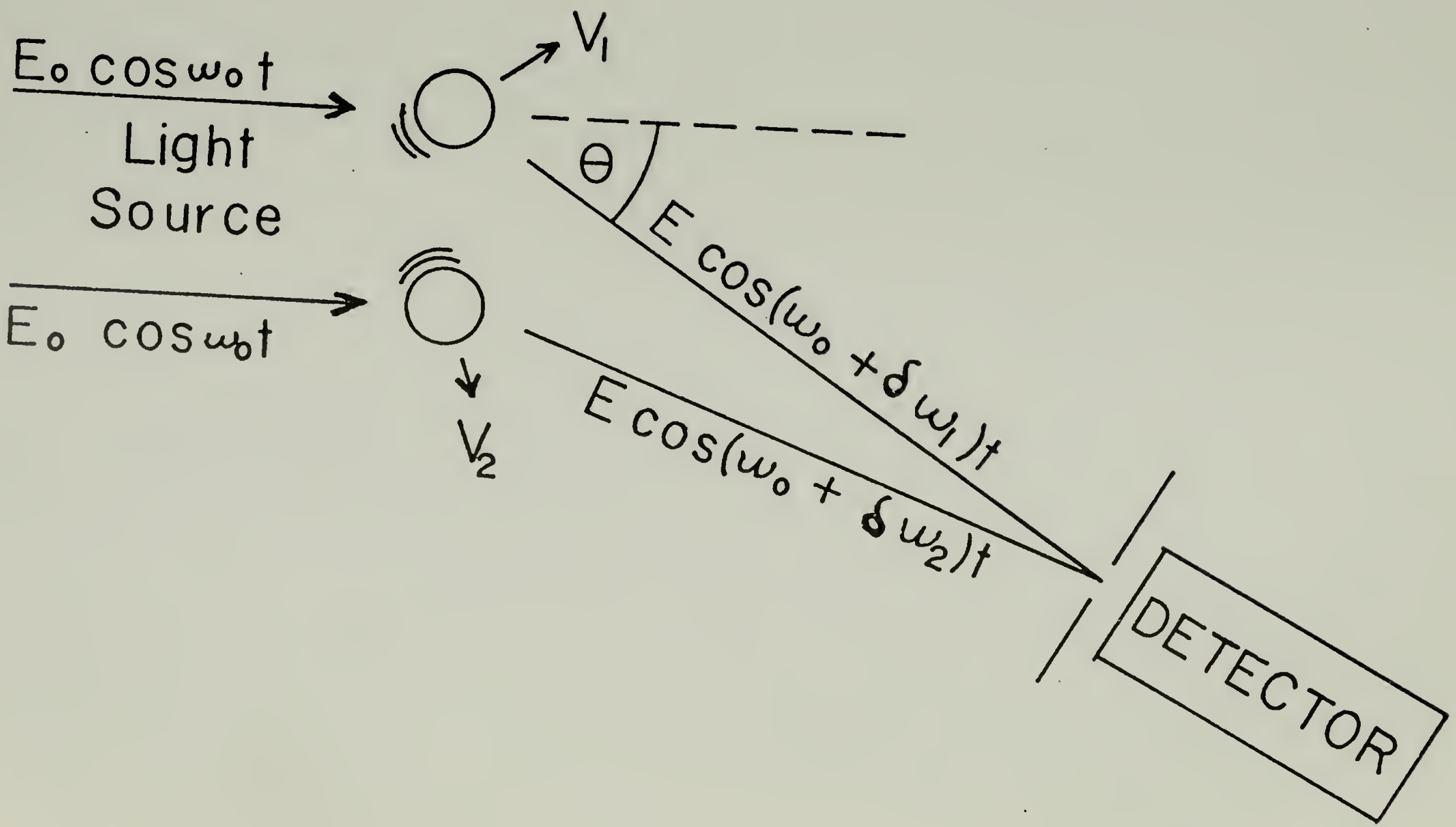
$E_o \cos\omega_o t$
Light
Source
$E_o \cos\omega_o t$
V_1
V_2
θ
$E \cos(\omega_o + \delta\omega_1)t$
$E \cos(\omega_o + \delta\omega_2)t$
DETECTOR

respond to frequencies in excess of 10^{10} Hz as a D.C. output current, Equation (2.20) reduces to

$$I \alpha \text{ D.C.} + E_o^2 \cos(\delta\omega_1 - \delta\omega_2)t \tag{2.21}$$

from which it can be seen that the photocurrent retains the information on the motion of the two molecules.

In order to discuss the more complex case of many macromolecules, it will be simpler at the outset to define all the quantities which are to be calculated and their interrelations.

The first-order field autocorrelation function is given by

$$G^{(1)}(\tau) = \langle E(t)\, E^*(t + \tau)\rangle \tag{2.22}$$

where * denotes the complex conjugate of a quantity. $G^{(1)}(\tau)$ is the Fourier transform of the spectral power density $S(\bar{K},\omega)$ given by Equation (2.19). The second-order or intensity correlation function is given by Equation (2.1) (or 2.2), which as mentioned previously is the Fourier transform of the power spectrum $I(\omega)$ (Equation (2.3)). These correlation functions may be written in normalized form as

$$g^{(1)}(\tau) = \frac{\langle E(t)E^*(t + \tau)\rangle}{\langle I\rangle} \tag{2.23}$$

and

$$g^{(2)}(\tau) = \frac{I(t)I(t + \tau)}{\langle I\rangle^2} \tag{2.24}$$

where I is the integrated intensity of light scattered at angle θ. For

a large class of fields having Gaussian statistics, the fields are completely specified by a knowledge of $G^{(1)}(\tau)$. Siegart (22) showed also that

$$g^2(\tau) = 1 + |g^{(1)}(\tau)|^2 \tag{2.25}$$

It should be stressed that under the experimental conditions of concern for the present experiments, relation (2.25) is always valid. Variations in the form of the measured intensity correlation function will just depend on the relation derived for the field correlation function. The latter will be discussed for the special cases of simple translational diffusion, interacting particles and polydisperse systems.

For light scattered from a solution of identical, noninteracting particles which are spherically symmetric and/or small compared to the wavelength of light, the substitution of Equation (2.18) for $\delta c(\bar{K},t)$ into Equation (2.14) for the scattered field results in

$$G^{(1)}(\tau) = (\text{constant})e^{-\Gamma\tau}e^{i\omega_o\tau} \tag{2.26}$$

$$G^{(2)}(\tau) = \langle I \rangle^2 [1 + e^{-2\Gamma\tau}] \tag{2.27}$$

and $$g^{(2)}(\tau) = 1 + e^{-2\Gamma\tau} \tag{2.28}$$

Thus the measured autocorrelation function results in single exponential decay.

The Fourier transform of Equation (2.27) is

$$I(\omega) = 2\pi\delta(\omega)\langle I \rangle^2 + 2\langle I \rangle^2 \frac{2\Gamma}{[\omega^2 + (2\Gamma)^2]} \tag{2.29}$$

which can be compared with Equation (2.3). The first term is just a D.C. photo current and the second term contains the information about the solute molecules. In addition, the crucial transformation has been made to a Lorentzian of half-width $2DK^2$ centered about zero frequency, where the narrowness of the spectrum is no longer an experimental problem.

Polydispersity

Since all macromolecular solutions are polydisperse to some degree, it becomes important to determine the effect of the polydispersity on the measured correlation function and hence on the time constants extracted from it. Macromolecules differing in molecular weight have different diffusion coefficients so that the correlation function should be a concentration weighted sum of exponents each with the decay constant dependent on the D of the corresponding molecule. Thus, the normalized field correlation function will be modified to give the following superposition of exponentials

$$|g^{(1)}(\tau)| = \int_{-\infty}^{\infty} G(\Gamma)e^{-\Gamma\tau}d\Gamma \tag{2.30}$$

where the distribution of decay rates is so defined that $G(\Gamma)d\Gamma$ is the fraction of the total intensity scattered due to molecules for which DK^2 lies between Γ and $\Gamma + d\Gamma$ and

$$\int_{-\infty}^{\infty} G(\Gamma)d\Gamma = 1 \tag{2.31}$$

Thus, for a system with, for example, two components, the correlation function is simply a weighted sum of two exponentials.

In addition, the mean value of the decay rate is given by

$$\bar{\Gamma} = \int G(\Gamma)\Gamma d\Gamma = \sum_i \Gamma_i G(\Gamma_i) \tag{2.32}$$

where discrete notation can also be used. Since the average intensity of light scattered by N macromolecules of molecular weight M is proportional to NM^2, for a polydisperse solution the weighting factor is

$$G(\Gamma_i) = \frac{N_i M_i^{\,2}}{\sum_i N_i M_i^{\,2}} \tag{2.33}$$

and therefore

$$\bar{\Gamma} = \frac{\sum_i N_i M_i^{\,2} \Gamma_i}{\sum_i N_i M_i^{\,2}} \tag{2.34}$$

If all the scatterers in the sample are small compared to 1/K and are noninteracting, for each species, $\Gamma_i = D_i K^2$ and hence

$$\bar{D} = \frac{\bar{\Gamma}}{K^2} = \frac{\sum_i N_i M_i^{\,2} D_i}{\sum_i N_i M_i^{\,2}} \tag{2.35}$$

Thus, for a polydisperse system, the diffusion constant obtained in an intensity fluctuation spectroscopy experiment is a z average diffusion constant, D_z.

In principle, $G(\Gamma)$ could be obtained by a Laplace inversion of the experimental estimate of $|g^{(1)}(\tau)|$ obtained from the measured intensity correlation function. Unfortunately, it turns out that this procedure is extremely sensitive to unavoidable statistical errors in the data, and, in general, data of unattainably high precision are needed to perform this inversion.

Two basic approaches have been adopted in attempting to characterize sample polydispersity. In one approach, a parametric form for $G(\Gamma)$ is assumed for the sample. In the other, the cumulants or moments of $G(\Gamma)$ about the mean for an arbitrary form of $G(\Gamma)$ are obtained. This latter method, developed by Koppel and Pusey (23,24) will be discussed first.

The basis of the derivation is an expansion of $e^{-\Gamma\tau}$ from Equation (2.31) around its mean value defined by Equation (2.33). Thus

$$\exp(-\Gamma\tau) = \exp(-\bar{\Gamma}\tau)\exp[-(\Gamma-\bar{\Gamma})\tau]$$

$$= \exp(-\bar{\Gamma}\tau)\left[1 - (\Gamma-\bar{\Gamma})\tau + \frac{(\Gamma-\bar{\Gamma})^2\tau^2}{2!} - \frac{(\Gamma-\bar{\Gamma})^3\tau^3}{3!} + \ldots\right] \quad (2.36)$$

Substituting Equation (2.37) into Equation (2.31) leads to

$$|g^{(1)}(\tau)| = \exp(-\bar{\Gamma}\tau)\left[1 + \frac{\mu_2\tau^2}{2!} - \frac{\mu_3\tau^3}{3!} + \ldots\right] \quad (2.37)$$

and thus

$$\ln[|g^{(1)}(\tau)|] = -\bar{\Gamma}\tau + \frac{1}{2!}\left(\frac{\mu_2}{\bar{\Gamma}^2}\right)(\bar{\Gamma}\tau)^2 - \frac{1}{3!}\left(\frac{\mu_3}{\bar{\Gamma}^3}\right)(\bar{\Gamma}\tau)^3 + \ldots \quad (2.38)$$

where

$$\frac{\mu_n}{\bar{\Gamma}^n} \equiv \frac{1}{\bar{\Gamma}^2} \int (\Gamma - \bar{\Gamma})^n \, G(\Gamma) d\Gamma \qquad (2.39)$$

are the nth normalized moments about the mean of $G(\Gamma)$.

Equation (2.38) is a polynomial in τ of infinite order, as compared with the linear function obtained for a monodisperse system. If all the terms were kept, i.e., if all the cumulants of the distribution were known, Equation (2.38) would be exact and $G(\Gamma)$ specified completely. As indicated before, inaccuracy of the data precludes this possibility. However, it turns out that for relatively narrow $G(\Gamma)$'s, $\mu_2/\bar{\Gamma}^2 < 0.25$, the experimental data are well described by just the first few terms of Equation (2.36). Thus data analysis consists of fitting the logarithm of the experimental electric field correlation function to a polynomial in τ of appropriate order. Where to truncate the polymomical actually becomes a matter of judgment, however. This is due to there being a trade off between systematic and random errors in the parameters $\bar{\Gamma}$, μ_2 and μ_3, whose relative magnitudes are not a priori known. As can be seen from Equation (2.39), as $\tau \to 0$ the higher order terms become less important. Thus the procedure suggested by Brown and Pusey (25) is to make a series of measurements over a range of τ_{max} where τ_{max} is the maximum delay time at which the correlator computes a value of the correlation function. The effective value of $\bar{\Gamma}$, μ_2, etc. obtained for each measurement are plotted against $\bar{\Gamma}\tau_{max}$ and extrapolated to $\bar{\Gamma}\tau_{max} = 0$, to give the true value.

By this procedure, the mean, variance, and occasionally the skewness of the distribution can be obtained. The main drawback is that

while the parameters obtained are well defined, they may not always be useful. That is, they are not related simply to the more usual indices of polydispersity, such as $\bar{M}w/\bar{M}n$. However, Pusey (25) has shown that for $\bar{M}w/\bar{M}n < 1.1$ the approximate relation

$$\frac{1}{b^2}\left(\frac{\mu_2}{\bar{\Gamma}^2} + 1\right) \approx \frac{\bar{M}z}{\bar{M}w} \approx \frac{\bar{M}w}{\bar{M}n} \tag{2.40}$$

can be used, where b is defined by $D = K_D M^{-b}$.

If it is simply desired to test the experimental results to determine if there is in fact nonexponential behavior, Equation (2.39) can also be used. If the experimental field correlation function is fit to a quadratic in τ the data can be said to fit a single exponential if the quadratic term is zero to within experimental error. Alternately, if Equation (2.9) is differentiated with respect to τ:

$$\frac{d}{d\tau} \ln|g^{(1)}(\tau)| = -\bar{\Gamma} + \left(\frac{\mu_2}{\bar{\Gamma}^2}\right)(\bar{\Gamma}\tau) - \frac{1}{2}\left(\frac{\mu_3}{\bar{\Gamma}^3}\right)(\bar{\Gamma}\tau)^2 + \ldots \tag{2.41}$$

Thus a plot of the first numerical derivative of the log of the experimental field correlation function as a function of τ will be a horizontal straight line for a single exponential.

In the other approach to sample polydisperity, a parametric form for $G(\Gamma)$ is assumed, often a Schultz distribution of the form

$$\omega(M) = \frac{1}{\Gamma(h+1)} \gamma^{h+1} M^h \exp[-\gamma M], \tag{2.42}$$

since this has proved to be a reasonable representation of a molecular

weight distribution of polymers. Here h is the width parameter and Γ is the gamma function, not the decay constant. The moments of the distribution can be found in Chapter V, Sample Characterization, and Chapter III, Heterogeneity Corrections.

Tagami and Pecora (26) have used the Schultz distribution to calculate by computer $|g^{(1)}(\tau)|$ for various values of h and b (from $D = K_D M^{-b}$). The experimental $|g^{(1)}(\tau)|$ can then be compared with those calculated to yield the best-fit values.

Ford (27), also using a Schultz distribution, derived an approximate theory relating a quantity, ΔD, to the polydispersity index, by analytically least squares fitting a single exponential to the expression

$$|g^{(1)}(\tau)| = [\int_0^\infty M\omega(M)e^{-D(M)K^2\Gamma}dM]^2 \tag{2.43}$$

The quantity ΔD is the fractional increase in the z average diffusion constant, D_z, obtained at $\tau \to 0$ over the long time apparent diffusion constant, obtained at $\tau \to \infty$. The results of this theory, derived in Appendix 6.1, are

$$\frac{D_z}{D_{eff}^{\infty}} = \frac{3 \pm 3[1 - \frac{4}{9}(Y + 1)^{1/2}}{Y + 1} \tag{2.44}$$

where

$$Y = \frac{\Gamma(2 - 2b + h)\Gamma(2 + h)}{\Gamma(2 - b + h)^2} \tag{2.45}$$

where $g_n^{(2)}$ are normalized values of the intensity correlation function in the nth correlation channel. For a Schultz distribution, the plot is a straight line. For particular values of h and b, the slope and intercept can be found and used to obtain Y at X = 0, [Y(0)] and Y at X = 1, [Y(1)], the ratio of which is then plotted as a function of b for varying values of h. This graph is plotted in Figure 8 of Ford. Experimental graphs of Y versus X, yielding experimental values of Y(1)/Y(0) can then be compared to this graph. If b is known, a value of h can thus be obtained.

For the case of two species of differing molecular weight, the field correlation function will be a weighted sum of two exponentials. The measured intensity correlation function will thus have five adjustable parameters. The difficulty in separating even two exponentials was demonstrated by Koppel (24), who showed that the composite diffusion constant of two species with diffusion constants of D_1 and 2.0 D_1, gave a good fit to a single exponential.

REFERENCES

1. Lord Rayleigh, Phil. Mag. 41, 107, 274, 447 (1871).

2. M. Smoluchowski, Ann. Phys., 25, 205 (1908).

3. A. Einstein, Ann. Phys., 33, 1275 (1910).

4. P. Debye, J. Phys. Coll. Chem., 51, 18 (1947).

5. P. Debye, J. Appl. Phys., 15, 338 (1944).

6. D. McIntyre and F. Gornick, "Light Scattering from Dilute Polymer Solutions," Gordon & Breach, New York (1964).

7. L. Brillouin, Compt. Rend., 158, 1331 (1914).

8. L. Brillouin, Ann. Phys. (Paris), 17, 88 (1922).

9. L.I. Mandel'shtam, Zh. Russ. Fit. Khim. Obshchest., 58, 381 (1926).

10. E.F. Gross, Nature 126, 201; 126, 400; 126, 603 (1930).

11. L. Landow and G. Placzek, Phys. Z. Sowjetunion 5, 172 (1934).

12. R. Pecora, J. Chem. Phys., 40, 1604 (1964).

13. P. Ribye, Phys. Rev. Letts., 14, 783 (1965).

14. H.Z. Cummins, N. Knable and Y. Yeh, Phys. Rev. Lett., 12, 150 (1964).

15. N.C. Ford, Jr. and G.B. Benedek, Phys. Rev. Lett., 15, 649 (1965).

16. N.C. Ford, Jr., Chemica Scripta., 2, 193 (1972).

17. P.N. Pusey, D.E. Koppel, D.N. Schaefer, R.D. Camerini-Otero, and S.H. Koenig, Biochem., 13, 952 (1974).

18. B. Berne and R. Pecora, "Dynamic Light Scattering," John Wiley, N.Y. (1976).

19. H.Z. Cummins and E.R. Pike (eds.), "Photon Correlation and Light Beating Spectroscopy," Plenum, New York (1974).

20. T. Olson, "Laser Light Scattering Studies of Transfer Ribonucleic Acid," Thesis, U. Mass., Amherst (1974).

21. J.D. Jackson, "Classical Electromagnetism," John Wiley, New York (1962).

22. A.J.F. Siegert, M.I.T. Rad. Lab. Rep. No. 465 (1943).

23. P.N. Pusey, D.E. Koppel, D.W. Schaeffer and R.D. Camerini-Otero, IBM Report No. RC3924, Yorktown Heights, New York (1972).

24. D.E. Koppel, J. Chem. Phys., 57, 4814 (1972).

25. J.C. Brown and P.N. Pusey, J. Chem. Phys., 62, 1136 (1975).

26. R. Pecora and Y. Tagami, J. Chem. Phys., 51, 3298 (1969).

27. Appendix 6.1, this thesis.

28. N.C. Ford, R. Gabler, and F.E. Karasz, Adv. in Chem. Ser. 125, 25 (1973).

CHAPTER III

DILUTE SOLUTION THEORY

Two Parameter Theory of Polymer Solutions

Introduction. Except when in the theta state, all equilibrium and nonequilibrium properties of dilute polymer solutions are influenced by the excluded volume effect. This effect may be treated within the framework of the two parameter theory of polymer solutions. It is not my intention to give a comprehensive review of this theory. Nevertheless, since the nomenclature and ideas involved will be referred to repeatedly, a brief summary of the salient features, taken principally from the book by Yamakawa (1), will be given.

The most general theory of dilute polymer solutions is described in terms of the conformational statistics of polymer chains in which the local chemical structure of a chain is considered in detail; that is, restrictions on the angles between successive bonds in the chain and steric hindrances to internal rotation about the bonds are explicitly taken into account. The configurational partition function for such a system can be written as

$$Z = \int \exp\left[- \frac{U(\{\phi_n\})}{kT} \right] d\{\phi_n\} \qquad (3.1)$$

where U is the energy of internal rotation, i.e., the potential of mean force, and ϕ_n are the rotation angles which are here chosen as the

internal coordinates of the chain. The energy U may be decomposed as

$$U(\{\phi_n\}) = \sum_{i=1}^{n} \mu_{1i}(\phi_i) + \sum_{i=1}^{n} \mu_{2i}(\phi_i, \phi_{i+1}) + \ldots \qquad (3.2)$$

Means of evaluating the partition function, and from this obtaining the unperturbed dimensions, $\langle R^2 \rangle_o$, and the distribution function, have been extensively investigated (2), by keeping only the first few terms of Equation (3.2), i.e., by including only short range interferences.

The excluded volume effect, on the other hand, is of long-range nature. Two or more segments remote from one another along the chain will repel each other when brought close together, since they both cannot occupy the same volume element at the same time. In addition, these repulsive forces will, to some extent, be altered by the existence of solvent molecules. Intramolecular interactions of this sort, usually referred to as the excluded volume effect or the long-range (intramolecular) interference effect, may be represented by higher-order terms in the expansion of Equation (3.2).

However, these is no fundamental way in which the intramolecular potential of Equation (3.2) may be split into the potentials corresponding to short-range and long-range interferences. In addition, the distribution function is very complicated even for unperturbed chains with only short-range interferences. Therefore, the evaluation of the excluded volume effect proceeds from a simplified molecular model of a polymer as a random-flight (Gaussian) chain of n identical segments with effective bond length l (i.e., an "equivalent chain" with "Kuhn statistical segment length" (3)). With his assumption, the configura-

tional partition function for the system may be given by

$$Z = \int [\prod_{i=1}^{n} \tau(\bar{r}_i)] \exp [- \frac{W(\{\bar{R}_n\})}{kT}] d\{\bar{r}_n\} \qquad (3.3)$$

where τ is the (effective) bond probability given by

$$\tau(\bar{r}) = \frac{1}{4\pi l^2} \delta(|r| - l) \qquad (3.4)a$$

(exact expression)

or

$$\tau(\bar{r}) = \left(\frac{3}{2\pi l^2} \right)^{3/2} \exp \left(- \frac{3r^2}{2l^2} \right) \qquad (3.4)b$$

(approximate expression)

and W represents only the potential of mean force due to long-range interferences. The effect of short-range interferences is absorbed into the parameter l. For the treatment of the partition function of Equation (3.3), it is necessary to make the superposition approximation in W,

$$W(\{\bar{R}_n\}) = \sum_{0 \le i \le j \le n} w(\bar{R}_{ij}) \qquad (3.5)$$

where $w(\bar{R}_{ij})$ is the pair potential of mean force between the i^{th} and j^{th} segments as a function of separation $\bar{R}_{ij}$, as well as to assume that the pair potential w is short-ranged. The potential w depends on solute-solute, solvent-solute, and solvent-solvent interactions, and is a complicated but undefined function of the separation distance. It is related to a pair correlation function $g(\bar{R}_{ij})$ for solute molecules (segments) at infinite dilution by the equation

$$g(\bar{R}_{ij}) = \exp\left[- \frac{w(\bar{R}_{ij})}{kT} \right] , \tag{3.6}$$

where the zero of w is chosen so that $g \to 1$ as $\bar{R}_{ij} \to \infty$. The binary cluster integral β is then defined as

$$X_{ij} \equiv g(\bar{R}_{ij}) - 1 = -\beta\delta(\bar{R}_{ij}) \tag{3.7a}$$

with

$$\beta = \int [1 - g(\bar{R}_{ij})] d\bar{R}_{ij} , \tag{3.7b}$$

and represents the effective volume excluded to one segment by the presence of another at infinite dilution. The assumption is also made that the mutual excluded volume β is significantly smaller than the volume occupied by a polymer coil. In addition, the instantaneous distribution for the entire chain may be written as

$$P(\{\bar{R}_n\}) = Z^{-1}\left[\prod_{i=1}^{n} \tau(\bar{r}_i) \right] \exp\left[- \frac{W}{kT} \right] \tag{3.8}$$

Then, with the assumptions that $n >> 1$ and (as stated above) $\beta << (nl^2)^{3/2}$ and the potential is pairwise additive, all the equilibrium and nonequilibrium properties of dilute polymer solutions may be expressed in terms of the two parameter combinations nl^2 and $n^2\beta$. The former quantity is just the unperturbed mean square end-to-end distance, $\langle R^2 \rangle_0$ (or 1/6 the unperturbed mean square radius of gyration, $\langle S^2 \rangle_0$), while the latter is just twice the total excluded volume between segments, which is related to the excluded volume parameter z by

$$z = \left(\frac{3}{2\pi \langle R^2 \rangle_o} \right)^{3/2} n^2 \beta = \left(\frac{3}{2\pi \langle R^2 \rangle_o} \right)^{3/2} M^2 B \qquad (3.9)$$

$$\langle R^2 \rangle_o = 6 \langle S^2 \rangle_o = n l^2 \qquad (3.10)$$

Thus these two equations represent long-range and short-range interferences in the chain, respectively. It is important to observe that the parameters n and l, and also n and β, never appear separately in the final equations. In other words, the final equations are invariant to the choice of n, which is thus arbitrary as long as the value of β is not discussed. In addition, it is important to note that the binary cluster integral and hence the excluded volume parameter are not directly observable quantities, whereas the unperturbed dimensions are directly measurable.

The central problem in the two parameter theory is thus to derive interrelations between the dilute solution properties and the parameters $\langle R^2 \rangle_o$ and/or z, in particular for linear flexible chains. Since the excluded volume effect describes the extent to which the coil dimensions are perturbed by the long-range interaction of the non-bonded segments, a relationship exists between z and the expansion factor, α. Various models and mathematical approximations have been used to derive the expansion factor as a function of z, and this provides an indirect method of determining β. Similarly, the second virial coefficient A_2, expressed as

$$A_2 = 4\pi^{3/2} N_A \left(\frac{\langle S^2 \rangle^{3/2}}{M^2} \right) \Psi \qquad (3.11)$$

where Ψ represents the degree of interpenetration of polymer molecules in dilute solution, is also a function of z:

$$\Psi = \bar{z}h_o(\bar{z}) \tag{3.12}$$

where

$$z = z|\alpha_s{}^3 \tag{3.13}$$

and α_s is defined by Equation (3.14)b.

Various expressions for Ψ have likewise been developed and can be used to determine z and thus β. As will be discussed later, since interaction between segments must be invarient to whether the segments occur on the same or different molecules, there should be self-consistency in the intramolecular and intermolecular theories; i.e., the value of z determined from observed values of α_S and from observed values of Ψ should be equivalent.

Expansion factors. The expansion factors α_R and α_s are defined by

$$\alpha_R{}^2 = \langle R^2 \rangle / \langle R^2 \rangle_o \tag{3.14}a$$

$$\alpha_S{}^2 = \langle S^2 \rangle / \langle S^2 \rangle_o \tag{3.14}b$$

Flory (4) was the first to calculate the expansion factors and thus demonstrate the excluded volume effect. In the model he used, the "smoothed-density model," the polymer molecule is regarded as a continuous cloud of segments whose distribution about the molecular center of mass is Gaussian. For this model, α_R and α_S are indistinguishable.

The equilibrium value of α is calculated from the balance between the osmotic force which tends to swell the molecule in solution and the elastic force arising from the resulting molecular expansion to a less probable configuration. This leads to the well-known Flory (F,o) equation for the expansion factor

$$\alpha^5 - \alpha^3 = 2C_M\Psi(1 - \frac{\theta}{T})M^{1/2} \qquad (3.15)$$

A correspondence exists between Flory's notation and that used in the two-parameter theory, namely that

$$z = (\frac{4}{3^{3/2}})C_M\Psi(1 - \frac{\theta}{T})M^{1/2} \qquad (3.16)a$$

$$\beta = 2V_o^{-1}V_s^{2}\Psi(1 - \frac{\theta}{T}) \qquad (3.16)b$$

where V_o is the molecular volume of the solvent and V_s is the volume of a segment.

Subsequently, the excluded volume effect was developed more rigorously through the formalism of statistical mechanics. For small values of z, perturbation theory techniques (5) were employed to evaluate the expansion factors, the most versatile of which was an application of the cluster expansion method of Ursell and Mayer in the theory of imperfect gases (6). The results, obtained in series form as

$$\alpha_R^2 = 1 + 1.333z - 2.075z^2 + 6.459z^3 - \ldots \qquad (3.17)a$$

$$\alpha_S^2 = 1 + 1.276z - 2.082z^2 + \ldots , \qquad (3.17)b$$

are exact equations for the excluded volume effect. However, the series are very slowly convergent and therefore their validity is confined to the range of small z, i.e., in the vicinity of the theta temperature.

Therefore, various attempts have been made to derive approximate closed expressions for α_R and α_S valid over a wider range of z. Two methods have been employed. One begins with the potential of mean force with the end-to-end distance, R, or the radius of gyration, S, fixed. In this approach the problem is to evaluate V(R) or V(S) (9). The other approach is a derivation of a differential equation for the expansion factor (8,10,11). Although all the theories predict that α increases with z without limit, in conformity with the Flory theory, there are differences among the values of α predicted by them. All expressions for α have the asymptotic form (1)

$$\lim_{z\to\infty} \alpha^{\nu} = \text{constant } z \tag{3.18}$$

but values for ν of between 1 and 5 have been predicted. An equation for α which gives α^{ν} at large z is referred to as an equation of the ν^{th} power type. In most of the approximate theories, adjustable constants are chosen to force agreement with the exact first-order perturbation theory at small z. When this is done to the original Flory theory (F,o), it is known as the modified Flory equation (F,m) (12). A partial list of the various equations derived for the expansion factor is given in Table 3.1.

For large excluded volume, an exact asymptotic solution for an

TABLE 3.1

Conjugate Pairs of $\alpha_s(z)$ and $\Psi(\bar{z})$

$\alpha_s(z)$	$\Psi(\bar{z})$	References
$\alpha_s^5 - \alpha_s^3 = 2.6z$ (3.19)	$\Psi(\bar{z}) = [\ln(1 + 2.3\bar{z})]/2.3$ (3.25)	Flory-Krigbaum-Orofino (FKO) (4,23,24)
$\alpha_s^5 - \alpha_s^3 = \frac{134}{105} z$ (3.20)	$\Psi(\bar{z}) = [\ln(1 + 5.73\bar{z})]/5.73$ (3.26)	Flory-Krigbaum-Orofino modified (FKO,m) (4,12,23,24)
$\alpha_s^2 = 0.541 + 0.459(1 + 6.04z)^{0.46}$ (3.21)	$\Psi(\bar{z}) = 0.783[1 - (1+4.454\bar{z})^{-0.2867}$ (3.27)	Yamakawa-Tanaka-Kurata (YT-KY) (8,26,27)
$\alpha_s^3 - 1 = 1.91z$ (3.22)	$\Psi(\bar{z}) = \bar{z}/(1 + 2.865\bar{z})$ (3.28)	Fixman-Stockmayer (F-S) (10,12,28)
$\alpha_s^3 - 1 = 1.91z$	$\Psi(\bar{z}) = (1 - e^{-5.73\bar{z}})/5.73$ (3.29)	Fixman-Casassa-Markovitz (F-CM) (10,25)
$\alpha_s^2 = \frac{1}{4.68}[3.68+(1+9.36z)^{2/3}$ (3.23)	"	Ptitsyn-Casassa-Markovitz (P-CM) (11,25)
"	$\Psi(\bar{z}) = [\ln(1 + 2.3\bar{z})]/2.3$	Ptitsyn-Flory-Krigbaum-Orofino (P-FKO) (11,23,24)
"	$\Psi(\bar{z}) = [\ln(1 + 5.73\bar{z})]/5.73$	Ptitsyn-Flory-Krigbaum-Orofino, modified (P-FKO,m) (11,12,23,24)

infinitely long chain has not yet been obtained. The problem has been attacked using the self-consistent field method (13-16). For the zeroth order field, a solution has been obtained with $\nu = 5$ and $C = .744$ in Equation (3.18).

Second virial coefficient. The study of the thermodynamic behavior of polymer solutions, which leads to expressions for the second virial coefficient, is necessary to complete the two-parameter theory for the equilibrium properties of dilute polymer solutions. It must take into account solute-solute (intermolecular) as well as solvent-solute and solvent-solvent interactions. There are two approaches to the problem. The older one (which will not be discussed) uses a discrete model and leads to a lattice theory which is useful over the whole concentration range (17). The second treatment is an application of the statistical mechanics of many-particle systems, e.g., the cluster theory of Mayer and McMillan (18), in which the osmotic pressure may be expressed in terms of the molecular distribution function.

In the expression for the second virial coefficient (Equation 3.11), the problem is to evaluate Ψ. For small z, a perturbation theory approach can again be employed, with the result that (19-21)

$$\Psi = \bar{z} \left(1 - 2.865\bar{z} + 14.278\bar{z}^2 - \ldots\right), \qquad (3.24)$$

The asymptotic solution for Ψ at large $\bar{z}$ has not yet been investigated. However (22), it may be expected that in the limit $z \to \infty$, polymer molecules behave like rigid spheres in dilute solutions, and therefore Ψ becomes a constant independent of z.

As in the case of the expansion factor, various approximate closed expressions for Ψ have been derived in order to cover a wide range of z. The methods used to evaluate Ψ employ smooth-density sphere models (12,23,24) or modifications of it (25), or use a differential-equation approach (26,27,12,28).

From Equations (3.12) and (3.13), it can be seen that $\Psi = \Psi(z,\alpha_s)$. Thus an expression for α_s must be chosen to be combined with a given expression for $h_o(\bar{z})$ in order to complete the form of Ψ as a function of z. This must be done with the view to maintaining self-consistency of the intramolecular and intermolecular theories, as proposed by Fujita et al. (29) and Yamakawa (1). Combinations which fulfill this criterion are known as "conjugate pairs" of $\Psi(\bar{z})$ and $\alpha_s(z)$; a list of these is given in Table 3.1. Thus, the Flory-Krigbaum-Orofino (FKO,o) equation for Ψ (23,24) and the original Flory (F,o) equation for α_s may be combined, since both are based on the smoothed Gaussian density model. Similarly, the modified Flory-Krigbaum-Orofino (FKO,m) equation for Ψ (12,23,24) should be combined with the modified Flory (F,m) equation for α_s (4,12). The Kurata-Yamakawa (KY) equation for Ψ (26,27) and the Yamakawa-Tanaka (YT) equation for α_s (8) are conjugate pairs, since they were both derived by an approach using a hierarchy of differential equations for α_R and α_S and the intramolecular and intermolecular hierarchies have been truncated in mathematically consistent closure approximations. Other combinations have been used, but there is no explicit justification for them.

Application to polyions. Dilute solutions of polyelectrolytes, when existing in the ionized form in aqueous media, increase in chain

dimension and tend toward a rodlike state owing to the strong electrostatic repulsion along the chain exerted by the charges on one another. This repulsion can be suppressed by the addition of a small amount of supporting electrolyte. Hence, equations describing the expansion factor and the second virial coefficient of non-ionic random coil molecules can also be applied to polyelectrolyte-salt systems, with the approximation that the excluded volume effect is predominantly the result of ionic interaction.

Solutions of polyions show large deviations from thermodynamic ideality. Most theoretical treatments have been focused on solving the equation for the free energy or for the electrostatic potential of the polyion by using some form of the Poisson-Boltzmann (30) equation. The physical models used are divided basically into two groups: spherical models and chain-like models, but cylinders have also been considered.

The extension of the excluded volume theory of non-ionic polymers to polyelectrolytes was first carried out by Ptitsyn (31). To calculate β, he assumed that the potential of average force is the sum of two terms, nonionic ($V_o(r)$) and ionic ($W(r)$). That is,

$$V(r) = V_o(r) + W(r)$$

and

$$\begin{aligned} V_o(r) &>> W(r) \qquad \text{for } r \leq a_o \\ V_o(r) &= 0 \qquad\quad\ \ \text{for } r > a_o \end{aligned} \tag{3.30}$$

where the distance of closest approach of segments is denoted by a_o. He assumed that $W(r)$ is given by the Debye-Hückel theory:

that is

$$W(r) = \frac{Z_s{}^2 e^2}{D} \quad \frac{e^{Ka_o}}{1 + Ka_o} \quad \frac{e^{-Kr}}{r} \tag{3.31)a}$$

with

$$K^2 = \frac{8\pi e^2 N_A C_s{}^o}{DkT \times 10^3} \tag{3.31)b}$$

where Z_s is the charge number of a segment, D the dielectric constant of the solvent, e the unit charge and $C_s{}^o$ is the concentration of added neutral salt of 1:1 type expressed in mole/l. If the concentration of added salt is high, it can be assumed that $W(r)/kT << 1$. Then the excluded volume parameter for polyelectrolytes is a sum of the excluded volume effect due to Van der Waals interactions of segments z_o, and that due to the ionic interaction of polyions and counterions, z_e. It can be expressed as

$$z = z_o + z_e = \left(\frac{3}{2\pi \langle R^2 \rangle_o} \right)^{3/2} n^2 \left(\beta_o + \frac{10^3 i^2}{2N_A C_s} \right) \tag{3.32}$$

where β_o is the binary cluster integral of the uncharged, non-bonded segments and i is the degree of ionization. With the approximation that $z_o << z_e$,

$$z \simeq z_e = \left(\frac{3}{2\pi \langle R^2 \rangle_o} \right)^{3/2} n^2 \left(\frac{10^3 i^2}{2N_A C_s} \right) \tag{3.33}$$

Several theories were subsequently derived with the above approximation to obtain α_s as a function of z_e, using the perturbation theory of

random coils. These are summarized in Table 3.2. As can be seen, the theories predict various functional forms for the proportionality between the concentration of added salt and the expansion factor.

For the theories developed thus far, the calculated expansions of the polyion are much larger than the experimentally observed ones if the analytical charge density of the polyion is used to calculate the repulsive force due to electric charges. The discrepancy is often explained by assuming that the effective charge density of the polyion is much smaller than the analytical one due to ion binding or low activity coefficient of the counterion in the polymer domain.

In addition, the discrepancy is probably due to the inadequacy of the assumption for polyions that the free energy of a coiled polymer can be expressed as the sum of pairwise interactions between segments (Equation 3.5). The electrostatic free energy of electrolyte solutions cannot be expressed in such a simple way but should contain all interactions among ions. Thus the neglect of counterion-counterion interaction and counterion-segment interaction may contribute to the disagreement between theory and experiment.

Theories of the second virial coefficient for polyelectrolyte-salt systems are rather limited due to the complexity involved in the nonideal nature of these systems contributed by both the electrostatic interaction and chain character. Since polyions are both linear polymers and electrolytes, the second virial coefficient is sometimes discussed as an extension of the theory of the second virial coefficient for nonionic linear polymers and sometimes by applying the theory for colloidal electrolyte solutions (30).

TABLE 3.2

The Effect of Ionic Strength on α_s

Workers	Equations for α_s
Flory (32)	$\alpha_s^5 - \alpha_s^3 = 2.67e\ \alpha \frac{1}{C_s}$ (3.34)a
Hill (33), Hermans and Overbeek (34)	$\alpha_s^5 - \alpha_s^3 \simeq 7.0z_e\ \alpha \frac{1}{C_s}$ (3.34)b
Katchalsky and Lifson (35)	$\alpha_s^3 - \frac{1}{\alpha_s} = 1.45z_e\ \alpha \frac{1}{C_s}$. (3.35)
Fixman (36)	$\alpha_s^3 - 1\ \alpha\ in^{1/2}/1 \cdot C_s^{1/2}$ (3.36)
Kurata (37,38)	$\alpha_s^3 - 1\ \alpha\ \Gamma(f)i^2M^{1/2}/C_s$ where $\Gamma(f) = 2f^{-2}[(1 + f^2)^{1/2} - 1]$ and $f = 3.38 \times 10^{-21}n^{-1/2}l^{-1}\alpha_s^{-1}(1 + 1/3\alpha_s^2)^{1/2}$ (3.37)
Ptitsyn (39-41)	$\alpha_s^2 - 0.786 + 0.95z_e^{2/3}$ (if $\alpha_s > 1.2$) $= 0.786 + 0.95(\frac{3}{2\pi})\ \frac{n^{1/3}}{l^2}\ (\frac{10^3i^2}{2N_AC_s})^{2/3}$ (3.38)
Alexandrowicz (42)	$\alpha_s^2 \simeq 1.7z_e^{1/2} + 0.35 \quad (\alpha_s \geq 2)$ (3.39)

Hill (43,44) applied the McMillan-Mayer theory (18) to spherical colloidal solutions in order to calculate the second virial coefficient, using the Donnan equilibrium and a Debye-Hückel ionic atmosphere. In this treatment, the macroion is considered as a point particle having z_p charges and the solution is thermodynamically ideal; that is, all the particles are distributed uniformly in the solution. The second virial coefficient of this ideal solution can be expressed as

$$A_2^o = \frac{10^3 z_p^2}{4M^2 C_s^o} \tag{3.40}$$

where it is to be noted that A_2^o is independent of the molecular weight of the polymer but is proportional to $1/C_s^o$.

However, the linear polyelectrolyte solution is extremely nonideal, both because there is electrostatic interaction between the charges of ions and because the macroion is not a point but a chain molecule. A correction factor to take account of the electrostatic interaction was reported by many workers (45-47) and is usually given as a constant, Γ_e, which is nearly independent of the molecular weight and the ionic strength so that

$$A_2 = A_2^o \Gamma_e \tag{3.41}$$

On the other hand, the nonideality in A_2 due to chain character was considered by Orofino and Flory (48). They obtained

$$A_2 \simeq \frac{16\pi N_A}{3^{3/2}} \frac{\langle S^2 \rangle^{3/2}}{M^2} \ln \left[1 + \frac{\pi^{1/2}}{2} (\alpha_s^2 - 1)\right]. \tag{3.42}$$

If α_s is given by Equation (3.34), Table 3.2, where the nonionic term has been neglected in comparison with the ionic term, then the above equation can be transformed to an equation of the form

$$A_2 = A_2^o \, h(\bar{z}) \tag{3.43}a$$

where

$$h(\bar{z}) = \frac{2}{\pi^{1/2}(\alpha^2-1)} \ln \left[1 + \frac{\pi^{1/2}}{2} (\alpha^2 - 1)\right] \tag{3.43}b$$

Thus A_2 becomes dependent on molecular weight and can deviate from the linearity against $1/C_s{}^o$.

Takahashi, Kato and Nagasawa (49) introduced the assumption that the two correction factors were independent, so that the second virial coefficient of linear polyelectrolytes can be expressed by

$$A_2 = A_2{}^o \Gamma_e h(\bar{z}) . \tag{3.44}$$

Alexandrowicz (50) also derived an approximate expression for $A_2(\alpha_s, z)$ in a good solvent ($\alpha_s \geq z$) by using the uniform segment cloud model. Equation (3.39), Table 3.2, was introduced into the expression for $A_2(\alpha_s, z)$ and a relation between A_2 and the ionic strength was obtained.

Empirically, it has been found (51) that log A_2 is linearly related to log C_s.

Nonequilibrium Properties

The nonequilibrium properties of dilute polymer solutions can also be accounted for within the framework of the two parameter theory.

There are three basic ideas in the development of the frictional properties of polymer solutions (1). The first is that the solvent is considered as a continuous viscous fluid. The second is the concept that a perturbation velocity is produced at the point of location of every segment of one polymer molecule by the presence of the remaining segments of the same molecule and of the segments of all the other molecules. The effects of these perturbations are cooperative, giving rise to intramolecular and intermolecular hydrodynamic interactions. The formulation of the hydrodynamic interaction is based on the Kirkwood-Riseman (2) method, which uses the Oseen tensor as a description of the interaction. Lastly, since it is necessary to take into account the random Brownian motion of the solute and for flexible-chain polymers the segmental Brownian motion, the analysis of the motion of the molecule can be carried out using the generalized diffusion equation which is satisfied by the molecular distribution function.

Although the theory of viscosity has been the most extensively discussed, the emphasis in this section will be on the theory of the frictional coefficient and hence the diffusion constant, of particular importance being the effects of excluded volume. The draining effect, that is, the dependence of Φ_0 and P_0 (the Flory-Fox constants in the unperturbed state) (3) or of Φ and P (the Flory-Fox constants in the perturbed state) on molecular weight will also be discussed.

The relationship between the diffusion coefficient and the frictional coefficient has been discussed by many authors (4-7). It has recently been pointed out by Vrentas and Duda (6) that the relationship utilized by Yamakawa (1) and Tanford (4) is derived from improper con-

stitutive equation which are not frame invariant. The equations arrived at by Vrentas and Duda are

$$D = D_o (1 + k_D C + \dots) \tag{3.45}$$

$$k_D = 2MA_2 - k_s - b_1 - 2\hat{V}_{20} \tag{3.46}$$

$$D_o = \frac{kT}{f_o} \tag{3.47}$$

Here f_o is the frictional coefficient at infinite dilution, k_s is the correction factor to the frictional coefficient, V_{20} is the partial specific volume of the solute at infinite dilution, b_1 is the coefficient in the series expansion for the partial specific volume of the solvent, k is Boltzmann's constant and T is the absolute temperature. For the present purpose, it should be noted that as $c \to 0$, the equations are formally equivalent to those of Yamakawa and Tauford. The discussion of k_D, where the differences actually occur, will be presented in this chapter, Concentration Dependence of Diffusion Constant.

The Kirkwood-Riseman equations (2) for the intrinsic viscosity and the translational diffusion coefficient of unperturbed chains are:

$$[\eta] = \frac{N_A \xi n^2 l^2 F(X)}{36 \eta_o M} \tag{3.48}$$

$$D_o = \frac{kT}{n\xi} \left(1 + \frac{8}{3}X \right) \tag{3.49}a$$

$$f_o = n\xi/\left(1 + \frac{8}{3}X\right) \tag{3.49}b$$

$$X = \left(\frac{n}{6\pi^3} \right)^{1/2} \frac{\xi}{\eta_o l} \qquad (3.50)$$

where l is the effective bond length of the chain, n is the number of effective segments in a chain, ξ is the translational friction coefficient of a segment, η_o is the solvent viscosity and X is the draining parameter. The latter is a measure of the hydrodynamic interactions between segments; values of XF(X) have been calculated and tabulated (2,8).

There are two limiting cases. In the free-draining case (X = 0, F(X) = 1), there are no hydrodynamic interactions between segments and the equations become

$$[\eta] = \frac{N_A \xi n \langle S^2 \rangle_o}{6 \eta_o M} \qquad (3.51)a$$

$$D_o = \frac{kT}{n\xi} \qquad (3.51)a$$

$$f_o = n\xi \qquad (3.51)a$$

The translational friction coefficient of the entire molecule is simply the sum of the friction coefficients of the individual segments. The frictional coefficient and the intrinsic viscosity are seen to be directly proportional to the molecular weight for the (unperturbed) free draining polymer chain.

At the other extreme, called the non-free-draining case ($X = \infty$, $XF(X) = 1.259$), the equations become

$$[\eta] = N_A \pi^{3/2} \chi F(\chi) \frac{\langle S^2 \rangle_o^{3/2}}{M} \qquad (3.51)b$$

$$D_o = \frac{.196}{\sqrt{6}} \frac{kT}{\eta_o \langle S^2 \rangle_o^{1/2}} \qquad (3.51)b$$

$$f_o = 6\pi\eta_o(.665) \langle S^2 \rangle_o^{1/2} \qquad (3.51)b$$

In this case there is dominant hydrodynamic interaction. The form of the intrinsic viscosity equation is equivalent to that for rigid sphere molecules obtained by Einstein with radius proportional to $\langle S^2 \rangle_o^{1/2}$, and leads to the concept of an equivalent hydrodynamic sphere, of radius $0.875 \langle S^2 \rangle_o^{1/2}$. The frictional coefficient and the intrinsic viscosity are seen to be directly proportional to $M^{1/2}$ for the (unperturbed) non-free-draining chain. In the equation for the friction coefficient 'Stokes' law is obeyed, indicating that here too the molecule behaves as a hard sphere, and the concept of an equivalent hydrodynamic sphere, defined as $R_H = .665 \langle S^2 \rangle_o^{1/2}$ can be applied.

Flory and Fox (3,9) and Mandelkern and Flory (10) proposed the following semi-empirical relations for the intrinsic viscosity and translational frictional coefficient, respectively.

$$[\eta] = 6^{3/2} \Phi_o \frac{\langle S^2 \rangle_o^{3/2}}{M} \qquad (3.54)a$$

$$f_o = 6^{1/2} \eta_o P_o \langle S^2 \rangle_o^{1/2} \qquad (3.54)b$$

These equations, as first proposed, neglected the excluded volume effect, which will be discussed below. They are introduced here since the nomen-

clature is that most commonly employed and therefore should be compared with the nomenclature of the Kirkwood-Riseman theory. Thus

$$\Phi_o = \left(\frac{\pi}{6}\right)^{3/2} \frac{N_A}{100} [XF(X)] \qquad (3.55)a$$

$$P_o = (6\pi^3)^{1/2} \frac{X}{1 + \frac{8}{3}X} \qquad (3.55)b$$

In the non-free-draining case, the values of these parameters are $\Phi_o = 2.87 \times 10^{21}$ and $P_o = 5.11$ (when $[\eta]$ is measured in dl/g and $\langle S^2 \rangle^{1/2}$ in cms). Other theories for the viscosity constant give limiting values of from 1.81 to 2.87×10^{21}, and there are similar fluctuations in P_o (1).

Intermediate values of the draining parameter X represent the degree of drainage of the solvent through the polymer chain. The ratio $\Phi_o(X) / \Phi_o(\infty)$ or $P_o(X) / P_o(\infty)$ may be regarded as the correction factors by which the hydrodynamic volumes of the molecule are decreased by the draining effect. Since X is proportional to $M^{1/2}$, both $\Phi_o(X)$ and $P_o(X)$ are predicted to increase with molecular weight. However, such an effect has never been observed experimentally (at least for unperturbed chains) and thus only the non-free-draining limit is valid for molecular weights of ordinary interest. It is interesting to note that according to the calculations of Edwards and Oliver (11), who obtained the frictional coefficient of a polymer chain based on a model for the latter as a cylinder of finite radius whose axis takes a random flight trajectory, the draining effect does not occur.

In general, both Φ and P depend on the excluded volume, although not on the draining parameter, and Equations (3.54a) and (3.54b)

become

$$[\eta] = 6^{3/2}\Phi \frac{S^2}{M}^{3/2} \tag{3.56}a$$

$$f = 6^{1/2}\eta_o P \langle S^2 \rangle^{1/2} \tag{3.56}b$$

If $[\eta]_\theta$ is the intrinsic viscosity of unperturbed chains, f_θ, the translational frictional coefficient of unperturbed chains, and the radii expansion factors are defined as

$$[\eta] = [\eta]_\theta \alpha_\eta^{\,3} \tag{3.57}a$$

$$f = f_\theta \alpha_f \tag{3.57}b$$

$$\langle S^2 \rangle^{1/2} = \alpha_s \langle S^2 \rangle_o^{1/2} \tag{3.57}c$$

then

$$\Phi = \Phi_o \left(\frac{\alpha_\eta}{\alpha_s}\right)^3 \tag{3.58}a$$

and

$$P = P_o\left(\frac{\alpha_f}{\alpha_s}\right) \tag{3.58}b$$

In the non-free-draining limit, α_η and α_f become functions of z alone. At small z, $\alpha_\eta^{\,3}$ may be expanded in the form

$$\alpha_\eta^{\,3} = 1 + c_1 z \ . \ . \ . \tag{3.59}$$

According to the semi-empirical theory of Flory and Fox (3), $\alpha_\eta^{\,3}$ is

equal to α_s^3, so that $c_1 = 1.914$. Kurata and Yamakawa (12,13) developed an approximate first-order perturbation theory for the intrinsic viscosity based on the theory of Kirkwood and Riseman and obtained a value of 1.55 for c_1. This result can be represented as

$$\alpha_\eta^3 = 1 + 1.55z \qquad (3.60)a$$

$$= \alpha_s^{2.43} \qquad \text{(closed form)} \quad (3.60)b$$

and can be combined with Equations (3.17b) and (3.58a) to yield

$$\Phi/\Phi_o = 1 - 0.46z \qquad (3.61)a$$

$$= \alpha_s^{-0.57} \qquad \text{(closed form)} \quad (3.61)b$$

Subsequently, Yamakawa and Tanaka (14) introduced exactly the excluded volume effect into Hearst's (15) dynamical theory of polymers, where the polymer chain is represented by a spring and bead model. In addition, they employed a procedure due to Fixman and Pyun (16) which avoids preaveraging the Oseen tensor. They obtained a value of 1.06 for c_1, which at present is regarded as the best value for this constant. However, there has not been derived an approximate closed expression for α_η which gives the first order perturbation theory of Yamakawa and Tanaka at small z.

In calculating the frictional coefficient, the starting point is Kirkwood's (17,18) general expression for the diffusion constant

$$D = \frac{kT}{\eta\xi}\left(1 + \frac{\xi}{6\pi\eta_o n}\sum_{\substack{i \\ i\neq j}}\sum_{j}\frac{1}{\langle R_{ij}\rangle}\right), \qquad (3.62)$$

and the problem becomes evaluating the average $\langle R_{ij}^{-1} \rangle$. For small values of z, Stockmayer and Albrecht (19) derived the exact first order perturbation theory value of α_f

$$\alpha_f = 1 + 0.609z \qquad (3.63)a$$

which combined with Equations (3.17b) and (3.58b) yields

$$P/P_o = 1 - 0.029z \qquad (3.63)b$$

Kurata and Yamakawa's (12,13) approximate first-order perturbation theory method using the Gaussian approximation that $\langle R_{ij}^{-1} \rangle = \tilde{\alpha}^{-1} \langle R_{ij}^{-1} \rangle_o$ yields

$$\alpha_f = 0.416z \qquad (3.64)a$$

$$= \alpha_s^{0.652} \qquad \text{(closed form)} \qquad (3.64)b$$

$$P/P_o = 1 - 0.222z \qquad (3.65)a$$

$$= \alpha_s^{-0.348} \qquad \text{(closed form)} \qquad (3.65)b$$

This gives a value too low for the coefficient of the linear term in z in the expression for α_f, when compared with the exact one. Horta and Fixman (20), using a boson operator formalism which was equivalent to the Gaussian approximation, also found a low value of 0.415 for the coefficient of z in α_f. Higher terms in the series have not been obtained, so application is limited to the region of the theta point.

Nevertheless, α_f or α_η are always smaller than α_s for positive

z, indicating that the effective hydrodynamic radius varies with varying excluded volume more slowly than the statistical radius does. Thus both P and Φ decrease with increasing z.

For large excluded volume, theories of the intrinsic viscosity and frictional coefficient are derived by a combination of the hydrodynamic treatment of Kirkwood and Riseman (2) with the normal coordinate analysis of the spring and bead model of a polymer chain, as developed by Rouse (21), Bueche (22), and Zimm (23). In addition, the deviation of the chain from Gaussian dimensions, whether due to excluded volume effects, drainage, polyelectrolyte effects, or actual mechanical stiffness, is expressed through a uniform expansion parameter ε such that

$$\langle R_{ij}^2 \rangle = l^2 |j-i|^{1+\varepsilon} \qquad (3.66)a$$

and thus

$$\langle R^2 \rangle = l^2 n^{1+\varepsilon} \qquad (3.66)b$$

This representation is due to Peterlin (24), who also showed that

$$\langle R^2 \rangle = (6 + 5\varepsilon + \varepsilon^2) \langle S^2 \rangle \qquad (3.67)$$

The parameter ε is a monotonically increasing function of z defined by

$$\varepsilon = \frac{1}{2} \frac{\partial \ln \alpha_R^2}{\partial \ln z} \qquad (3.68)$$

It can thus be determined from any of the expressions for α_R listed in

Table 3.1. It can also be related to the Mark-Houwink-Sakurada (25, 26) exponent in the empirical expression for the intrinsic viscosity ($[\eta] = K_\eta M^a$) as $a = 0.5 + 3\varepsilon/2$, if the non-Gaussian nature of the polymer chain arises solely from the excluded volume effect.

Ptitsyn and Eizner (27), Tschoegl (28), and Bloomfield and Zimm (29) calculated $\Phi(\varepsilon)$ as a function of ε for values of ε ranging from 0 to 0.5. A new hydrodynamic interaction parameter was defined as

$$X(\varepsilon) = \frac{2^{\varepsilon/2}\eta^{\frac{1-\varepsilon}{\varepsilon}}\xi}{(6\pi^3)^{1/2}\ln_0} \tag{3.69}$$

which reduces to Equation (3.50) when $\varepsilon \to 0$. Only Tschoegl (28) considered both the effects of excluded volume and hydrodynamic interaction, and obtained families of curves with partial draining. For the non-free draining case, Φ decreases from 2.81×10^{21} at $\varepsilon = 0$ to $.686 \times 10^{21}$ at $\varepsilon = 0.5$, with the values decreasing as the drainage increases. For the frictional coefficient, only the non-free draining case has been considered, with the results that (29)

$$P/P_0 = \frac{1}{3\sqrt{6}}\ (1 - \varepsilon)(3 - \varepsilon)(6 + 5\varepsilon + \varepsilon^2)^{1/2} \tag{3.70}$$

where P decreases from a value of 5.11 at $\varepsilon = 0$ to that of 2.57 at $\varepsilon = 0.5$ and (27)

$$P/P_0 = [1 - 0.083(2a - 1)] = [1 - 0.25\varepsilon]. \tag{3.71}$$

For small z, it can be shown* that the Equations (3.70) and (3.71) reduce to

$$P/P_o = 1 - 0.25z \tag{3.72}$$

$$P/P_o = 1 - 0.17z \tag{3.73}$$

These results can be compared to Equations (3.63b) and (3.65c). Thus, all theories which use a Gaussian approximation predict a value for α_f which is too small compared to the exact value of Equation (3.63a).

From measurements of P for polymers in organic solvents reported in the literature, Meyerhoff (30) proposed a semiempirical relation

$$P/P_o = 1.31\,[1 - 0.33(2a - 1)] \tag{3.74}$$

to explain the existing experimental data.

Another parameter of interest is that derived from a combination of Equations (3.56a) and (3.56b), which lead Mandelkern and Flory (31) to

$$\beta = \Phi^{1/3}P^{-1} = \left(\frac{\eta_o}{T}\right)D_o([\eta]M)^{1/3} \tag{3.75}$$

The parameter β is more insensitive to excluded volume and draining effects than are either Φ or P evaluated separately. From Equations (3.58a) and (3.58b)

---

*For small ε, Equation (3.70) reduces to $P/P_o = 1 - 0.37\varepsilon$ after neglect of the ε^2 terms and expansion of the square root. For small z, $\alpha_R^2 = 1 + 4/3z$. Employing Equation (3.68) yields $\varepsilon = 2/3z$, thus $P/P_o = 1 - 0.25z$.

$$\beta = \Phi_o^{1/3} P_o^{-1} \frac{\alpha_\eta}{\alpha_f} \tag{3.76}$$

The Kirkwood-Riseman value of $\Phi_o^{1/3} P_o^{-1}$ is calculated to be 2.78×10^6. For small values of z, from Equations (3.60) and (3.64)

$$\beta = \Phi_o^{1/3} P_o^{-1}(1 + 0.1z) = \Phi_o^{1/3} P_o^{-1} \alpha_s .158 \tag{3.77}$$

For large values of z, Bloomfield and Zimm numerically obtained β as a function of the parameter ε described previously, and these values are tabulated below:

ε	$\beta \times 10^{-6}$
0	2.759
.1	2.776
.2	2.846
.3	2.956
.4	3.135
.5	3.426

For "normal" ranges of ε, 0 to .2, there is thus only a 3% change in β.

The question of whether the draining effect exists for $z > 0$ has been discussed by Yamakawa (32), using data (33) for monodisperse polystyrenes prepared anionically. As suggested by Fujita et al. (34), if α_η is a function of α_s only, then α_η must be a function of z only, since α_s is a function of z only. Plots of $\log \alpha_\eta^3$ against $\log \alpha_s^3$ for the polystyrenes studied formed a single-composite curve, indicating the absence of the draining effect for flexible chains irrespective of the value of z.

Intrinsic viscosity data is frequently analyzed using Stockmayer-Fixman (35) plots of the form

$$\frac{[\eta]}{M^{1/2}} = K_{\theta\eta} + 0.51\Phi_o B M^{1/2} \qquad (3.78)a$$

where

$$K_{\theta\eta} = [\eta]_\theta / M^{1/2} = \Phi_o 6^{3/2} \left(\frac{\langle S^2\rangle_o}{M}\right)^{3/2} \qquad (3.78)b$$

Thus intercepts of these plots yield unperturbed dimensions of the polymer and the slopes are proportional to the long range interaction parameter. Equation (3.78) is based on the first order perturbation theory expression for α_η^3 of Kurata and Yamakawa (Equation 3.60a) and the factor 0.51 will thus change depending upon which expansion for α_η^3 is used. Plots of α_η^3 against z for polystyrene (30,31) over a large range of z (0 to 6) have only slight curvature. This characteristic accounts for why there is a linearity between $[\eta]/M^{1/2}$ and $M^{1/2}$ over a relatively wide range of M.

An equation analogous to Equation (3.78) can be derived for the frictional coefficient as follows (36,37). Since $f = 6^{1/2}\eta_o P_o \langle S^2\rangle_o^{1/2} \alpha_f$ (Equations 3.65b and 3.57b), then

$$\frac{f}{M^{1/2}} = 6^{1/2}\eta_o P_o \left(\frac{\langle S^2\rangle_o}{M}\right)^{1/2} \alpha_f \, . \qquad (3.79)$$

Using Equation (3.63)a for α_f and the definition of z (Equation 3.9), Equation (3.79) becomes

$$\frac{f}{M^{1/2}} = K_{\theta f} + 2B \frac{P_o^3}{K_{\theta f}^2} M^{1/2} \qquad (3.80)a$$

where

$$K_{\theta f} = 6^{1/2} P_o \left(\frac{\langle S^2 \rangle_o}{M}\right)^{1/2} \eta_o \qquad (3.80)b$$

If Equation (3.64a) is used for α_f the numerical coefficient for the slope becomes 1.37. It should be emphasized that these equations are valid only for small values of excluded volume. For large values of z, combining Equations (3.56b, 3.67, and 3.70) gives

$$f = 6^{1/2} P_o \langle S^2 \rangle_o^{1/2} \eta_o \alpha_R \left(1 - \frac{4}{3}\varepsilon + \frac{\varepsilon^2}{3}\right) \qquad (3.81)$$

If a commonly used expression for α_R, the Flory modified (F,m)

$$\alpha_R^5 - \alpha_R^3 = 4/3z \qquad (3.82)$$

and Equation (3.68) for ε are used, it can be seen that f will be a complicated function of z and hence M. Plots of $f/M^{1/2}$ versus $M^{1/2}$ would thus not be expected to be linear.

However, a modification of the procedure due to Ford et al. (36) can be adopted. By substituting Equation (3.81) into Equation (3.82) and using the definition of z (Equation 3.9) results in

$$\frac{1}{(D^2M)} \frac{1}{\phi(\varepsilon)^2} \left(\frac{kT}{\eta_o}\right)^2 = (K_{\theta f})^2 + (D^3M^2)\phi(\varepsilon)^3 \left(\frac{\eta_o}{kT}\right)^3 K_{\theta f}^2 P_o^3 2^2 \frac{(6)^{1/2}}{\pi^{3/2}} B \qquad (3.83)$$

where

$$\phi(\varepsilon) = \left(1 - \frac{4}{3}\varepsilon + \frac{\varepsilon^2}{3}\right) \qquad (3.84)$$

Thus Equation (3.83) should be a straight line with intercept proportional to the unperturbed dimensions and slope proportioned to the interaction parameter B. Values of ε can be determined from the empirical

relation $a = (.5 + 3\varepsilon/2)$.

Concentration Dependence of Diffusion Constant

Introduction. The concentration dependence of the diffusion constant in dilute polymer solutions has been discussed by several authors (1,2), most recently by Vrentas and Duda (3). Their modified form of the series expansion which describes the concentration dependence is the most rigorous, since it is derived using constitutive equations for the diffusion flux and for the frictional force term which are frame invarient. The equation they arrive at is

$$D \simeq D_o[1 + k_D C + \ldots] \tag{3.85}$$

where D_o is the mutual diffusion coefficient at infinite dilution and the coefficient k_D is given by

$$k_D = 2MA_2 - k_f - b_1 - 2\hat{V}_{20} \tag{3.86}$$

Here, A_2 is the second virial coefficient, M is the molecular weight of the polymer, and $\hat{V}_{20}$ is the partial specific volume of the polymer on the limit of zero polymer concentration. Furthermore, b_1 is defined by the series expression

$$\hat{V}_1 = \hat{V}_{10}[1 + b_1 c + \ldots] \tag{3.87}$$

where $\hat{V}_1$ is the partial specific volume of the solvent and $\hat{V}_{10}$ is the specific volume of the solvent. Similarly, k_f is defined by

$$f_{12} = (f_{12})_o[1 + k_f c] \tag{3.88a}$$

where f_{12} is the friction coefficient based on the relative velocities of the components. Henceforth, the subscripts will be dropped, so

$$f = f_o[1 + k_f c] \tag{3.88b}$$

The effect of $\hat{V}_{20}$ and b_1 on k_D can usually be ignored, but becomes important when k_D is less than 20 ml/g. When volume change on mixing effects are small, b_1 can be set equal to zero, but the term $-2V_{20}$ is of the order of 2 ml/g for most polymers, and so can introduce at least a 10% error.

It should be noted that the more common expressions do not include b_1 and have $\hat{V}_{20}$ multiplied by 1 instead of 2. These modifications are not too important in here, but the use of correct constitutive equations becomes important when theories of k_f are transformed to laboratory frames, as will be discussed later. The modified equations are introduced here for consistency.

The prediction of the coefficient k_D involves experimental measurements of the quantities b_1 and $\hat{V}_{20}$ (or adequate approximations) and expressions or experimental determinations of the quantities A_2 and k_f. The second virial coefficient has in the present case been determined experimentally by light scattering disymmetry data and been found to be of the form

$$A_2 = aM^{-\delta} \tag{3.89}$$

As briefly discussed in Chapter III, Literature Survey for Polyions

subsection Na-copoly (ethyl acrylate-acrylic acid), the measured A_2 were compared with various expressions which were derived utilizing the two-parameter theory of dilute polymer solutions.

The correction factor to the friction coefficient, k_f , has been measured in the present experiments. It is the same coefficient which can be obtained from the concentration dependence of the sedimentation constant, where it is usually labeled k_s. Three theories have been proposed to predict this hydrodynamic constant and these will be compared below.

As can be seen from Equation (3.86), k_D is the sum of positive and negative factors. It is thus expected that the diffusion coefficient will either increase or decrease with concentration, depending on the relative contributions of the various terms. Since, as will be later discussed, k_f in each of the theories is some function of A_2, and A_2 is known experimentally, it should be possible to predict the cross-over point for the change in sign in k_D as a function of both molecular weight and A_2.

Theories of k_f. Of the three theories which presently exist to predict k_f, those of Yamakawa (6) and Imai (5) both give $k_f = 0$ at the theta temperature, whereas that of Pyun and Fixman (4) predicts non zero k_f under theta conditions. The latter theory is based on the uniform density sphere model of polymers, which is less realistic than the Gaussian model used in deriving the former two theories. Nevertheless, its prediction of non zero k_f at the theta point is supported by the bulk of experimental evidence accumulated so far.

As pointed out by Yamakawa (2), the basic problem in the theory of k_f is due to the fact that the velocity perturbation around a sphere moving in a fluid is asymptotically proportional to r^{-1} in the Stokes approximation, where r is the distance from the center of the sphere. Thus a direct summation of this long-ranged perturbation for a finite system results in a coefficient k_f which depends on the size and shape of the system. Since constitutive properties such as the frictional coefficient should be independent of surface effects, Yamakawa, and Pyun and Fixman (4,6) eliminated the surface effect by defining the frictional coefficient as the ratio of the external force on a polymer molecule to the drift velocity; i.e., the average translational velocity of the polymer molecule relative to the solvent, rather than to the simple average velocity of polymer molecules. It then becomes necessary to transform the frictional coefficient thus obtained to a laboratory coordinate system, since in experiments the frictional coefficient is based on the average sphere velocity rather than the drift velocity.

According to Vrentas and Duda (7), since the constitutive equations used by Yamakawa (2) are incorrect, when the coordinate transformation is used to go from the molecular frame to the laboratory frame to eliminate the surface effect and conserve solution volume, the resulting equations for k_f are also incorrect. The error involves the use of an expression for the volume fraction of spheres of solute and trapped solvent (Equation 36.9 of Yamakawa (2)), whereas the correct expression should be for just the volume fraction of solute. In addition, King et al. (8) corrected the results of Yamakawa and Imai for k_f and these results do not need correction. The theories of k_f presented

in this section will be the correct ones of Vrentas and Duda.

The correction factor to the frictional coefficient can be defined with the concentration expressed either as a weight percent or as a volume fraction of spheres in solution. In what follows, the nomenclature for the former coefficient will be k_f^c and for the latter k_f^ϕ. Thus

$$f = f_o(1 + k_f^c c) \quad \text{where } c = \text{concentration (grams/100 ml.)} \tag{3.90a}$$

$$f = f_o(1 + k_f^\phi \phi) \quad \text{where } \phi = \text{volume fraction of polymer} \tag{3.90b}$$

The relationship between the two coefficients is (4)

$$k_f^c = \frac{k_f^\phi (\frac{4\pi}{300}) \; R_H^3 N_A}{M} \tag{3.91}$$

where R_H is the hydrodynamic radius of a polymer molecule in solution at infinite dilution.

In the derivation of k_f by Pyun and Fixman (4), the model employed was that of hard (i.e., impenetrable) and soft (i.e., interpenetrable) spheres of uniform segment density. For hard spheres, a values of 7.157 was found for k_f^ϕ. The value for soft spheres was smaller and was dependent on the segment-segment interaction constant. With the slight modification of Vrentas and Dudas (7), k_f^c for soft spheres is given by

$$k_f^c = [7.16 - K(A)] \frac{4\pi R_H^3 N_A}{3M} - \hat{V}_{20} - b_1 \tag{3.92}$$

In Equation (3.92) K(A) is a monotonically decreasing function of the parameter A which is given by

$$A = \frac{3n^2\beta}{8\pi R_H{}^3} \tag{3.93}$$

where n is the number of equivalent segments per molecule and β is the binary cluster integral for a pair of segments. The evaluation of K(A) depends upon the numerical evaluation of an integral of the type

$$K(A) = \int_0^1 R(x)e^{-A(1-x)^2(2+x)}dx \tag{3.94}$$

where R(x) depends upon the model chosen to approximate the hydrodynamic interaction between two spheres. The dumbbell shape form is approximated by a prolate ellipsoid of varying axial ratio, 1 + x, or by ellipsoids whose volume is that of the dumbbell. The behavior of K(A) for small value of A is shown in Figure 3.1 taken from the paper of Pyun and Fixman (4). An asymptotic formula for K(A) (4)

$$K(A) = \frac{6.39}{(A + 2.6)\ 1/2} \tag{3.95}$$

fits well for larger values of A, and gives a value of K(A) which is good to within a few percent even for values of A as low as 4 or 5.

The value of K(A) at the theta temperature (A = 0) depends upon R(x), and was found to be 4.93, 4.56, and 4.20 for three models chosen. Thus, since $k_f{}^{\phi}$ = [7.16 - K(A)], $k_f{}^{\phi}$ is 2.23, 2.60, or 2.96, respectively, and is definitely positive for a theta solvent. It

Figure 3.1

Behavior of K(A) for small values of A, taken from Pyun and Fixman (4).

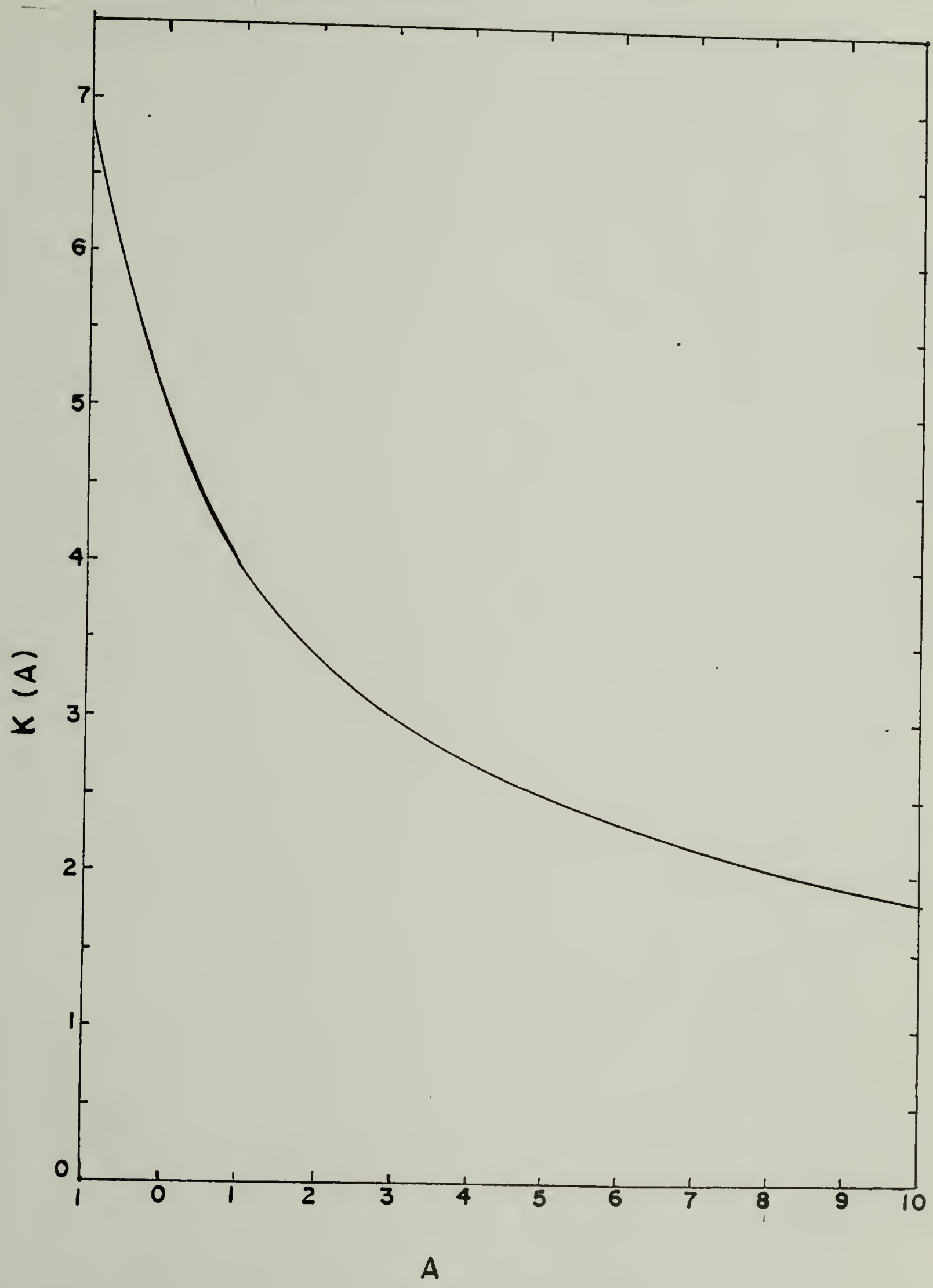
K (A)
7
6
5
4
3
2
1
0
1
0
1
2
3
4
5
6
7
8
9
10
A

disappears only when K(A) = 7.16, which occurs at about A = -1. At the other extreme, A = ∞, K(A) = 0, the hard sphere value of 7.16 is obtained.

For intermediate values of interaction, it is necessary to put A in a useful form, by relating it to measurable quantities such as A_2. This may be done via the two parameter theory of polymer solutions. Using the relation between the parameters z and β from Equation (3.9), but substituting $\langle R^2 \rangle_o = 6 \langle S^2 \rangle_o$, yields

$$z = \left(\frac{1}{4\pi \langle S^2 \rangle_o} \right)^{3/2} n^2 \beta \qquad (3.96)$$

which, upon insertion into Equation (3.93), gives

$$A = 3\pi^{1/2} z \frac{(\langle S^2 \rangle_o)^{3/2}}{R_H^3} . \qquad (3.97)$$

R_H is the hydrodynamic radius which can be determined experimentally from $R_H = kT/6\pi\eta_o D_o$ and $\langle S^2 \rangle_o^{1/2}$ is the root-mean-square end to end distance which can be determined from light scattering. In addition, z can be related to A_2 by the approximate theory of Yamakawa (2) given in Chapter III, Two Parameter Theory (α, A_2), and summarized here by the following set of equations

$$A_2 = \frac{N_A h_o (\bar{z})_n^2 \beta}{2M^2} . \qquad (3.98)a$$

$$\bar{z} = z/\alpha_s^3 \qquad (3.98)b$$

$$\alpha_s^3 = 0.541 + .459(1 + 6.04z)^{.46} \qquad (3.98)c$$

$$h_o(\bar{z}) = \frac{.547[1 - (1 + 3.903\bar{z})^{-.4683}]}{\bar{z}} \qquad (3.98)d$$

Then, substituting β from Equation (3.96) into Equation (3.98a) and using $\langle S^2 \rangle = \alpha_s^2 \langle S^2 \rangle_o$, the following relation is obtained

$$A_2 = \frac{4\pi^{3/2} N_A}{M^2} (\langle S^2 \rangle)^{3/2} \left\{ 0.547[1 - (1 + 3.903\bar{z})^{-.4683}] \right\} \qquad (3.99)$$

Thus, by using experimental values of A_2, α_s, $\langle S^2 \rangle^{1/2}$, and $\langle S^2 \rangle_o^{1/2}$, obtained from light scattering data, z can be calculated and used in Equation (3.97) to determine A. Then Equation (3.95) can be used to evaluate K(A), or for smaller values of A, Figure 3.1 can be employed.

At the theta point, from Equation (3.92) and the evaluation of R_H at the infinite dilution value of the diffusion constant determined at theta conditions, $D_o = K_D M^{1/2}$, i.e.,

$$R_H = \frac{kT}{6\pi\eta_o K_D M^{-1/2}} ,$$

yields

$$(k_f^c)_\theta = 2.23 \frac{4\pi N_A}{3K_D^3} M^{1/2} - \hat{V}_{20} - b_1 \quad . \qquad (3.100)$$

Thus Pyun and Fixman's (4) results predict that k_f^c will have a square

root dependence on M at the theta point.

For small values of A, Billick (9) suggested expanding the exponential term of Equation (3.94) in a power series

$$K(A) = \int_0^1 R(x)\{1-A(1-x)^2(2+x) + \frac{A^2}{2}[(1-x)^2(2+x)]^2 + \ldots\}\, dx \qquad (3.101)$$

or

$$K(A) = K_o - AK_1 + A^2K_2 + \ldots$$

where K_o, K_1, K_2 are constants and K_o is the value of K(A) at the theta temperature, which as previously mentioned, is between 4.2 and 4.93. Then, using Equation (3.93) and assuming that β is proportional to A_2, gives the result

$$K(A) = K_o - \frac{M^2A_2}{a^3}K_1' + \frac{M^4A_2^2}{a^6}K_2' + \ldots \qquad (3.102)$$

where K_1' and K_2' are now constants. Substituting this result for K(A) into Equation (3.92) and subtracting (k_f^c) from Equation (3.100) yields for small values of A_2

$$k_f^c - (k_f^c)_\theta = (MA_2)\frac{4\pi}{3}N_AK_1' \qquad (3.103)$$

Thus a plot of $k_f^c - (k_f^c)_\theta$ versus MA_2 should be linear over the range of small values of MA_2.

The concentration dependence of the frictional coefficient by Yamakawa (6) was calculated on the basis of the Kirkwood-Riseman (10) approach, taking into account the intramolecular and intermolecular

hydrodynamic interactions. A random flight model of a polymer with a Gaussian segment distribution was used and the intermolecular potential needed to evaluate the mean perturbation field was taken as the one proposed by Flory and Krigbaum (11). They obtained

$$k_f = \frac{4f_o A_2 M \lambda(\bar{z})}{9\pi^{3/2} \langle S^2 \rangle^{1/2} \eta_o} \qquad (3.104)a$$

where

$$f_o = \eta\xi/(1 + \frac{8X}{3\alpha_o}) \qquad (3.104)b$$

and

$$\lambda(\bar{z}) = \frac{f(\bar{z})}{h_o(\bar{z}) - \phi(\bar{z})} \qquad (3.104)c$$

The expression for f_o is the same one which occurs on the original Kirkwood-Riseman (9) derivation (Equation 3.49) and contains the draining parameter X (Equation 3.50). Thus, in the non-free draining limit, $X \to \infty$, Equations (3.104a) and (3.104b) reduce to

$$k_f = \lambda(\bar{z}) A_2 M \qquad (3.104)a'$$

$$f_o = (\frac{9\pi^{3/2}}{4}) \eta_o \langle S^2 \rangle^{1/2} \qquad (3.104)b'$$

What is important about $\lambda(\bar{z})$ is that it is a decreasing function $\bar{z}$, whose values have been tabulated by Yamakawa and which range from 1.345 for the theta state to 1.06 for the largest exclude volume calculated. The function $\phi(\bar{z})$ is part of the virial expansion factor as a function

of concentration

$$\alpha = \alpha_o[1 - A_2M\phi(\bar{z})c + \ldots] \tag{3.105}$$

where α_o is the expansion factor at infinite dilution. A closed expression for $\phi(\bar{z})$ was used, but the exact form is not too important since the contribution of $\phi(\bar{z})$ to $\lambda(\bar{z})$ is small. However, the expression for $h_o(z)$ is taken from first order perturbation theory.

The Yamakawa theory is thus limited to the vicinity of the theta point. It predicts in addition that k_f vanishes at the theta point. Since A_2 is an increasing function of z and $\lambda(\bar{z})$ is a decreasing function of z, k_f^c changes less with z than the corresponding expression in the Pyun and Fixman theory (Equation 3.92).

The concentration dependence of the frictional constant derived by Imai (5) relates k_f^c to the expansion coefficient α_η in the following manner:

$$k_f^c \sim \left(\frac{z}{\alpha_\eta^5}\right) M^{1/2}\alpha_\eta \tag{3.106}$$

Since Imai also demonstrated (12) that

$$\alpha_\eta^5 - \alpha_\eta^3 = \text{constant } z, \tag{3.107}$$

the following expression was obtained:

$$k_f^c = C_oM^{1/2}(\alpha_\eta - \alpha_\eta^{-1}), \tag{3.108}$$

where C_o is a constant dependent on the unperturbed dimensions of the polymer coil. Thus Imai's theory predicts that k_f^c vanishes at the

theta point, and that there should be a linear increase of k_f^c with $(\alpha_\eta - \alpha_\eta^{-1})$.

Heterogeneity Corrections

For heterogeneous polymers, equations derived for monodisperse systems must be corrected for the effects of polydispersity. Often, it is found that the molecular weight distribution can be adequately described by a Schultz distribution whose weight fraction is given by

$$\omega(M) = \frac{1}{\Gamma(1+h)} \gamma^{h+1} M^h \exp[-\gamma M] \tag{3.109}$$

where h is the width parameter of the distribution defined as

$$h = \left| \frac{M_w}{M_n} - 1 \right|^{-1} \tag{3.110}$$

The Schultz distribution will be used to evaluate the various molecular averages needed in this section.

It has been shown (1) that the diffusion constant obtained for polydisperse systems is a z average diffusion constant, D_z. The correct equations to use for polydisperse systems are thus

$$D_z = D_{z_o}[1 + (2M_\nu A_2 - k_f^c)c] \tag{3.111}$$

$$k_f^c = k_f \phi \frac{4\pi N_A}{3M_f} \left(\frac{kT}{6\pi\eta_o D_{z_o}} \right)^3 \tag{3.112}$$

$$D_{z_o} = K_D M_D^{-b} \tag{3.113}$$

where the correct molecular weight averages to be used, designated as M_ν, M_D, and M_f have been derived in Appendix 3.1, and the results summarized below.

$$M_D = \frac{1}{1+h}\left[\frac{\Gamma(h+2)}{\Gamma(h+2-b)}\right]^{1/b} M_w = \phi_D M_w \tag{3.114}$$

$$M_\nu = \left(\frac{1}{1+h}\right)^{1-\delta}\left[\frac{\Gamma(h+3-\delta-b)}{\Gamma(h+2-b)}\right] M_w = \phi_\nu M_w \tag{3.115}$$

$$M_f = \frac{(h+1)^2\Gamma(h+1)^3}{\Gamma(h+1+2b)\Gamma(h+2-b)^2} = \phi_f M_w \tag{3.116}$$

Here δ is defined by $A_2 = aM_w^{-\delta}$.

The equations for intrinsic viscosity and frictional coefficient obtained in Chapter III, Nonequilibrium Properties (f, [n]), were derived for monodisperse polymers. However, it has been shown by Newman et al. that the correct averages to be used in the relation $[n] = \Phi_o \langle R^2_o \rangle_n^{3/2}/M_n$ are number averages, and they proposed introduction of a factor to correct for sample heterogeneity when the ratio $\langle R^2 \rangle_z^{3/2}/\langle M \rangle_w$ was determined from light scattering experiments. Thus, for a heterogeneous polymer,

$$[n] = \frac{\Phi_o}{q_\phi}\frac{\langle R^2_o \rangle_z^{3/2}}{M_w} = \Phi_{APP}\frac{\langle R_o^2 \rangle_z^{3/2}}{M_w} \tag{3.117}$$

where

$$q_\phi = \frac{(\langle \bar{R}^2_o \rangle_z)^{3/2}}{\langle (\bar{R}^2_o)^{3/2} \rangle_n}\frac{M_n}{M_w} \tag{3.118}$$

If the molecular weight distribution is represented by a Schultz

distribution, then

$$q_\phi = \frac{\Gamma(h+1)(h+2)^{3/2}}{\Gamma(h+1.5)(h+1)} \tag{3.119}$$

Thus the apparent value of Φ measured must be multiplied by the correction factor q_ϕ, which is always greater than unity, to obtain the value which would be observed for a polymer consisting of a single species.

In addition, the measured value of Φ must be corrected for excluded volume effects to obtain the limiting value of the viscosity constant. For small values of excluded volume, Equation (3.61) can be used to obtain

$$\Phi_o = \Phi_{APPARENT} q_\phi \alpha_s^{+.57} \tag{3.120}$$

For large values of excluded volume, Schultz included the effect by setting $R_i^2 \sim M_i^{1+2\varepsilon}$, where the ε he employs is one half that defined by Peterlin (Equation 3.66). For a Schultz distribution, Equation (3.118) is modified to become

$$q_\phi(\varepsilon) = \frac{\Gamma(h+1)\Gamma(h+3+2\varepsilon)^{3/2}}{(h+1)\Gamma(h+3/2+3\varepsilon)\Gamma(h+2)^{3/2}} \tag{3.121}$$

It reduces to Equation (3.119) for $\varepsilon = 0$.

Then, using Peterlin's relation between $\langle R^2 \rangle$ and $\langle S^2 \rangle$, Equation (3.67), with the present definition of ε, leads to

$$[\eta] = \frac{\Phi_o 6^{3/2}(6+10\varepsilon+4\varepsilon^2)^{3/2} \langle S^2 \rangle z_o^{3/2}}{q_\phi \quad M_w} \tag{3.122}$$

Thus

$$\Phi_o = \Phi_{APPARENT} \frac{q_\phi(\varepsilon)}{(6 + 10\varepsilon + 4\varepsilon^2)^{3/2}} \qquad (3.123)$$

The value of ε to use depends upon the form of the expansion factor, but can also be related to the Mark-Houwink-Sakurada exponent as discussed in Chapter III, Nonequilibrium Properties (f, [n]).

It should be noted that reported values of Φ in the literature are often not corrected for polydispersity nor for excluded volume effects. This could easily lead to errors of 30% in the values of Φ for M_w/M_n ratios of only 1.5.

In the equation for the frictional coefficient, since the diffusion constant and hence f are z averages, the correct average for the macromolecular radius is a "diffusion average" radius defined as

$$R_D = \frac{\sum N_i M_i^2}{\sum N_i M_i^2 R_i^{-1}} \qquad (3.124)$$

Since the radius obtained from light scattering is a z average, $\langle S^2 \rangle_z^{1/2}$, a correction factor must be introduced as

$$f = \frac{P n_o}{q_p} \langle S^2 \rangle_z^{1/2} \qquad (3.125)$$

so that

$$P_{APPARENT} = P/q_p \qquad (3.126)$$

where

$$q_p = \frac{\langle S^2 \rangle_z^{1/2}}{R_D} = \langle S^2 \rangle_z^{1/2} D_z \qquad (3.127)$$

For a theta solvent, using a Schultz distribution, this becomes

$$q_p = \frac{\Gamma(h + 3/2)\Gamma(h + 3)^{1/2}}{[\Gamma(h + 2)]^{3/2}} \qquad (3.128)$$

The derivation of this result is given in Appendix 3.2.

Here, too, the apparent value of P must be corrected for excluded volume effects. For small values of excluded volume, Equation (3.65) can be used to obtain

$$P_o = P_{APPARENT}\, q_p \alpha_s^{.348} \qquad (3.129)$$

For large excluded volume, Equation (3.128) can be modified again using $R_i^2 \sim M_i^{1+2\varepsilon}$ to yield

$$q_p = \frac{\Gamma(h + 3/2 - \varepsilon)[\Gamma(h + 3 + 2\varepsilon)]^{1/2}}{\Gamma(h + 2)^{3/2}} \qquad (3.130)$$

as shown in Appendix 3.2, and thus

$$P_o = P_{APPARENT}\, q_p(\varepsilon) \qquad (3.131)$$

The heterogeneity correction factor to β has also been obtained by combining Equations (3.121) and (3.128) to yield

$$q_\beta = q_\phi^{1/3} q_p^{-1} \frac{(h + 1)^{2/3}\,[\Gamma(h + 1)]^{4/3}}{\Gamma(h + 3/2 - \varepsilon)[\Gamma(h + 3/2 + 3\varepsilon)]^{1/3}} \qquad (3.132)$$

Literature Survey for Polyions

General. Results of intrinsic viscosity and light scattering data which have appeared in the literature (1-14) on polyelectrolyte-salt systems generally support the view that the electrostatic repulsion in a polyion is sufficiently suppressed by the addition of low molecule weight electrolytes so that the excluded volume theories applicable to nonionic polymers are also valid for polyelectrolyte-salt-systems. Thus, tests of the two parameter theory for polyelectrolytes proceed by the same methods which are used for nonionic polymers.

When light scattering measurements have been performed, values of A_2 and α_s are obtained. It is thus possible to test the validity of various theories by checking the consistency in the values of z determined from observed values of α_s and from observed values of Ψ using the theoretical expressions for α_s and Ψ. Theoretical curves for "conjugate pairs" of $\Psi(\bar{z})$ and $\alpha_s(z)$ are shown in Figure 3.2, where the curves are identified by the abbreviated symbols listed in Table 3.1. Experimental values of $\Psi(\bar{z})$ calculated from observed A_2, M, and $\langle S^2 \rangle^{1/2}$ using Equation (3.11) are shown for various polyelectrolyte systems taken from Tan (15). The scatter of the experimental points is larger than those of nonionic polymers ($\alpha_s < 1.5$).

In addition, the validity of a theory can be tested by the linearity between $M^{1/2}$ and z determined from observed values of α_s using its theoretical expression. This condition arises simply from the definition of z (Equation 3.9). From the slope of a plot of $M^{1/2}$ versus z, values of β can be determined.

Figure 3.2 (a-b)

Theoretical curves for "conjugate pairs" of $\Psi(\bar{z})$ and $\alpha_s(z)$, where the curves are identified by the abbreviated symbols listed in Table 3.1.

Experimental points are:

(a) △ Na-polyacrylate

● Na-polyphosphate

□ Na-carboxymethyl cellulose

o Li-polyphosphate

(b) Fractions of Na-copoly (ethyl acrylate-acrylic acid)

o F1
△ F2
● F4

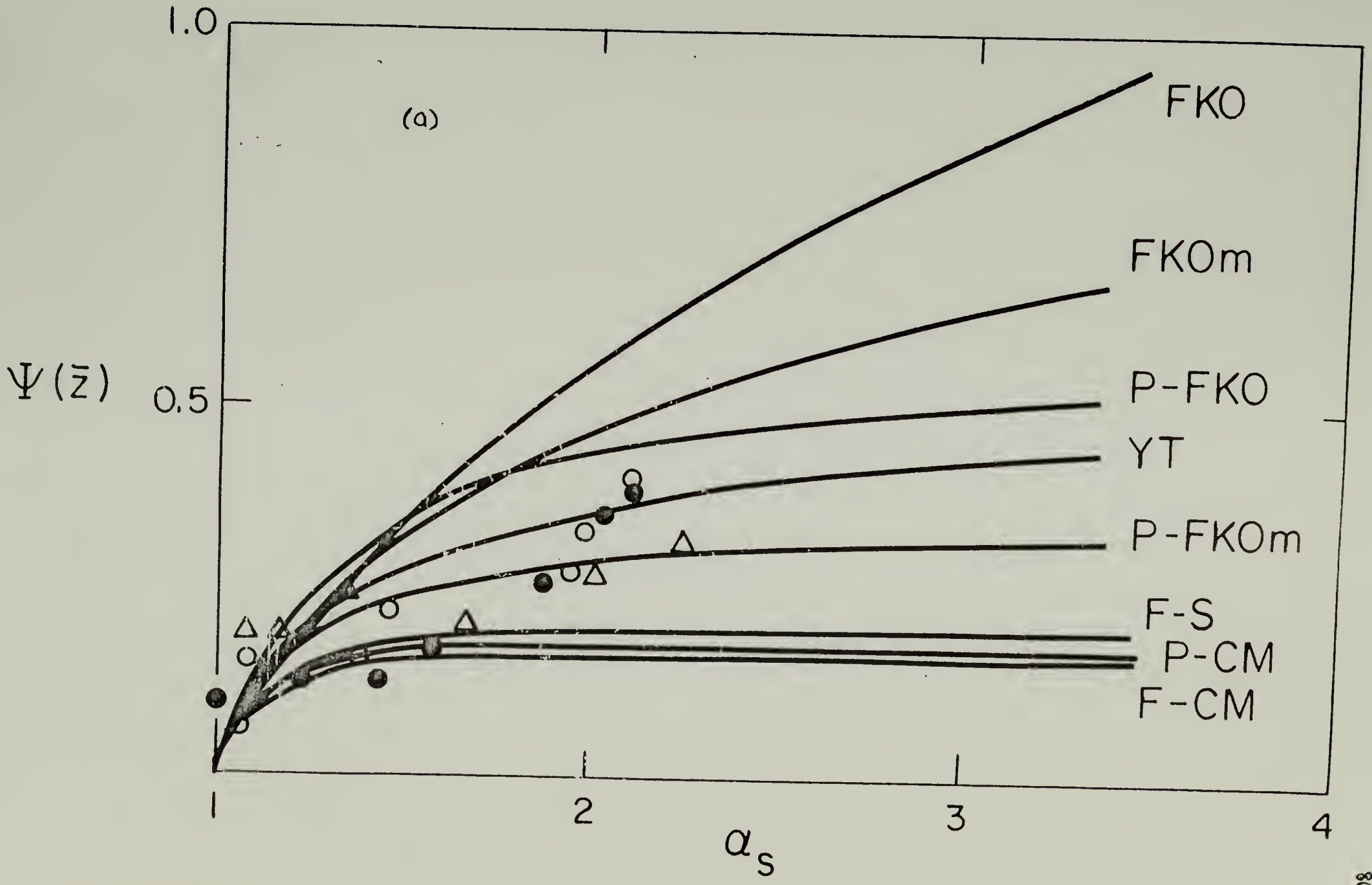
1.0
0.5
Ψ(z̄)
(a)
FKO
FKOm
P-FKO
YT
P-FKOm
F-S
P-CM
F-CM
1
2
3
4
α_s

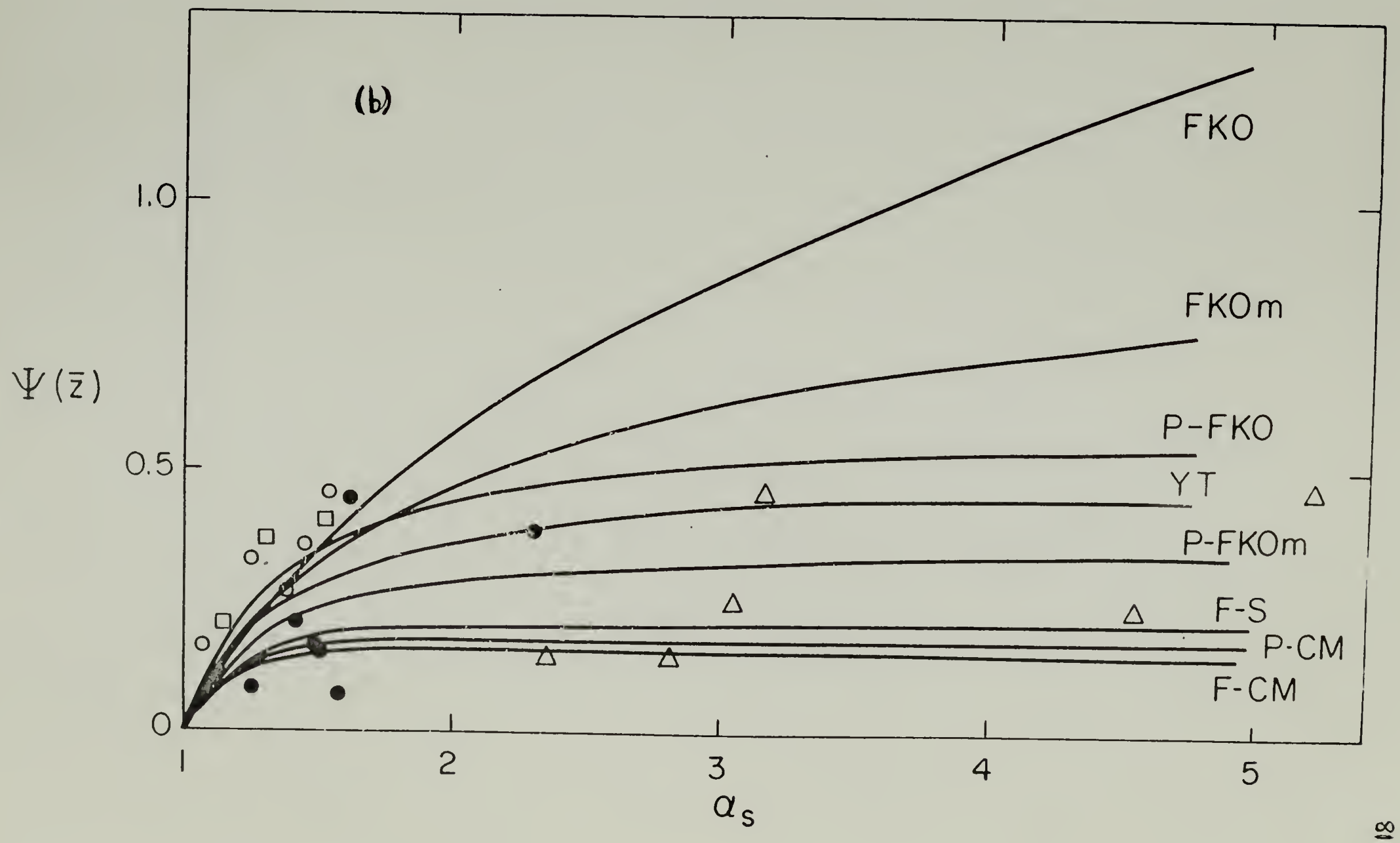
(b)
FKO
FKOm
P-FKO
YT
P-FKOm
F-S
P-CM
F-CM
1.0
0.5
0
1
2
3
4
5
$\Psi(\bar{z})$
α_s

To test approximate two-parameter theories of the intrinsic viscosity or frictional coefficient, it is convenient to plot Φ/Φ_o or P/P_o against α_s (α_η or α_f can also be used). The former are plotted for various polyelectrolytes as well as for nonionic polymers in Figure 3.3, taken from Tan (15). Even for nonionic polymers there is an increase in Φ/Φ_o at large α_η which is, however, larger for polyions, and which is not predicted by any of the theories of viscosity so far developed.

Values of β can also be obtained from viscosity measurements by the indirect method of using Stockmayer-Fixman plots. As is evident from Equation (3.78), B can be determined from the slope of a plot of $[\eta]/M^{1/2}$ versus $M^{1/2}$ and if a suitable value of n is chosen, β (which is equal to M^2B/n^2) can be estimated. The intercepts of these plots can be used to obtain unperturbed dimensions.

It is found for some polyelectrolyte systems that the intercepts for various ionic strengths do not agree (11,14,15). Thus the values of the unperturbed dimensions and hence the expansion factors are not well defined. Patel and Patel (16) reanalyzed the data of Nagasawa et al. (13) for the second virial coefficient of sodium polystyrene-sulfonate (NaPSS) using different criteria for determining unperturbed dimensions, and came to different conclusions. In work on sodium carboxymethyl amylose (Na-CMA), Patel and Patel (4) found that values of a (from $[\eta] = KM^a$) were constant between 0.65N NaCl and 1.5N NaCl and concluded that to obtain exact theta conditions is difficult with polyelectrolytes. Tan (15), on the other hand, found with aqueous salt solutions of sodium poly-3-methyl-acryloyloxy propane-1-sulfonate

Figure 3.3

Viscosity constant Φ/Φ_0 versus α_η for several polyelectrolytes.

——— experimental

-o-o-o- theoretical

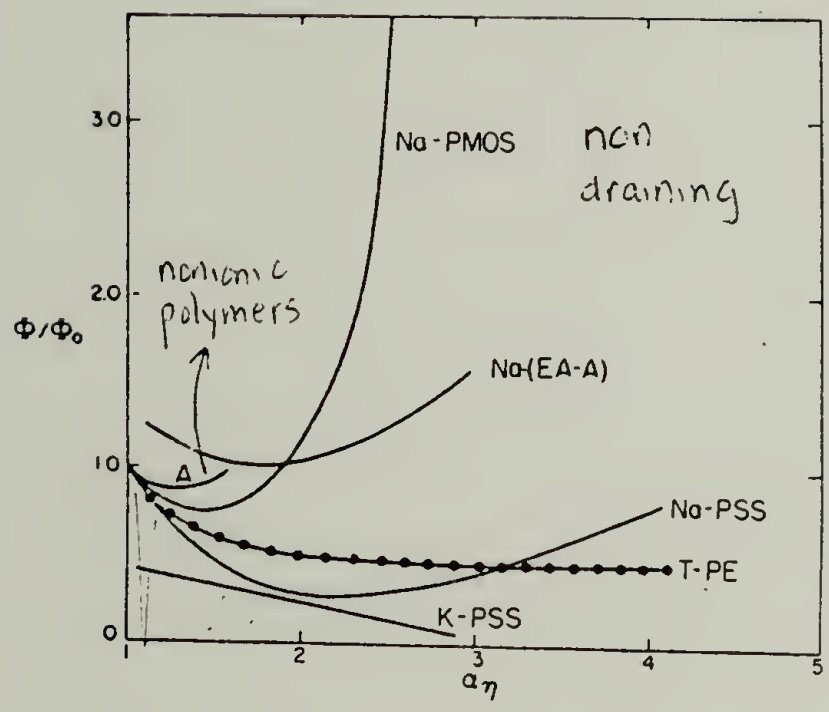
30
20
10
0
Φ/Φ₀
Na-PMOS
non draining
nonionic polymers
Na-(EA-A)
A
Na-PSS
T-PE
K-PSS
1
2
3
4
5
aη

partially

(Na-PMOS) that even salt concentrations of 13N LiCl, 12N NaI or 7.5N KI were not theta solvents for the system.

The empirical linear relation between log A_2 and log C_s proposed by Trap and Hermans (1) is found to be a good description for many systems. Data on Na-copoly (ethyl acrylate-acrylic acid) (14), Na-poly(styrene sulfonate) (13,16), Na-carboxymethyl cellulose (1), and Na-carboxymethyl amylose, are plotted (4) in Figure 3.4, taken from Tan (14).

Na-copoly (ethyl acrylate-acrylic acid) (14). For the polymer in the present study, Na-copoly (ethyl acrylate-acrylic acid), for degrees of expansion within the ionic strength range 0.05 - 0.5N NaCl, the linear relation between α_s^2 and $C_s^{-2/3}$ proposed by Ptitsyn (Table 3.2, Equation 3.38), which precludes points with $\alpha_s < 1.2$ (i.e., points beyond C_s = 0.5N for this system), provides the best description of the data as discussed by Tan (14). Figures 3.5a-c are plots of α_s^2 versus $C_s^{-2/3}$ for three factions of the copolymer taken from Tan (14). In addition to the linearity exhibited by the data, the common intercept of 0.78 is the same as that predicted by Equation (3.38).

Combining the experimental slope of approximately 0.5 in Figures 3.5a-c and Equation (3.38) (Table 3.2) it is possible to write

$$\left[0.95 \left(\frac{3}{2\pi}\right)\left(\frac{n^{1/3}}{l^2}\right) \frac{10^2}{(2N_A)^{2/3}}\right] i^{4/3} = 0.5 \qquad (3.133)$$

Since $6\langle S^2\rangle_o = nl^2$, l can be estimated and the quantity in brackets of Equation (3.133) evaluated. Thus the effective degree of ionization

Figure 3.4

Double logarithmic plots of the second virial coefficient versus ionic strength from Tan (14):

Line A

Na-carboxymethyl cellulose
o from osmotic pressure
Δ,□ from light scattering

Lines B and C

Na-polystyrene sulfonate

Lines D and E

Na-copoly (ethyl acrylate-acrylic acid)
(o, F1; Δ, F2; ●, F4)

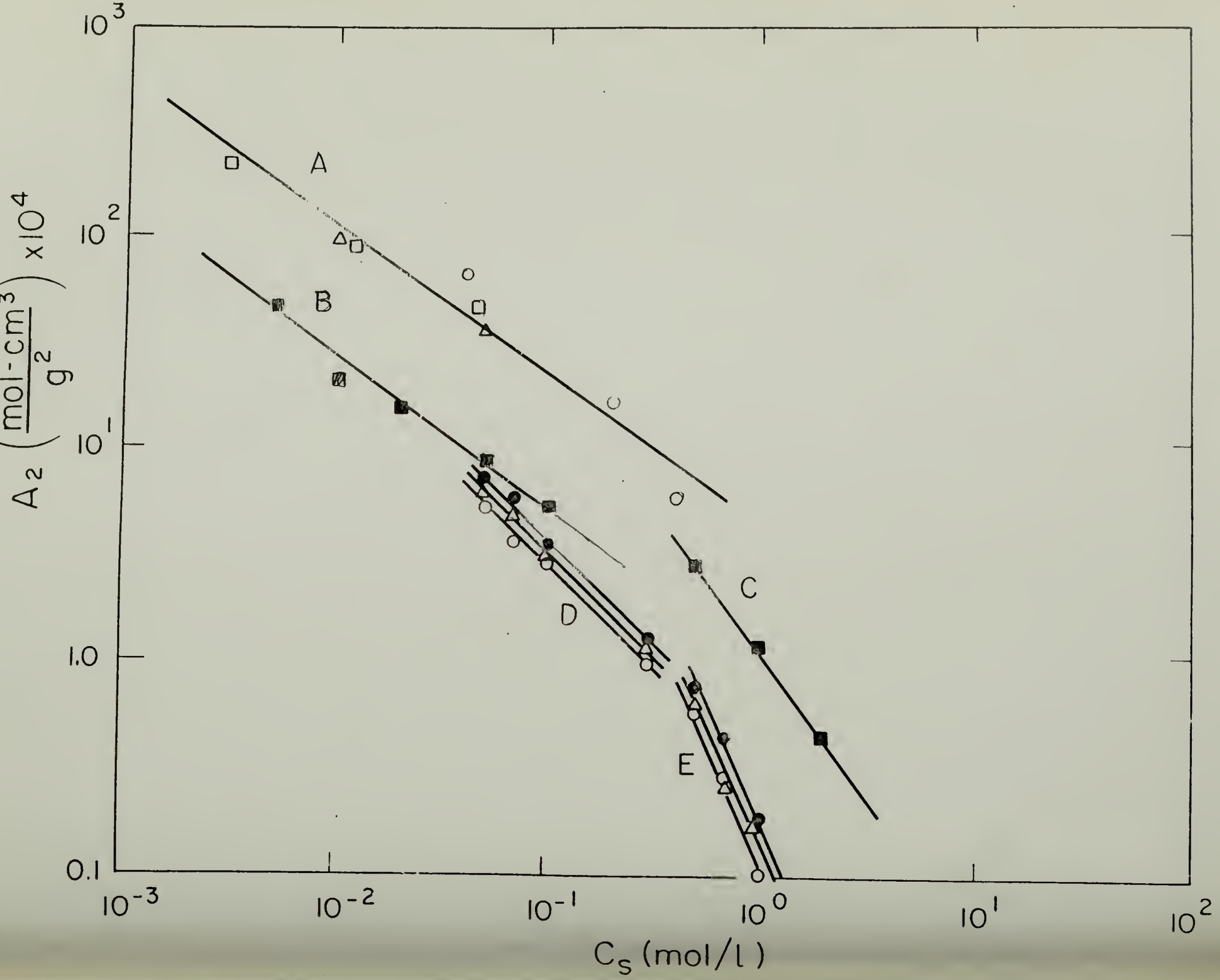
$A_2\left(\frac{\text{mol-cm}^3}{g^2}\right) \times 10^4$
10^3
10^2
10^1
1.0
0.1
A
B
C
D
E
10^{-3}
10^{-2}
10^{-1}
10^0
10^1
10^2
C_s (mol/l)

Figure 3.5

Plots of α_s^2 versus $C_s^{-2/3}$ for fractions of Na-copoly (ethyl acrylate-acrylic acid) from Tan (14).

(a) F1

(b) F2

(c) F4

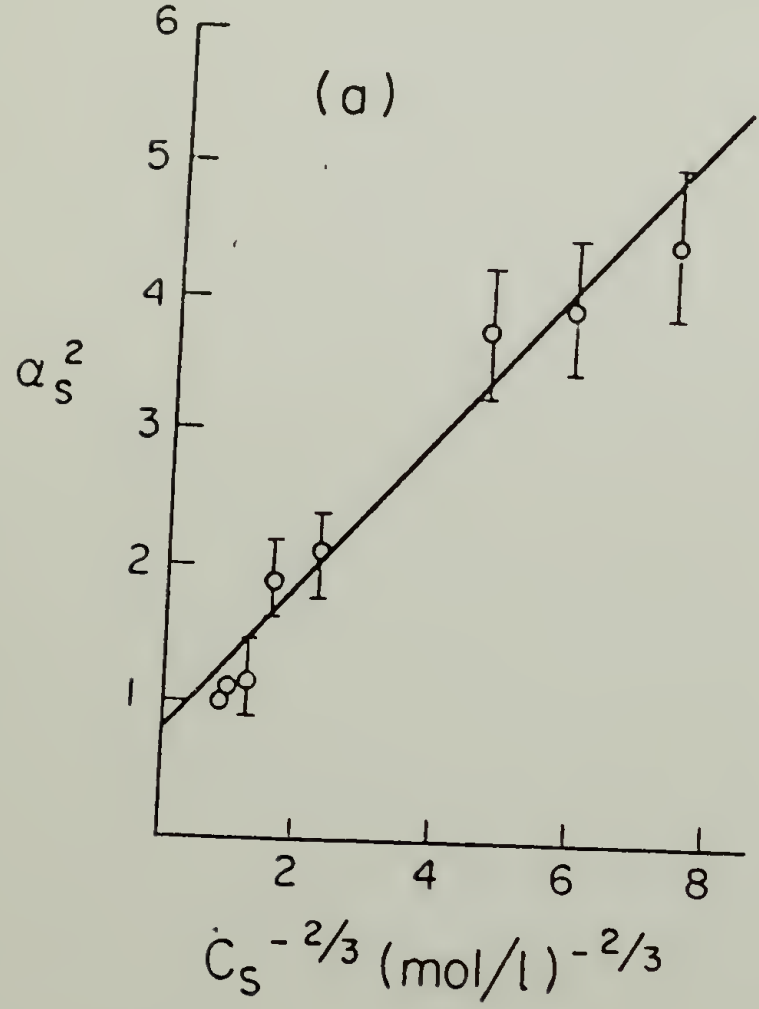
(a)
6
5
4
3
2
1
α_s^2
2
4
6
8
$C_s^{-2/3}$ (mol/l)$^{-2/3}$

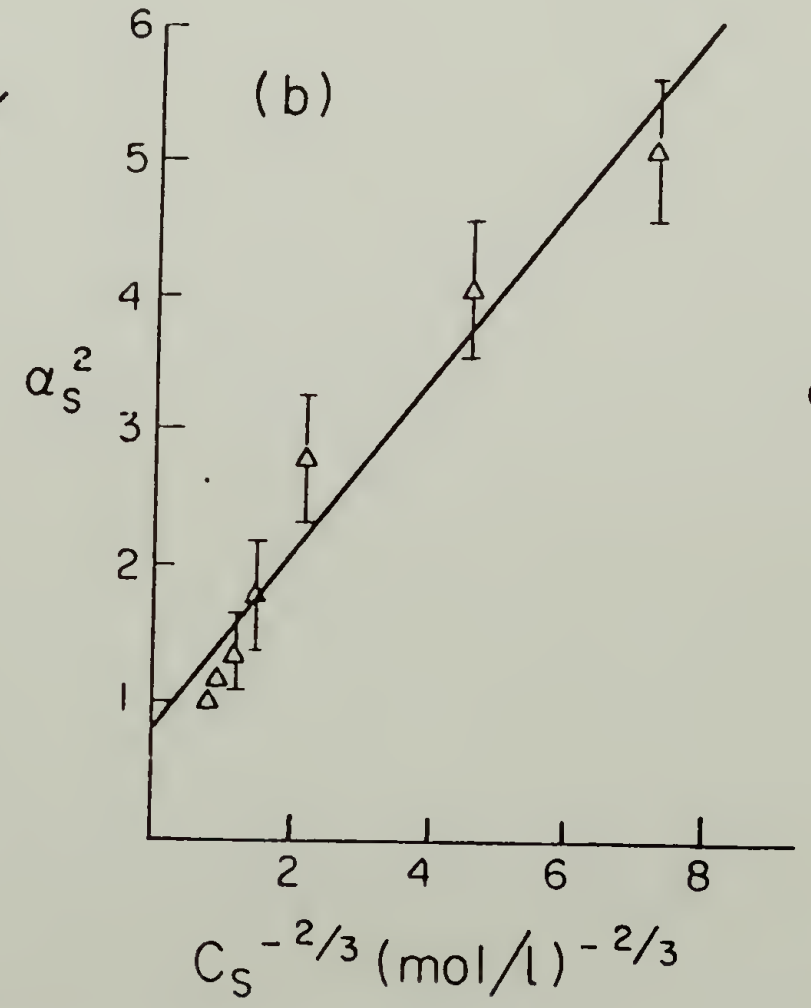
(b)
6
5
4
3
2
1
α_s^2
2
4
6
8
$C_s^{-2/3}$ (mol/l)$^{-2/3}$

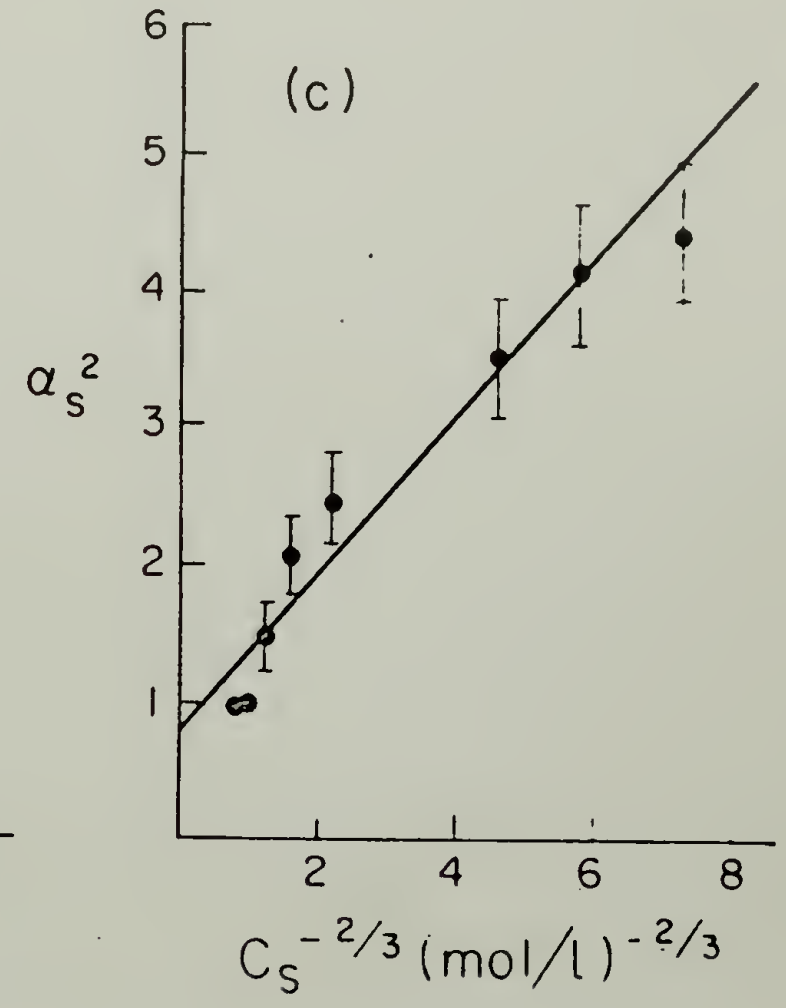
(c)
6
5
4
3
2
1
α_s^2
2
4
6
8
$C_s^{-2/3}$ (mol/l)$^{-2/3}$

calculated in this manner is 0.044, which is substantially smaller than the apparent value of unity assumed for the experimental conditions of pH 7. As mentioned in Chapter III, Two Parameter Theory (α, A_2), Application to polyions, this can be attributed to counterion binding to the charged groups on the polyions.

As can be seen from Figure 3.2, the experimental values of $\Psi(\bar{z})$ calculated from observed A_2, M, and $\langle S^2 \rangle^{1/2}$ for the fractions of Na-copoly (ethyl acrylate-acrylic acid) can be described approximately either by P-FKOm or YT theories.

Since α_s^2 is linearly proportional to $C_s^{-2/3}$ for $C_s \leq 0.5N$, the ionic strength dependence of A_2 can be obtained as follows. Using Equation (3.38), Table 3.2 and the slope of 0.5 from Figures 3.5a-c, $0.95\ z^{2/3} = 0.5\ C_s^{-2/3}$ and $z \sim 1/C_s$. Therefore, z can be calculated from each C_s. By substituting these z values into Equation (3.38), α_s can be calculated and hence $\bar{z}$ $(=z/\alpha_s^3)$ can be obtained. If the combination of Ptitsyn's $\alpha_s(z)$ and FKOm's $\Psi(\bar{z})$ is chosen to describe the universal curve in Figure 3.2, $\Psi(\bar{z})$ can be calculated using values of $\bar{z}$ for each C_s. Therefore, A_2 can be obtained from Equation (3.11). The calculated and observed A_2 for three fractions of Na-copoly (ethyl acrylate-acrylic acid) are listed in Table 3.3 where it can be seen that the agreement is reasonable.

TABLE 3.3

Second Virial Coefficients, $A_2 \times 10^4$ (mol·cm^3/g^2), for Na-Copoly (ethyl acrylate-acrylic acid) in NaCl Solutions from Tan (14)

Ionic Strength	Fraction F1		Fraction F2		Fraction F3	
(mol/l)	calc.	obs.	calc.	obs.	calc.	obs.
0.05	3.94	5.25	4.08	6.00	5.37	7.00
0.07	3.11	3.55	--	--	4.71	5.74
0.1	2.86	2.84	2.61	3.10	3.56	3.38
0.3	0.99	0.95	1.23	1.11	1.73	1.21
0.5	0.77	0.59	0.56	0.57	1.15	0.72

REFERENCES

Two Parameter Theory of Polymer Solutions

1. H. Yamakawa, "Modern Theory of Polymer Solutions," Harper and Row, New York (1971).

2. P.J. Flory, "Statistical Mechanics of Chain Molecules," John Wiley & Sons, New York (1969).

3. W. Kuhn, Kolloid Z., 87, 3 (1939).

4. P.J. Flory, J. Chem. Phys., 17, 303 (1949).

5. B.H. Zimm, W.H. Stockmayer & M. Fixman, J. Chem. Phys., 21, 1716 (1953).

6. E. Teramoto, Proc. Intern. Conf. Theoret. Phys., Kyoto Tokyo (1953).

7. M. Fixman, J. Chem. Phys., 23, 1656 (1955).

8. H. Yamakawa & G. Tanaka, J. Chem. Phys., 47, 3991 (1967).

9. H. Fujita, K. Okita & T. Norisuye, J. Chem. Phys., 47, 2723 (1967).

10. M. Fixman, J. Chem. Phys., 36, 3123 (1962).

11. O.B. Ptitsyn, Vysokomolekul. Soedin., 3, 1673 (1961).

12. W.H. Stockmayer, Makromol. Chem., 35, 54 (1960).

13. S.F. Edwards, Proc. Phys. Soc. (London), 85, 613 (1965).

14. H. Reiss, J. Chem. Phys., 47, 186 (1967).

15. H. Yamakawa, J. Chem. Phys., 48, 3845 (1968).

16. H. Yamakawa, J. Chem. Phys., 54, 2484 (1968).

17. P.J. Flory, "Principles of Polymer Chemistry," Ch. 12, Cornell Univ. Press, Ithaca, N.Y. (1953).

18. W.G. McMillan & J.E. Mayer, J. Chem. Phys., 13, 276 (1945).

19. B.H. Zimm, J. Chem. Phys., 14, 164 (1946).

20. M. Kurata & H. Yamakawa, J. Chem. Phys., 29, 311 (1958).

21. Y. Tagami & E.F. Casassa, J. Chem. Phys., 50, 2206 (1969).

22. H. Yamakawa, Pure & Appl. Chem., 31, 179 (197).

23. P.J. Flory & N.R. Krigbaum, J. Chem. Phys., 18, 1086 (1950).

24. T.A. Orofino & P.J. Flory, J. Chem. Phys., 26, 1067 (1957).

25. E.F. Casassa & H. Markovitz, J. Chem. Phys., 29, 493 (1958).

26. M. Kurata, M. Fukata, H. Sotobayashi & H. Yamakawa, J. Chem. Phys., 41, 139 (1964).

27. H. Yamakawa, J. Chem. Phys., 48, 2103 (1968).

28. W.H. Stockmayer & M. Fixman, J. Polym. Sci., Pt. C, 1, 137 (1963).

29. T. Norisuye, K. Kawahara, A. Teramota & H. Fujita, J. Chem. Phys., 49, 4330 (1968).

30. S.A. Rice and M. Nagasawa, "Polyelectrolyte Solutions," Academic Press, Inc., New York (1961).

31. O.B. Ptitsyn, Vysokomol. Soedin., 3, 1251 (1961).

32. P.J. Flory, J. Chem. Phys., 21, 162 (1953).

33. T.L. Hill, J. Chem. Phys., 20, 1173 (1952).

34. J.J. Hermans & J. Th. G. Overbeek, Rec. Trav. Chim., 67, 761 (1948).

35. A. Katchalsky & S. Lifson, J. Polym. Sci., 11, 409 (1953).

36. M. Fixman, J. Chem. Phys., 41, 3772 (1964).

37. M. Kurata, J. Polym. Sci., C15, 347 (1966).

38. M. Kurata, W.H. Stockmayer & A. Roig, J. Chem. Phys., 33, 151 (1960).

39. O.B. Ptitsyn, Vysokomol. Soedin., 3, 1673 (1961).

40. O.B. Ptitsyn, Vysokomol. Soedin., 3, 1251 (1961).

41. O.B. Ptitsyn, Ukr. Fiz. Zh., 7, 702 (1962).

42. Z. Alexandrowicz, J. Chem. Phys., 46, 3789 (1967).

43. T.L. Hill, Disc. Faraday Soc., 21, 31 (1956).

44. T.L. Hill, J. Phys. Chem., 61, 548 (1952).

45. D.T.F. Pals & J.J. Hermans, Rec. Trav. Chim., 71, 469 (1952).

46. A. Katchalsky, Z. Alexandrowicz and O. Kedem, in B.E. Conway and R.G. Barradas, Eds., "Chemical Physics of Ionic Solutions," John Wiley & Sons, Inc., New York, 295 (1966).

47. G.S. Manning and B.H. Zimm, J. Chem. Phys., 43, 4250, 4260 (1965).

48. T.A. Orofino & P.J. Flory, J. Phys. Chem., 63, 283 (1959).

49. A. Takahashi, T. Kato and M. Nagasawa, J. Phys. Chem., 71, 2001 (1967).

50. Z. Alexandrowicz, J. Polym. Sci., Part A-2, 6, 1227 (1968).

51. H.J.L. Trap and J.J. Hermans, J. Phys. Chem., 58, 757 (1954).

Nonequilibrium Properties

1. H. Yamakawa, "Modern Theory of Polymer Solutions," Harper & Row, New York (1971).

2. J.G. Kirkman & J. Riseman, J. Chem. Phys., 16, 565 (1948).

3. P.J. Flory & T.G. Fox., Jr., J. Am. Chem. Soc., 73, 1904 (1951).

4. C. Tanford, "Physical Chemistry of Macromolecules," Wiley, New York (1961).

5. R.J. Bearman, J. Phys. Chem., 65, 1961 (1961).

6. J.S. Ventas & J.L. Duda, J. Appl. Polym. Sci., 20, 2569 (1976).

7. N.C. Ford, Jr., Chemica Scripta, 2, 193 (1972).

8. J.G. Kirkwood, R.W. Zwanzig & R.J. Plock, J. Chem. Phys., 23, 213 (1955).

9. P.J. Flory, "Principles of Polymer Chemistry," Cornell Univ. Press, Ithaca, New York, Ch. XIV (1953).

10. L. Mandelkern & P.J. Flory, J. Chem. Phys., 20, 212 (1952).

11. S.F. Edwards & M.A. Oliver, J. Phys. A, 4, 1 (1971).

12. M. Kurata & H. Yamakawa, J. Chem. Phys., 29, 211 (1958).

13. H. Yamakawa & M. Kurata, J. Phys. Soc. Japan, 13, 94 (1958).

14. H. Yamakawa & G. Tanaka, J. Chem. Phys., 55, 3188 (1971).

15. J.E. Hearst, J. Chem. Phys., 37, 2547 (1962).

16. C.W. Pyun and M. Fixman, J. Chem. Phys., 42, 3838 (1965) and 44, 2107 (1966).

17. J.G. Kirkwood, Rec. Trav. Chim., 68, 649 (1949).

18. J.G. Kirkwood, J. Polym. Sci., 12, 1 (1954).

19. W.H. Stockmayer & A.C. Albrecht, J. Polym. Sci., 32, 215 (1958).

20. A. Horta & M. Fixman, J. Am. Chem. Soc., 90, 2048 (1968).

21. P.E. Rouse, Jr., J. Chem. Phys., 21, 1272 (1953).

22. F. Bueche, J. Chem. Phys., 22, 603 (1954).

23. B.H. Zimm, J. Chem. Phys., 24, 269 (1956).

24. A. Peterlin, J. Chem. Phys., 23, 2464 (1955).

25. R. Houwink, J. Prakt. Chem., 157, 15 (1940).

26. I. Sakurada, Kasen Koenshu, 5, 33 (1940); 6, 177 (1941).

27. O.B. Ptitsyn and Yu.E. Eizner, Zh. Fiz. Khim., 32, 2464 (1958); 29, 1117 (1959).

28. N.W. Tschoegl, J. Chem. Phys., 39, 149 (1963); 40, 473 (1964).

29. V.A. Bloomfield & B.H. Zimm, J. Chem. Phys., 44, 315 (1966).

30. G. Meyerhoff, Makromol. Chem., 72, 214 (1964).

31. L. Mandelkern & P.J. Flory, J. Chem. Phys., 20, 212 (1952).

32. H. Yamakawa, Pure and Appl. Chem., 31, 179 (1973).

33. A. Yamamoto, M. Fujii, G. Tanaka and H. Yamakawa, Polymer J., 2, 799 (1971).

34. K. Kawahara, T. Norisuye, and J. Fujita, J. Chem. Phys., 49, 4339 (1968).

35. W. Stockmayer & M. Fixman, J. Polym. Sci., C1, 137 (1963).

36. N.C. Ford, Jr., F.E. Karasz and J.E.M. Owen, Disc. Faraday Soc., 49, 228 (1970).

37. J.M.G. Cowie and S. Bywater, Polymer, Lond., 6, 197 (1965).

Concentration Dependence of Diffusion Constant

1. C. Tanford, "Physical Chemistry of Macromolecules," Wiley, New York (1961).

2. H. Yamakawa, "Modern Theory of Polymer Solutions," Harper & Row, New York (1971).

3. J.S. Vrentas and J.L. Duda, J. Appl. Polym. Sci., 20, 2569 (1976).

4. C.W. Pyun and M. Fixman, J. Chem. Phys., 41, 937 (1964).

5. S. Imai, J. Chem. Phys., 50, 2116 (1969).

6. H. Yamakawa, J. Chem. Phys., 36, 2995 (1962).

7. J.S. Vrentas and J.L. Duda, J. Polym. Sci., Polym. Phys. Ed., 14, 101 (1976).

8. T.A. King, A. Knox, W.I. Lee and J.D.G. McAdam, Polymer, 14, 151 (1973).

9. I.H. Billick, Preprints (Am. Chem. Soc. Polym. Div.), 5, 855 (1964).

10. J.G. Kirkwood and J. Riseman, J. Chem. Phys., 16, 565 (1948).

11. P.J. Flory and W.R. Krigbaum, J. Chem. Phys., 18, 1086 (1950).

12. S. Imai, J. Chem. Phys., 50, 2107 (1969).

Heterogeneity Corrections and Literature Survey for Polyions

1. H.J.L. Trap and J.J. Hermans, J. Phys. Chem., 58, 757 (1954).

2. N.S. Schneider and P. Doty, J. Phys. Chem., 58, 762 (1954).

3. R.M. Fuoss and V.P. Strauss, J. Polym. Sci., 3, 602 (1948); Ann. N.Y. Acad. Sci., 12, 48 (1949).

4. J.R. Patel and R.D. Patel, Polymer, 10, 167 (1969); Ind. J. Chem., 7, 1225 (1969).

5. A. Silberberg, J. Elliassaf, and A. Katchalsky, J. Polym. Sci., 23, 253 (1957).

6. T.N. Nekrasova, O.B. Ptitsyn, and M.S. Shikanova, Vysokomol. Soedin, A10, 1530 (1968).

7. P.J. Flory and J.E. Osterheld, J. Phys. Chem., 58, 653 (1954).

8. T.A. Orofino & P.J. Flory, J. Phys. Chem., 63, 283 (1959).

9. H. Eisenberg & D. Woodside, J. Chem. Phys., 36, 1844 (1962).

10. A. Raziel and H. Eisenberg, Israel J. Chem., 11, 183 (1973).

11. A. Takahashi and M. Nagasawa, J. Amer. Chem. Soc., 86, 543 (1964).

12. I. Noda, T. Tsuge & M. Nagasawa, J. Phys. Chem., 74, 710 (1970).

13. A. Takahashi, T. Kate, and M. Nagasawa, J. Phys. Chem., 71, 2001 (1967).

14. J.S. Tan & S.P. Gasper, J. Polym. Sci., Polym. Phys. Ed., 12, 1785 (1974).

15. J.S. Tan & S.P. Gasper, J. Polym. Sci., Polym. Phys. Ed., 13, 1705 (1975).

16. J.R. Patel and R.D. Patel, Makromol. Chem., 120, 103 (1968).

CHAPTER IV

CONFORMATIONAL TRANSITIONS

Literature Survey

Studies of polymers containing both hydrophilic and hydrophobic groups have revealed that under certain conditions the molecules undergo a conformational transition. Extensive work on the conformational transition in polymethacrylic acid (PMAA) has been reported in the literature (1-14). The most commonly used measurements include (a) the intrinsic viscosity, [n], as a function of the degree of ionization (1-3), the composition of the alcohol-water mixed solvent (2-5) or temperature (6); (b) pK as a function of the degree of ionization (7-11); (c) the fluorescence intensity or the dielectric loss tangent as a function of the composition of alcohol-water mixed solvent (4); (d) the hydrocarbon solubilities in different media (12,13); and (e) low angle x-ray scattering in water-methanol mixed solvent (14).

It has been concluded that a cooperative transition from a compact coiled state to an extended rod-like state occurs in PMAA. This transition is attributed to a cooperative rupture of hydrophobic attraction among the $-CH_3$ groups and to the increase in hydrogen bonding among the -COOH groups along the chain as the solvent is changed from aqueous media to methanol. This type of transition was not observed in polyacrylic acid (PAA) (1,2,8).

In the copolymer Na-copoly (ethyl acrylate-acrylic acid) 75% of the side chains are ethyl ester groups. In aqueous salt solutions, strong hydrophobic attraction among these ester groups should prevail, and attraction should increase with an increase in ionic strength. On the other hand, the electrostatic repulsion between the charged groups on the chain should decrease with an increase in ionic strength owing to a stronger counterion screening. As a result, a transition similar to that observed in PMAA should occur, but less well defined because of the smaller charge density along the chain.

Na-copoly (ethyl acrylate-acrylic acid)

Previous work on Na-copoly (ethyl acrylate-acrylic acid) probed the transition using light scattering (15), intrinsic viscosity (15), potentiometric titration (16) and dye binding studies (17).

Changes in molecular parameters as a function of ionic strength exhibited unusual polyelectrolyte behavior. Figure 4.1a shows $\langle s^2 \rangle^{1/2}$ versus C_s, Figure 4.1b shows α_s^2 versus $C_s^{-2/3}$, and Figure 4.2 shows $[\eta]$ versus C_s as well as $\ln[\eta]$ versus $\ln C_s$ for fractions of this copolymer. Although Figures 4.1 and 4.2 do not show typical cooperative transition curves (it is noted, however, that experiments in the low-ionic-strength region are difficult to perform), changes in $\langle s^2 \rangle^{1/2}$ and $[\eta]$ are pronounced from low C_s up to $C_s \simeq 0.1N$ to 0.3N and level off beyond 0.3N. Changes in magnitude of $\langle s^2 \rangle^{1/2}$ and $[\eta]$ with C_s within the same molecular weight and ionic-strength regions for other typical polyelectrolytes, e.g., Na-PAA in NaBr solutions (18,19), are considerably smaller than those for this copolymer. Figure 3.4 shows a double loga-

Figure 4.1

a. Radius of gyration versus ionic strength for fractions of Na-copoly (ethyl acrylate-acrylic acid), from Tan (15).

b. The expansion factor, α_s^2 versus $C_s^{-2/3}$ for three fractions of Na-copoly (ethyl acrylate-acrylic acid), from Tan (15).

(a)

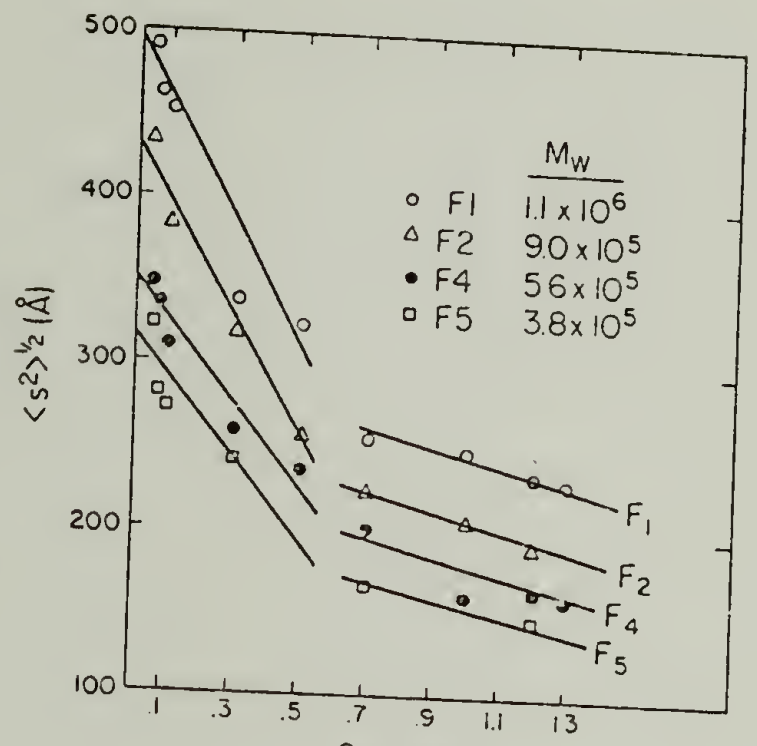
500
400
300
200
100
$\langle s^2 \rangle^{1/2}$ (Å)
M_w
F1 1.1×10^6
F2 9.0×10^5
F4 5.6×10^5
F5 3.8×10^5
F_1
F_2
F_4
F_5
.1
.3
.5
.7
.9
1.1
1.3
C_S (mol/l)

(b)

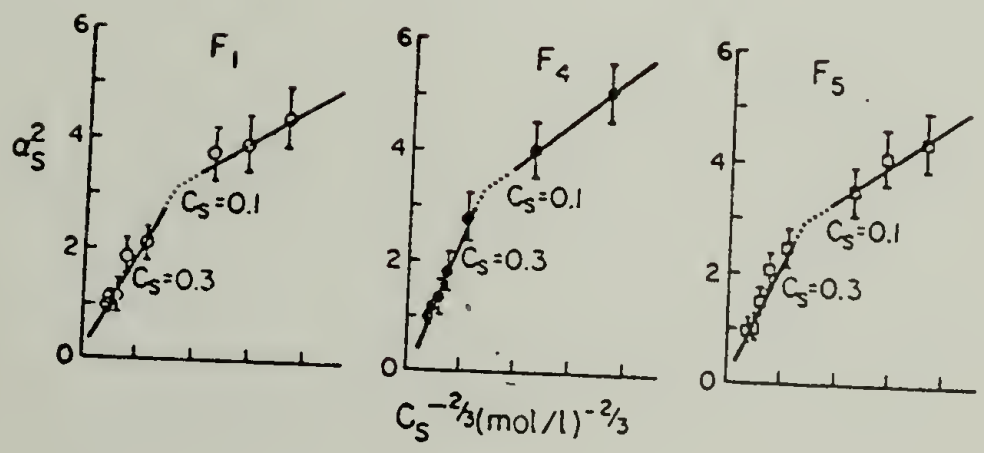
F_1
F_4
F_5
α_S^2
C_S=0.1
C_S=0.3
0
2
4
6
$C_S^{-2/3}$(mol/l)$^{-2/3}$

Figure 4.2

a. Intrinsic viscosity versus ionic strength for fractions of Na-copoly (ethyl acrylate-acrylic acid), from Tan (15).

b. Intrinsic viscosity versus $C_S^{-1/2}$ for four fractions of Na-copoly (ethyl acrylate-acrylic acid), from Tan (15).

(a)

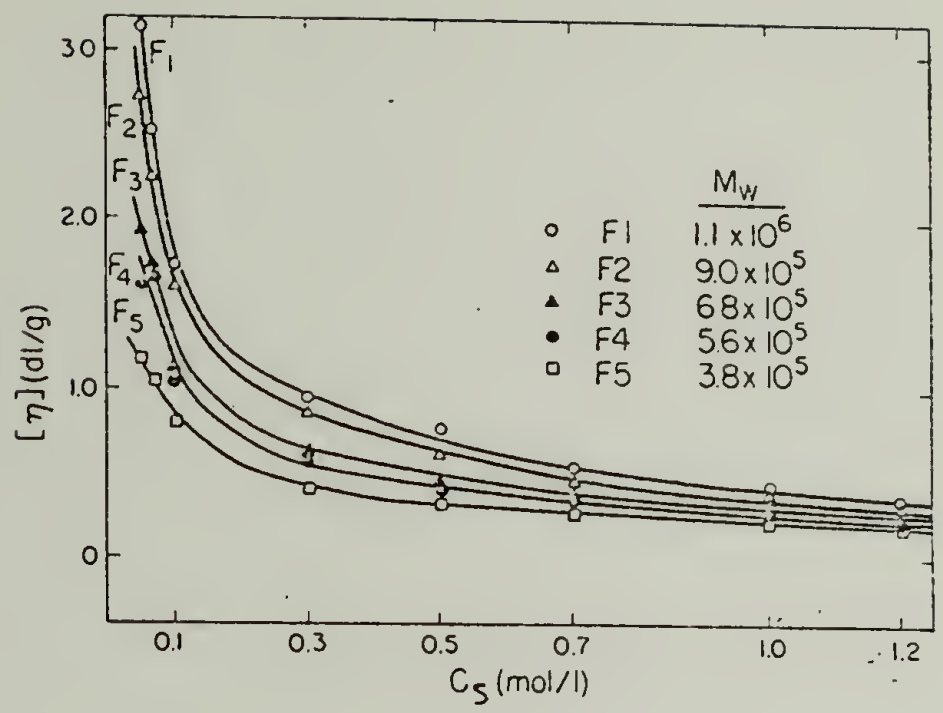
3.0
2.0
1.0
0
[η](dl/g)
F1
F2
F3
F4
F5
Mw
F1 1.1 x 10^6
F2 9.0 x 10^5
F3 6.8 x 10^5
F4 5.6 x 10^5
F5 3.8 x 10^5
0.1
0.3
0.5
0.7
1.0
1.2
Cs (mol/l)

(b)

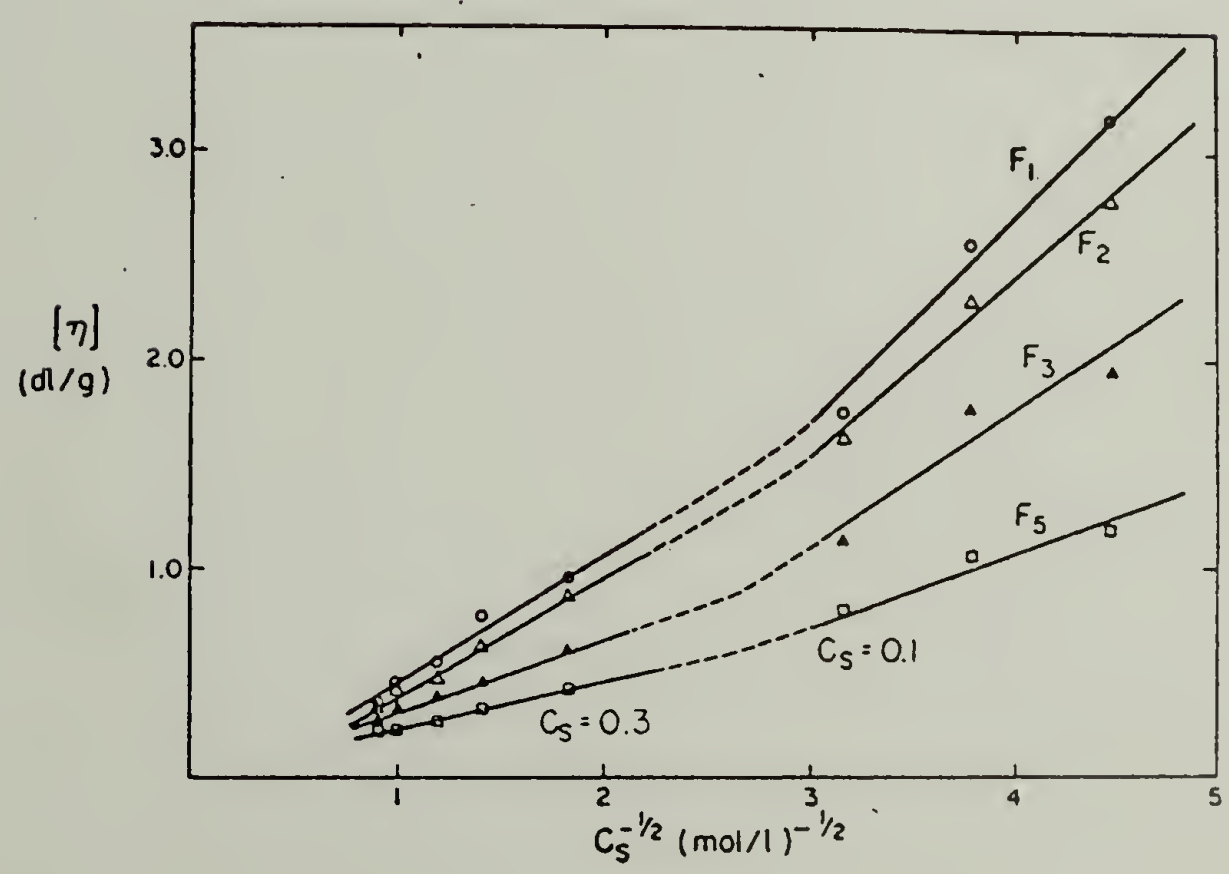
3.0
2.0
1.0
[η]
(dl/g)
F1
F2
F3
F5
Cs = 0.1
Cs = 0.3
1
2
3
4
5
Cs^-1/2 (mol/l)^-1/2

rithmic plot of the second virial coefficient against ionic strength. The break in the curves in the region $C_s \simeq 0.1N$ to 0.3N and their change in slope, which does not occur for polyelectrolytes without hydrophobic groups along the chain, suggest the existence of a structural transition region in this system. Thus although cooperativity is not evident, the trend of the data indicates that the copolymer molecules undergo conformational changes in the ionic strength region of 0.1N to 0.3N NaCl, and this less well defined transition is confirmed both thermodynamically ($\langle s^2 \rangle^{1/2}$ and A_2) and hydrodynamically ([η]). This transition can be interpreted as a result of an increase of hydrophobic attraction and decrease of electrostatic repulsion within the coil going from a low ionic strength to a high ionic strength medium. With this change in environment, the molecule will go through a transition from an extended, swollen state to a tightly coiled state.

The possibility of two different conformations was further verified by direct measurements of the unperturbed dimensions of this system in an aqueous salt solution and in an organic solvent. Observed values for the second virial coefficient are nearly zero for solutions in 1.2N NaCl and negative in 1.3N NaCl indicating that a solution between these normalities is a θ-solvent for this copolymer. In addition, the exponent a in the Mark-Houwink-Sakorada equation is 0.50 in 1.2N NaCl. Therefore, on the basis of light scattering and viscosity measurements, molecular dimensions in 1.2N NaCl were used as "unperturbed dimensions" in aqueous media. In organic media, A_2 values are nearly zero and a is 0.50 for methyl-butyrate (MeBu) at 40°C which is therefore designated as the theta solvent. It was found that unperturbed radii

of gyration for the copolymer in MeBu are 1.3 to 1.4 times greater than the unperturbed radii of gyration observed in 1.2N NaCl solution. Thus the unperturbed dimension of a polymer can differ considerably, depending on the polarity of both the polymer and the solvent. Figure 4.3 (15) shows sketches of the structures of a typical polyelectrolyte and an atypical polyelectrolyte in solutions. In the case of a typical polyelectrolyte without hydrophobic groups in the chain (e.g., PAA), its unperturbed dimension in the ionized form in an aqueous salt θ-solvent can be greater than that in the unionized form in an organic θ-solvent. This expansion is attributed to the residual electrostatic repulsive force between the charged groups. In the case of an atypical polyelectrolyte containing some hydrophobic groups on the side chains, its unperturbed dimension in the ionized form in an aqueous salt θ-solvent is expected to be smaller than that in the unionized form in an organic θ-solvent. This contraction is attributed to the strong hydrophobic attraction within the coil which surpasses the relatively weak residual repulsive force between the charged groups.

The existence of a conformational transition was also investigated by potentiometric titration and dye binding. In the potentiometric study (16), the copolymer was dissolved in a mixed solvent, isoproponal-H_2O (4:1) and a conformational change was induced by the addition of NaOH. This was observed by the shape of the plots of experimental values of pKa against α. For polyelectrolytes which do not undergo conformational transitions during ionization pKa is a monotonic increasing function of α. For polyelectrolytes which are believed to undergo configurational transitions, the curve of such plots has a sharp rise

Figure 4.3

Conformations of polyelectrolytes in different solvents, from Tan (15).

i. Flexible coil in organic solvent.

ii. Rodlike state in H_2O.

iii. Flexible coil in aqueous NaCl solution.

The symbols on the coils are:

- o -COOH groups
- ● Hydrophobic groups
- ⊖ $-COO^-$ groups with strong electrostatic repulsion
- ⊖ $-COO^-$ groups almost shielded by counterions

	(i) nonionized (organic solvent)	(ii) ionized (water)	(iii) ionized (aq. NaCl)
a) Typical polyelectrolyte			
b) Atypical polyelectrolyte	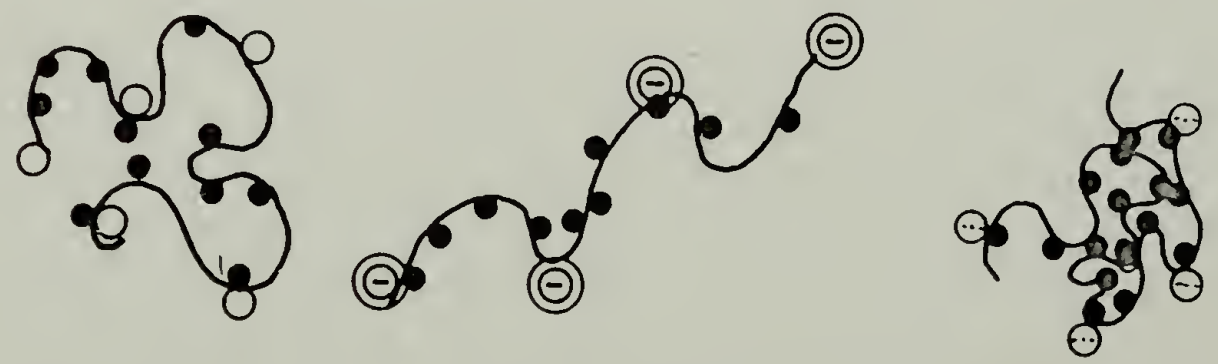		

at low α followed by a maximum, or plateau region, and rises again at high α. A transition region was observed over the range of degree of ionization from 0.2 to 0.6. In addition, the titration behavior of three copolymers of the same chain length but different acid contents was compared. The data suggest that the start of the transition region occurs at a lower degree of ionization for chains with higher acid content. However, the fraction of charge per residue at the onset of the transition is about 0.10 for the three copolymers studied.

In the dye binding study (17), 2-p-toluidinyl naphthalene-6-sulfonate (TNS) was used as a fluorescent probe for the copolymer. The emission of this probe is completely quenched in water or aqueous sodium chloride medium, but gives a very intense emission band peaking at 440 nm in alcohols, other organic solvents or when it is bound to hydrophobic sites of proteins, when excited by ultraviolet radiation. Thus the probe would be responsive to the amount of hydrophobic region available to it within the copolymer coil when the solvent is changed from low C_s to high C_s. The study indicated that the hydrophobic character of the copolymers becomes increasingly more pronounced as the ionic strength is increased. This is demonstrated in Figure 4.4. The zero intensity at $C_s = 0$ is due to the masking of the interaction between TNS and the copolymer, if present, by the strong repulsion between the similarly charged sulfonate groups on the dye molecule and the carboxylic sites on the copolymer. The interaction increases with an increase in C_s due to the shielding effect of the counterions around the polyion. However, instead of a leveling off of intensity once the polymer sites are completely shielded by the counterions (at C_s = 0.2-

Figure 4.4

Relative fluorescence intensity of TNS in aqueous solutions of Na-copoly (ethyl acrylate-acrylic acid) and NaCl versus log C_s, from Tan (17).

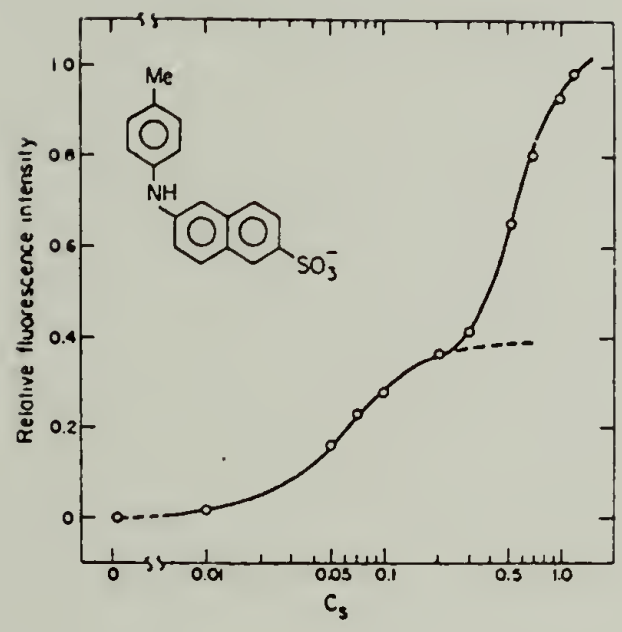
Me
NH
SO_3^-
Relative fluorescence intensity
1.0
0.8
0.6
0.4
0.2
0
0
0.01
0.05
0.1
0.5
1.0
C_s

0.3), a rapid increase in intensity beyond this region was observed, which has to be accounted for by additional modes of dye binding. The model of a conformational transition region from an extended coil to a compact coil could explain the results. In addition, after the transition occurs, the strength of hydrophobic clustering increases rapidly with C_s and hence interaction between the dye and hydrophobic parts of the copolymer is increased.

Although two types of conformations are proposed for this hydrophobic copolymer, it is believed that both the swollen-coil and the compact-coil structures are random coils. With decreasing ionic strength below the transition, the molecule keeps expanding and does not reach the rodlike state even in extremely low C_s media, presumably because this copolymer lacks a high charge density along the chain.

REFERENCES

1. T.N. Nekrasova, O.B. Ptitsyn, and M.S. Shikanova, Vysokomol. Soedin., A10, 1530 (1963).

2. T.N. Nekrasova and E. Churylo, Vysokomol. Soedin., A11, 1103 (1969).

3. Z. Priel and A. Silberberg, J. Polym. Sci., Part A-2, 8, 689 (1970).

4. T.M. Birshtein, Ye.V. Anufriyeva, T.N. Nekrasova, O.B. Ptitsyn, and T.V. Sheveleva, Vysokomol. Soedin., 7, 372 (1965).

5. E.V. Frisman, M.A. Sibileva, Nhuen Tkhi, Kim Ngan, and T.N. Nekrasova, Vysokomol. Soedin., A10, 1834 (1968).

6. S.S. Urazovskii and I.T. Slyusarov, Vysokomol. Soedin., 3, 420 (1961).

7. M. Mandel and M.G. Stadhouder, Makromol. Chem., 80, 141 (1964).

8. T.N. Nekrasova, Ye.V. Anufriyeva, A.M. Yel'yashevich, and O.B. Ptitsyn, Vysokomol. Soedin., 7, 913 (1965).

9. A.M. Liquori, G. Barone, V. Crescenzi, F. Quadrifoglio, and V. Vitagliano, J. Macromol. Chem., 1, 291 (1966).

10. M. Mandel, J.C. Leyte and M.G. Stadhouder, J. Phys. Chem., 71, 603 (1967).

11. T.N. Nekrasova, A.G. Gabrielyan, and O.B. Ptitsyn, Vysokomol. Soedin., A10, 290 (1963).

12. G. Barone, V. Crescenzi, B. Pispisa, and F. Quadrifoglio, J. Phys. Chem., 1, 761 (1966).

13. G. Barone, V. Crescenzi, A.M. Liquori, and F. Quadrifoglio, J. Phys. Chem., 71, 2341 (1967).

14. A.I. Grigorev, L.A. Volkova, and O.B. Ptitsyn, Vysokomol. Soedin., B11, 232 (1969).

15. J.S. Tan and S.P. Gasper, J. Polym. Sci., Polym. Phys. Ed., 12, 1785 (1974).

16. J.S. Tan and S.P. Gasper, Macromolecules, 6, 741 (1973).

17. J.S. Tan and R.L. Schneider, J. Phys. Chem., 79, 1380 (1975).

18. A. Tokahashi, T. Kato and M. Nagasawa, J. Phys. Chem., 71, 2001 (1967).

19. A. Takahashi and M. Nagasawa, J. Amer. Chem. Soc., 86, 543 (1964).

CHAPTER V

EXPERIMENTAL METHODS

Apparatus

A schematic diagram of the apparatus for the intensity fluctuation spectroscopy experiments used for the diffusion constant measurements is shown in Figure 5.1 (1,2,3). The light source is a Spectra-Physics model 125 helium-neon laser of wavelength 6328 Å whose electric field vector is polarized perpendicular to the scattering plane. The power output is approximately 50 mw, and was always operated at peak power, since as can be seen from Equation (2.27), the rate at which the correlation function accumulates is proportional to $\langle I \rangle^2$.

The laser beam is focused into the sample cell by a 10 cm. focal length lens. The sample cell is housed in a cylindrical copper block containing a square hole which is parallel to the cylinder axis and which is slightly larger than the diameter of the cell (~1 cm.) aiding in its positioning. There is also a slot perpendicular to the axis which allows the incident light to enter the cell and be scattered back out. The copper block has soldered to it a coil of copper tubing which is attached to a constant temperature bath. The scattered light passes through to the scattering arm which contains an adjustable aperture, in back of which is a lens of focal length 8 cm. which focuses an image of the scattering volume on a pinhole of variable size. In back of the

Figure 5.1

Block diagram of the light scattering apparatus, taken from Olson (3).

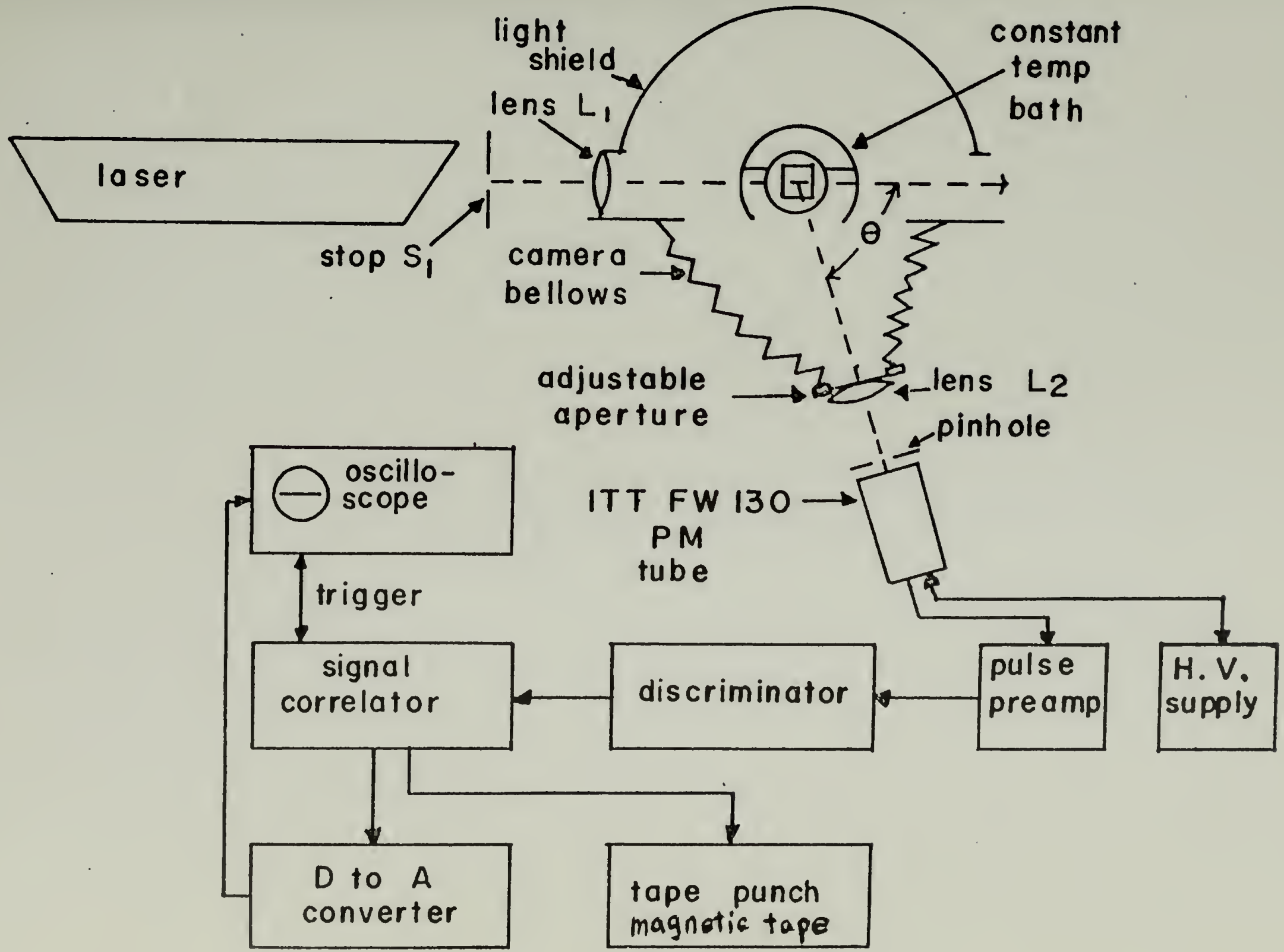
light shield
lens L_1
constant temp bath
laser
stop S_1
camera bellows
θ
adjustable aperture
lens L2
pinhole
oscillo-scope
ITT FW 130 PM tube
trigger
signal correlator
discriminator
pulse preamp
H. V. supply
D to A converter
tape punch magnetic tape

pinhole is a mirror which can be rotated to send the image of the scattering volume either to the photomultiplier or up into a microscope lens which makes possible the direct observation of the illuminated scattering volume. The whole scattering arm is rotatable so that the scattered light can be viewed as a function of the angle θ. In the present experiments, the scattered light was observed at $\theta = 90°$.

Equation (2.11) gives an expression for the scattered electric field at a single point in the far field but real detectors have finite area. The scattered field is coherent on an area called the "coherence area," which is the first bright spot of the diffraction pattern of the scattering volume. When the source and detector have a finite size the intensity correlation function, Equation (3.25) is modified to (4)

$$g^{(2)}(\tau) = 1 + f(A)|g^{(1)}(\tau)|^2. \tag{5.1}$$

The term f(A) is a function of the number of coherence areas accepted by the detector which in turn depends on the pinhole and aperture sizes. Values of f(A) as a function of the number of coherence areas are calculated by a theory of Jakeman (5) and listed in Table 5.1 for the apparatus used here.

The signal-to-noise ratio is the determinant factor in the accuracy of the decay rate $\Gamma(\tau)$ and is defined as (6,7)

$$\frac{\text{signal}}{\text{noise}} = \frac{G(\infty)e^{-\Gamma(0)}}{[G(\infty)(1 + e^{-2\Gamma(0)})]^{1/2}}. \tag{5.2}$$

Discussions of ways to optimize it can be found in several review arti-

TABLE 5.1

Values of f(A) Calculated as a Function of Aperture and Pinhole Size

Aperture Diameter (mm)	Pinhole Diameter (μm)			
	45	100	200	250
.5	.004	.02	.08	.12
1	.016	.08	.32	.50
2	.064	.32	1.3	2.0
3	.146	.72	2.9	4.5
5	.405	2.0	8.0	12.5

cles (4,7-10).

The choice of pinhole size and aperture size affect the signal-to-noise ratio. In Table 5.1, the values to the right of the vertical dashed line give unacceptable signal-to-noise ratios. In the present experiments, the largest pinhole was used and the smallest aperture chosen which provided an acceptable photon count rate.

As indicated earlier, the scattered light could be viewed through a microscope. When a sample was ready for study, it was typically viewed first this way. This allowed for observation of the cleanliness of the sample. The cuvette was positioned with its sides parallel to the incoming laser, to avoid scattering of stray light from the cell walls. This problem was increased when the cells were scratched, so they had to be positioned to minimize this effect. The diffuse stray light showed up as a halo surrounding the image of the laser beam passing through the cell. It was decreased substantially by placing a piece of black cloth on the back face of the cuvette (relative to the observed light). These precautions are essential, because as shown by Ford (7), an error in the time constant due to stray light (that is, coherent stray light), scattered either from the walls or from dust or bubbles is given by approximately

$$\frac{\Delta\Gamma}{\Gamma} = -\frac{16}{9}\frac{N_{coh}}{N_s} \qquad (5.3)$$

where N_s are the number of photons due to the signal and N_{coh} are the number of photons due to the stray light. Thus only 1% of stray light can produce an error of 2% in the decay constant.

The photomultiplier used as a detector was an ITT FW 130, which has a very low dark current (1). It has a small photocathode of about 2.54 mm. The pulses from the photomultiplier tube were amplified and then fed into a discriminator which produced uniform output logic pulses for input pulses of sufficient magnitude.

The apparatus needed to measure the correlation function of the photodetections, or the digital autocorrelation function, is a correlation function computer. The correlator used for the present experiments is a real time autocorrelator which was designed and built in this laboratory (12). It counts the number of photons detected, N_i, during each time interval, ΔT, and calculates the sum

$$G^{(2)}(\tau) = G^{(2)}(j\Delta T) = \langle n(t)n(t+\tau)\rangle = \sum_{i=1}^{T/\Delta T} n_i n_{i+j} \qquad (5.4)$$

where T is the total duration of the experiment and $j = \tau/\Delta T$.

In order to simplify Equation (5.4) it is necessary to find $G^{(2)}(\tau)$ when $\tau \to \infty$. In this case n_i and n_{i+j} are uncorrelated and can be replaced by their average values. Therefore $\bar{n}_i = \bar{n}_{i+j} = (NT)/(T\Delta T) = N\Delta T$, where N is the average number of photons detected each second. Thus

$$G^{(2)}(\infty) = (N\Delta T)^2 T/\Delta T = N^2 T\Delta T \qquad (5.5)$$

which combined with Equation (2.27) yields

$$G^{(2)}(\tau) = N^2 T\Delta T (1 + e^{-\Gamma\tau}). \qquad (5.6)$$

The clock in the correlator is provided by a crystal oscillator with a fundamental frequency of 10 MHz, which is subdivided by a series of flip-flops to give ΔT a range from a 0.1 second to 0.05×10^{-6} second (old correlator) or 0.01×10^{-6} second (new correlator), where the two correlators will be described later.

The output of the correlator was fed into a digital to analog converter and displayed on an oscilloscope screen. It was thus possible to observe the evolution of the signal and the cleanliness of the sample being studied. The latter could be monitored for dirt, which manifested itself by erratic jumping of the signal.

Once the correlation function was obtained it was read out onto magnetic tape where it could be stored and/or fed into the university computer where it was analyzed.

Two correlators were used for the present experiments. The older one had 58 total channels with 21 active. The active channels were distributed such that the first 10 channels would obtain $G(\tau)$ at intervals of $1\Delta T$, the next six at values of $2\Delta T$ and the last 5 at intervals of $5\Delta T$. The newer correlator had 64 active data channels with two possibilities of their distribution. When a toggle switch was set to "no delay," $G(\tau)$ was obtained at intervals of $1\Delta T$. When the switch was in the position "delay" the first 56 were spaced at intervals of $1\Delta T$, the last 8 were delayed by $64\Delta T$ and then spaced at intervals of $1\Delta T$ again.

The spacing of the active data channels has to take into consideration both the need for accurate determination of the baseline and the importance of the first channels in an exponential signal. Both

correlators space the first channels equally, although the newer one has more channels. The delayed channels on the new correlator are a real advantage in baseline determination, without loss in accuracy of the first channels.

Inaccurate baseline determination will lead to erroneous time constants in a single exponential fit or extra time constants in the analysis of multiple exponentials. For the present experiments, two methods of determining the baseline were used. In one method the full correlation function was fit to the sum of a constant and exponential function using a least squares fitting procedure. The new correlator was better suited for this procedure since the last eight delayed channels could be chosen to be at their baseline value. In principle, the baseline could have been obtained from these last eight channels. However, for the samples studied, the computer fit using this three parameter fitting procedure predicted for the baseline the same values as were experimentally obtained for the last eight channels. However, it should be noted that in a situation where a long and short time constant are present simultaneously, this method would not work as well. It is also very inaccurate at short sample times when there is multiple exponential behavior.

The baseline can also be determined from Equation (5.5), which is derived, however, for an ideal correlator. It can be calculated from the square of the total number of photons detected during the experiment divided by the total number of sample times $T/\Delta T$. Equation (5.5) is true only if the laser intensity and detector sensitivity are constant during the course of the experiment, and no large dust particles have

scattered light into the detector. It is useful when measurements are performed at short sample times. At long sample times, when the last eight channels are at their baseline value, the experimental value of $G^{(2)}(\infty)$ calculated by the above procedure and that determined by a 3 parameter fit agreed to within experimental error.

Sample Characterization

Polymerization and preparation. The polymer used in the present study, sodium copoly (ethyl acrylate-acrylic acid), is a random copolymer of ethyl acrylate and acrylic acid in a mole ratio of 3 to 1. It thus contains both hydrophobic and hydrophilic groups and can exist in ionic or nonionic forms depending on the solvent.

The samples were prepared at Eastman Kodak (1) by solution polymerization of 30 g. of ethyl acrylate and 20 g. of acrylic acid dissolved in 500 ml. of acetone, with 0.25 g. of 2,2-azo-bis-(2-methyl-propionitriol) added as catalyst. The mixture was heated overnight in order to reach 85% completion. The copolymer was then precipitated in water and dried under vacuum at room temperature. Fractions of the copolymer were obtained by a scheme of repeated precipitation fractionations using dioxane as the solvent and hexane as the precipitant. Stepwise addition of the precipitant to an initial polymer-dioxane solution (10%) up to turbidity was followed by heating of the mixture to 35°C to re-dissolve the precipitate. Subsequent slow cooling to 20°C was carried out to precipitate each fraction. Ten fractions were collected with a polymer recovery of 99%. Solvents were evaporated and the polymer fractions were recovered by freeze-drying overnight. Each fraction

was analyzed for acrylic acid content by titration. The percentage of acrylic acid content for all the fractions were found to be constant at 20% by weight.

A copolymer of this composition was not readily soluble in water but was put into solution by being dissolved first in methanol, either as 1% or 2% weight percent solutions. The methanol solutions were then neutralized with dilute sodium hydroxide and diluted with water. Methanol was removed by evaporation under vacuum at 35°C to give aqueous stock solutions of 2.0% polymer concentration of pH 7.0. All subsequent measurements in aqueous media were made with these stock solutions, maintaining pH 7.0 ± 0.1, since previous titrations had shown that ionization of the polymer was essentially complete under these conditions.

The copolymer could be dissolved directly in the organic solvent, 2-heptanone, although the highest molecular weight fraction did not dissolve completely.

Polydispersity index. The determination of the polydispersity of the fractions was carried out by gel permeation chromatography (GPC), also at Eastman Kodak. Since GPC of polymers containing polar groups such as carboxylic acid has been unsuccessful, the free acid groups of this copolymer were converted to the methyl ester by chemical reaction with diazomethane. The GPC traces of the methylated fractions were then obtained using a Waters Associate M-100 chromatograph. Tetrahydrofuran was used as the solvent at a flow rate of 1.0 ml/min. A series of Styrogel columns of 10^6, 10^5, 10^4, and 10^3 Å nominal porosities were

used to determine the molecular weight distribution. The ratios of polystyrene weight average to number average equivalent weights corrected for instrumental spreading were used to determine the polydispersity of each fraction.

The samples whose diffusion coefficients were measured were not from the same batch used in the previous publications of Tan. For the latter, the polydispersity index, M_w/M_n of the original polymer was 3.5 and the value for the fractions was 1.5 ± 0.1. Unfortunately, the polydispersity index of the fractions for the present study ranged from 1.50 to 2.27, as presented in Table 5.2.

Intrinsic viscosities and viscosity average molecular weights. Intrinsic viscosities of the original fractions were determined by Tan (1) using Ubbelohde capillary viscometers. It was determined that kinetic energy corrections were not significant enough to affect the linear dependence of viscosity on flow time. Intrinsic viscosities of aqueous solutions at ionic strengths of .05N and .07N NaCl were carried out with dialyzed samples, whereas with solutions of higher ionic strength dialyzed and undialyzed samples yielded essentially the same intrinsic viscosity. Thus dilutions could be made with NaCl solutions of molarities identical with the total ionic strength. All measurements were made at 25.0° ± 0.1. The results of these viscosity studies are found in Table 5.3, which lists the parameters in the Mark-Houwink-Sukurada relation, $[\eta] = K_\eta M_w^a$. The weight average molecular weights used in the equation were determined from light scattering studies. This is standard procedure since the weight average and viscosity average molecular

TABLE 5.2

Molecular Weight x 10^{-5} and Polydispersity Index, M_w/M_n

Fraction PC-80	Light Scattering		[η] in THF		[η] in 0.1N NaCl		M_w/M_n
	M_w	M_D	M_ν	M_D	M_ν	M_D	
F8	1.85	2.13	2.09	2.58	2.1	2.61	2.27
FD	4.8	4.17	3.4	5.50	3.1	3.80	2.21
F9	---		2.95	3.62	4.2	5.08	
F4	5.6	6.08	---		5.8	6.53	1.50
F1	13.0	14.50	7.2	8.53	7.2	8.37	1.8

TABLE 5.3

The Mark-Houwink Constants K_η and a in $[\eta] = K_\eta M_w^{-a}$

For Na-copoly (ethyl acrylate-acrylic acid)

in Various Media

Solvent	$K_\eta \times 10^5$	a
THF	11.0	0.73
2-Heptanone	61.9	0.52
MeBu	75.0 ± 0.5	0.50
0.05N NaCl	0.90	0.92
0.07N NaCl	1.59	0.86
0.1N NaCl	3.06	0.79
0.3N NaCl	4.41	0.72
0.5N NaCl	4.76	0.69
0.7N NaCl	4.32	0.68
1.0N NaCl	11.8	0.59
1.2N NaCl	34.5 ± 0.5	0.50

weights are very close for reasonably monodisperse polymers. For the original fractions, whose polydispersity index was 1.5 ± 0.1, the two averages can differ by 10%.

Intrinsic viscosity measurements on the samples used in the present study were made using Ubbelohde capillary viscometers chosen to ensure solvent flow times of at least 100 seconds. The usual precautions were taken in cleaning the viscometers. The purpose of the measurements was to determine the molecular weights of the fractions, in particular that of the highest molecular weight, since previous light scattering and viscosity measurements done at Eastman Kodak had been in disagreement as discussed later. The highest molecular weight fraction was very difficult to dissolve in tetrahydrofuran (THF), a good solvent for which K_η and a had been determined; the sample remained as a gel after a period of one month. Therefore, the measurements were performed using 0.1N NaCl, a good solvent for which K_η and a had also been determined and for which dialysis was unnecessary. The initial polymer concentrations were approximately 0.5% and successive dilutions were made with 0.1N NaCl solutions to approximately 0.1% for each run. The temperature of the thermostatted bath was maintained at 25.00 ± .02. The solutions were filtered through Millipore filters of 0.65μ pore size. To avoid excessive bubbling of the solutions which was sometimes a problem, and to avoid particulate contamination which sometimes occurred when pipet bulbs were used to mix the successive dilutions, very slightly pressurized clean nitrogen gas was used to mix the solutions and push the liquid past the viscometer bulb. Flow times were taken for each run until three successive readings were within 0.2 seconds of

each other.

The concentrations of the solutions were determined by UV spectroscopy using the end absorption of the carbonyl group at 220 nm, with the slitwidth set at .35 nm at 300 nm. Aliquots were not evaporated to dryness as is conventionally done because the residue of salt which was constant for all the solutions decreased the relative accuracy of the lower concentration solutions. Since the amount of polymer available was small it was not possible to simply use larger aliquots. Instead, an approximately 1% stock solution of the unfractionated polymer, which was easier to obtain, was prepared in 0.1N NaCl, and three 10 ml aliquots were evaporated to dryness. After subtraction of the weight percent salt, the exact concentration was determined. Dilutions of the stock solution were used to obtain a UV calibration curve, which is shown in Figure 5.2. In addition, some of the dilutions were evaporated to dryness and the concentrations when compared to those predicted from the UV calibration curve agreed to within 10%.

Intrinsic viscosities were obtained by extrapolation of η_{sp}/c against c, and $\ln\eta_{rel}/c$ against c, to zero polymer concentration c in 0.1N NaCl, where η_{sp} and η_{rel} are the specific and relative viscosities, respectively; these extrapolations appear in Figures 5.3a-d. The intrinsic viscosities determined in this way were used in the relation $[\eta] = 3.06 \times 10^{-5} M^{-79}$ from Table 5.3 to obtain the viscosity average molecular weights, M_v.

Solvent viscosity. It was necessary to know the viscosities of the solvents for the diffusion studies, since the value of the viscosity is

Figure 5.2

UV Calibration Curve. Absorbance at 220 nm versus concentration of unfractionated Na-copoly (ethyl acrylate-acrylic acid).

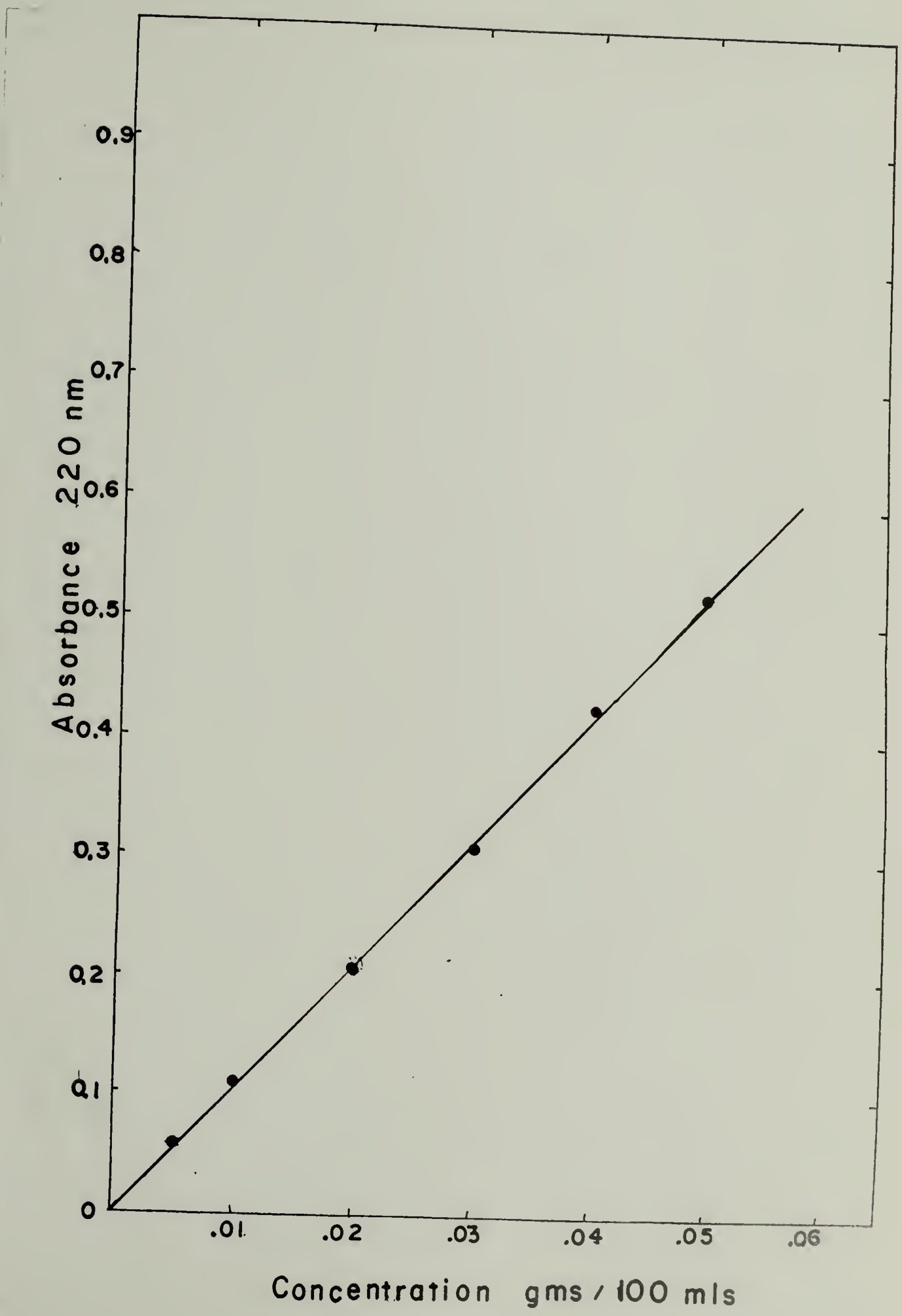
Absorbance 220 nm
0
0.1
0.2
0.3
0.4
0.5
0.6
0.7
0.8
0.9
.01
.02
.03
.04
.05
.06
Concentration gms / 100 mls

Figures 5.3a-d

Intrinsic viscosity plots of $\ln \eta_r / c$ or $(\eta_r - 1)/c$ versus concentration of Na-copoly (ethyl acrylate-acrylic acid) in 0.1N NaCl for four polymer fractions:

a. PC-80 F8 $M_D = 2.5 \times 10^5$

b. PC-80 FD $M_D = 4.0 \times 10^5$

c. PC-80 F9 $M_D = 6.0 \times 10^5$

d. PC-80 F1 $M_D = 8.4 \times 10^5$

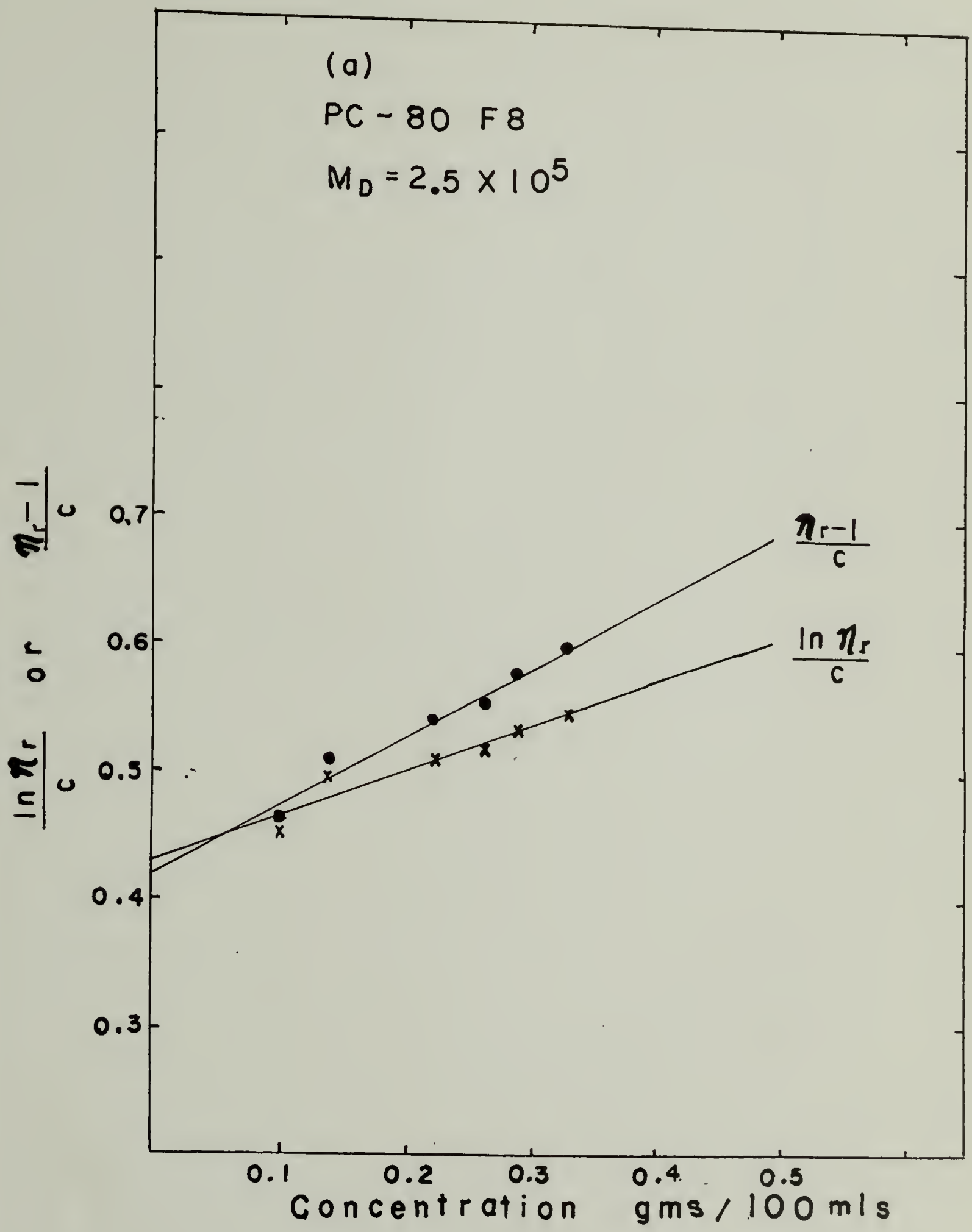
(a)
PC - 80 F8
$M_D = 2.5 \times 10^5$
$\frac{\eta_r - 1}{c}$ or $\frac{\ln \eta_r}{c}$
0.7
0.6
0.5
0.4
0.3
$\frac{\eta_r - 1}{c}$
$\frac{\ln \eta_r}{c}$
0.1
0.2
0.3
0.4
0.5
Concentration gms / 100 mls

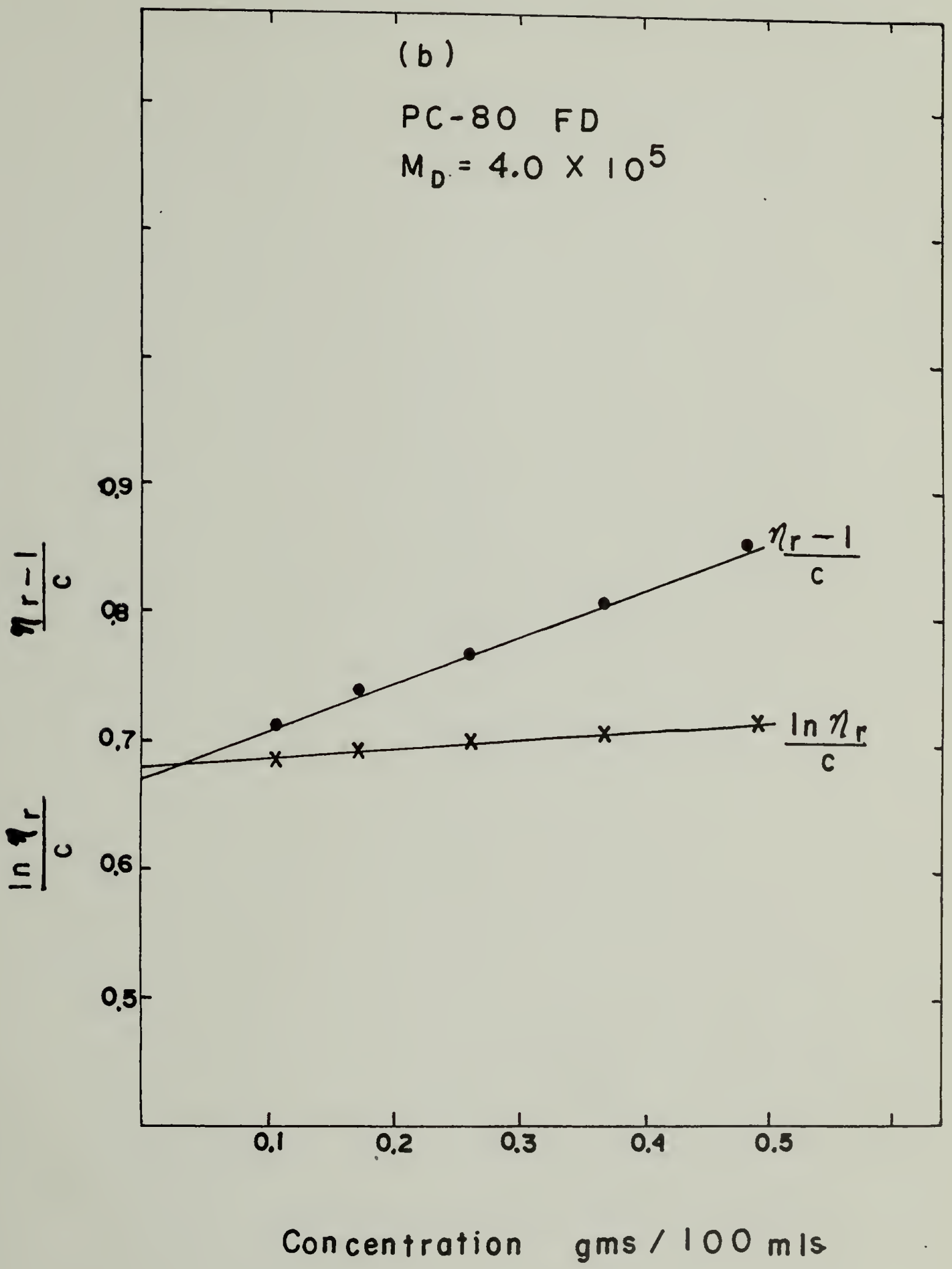
(b)
PC-80 FD
$M_D = 4.0 \times 10^5$
$\frac{\eta_r - 1}{c}$
$\frac{\ln \eta_r}{c}$
0.9
0.8
0.7
0.6
0.5
0.1
0.2
0.3
0.4
0.5
Concentration gms / 100 mls

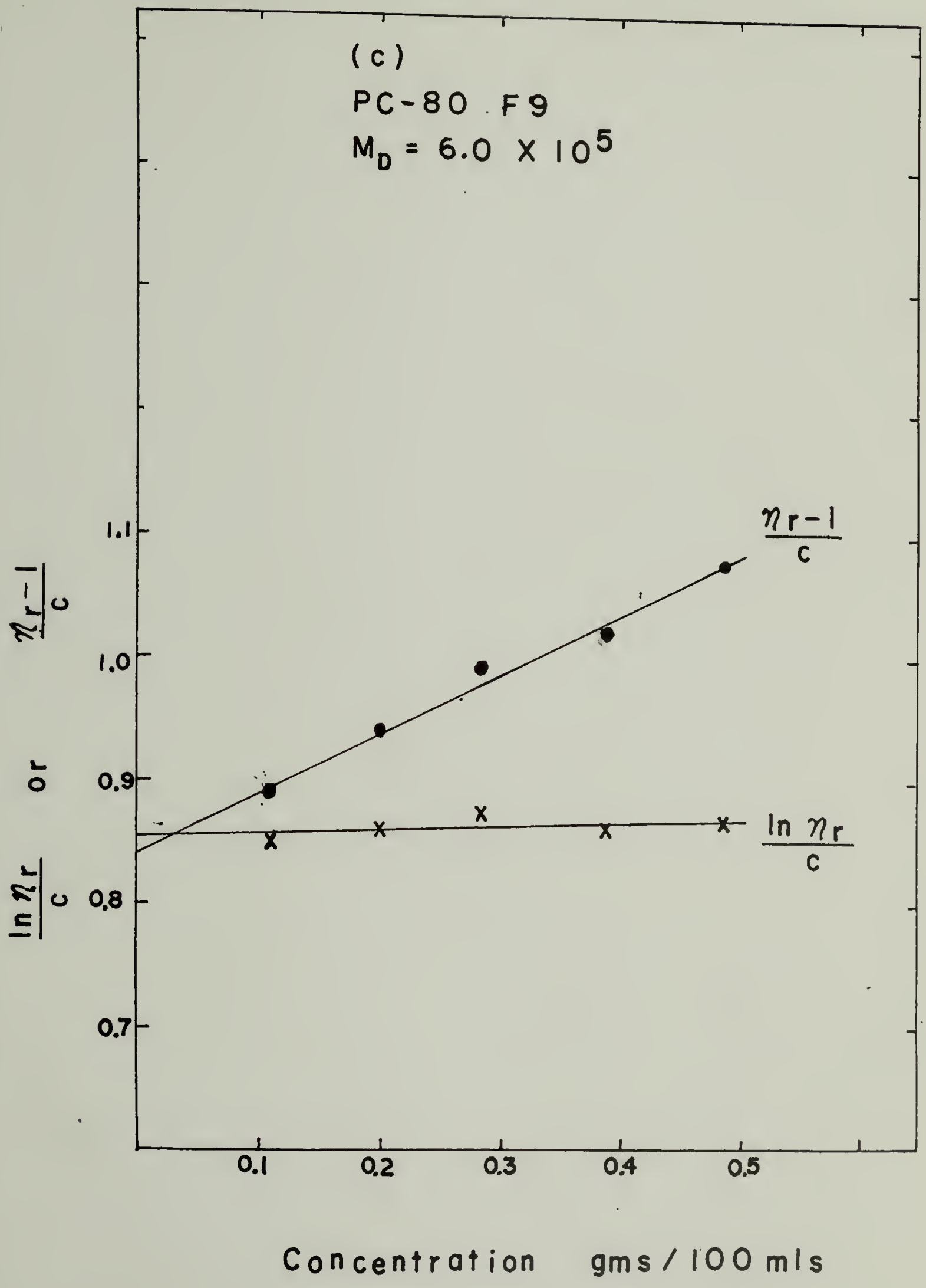
(c)
PC-80 . F9
$M_D = 6.0 \times 10^5$
$\frac{\eta r - 1}{c}$
1.1
1.0
0.9
0.8
0.7
or
$\frac{\ln \eta r}{c}$
$\frac{\eta r - 1}{c}$
$\frac{\ln \eta r}{c}$
0.1
0.2
0.3
0.4
0.5
Concentration gms / 100 mls

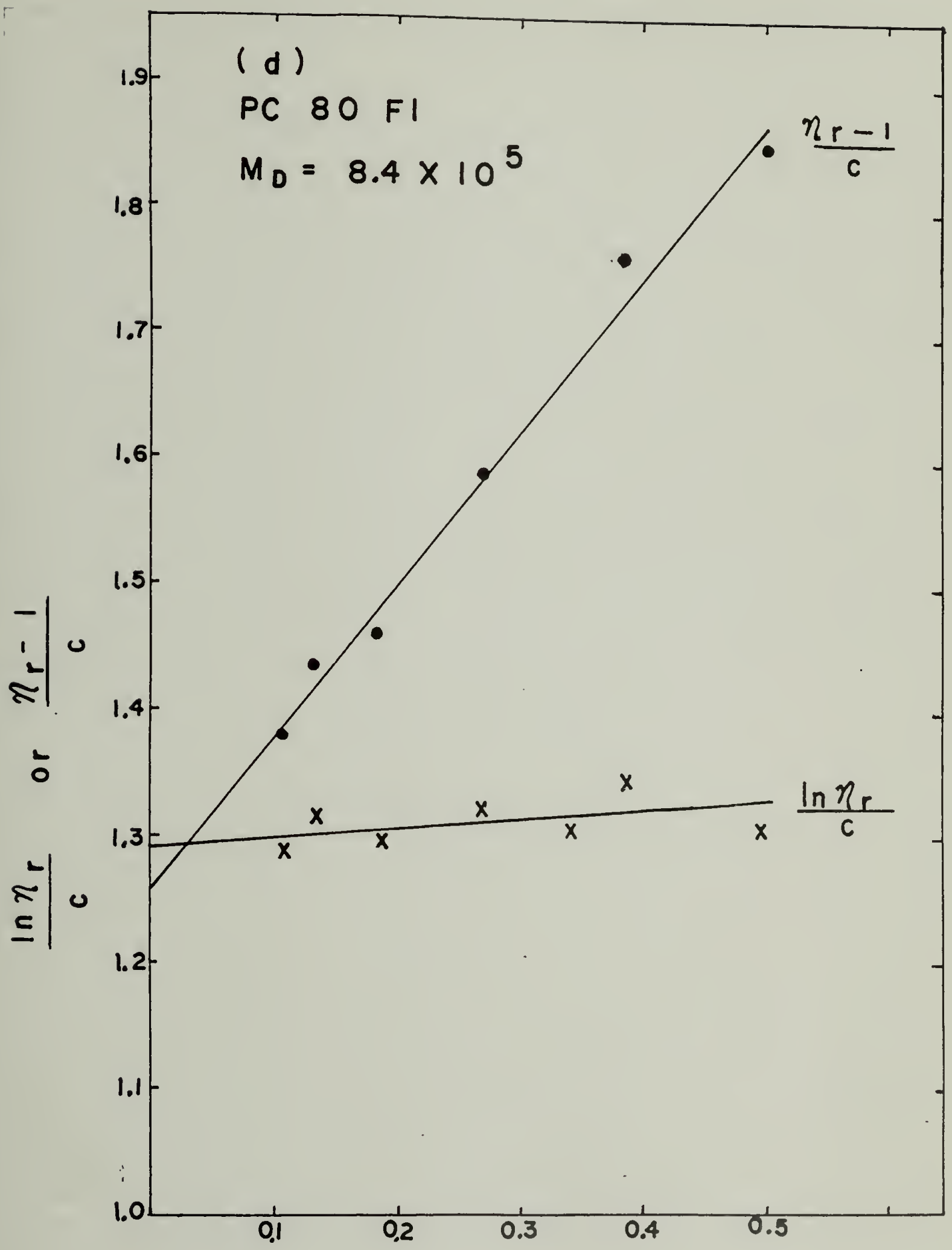
(d)
PC 80 F1
$M_D = 8.4 \times 10^5$
$\frac{\eta_r - 1}{c}$
$\frac{\ln \eta_r}{c}$
$\frac{\ln \eta_r}{c}$ or $\frac{\eta_r - 1}{c}$
1.9
1.8
1.7
1.6
1.5
1.4
1.3
1.2
1.1
1.0
0.1
0.2
0.3
0.4
0.5
Concentration gms / 100 mls

needed in the equation $D = kT/6\pi\eta_0 R_H$. Values of η_0 for water can be found in the Handbook of Chemistry and Physics, but those for 2-heptanone are not listed and must be measured. This was done at 20°C and 25°C by comparing the flow times of 2-heptanone with the flow times of water in Ubblehode capillary viscometers chosen to ensure flow times of at least 200 seconds. The equation

$$\frac{\eta_1}{\eta_2} = \frac{\rho_1 t_1}{\rho_2 t_2} \qquad (5.7)$$

was used where η is the viscosity, ρ is the density and t is the flow time, and the subscripts 1 and 2 refer to the unknown and the standard (here chosen to be water), respectively. The densities were obtained from the Handbook of Chemistry and Physics. The viscosity of water was taken to be 1.002 cp at 20°C and 0.89 cp at 25°C.

To check the accuracy of viscosity data obtained by this method, the viscosity of acetone, for which the value at 25°C is known to be 0.316 cp, was compared with the measured value of 0.318 cp. There was thus only a 0.6% error. The viscosity of 2-heptanone obtained this way was found to be 0.789 cp at 25°C and 0.849 cp at 20°C.

Molecular weight from light scattering. The weight average molecular weights were determined at Eastman Kodak with a SOFICA photometer using unpolarized light of 436 nm. The Zimm method of data treatment was used and the molecular weights used for the present study were determined from samples dissolved in methyl butyrate. The weight average molecular weights obtained this way, as well as the viscosity average molecular

weights are listed in Table 5.2.

Sample polydispersity. Since the samples were heterogeneous, some form for the molecular weight distribution had to be assumed. As discussed by Flory (2), a Schultz distribution is a good approximation for a molecular weight distribution for fractionated samples. With this assumption, the molecular weights obtained by light scattering and viscosity can be compared. Since the diffusion average molecular weight, M_D, defined by Equation (3.114) will be needed in later calculations, both M_w and M_v are normalized to the diffusion average here. This can be easily done using the polydispersity index M_w/M_n, the defining equations for the molecular weight averages and assuming a Schultz distribution. Thus

$$M_w = (h + 1)/\gamma \qquad M_n = h/\gamma \qquad M_w/M_n = (h + 1)/h \tag{5.8}$$

$$M_v = \frac{1}{\gamma}\left[\frac{\Gamma(h + a + 1)}{\Gamma(h + 1)}\right]^{1/a} \tag{5.9}$$

$$M_D = \frac{1}{\gamma}\left[\frac{\Gamma(h + 2)}{\Gamma(h + 2 - b)}\right]^{1/b} \tag{5.10}$$

The results are given in Table 5.2. The molecular weights used in later calculations are taken as weighted averages of the two closest values in the table, except for F4 where the value obtained from light scattering was used. This was done since F4 was a fraction from the original batch used for the publications of Tan, for which only M_w were reported.

Light scattering studies. Radii of gyration and second virial coeffi-

cients of the copolymer were determined by light scattering at Eastman Kodak (1). Since values of A_2, $\langle s^2 \rangle^{1/2}$ and the expansion factors are needed for later calculations, the results of the studies are given in Tables 5.4 and 5.5. The radii of gyration were determined from the slopes of linear plots of $(Kc/R_\theta)^{1/2}_{c=0}$ against $\sin^2 \frac{\theta}{2}$ and the second virial coefficients from slopes of linear plots of $(Kc/R_\theta)^{1/2}_{\theta=0}$ against concentration. Here K is the Rayleigh optical constant and R_θ is the excess scattering of polymer solute at the scattering angle θ, which was varied from 35° to 135°.

Diffusion Constant Measurements

Sample Preparation. Samples of Na-copoly (ethyl acrylate-acrylic acid) which were used for diffusion constant measurements are characterized in Table 5.2. The samples to be studied were prepared from the 1 or 2% aqueous stock solutions maintained at pH 7.0 ± 0.1 or from solid fractions directly dissolved in 2-heptanone. The ionic strength of the aqueous solutions was varied from 0.05N to 1.2N NaCl. The measurements were made over a range of concentrations which varied from approximately 0.5% to 0.05%, in order to be in the dilute solution region.

In order to fulfill the conditions for dilute solution, so that only terms linear in concentration need to be taken into account in the concentration dependence of the diffusion constant, the criterion of T.A. King et al. (3) was adopted. A maximum useful concentration, C_m, is defined such that the distance between the neighboring centers of mass of two polymers is at least twice the linear effective diameter of the polymer. Alternatively, the total volume occupied by the polymer

TABLE 5.4

a and δ Values in the Relationship, $A_2 = aM_w^{-\delta}$, for Copoly (ethyl acrylate-acrylic acid) in Various Media

Solvent	$a \times 10^2$ ($mol^2 cm^2/g^3$)	δ
THF	5.13	0.373
2-Heptanone	0.84	0.383
0.05 N NaCl	9.59	0.372
0.07 N NaCl	7.59	0.375
0.1 N NaCl	5.40	0.376
0.3 N NaCl	2.00	0.382
0.5 N NaCl	1.28	0.389
0.7 N NaCl	0.49	0.370
1.0 N NaCl	0.26	0.369
1.2 N NaCl	0.18	0.368

TABLE 5.5

K and ν Values in the Relationship, $\langle s^2 \rangle = KM_w^{\nu}$, for Na-copoly (ethyl acrylate-acrylic acid) in Various Media

Solvent	$K \times 10^{18}$ (cm^2/g mol)	ν
THF	20.4	1.00
2-Heptanone	13.2	0.981
0.05 N NaCl	3.82	1.128
0.07 N NaCl	3.31	1.132
0.1 N NaCl	4.79	1.092
0.3 N NaCl	2.98	1.095
0.5 N NaCl	3.43	1.068
0.7 N NaCl	3.17	1.045
1.0 N NaCl	3.03	1.035
1.2 N NaCl	3.62	1.014

molecules should not be greater than 10% of the volume of the solution. Thus the condition can be written as

$$\frac{N_A C_m V_H}{M} \leq 0.1 \tag{5.11}$$

where V_H is the hydrodynamic volume of the solute, equal to $\frac{4}{3}\pi R_H^3$. Combining Equations (3.56a) and (3.56b) and using $R_H = P\langle s^2\rangle^{1/2}/6^{1/2}\pi$ leads to

$$\frac{N_A V_H}{M} = \frac{N_A (P^3/\Phi)[\eta]}{162\pi^2} . \tag{5.12}$$

If the dependence of P and Φ on excluded volume is neglected, then with their unperturbed values of $P_0 = 5.1$ and $\Phi_0 = 2.5 \times 10^{23}$,

$$\frac{N_A V_H}{M} = 0.2[\eta] , \tag{5.13}$$

and the limiting concentration becomes

$$0.2[\eta]C_m \leq .1$$

$$C_m \leq .5[\eta]^{-1} . \tag{5.14}$$

In addition, $[\eta] = K_\eta M^a$ so that

$$C_m \leq .5K_\eta^{-1} M^{-a} .$$

Using the values of K_η and a listed in Table 5.3, the limiting concentrations, expressed as a weight percent, in the various ionic strength

solutions for the fractions of Na-copoly (ethyl acrylate-acrylic acid) are given in Table 5.6, and provide a useful guide to the concentrations to be used in investigating Equation (5.11).

The aqueous solutions consisted of three components: water, polymer and supporting electrolyte. It has been shown (4,5) that light-scattering measurements on such a system can be interpreted as if made on a two-component system if constant chemical potential of the low molecular weight salt is maintained in the solution. Tan (1) measured scattering intensities at various angles for an undialyzed polymer solution against 0.1N NaCl and for the sample dialyzed for four days against 0.1N NaCl. Almost identical results were obtained in the plots of Kc/R_θ versus $\sin^2(\theta/2)$. Therefore, it can be assumed that dialysis has very little effect on light-scattering results for the range between 0.1N and 1.2N NaCl. Samples in this ionic strength range were prepared by making 0.5% polymer solutions of XN NaCl from the 1 or 2% stock solutions and successively diluting these with XN NaCl to 0.05%. In the ionic strength region below 0.1N NaCl, the contribution to ionic strength by the polyelectrolyte is more important, and hence, samples dialyzed against solvent for at least 2 days were used. However, it has been shown (4) that for practical purposes, if the polymer solution is equilibrated against a given electrolyte solution at one polymer concentration, dilution at constant activity of the supporting electrolyte may be achieved simply by diluting with the "outside" polymer-free equilibrium solution of the supporting electrolyte. Thus even for the low ionic strength solutions, only the 0.5% solutions were dialyzed and this was isoionically diluted to lower concentrations.

TABLE 5.6

Limiting Concentrations, C_m, for Na-copoly (ethyl acrylate-acrylic acid) in Various Media

Solvent	Fraction F8	F9	FD	F4	F1
1.2 N	3.5%	2.2%	2.6%	1.9%	1.7%
1.0 N	3.4%		2.4%	1.7%	1.5%
0.7 N	3.2%		2.1%	1.4%	1.2%
0.5 N	2.6%		1.7%	1.1%	1.0%
0.3 N	1.9%		1.2%	.80%	.70%
0.1 N	1.2%		.7%	.46%	.39%
0.07 N	1.0%		.6%	.35%	.29%
0.05 N	.84%		.5%	.28%	.23%

The organic solvent, 2-heptanone, was obtained as an Eastman reagent chemical. The solvent purity was determined by gas chromatography. Since the most likely contaminant was water or methanol, the 2-heptanone was stored over "drierite." A gas chromatograph of the solvent kept this way showed no traces of impurity, making fractional distillation of the solvent prior to use unnecessary. Weighed amounts of dried copolymer fractions were dissolved in the 2-heptanone to make 0.5% solutions. These were then successively diluted with 2-heptanone to 0.1%.

Sample cleaning.

Cleaning procedures, still. The preparation of clean samples, free of particulate contamination and air bubbles, is essential in photon correlation spectroscopy as in conventional Rayleigh scattering. To minimize the amount of dirt and bubbles, it was necessary to clean cuvettes and glassware with "super-water," described below, and to use filtration techniques to get the final samples into the cleaned cuvettes.

"Super-water," water of exceptionally high purity and cleanliness, was prepared in the all glass still shown in Figure 5.4 taken from Olson (6) and according to the design of Timashoff and Townend (7). The stainless steel container was itself filled with water which had been doubly distilled or deionized and distilled. The water in the container was pressurized with nitrogen gas which was filtered through a sintered glass filter, at about 2 psi. This was sufficient pressure to push the water through two Millipore filters which were in series. The first was

Figure 5.4

Diagram of the glass water still and filtration apparatus, taken from Olson (6).

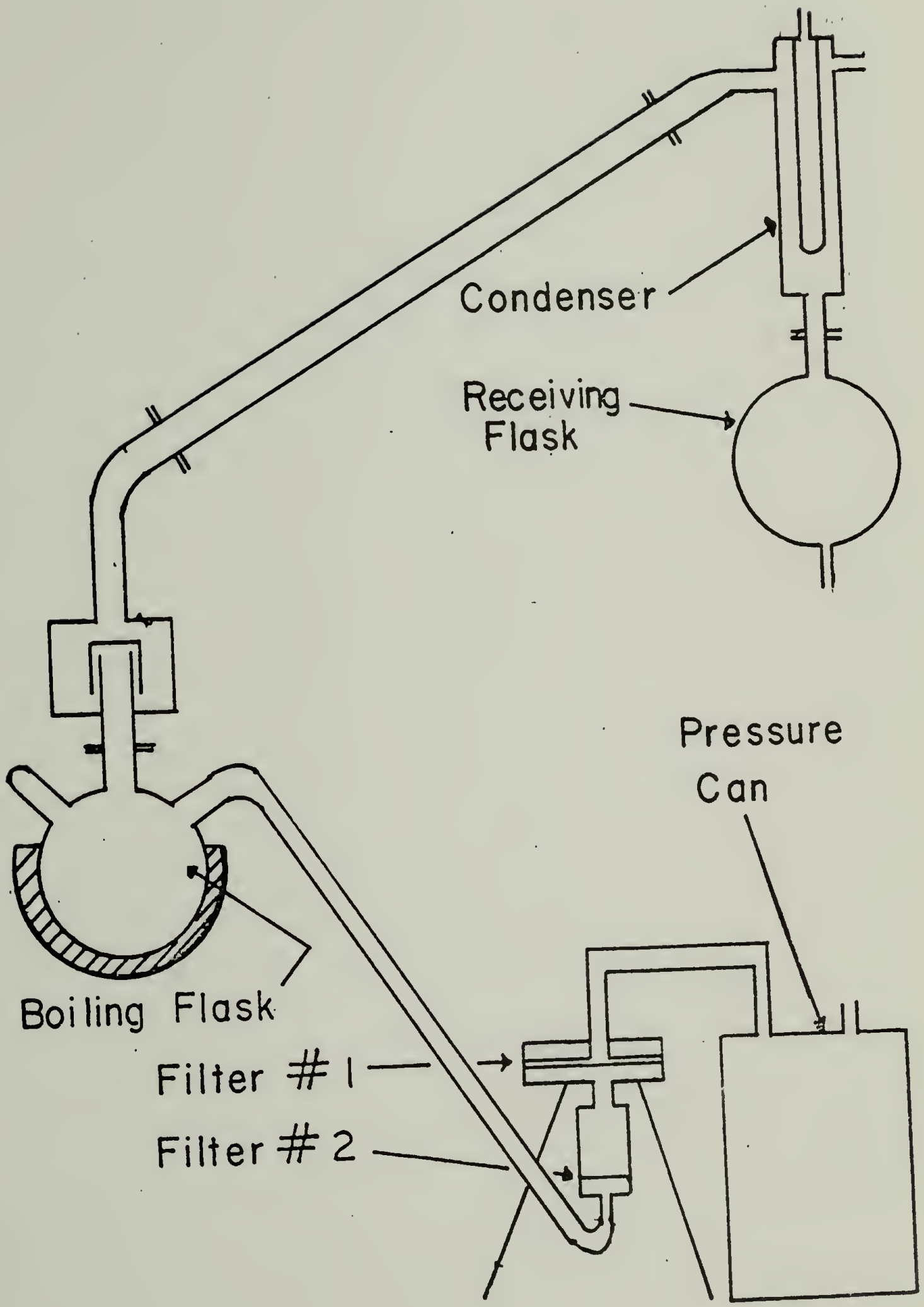
Condenser
Receiving Flask
Pressure Can
Boiling Flask
Filter #1
Filter #2

a 142mm filter with a pore size of 0.22μ which removed larger contaminants and the second was a 142mm filter with a pore size of 0.025μ to remove whatever passed through the first filter. With this arrangement, the larger pore size, less expensive filter becomes blocked sooner, having to be replaced approximately every three weeks, and provides a margin of safety in case the water from the stainless steel container was accidentally contaminated. The doubly filtered water was fed into a standard 3000 ml round bottom boiling flask with three openings. It was heated by an electric heating mantel and contained teflon boiling chips. One side opening served as the entrance for the doubly filtered water, the top opening allowed the exiting steam to pass to the condenser, and the other side opening was for overflow. This was necessary in case the water entered the flask at a faster rate than it would be boiled off. It was undesirable to have more than about 2000 ml of water in the boiling flask. If the water level reached the top of the flask, there was risk of contamination to the super-water in the receiving bulb.

The exiting steam passed through a spray trap and then up an uninsulated tube 20 inches long and approximately 2 inches in diameter, which prevented dirt from reaching the receiving side. The tube was attached to a Friedrichs condenser, which in turn was connected to the 3000 ml round bottomed receiving flask, containing the super-water. A small glass rod was attached to the condenser between the center section and the outerwall, permitting the condensed water to run down both the outer wall of the condenser and the sides of the receiving flask, rather than drip into it. This helped prevent the formation of microbubbles in

the super-water.

The receiving flask contains a small vent at the top to allow air to escape. The water is dispensed from the bottom of the flask which was modified to allow for a small tapered opening to which teflon tubing is attached.

The separate sections of the still are connected by rubber or teflon O-rings rather than ground glass joints. The abrasion of the latter can cause contamination by glass dust, which is very difficult to remove.

If accidentally contaminated, as for example, by running the still dry or microbial attack, the still can be taken apart, cleaned with glass cleaning solution, rinsed with distilled deionized water and reassembled. After about two days of continuous operation, super-water can be produced.

The super-water thus prepared is used to clean cuvettes, as the final rinse in cleaning glassware and for preparing the solvents and solutions to be used for diffusion measurements.

The glassware was typically cleaned by soaking overnight in glass cleaning solution. If organic material was suspected to be present, the glassware was first washed with Acctinox soap. After rinsing with tap water, the glassware was soaked for 24 hours in distilled deionized water. This was necessary to remove chromate ions from the glass cleaning solution, which adhere to glass surfaces. This step is probably not crucial in ordinary work, but is done here as a precaution to prevent contributions of the chromate ions to the ionic strength of the polyelectrolyte solutions. The glassware was then rinsed, perhaps

ten times with distilled deionized water and given a final rinse with super-water. Drying was accomplished in an oven or by leaving overnight to dry.

The cuvettes which were Hellma standard 1 cm. path length glass cells were treated similarly except that the rinsing stage was more extensive. A cuvette cleaner was used which speeded up the process and provided a slightly pressurized spray of water facilitating removal of dust. The cuvette had a capacity of about 3 mls., and perhaps 50 mls. of distilled deionized water and the same amount of super-water were used during the rinsing stage. Although the cuvettes were clean at this point, it was found that drying them, either naturally or in an oven, gave the most consistently good results. When wet, dirt entering from the top was more easily conducted to the sample solution by water along the sides of the cuvette. Cuvettes for use with organic solvents had to of course be dried to prevent contamination with water.

The actual filtration was done with a disposable or glass syringe attachable to a stainless steel filter holder. A needle tipped with teflon tubing was attached to the end of the filter holder. This made it possible to filter directly to the bottom of the cuvette so that dripping, causing the formation of microbubbles, would not occur. The teflon tubing was used to avoid scratching the cuvette glass. For aqueous solutions, Millipore filters were used. These had to be flushed several times with super-water to wash off residual surfactant. This process also served to clean the syringe needle and teflon tubing. It took approximately 50 mls. of super-water passed through the filter to get the water coming out of the teflon tubing perfectly clean. Filters

without surfactant were obtainable from Millipore and were sometimes used, but they were found to be weaker mechanically; that is, they were more prone to break or tear under pressure.

The cuvette was checked for cleanliness by filtering super-water into the cell with a 0.22μ Millipore filter through which 50 mls. of super-water had already been passed. The cuvette could then be observed in the laser beam and checked for contamination, which showed up as sparkles.

Sample filtration. The aqueous NaCl solutions were filtered through 0.22μ Millipore filters. The polymer-salt solutions were filtered through 0.65μ and then through 0.45μ and/or 0.22μ Millipore filters. The last filtration was done directly into a cleaned cuvette. Except through occasional carelessness, dirt was easily eliminated from the aqueous solutions. The more troublesome source of contamination was from microbubbles, which occurred because the polyelectrolyte itself was a surfactant. The problem became critical for the lowest ionic strength solutions. The lower the ionic strength, the more expanded the polymer coil and the more difficult it became to push the polyelectrolyte through the filter; this effect was of course a function of molecular weight. The large coil size necessitated the use of larger pore size filters for the final filtration. The samples could always be filtered through the 0.65μ Millipore filter. However, for the lowest ionic strengths, it was impossible to filter through the 0.22μ pore size and sometimes even impossible to filter through the 0.45μ pore size. After filtering the low ionic strength solutions through the 0.45μ or 0.65μ

filters, often nothing but a mass of sparkles could be observed under the laser beam. It should be remarked that the solutions after filtration were of the same concentration as before the filtering procedure. This was checked by measuring the UV absorption at 220 nm both before and after filtration and observing no change in the absorption within the experimental uncertainty of the reading.

The organic solvent 2-heptanone had to be filtered through fluoropore filters made of teflon. Ultrafine sintered glass filters could also be used but were cumbersome, especially upon final filtration into the small opening of the cuvette. 2-Heptanone dissolved Millipore filters instantaneously and swelled nucleopore filters. It was found undesirable to use disposable plastic syringes with organic solvents due to the possibility that additives or traces of monomer could be leached out. Therefore, glass syringes were used. If too much pressure was required to push the solution through the filter, the solution would instead rise up between the finite space between the glass plunger and the syringe. This made it necessary to replace the glass plunger with a rubber stopper with a hole bored through it, into which was pushed a piece of tight fitting stainless steel tubing. The stopper was then clamped to the glass syringe and the solution pushed through the filter by pressurized nitrogen gas.

REFERENCES

Apparatus

1. N.C. Ford, W. Lee, and F.E. Karasz, J. Chem. Phys., 9, 3098 (1969).
2. N.C. Ford, F.E. Karasz, and J.E. Owen, Disc. Faraday Soc., 49, 228 (1970).
3. T. Olson, "Laser Light Scattering Studies of Transfer Ribonucleic Acid," Thesis, UMass, Amherst (1974).
4. H.Z. Cummins and E.R. Pike, eds., "Photon Correlation and Light Beating Spectroscopy," Plenum, NY (1973).
5. Ibid., p. 117.
6. V. Degiorgio and J.B. Lutovka, Phys. Rev. A, 4, 2033 (1971).
7. N.C. Ford, Chemica Scripta, 2, 193 (1972).
8. B. Chu, Ann. Rev. Phys. Chem., 21, 145 (1970).
9. H.Z. Cummins and H.L. Swinney, in "Progress in Optics," ed. E. Wolf, 8, 133 (1970).
10. R. Pecora, Ann. Rev. Biophys. Bioeng., 1, 257 (1972).
11. R. Foord, R. Jones, C.J. Oliver, and E.R. Pike, Appl. Opt., 8, 1975 (1969).
12. R. Asch and N.C. Ford, Rev. Sci. Instrum., 44, 506 (1973).

Diffusion Constant Measurements

1. J.S. Tan and S.P. Gasper, J. Polym. Sci. Polym. Phys. Ed., 12, 1785 (1974).
2. P.J. Flory, "Principles of Polymer Chemistry," Cornell University Press, Ithaca (1953).
3. T.A. King, A. Knox, W.I. Lee and J.D.G. McAdam, Polymer, 14, 151 (1973).

4. E.F. Cassasa and H. Eisenberg, J. Phys. Chem., 64, 753 (1960); J. Phys. Chem., 65, 427 (1961); H. Eisenberg, J. Chem. Phys., 36, 1837 (1962).

5. H. Eisenberg and D. Woodside, J. Chem. Phys., 36, 1844 (1962).

6. T. Olson, "Laser Light Scattering Studies of Transfer Ribonucleic Acid," Thesis, UMass, Amherst (1974).

7. S.N. Timasheff and R. Townend, "The Physical Principles and Techniques of Protein Chemistry," Part B, Academic Press, New York, 147 (1970).

CHAPTER VI

RESULTS AND DISCUSSION

The raw data for the diffusion constant measurements of Na-copoly (ethyl acrylate-acrylic acid) as a function of concentration and ionic strength for the five molecular weight fractions studied are shown in Figures 6.1a-e. Figure 6.2 shows the concentration dependence of two fractions in 2-heptanone. As can be observed, the diffusion constant is a very strong function of concentration and changes slope for the molecular weight fractions at different values of ionic strength. In order to obtain the intercepts and slopes of these plots, it was sometimes found useful to linearize them by inverting the relationship $D = D_0(1 + 2MA_2c)/(1 + k^c c)$ to obtain

$$\frac{(1 + 2MA_2c)}{D} = \frac{1}{D_0}(1 + k_f^c c) \tag{6.1}$$

so that the intercept gave $1/D_0$ and the slope k_f/D_0. These plots are shown in Figures 6.3a-e.

In order to use this raw data, modifications had to be made to take into account the polydispersity of the samples. For polydisperse samples, the least square diffusion constant, D_{LS}, obtained by fitting the measured correlation function to a function of the form

$$G(\tau) = A + Be^{-c\tau} \tag{6.2}$$

Figures 6.1a-e

Plots of diffusion constants versus concentration of Na-copoly (ethyl acrylate-acrylic acid) for ionic strengths between 0.05N NaCl and 1.2N NaCl. Graphs a-e are for the five fractions:

a. PC-80 F8 $M_D = 2.5 \times 10^5$

b. PC-80 FD $M_D = 4.0 \times 10^5$

c. PC-80 F9 $M_D = 5.1 \times 10^5$

d. PC-80 F4 $M_D = 6.0 \times 10^5$

e. PC-80 F1 $M_D = 8.4 \times 10^5$

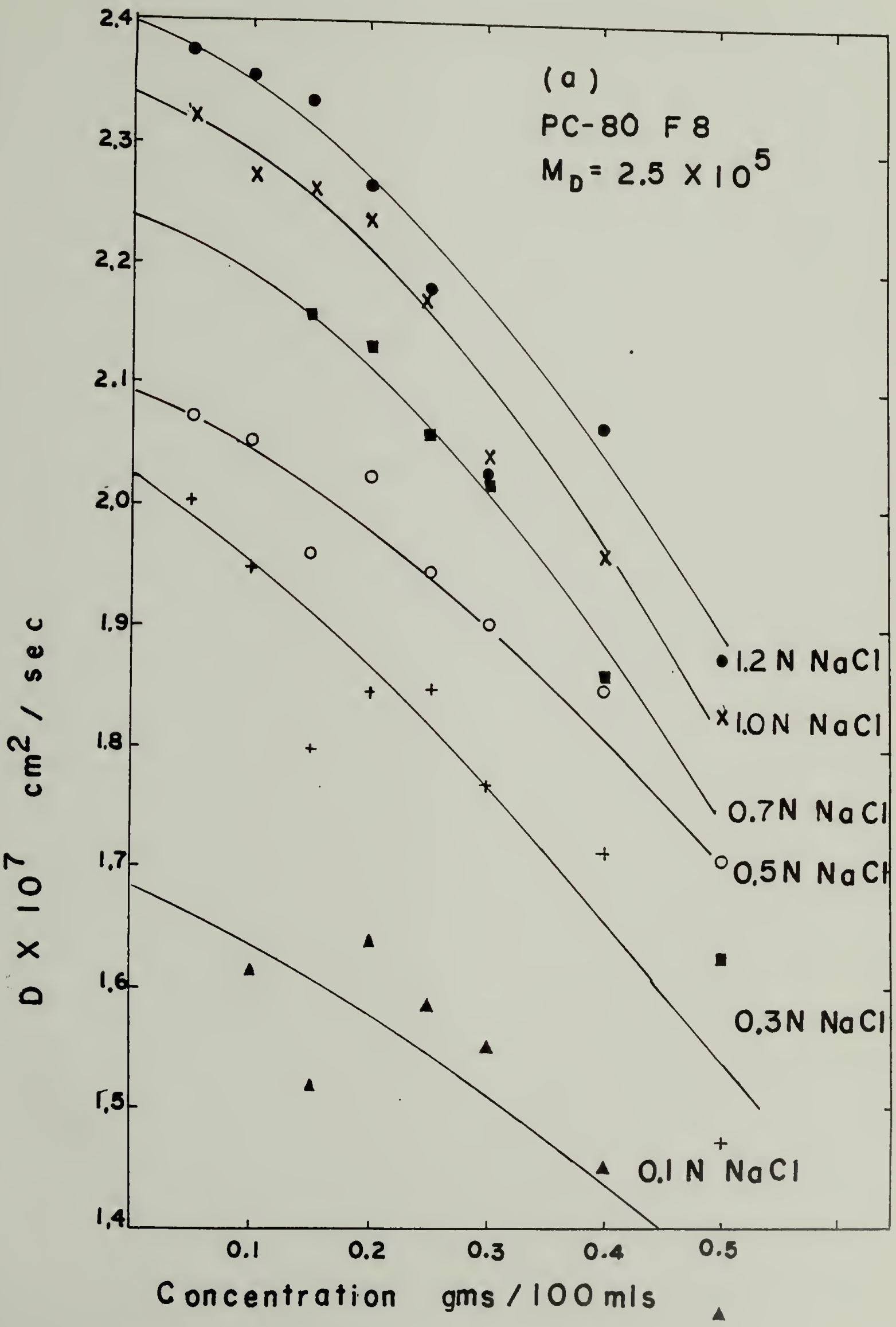
(a)
PC-80 F 8
$M_D = 2.5 \times 10^5$
1.2 N NaCl
1.0 N NaCl
0.7N NaCl
0.5N NaCl
0.3N NaCl
0.1 N NaCl
D X 10^7 cm^2 / sec
2.4
2.3
2.2
2.1
2.0
1.9
1.8
1.7
1.6
1.5
1.4
0.1
0.2
0.3
0.4
0.5
Concentration gms / 100 mls

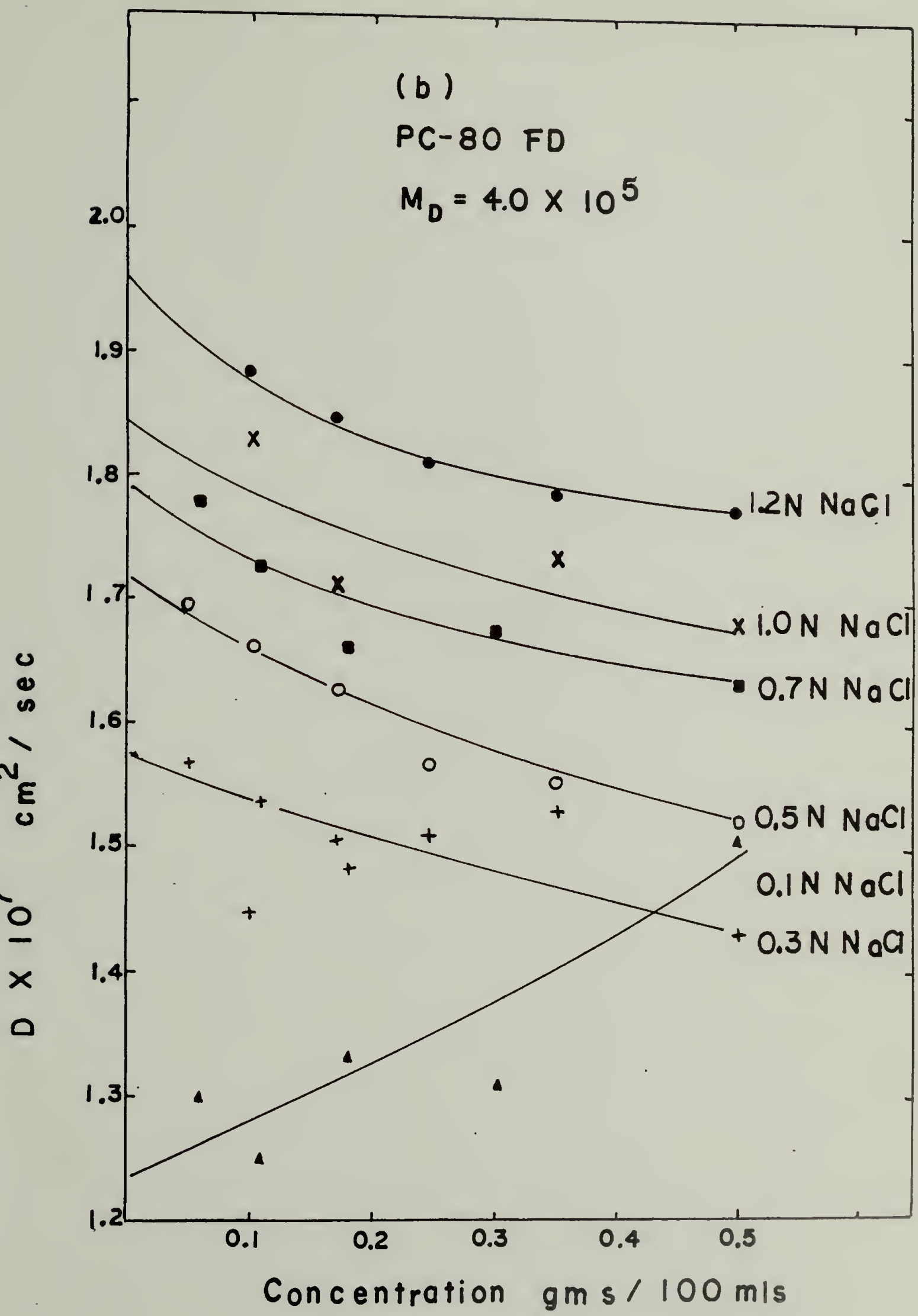
(b)
PC-80 FD
$M_D = 4.0 \times 10^5$
1.2N NaCl
1.0N NaCl
0.7N NaCl
0.5N NaCl
0.3N NaCl
0.1N NaCl
$D \times 10^7$ cm^2 / sec
2.0
1.9
1.8
1.7
1.6
1.5
1.4
1.3
1.2
0.1
0.2
0.3
0.4
0.5
Concentration gms / 100 mls

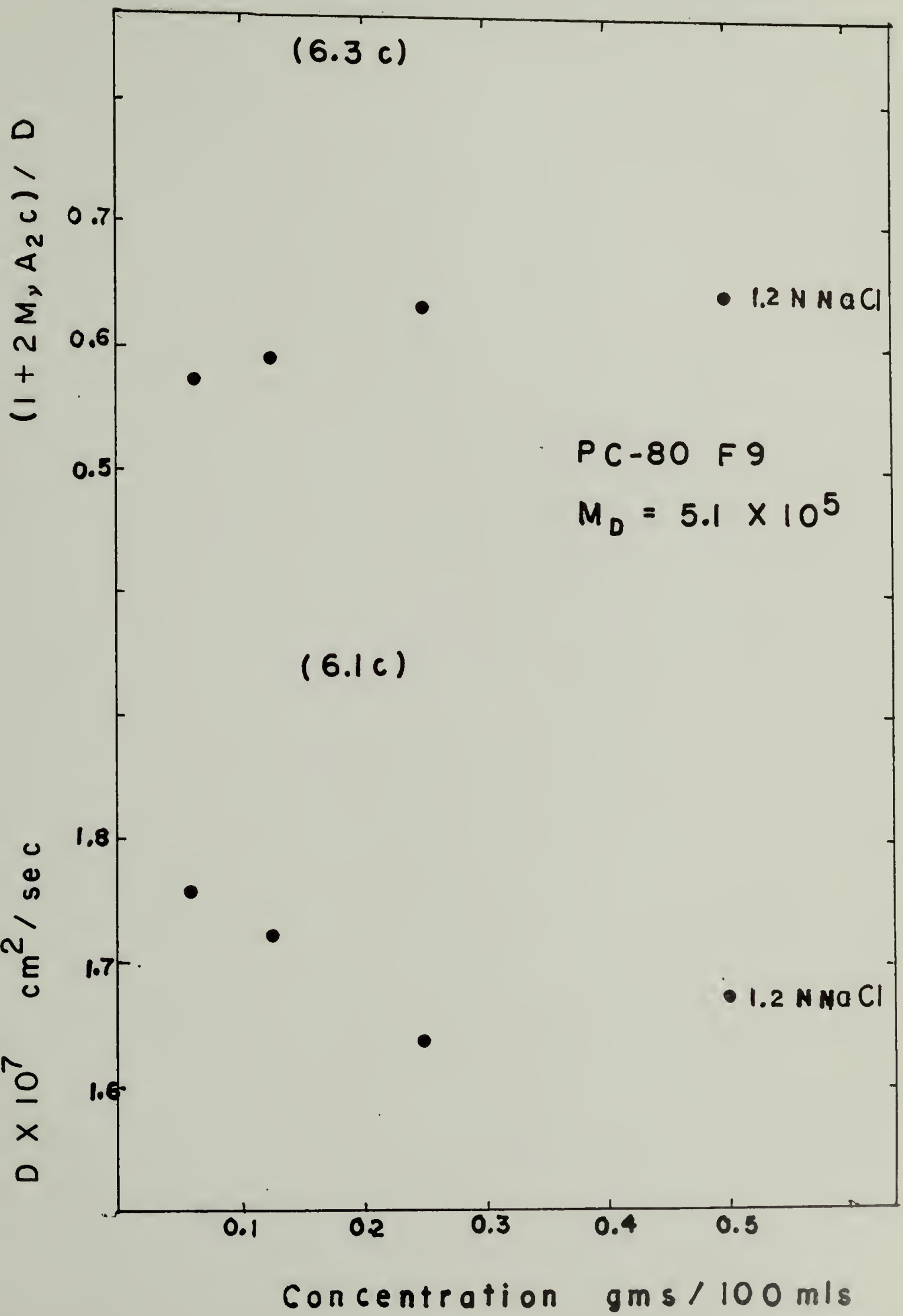
(6.3 c)
(1 + 2 M_y A_2 c) / D
0.7
0.6
0.5
1.2 N NaCl
PC-80 F9
M_D = 5.1 X 10^5
(6.1 c)
1.8
1.7
1.6
D X 10^7 cm^2 / sec
1.2 N NaCl
0.1
0.2
0.3
0.4
0.5
Concentration gms / 100 mls

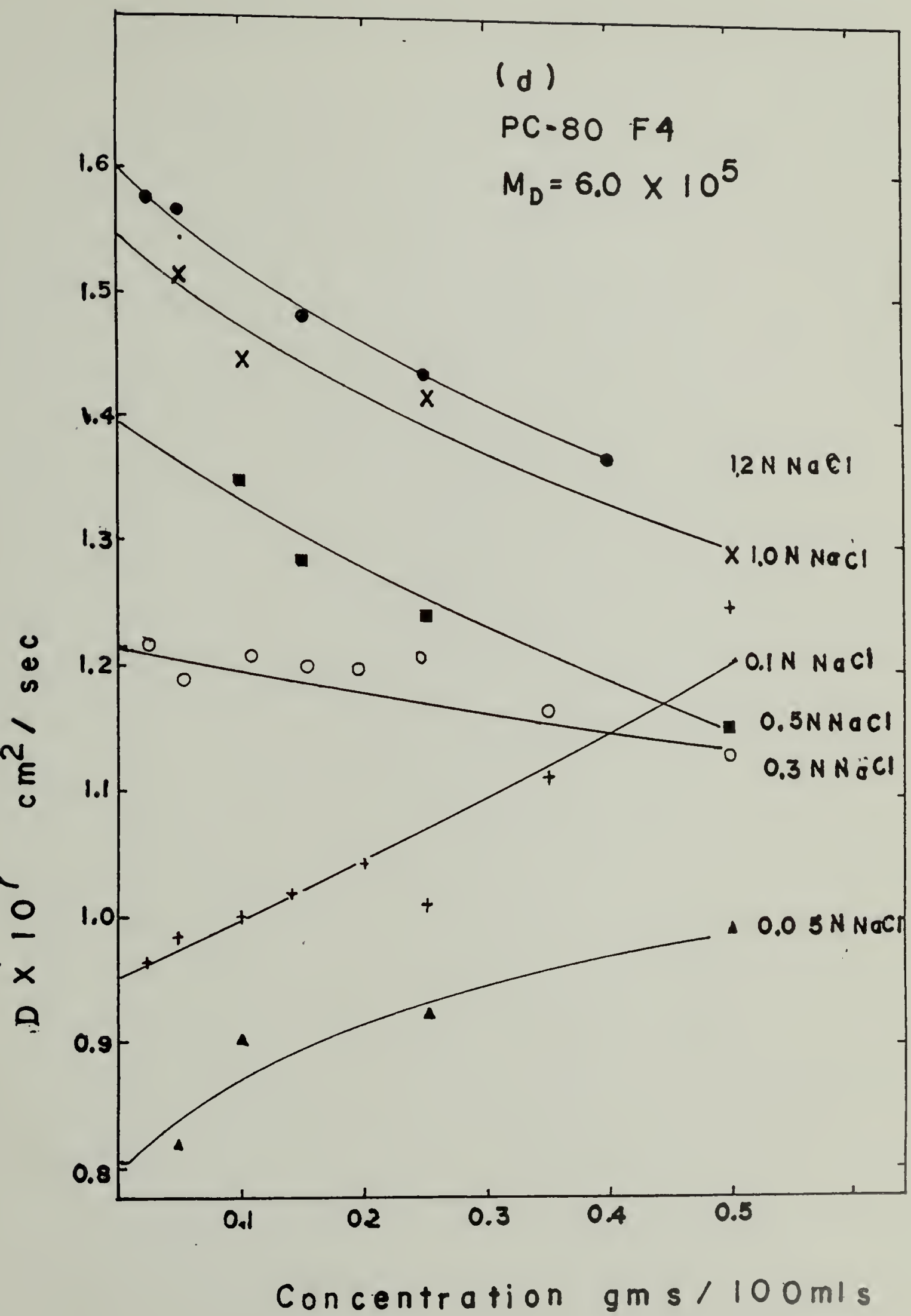
(d)
PC-80 F4
$M_D = 6.0 \times 10^5$
1.2 N NaCl
1.0 N NaCl
0.5 N NaCl
0.3 N NaCl
0.1 N NaCl
0.05 N NaCl
D X 10^7 cm^2 / sec
1.6
1.5
1.4
1.3
1.2
1.1
1.0
0.9
0.8
0.1
0.2
0.3
0.4
0.5
Concentration gms / 100mls

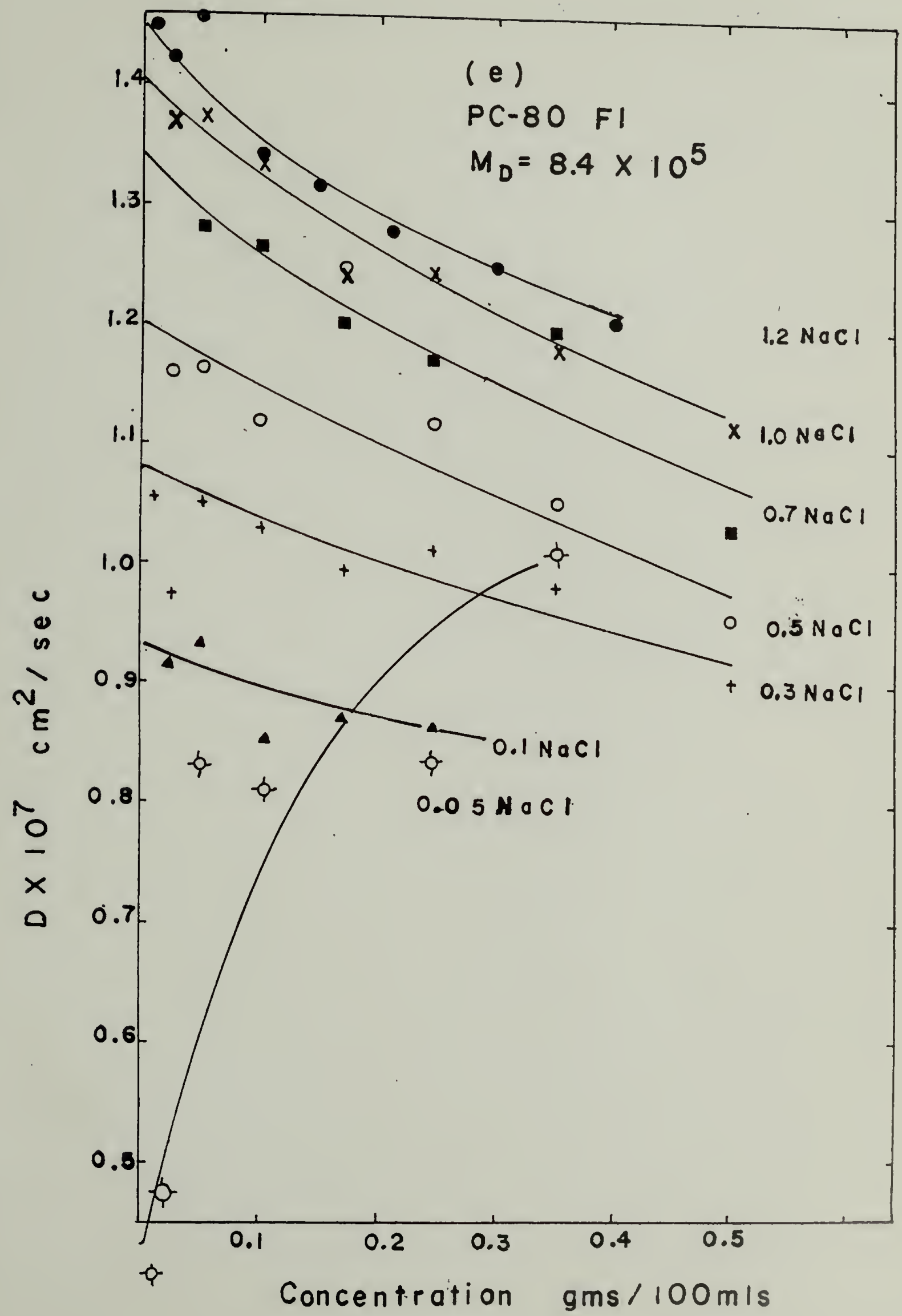
(e)
PC-80 FI
$M_D = 8.4 \times 10^5$
1.2 NaCl
1.0 NaCl
0.7 NaCl
0.5 NaCl
0.3 NaCl
0.1 NaCl
0.05 NaCl
$D \times 10^7$ cm^2/sec
1.4
1.3
1.2
1.1
1.0
0.9
0.8
0.7
0.6
0.5
0.1
0.2
0.3
0.4
0.5
Concentration gms/100mls

Figure 6.2

Plots of diffusion constant measurements versus polymer concentration for two fractions of Na-copoly (ethyl acrylate-acrylic acid) in 2-heptanone.

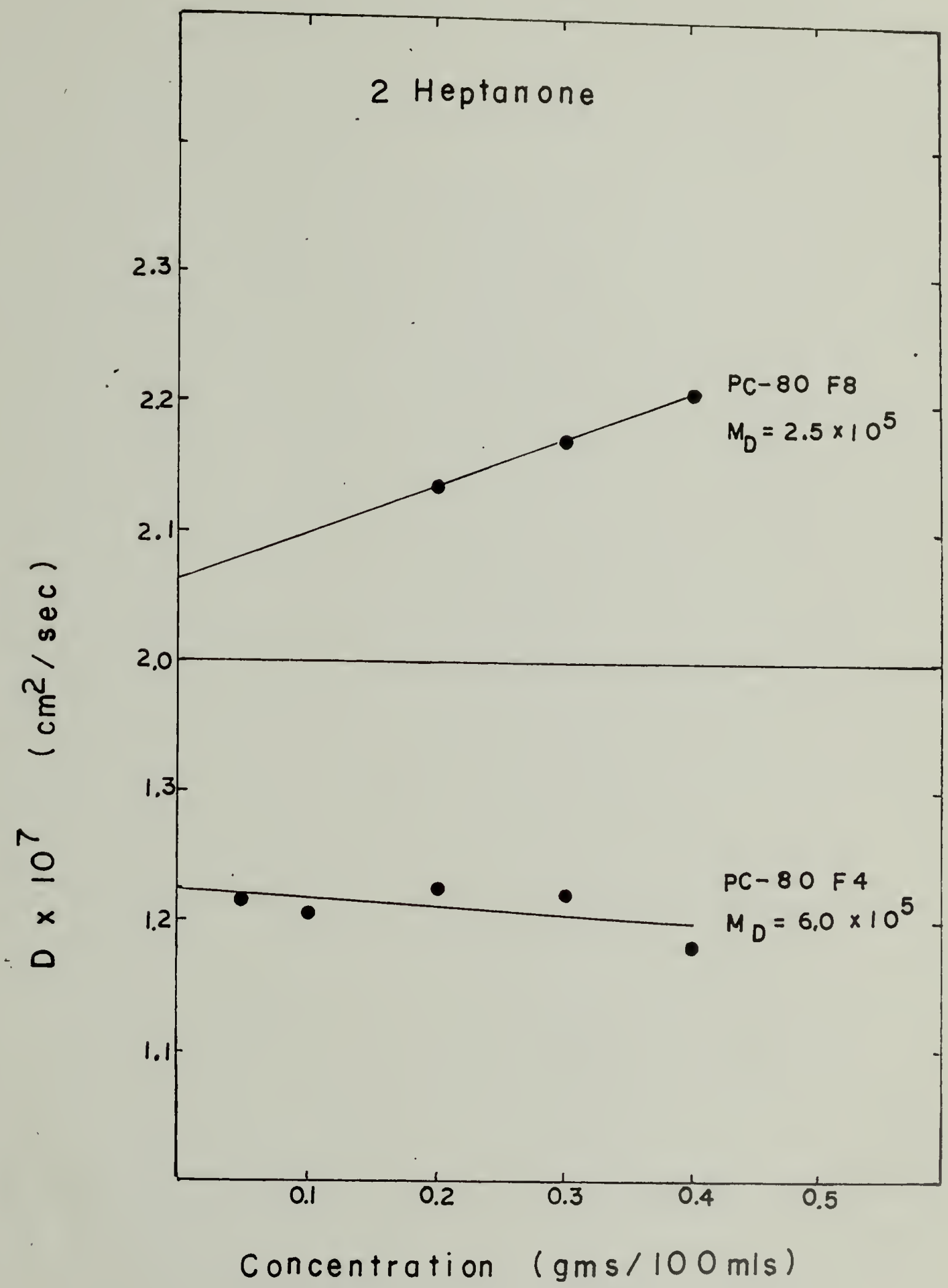
2 Heptanone
PC-80 F8
$M_D = 2.5 \times 10^5$
PC-80 F4
$M_D = 6.0 \times 10^5$
$D \times 10^7$ (cm^2/sec)
2.3
2.2
2.1
2.0
1.3
1.2
1.1
0.1
0.2
0.3
0.4
0.5
Concentration (gms/100mls)

Figures 6.3a-e

Plots of $(1 + 2M_\nu A_2 c)/D$ versus polymer concentration for five fractions of Na-copoly (ethyl acrylate-acrylic acid) in ionic strength solutions from 0.5N NaCl to 1.2N NaCl.

a. PC-80 F8 $M_D = 2.5 \times 10^5$

b. PC-80 FD $M_D = 4.0 \times 10^5$

c. PC-80 F9 $M_D = 5.1 \times 10^5$ (see Figure 6.1c)

d. PC-80 F4 $M_D = 6.0 \times 10^5$

e. PC-80 F1 $M_D = 8.4 \times 10^5$

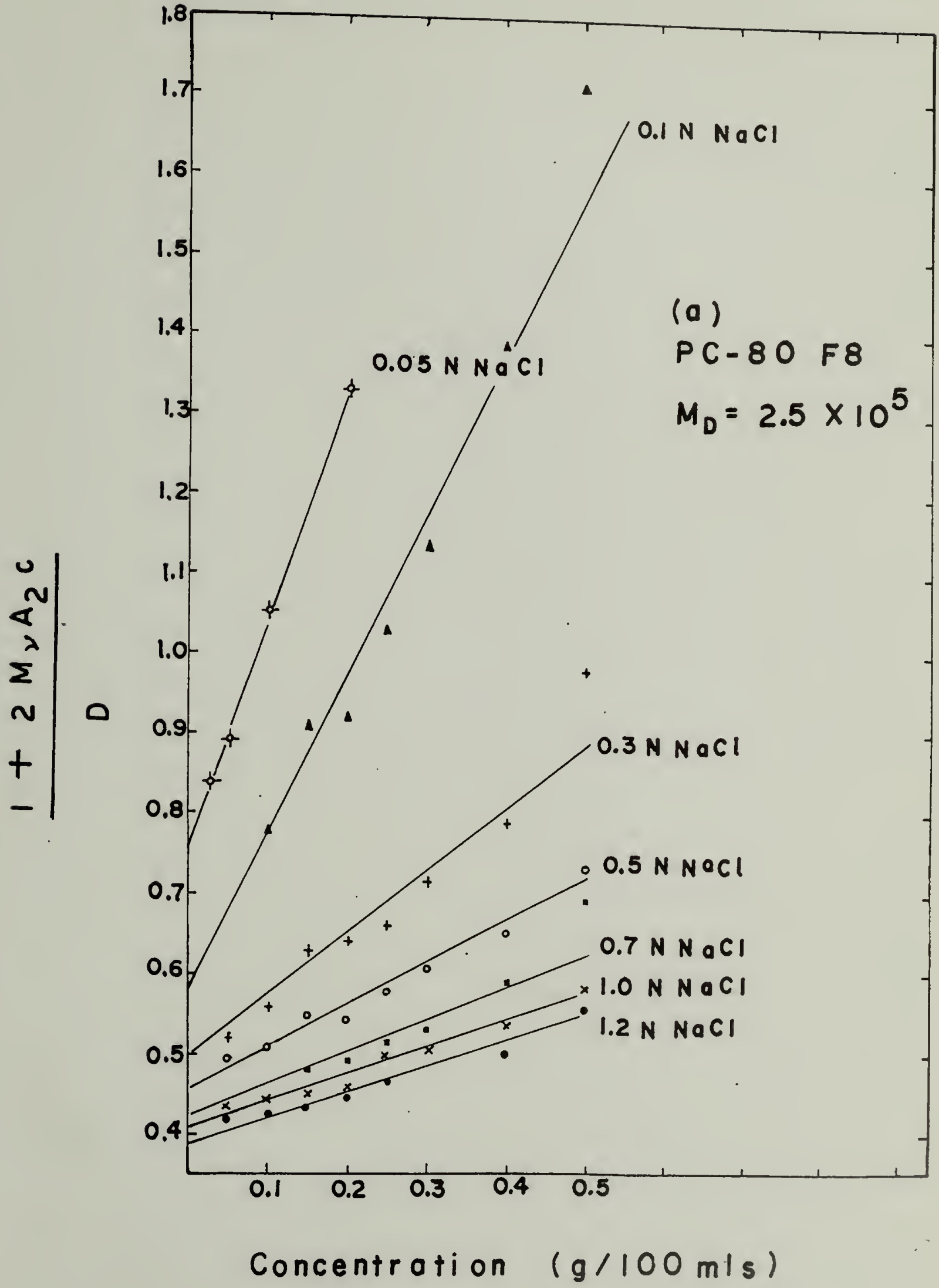
1.8
1.7
1.6
1.5
1.4
1.3
1.2
1.1
1.0
0.9
0.8
0.7
0.6
0.5
0.4
0.1
0.2
0.3
0.4
0.5
0.1 N NaCl
0.05 N NaCl
0.3 N NaCl
0.5 N NaCl
0.7 N NaCl
1.0 N NaCl
1.2 N NaCl
(a)
PC-80 F8
$M_D = 2.5 \times 10^5$
$\frac{D}{1 + 2 M_\nu A_2 c}$
Concentration (g/100 mls)

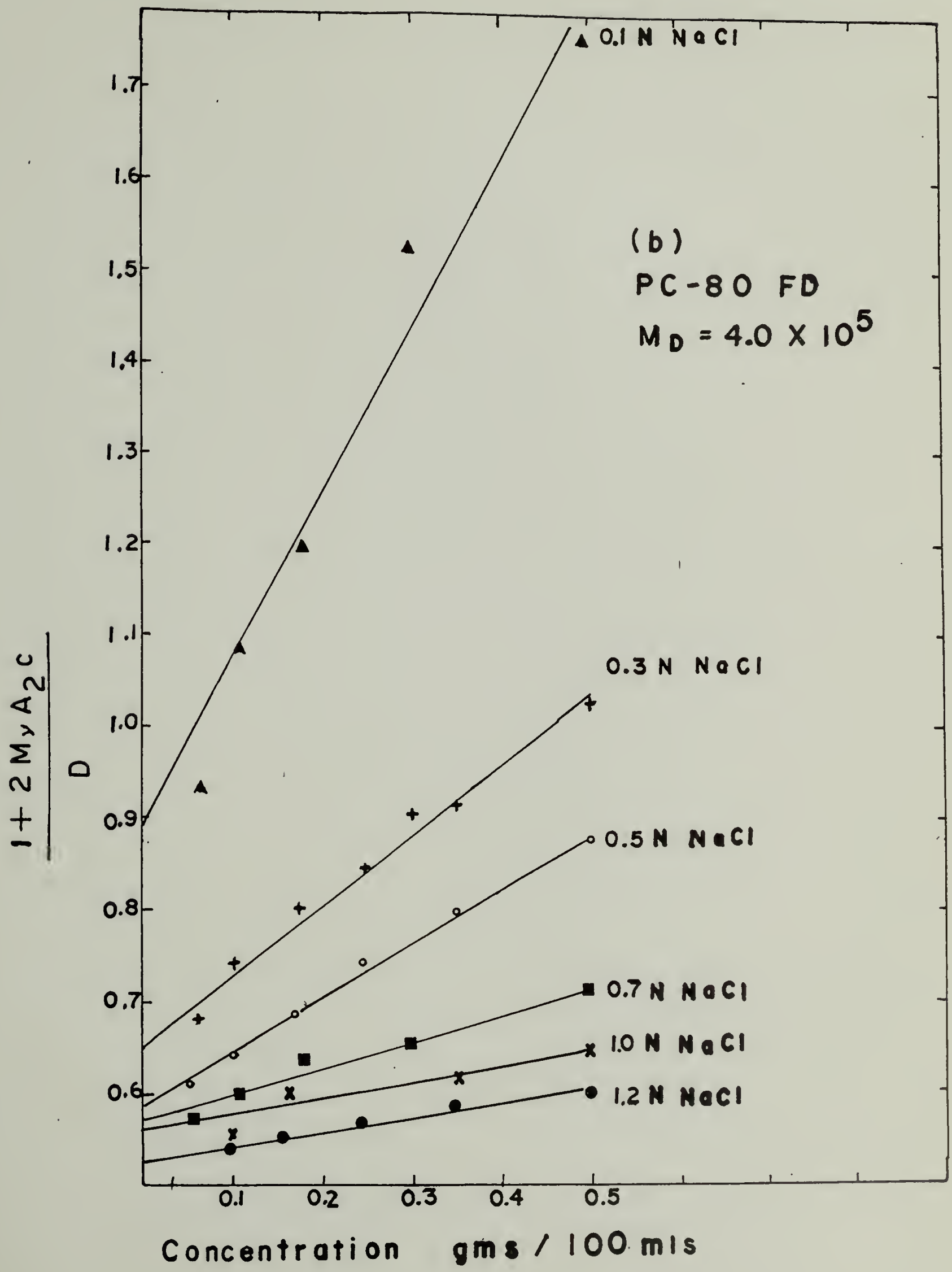
0.1 N NaCl
(b)
PC-80 FD
$M_D = 4.0 \times 10^5$
0.3 N NaCl
0.5 N NaCl
0.7 N NaCl
1.0 N NaCl
1.2 N NaCl
$\frac{1+2M_yA_2c}{D}$
1.7
1.6
1.5
1.4
1.3
1.2
1.1
1.0
0.9
0.8
0.7
0.6
0.1
0.2
0.3
0.4
0.5
Concentration gms / 100 mls

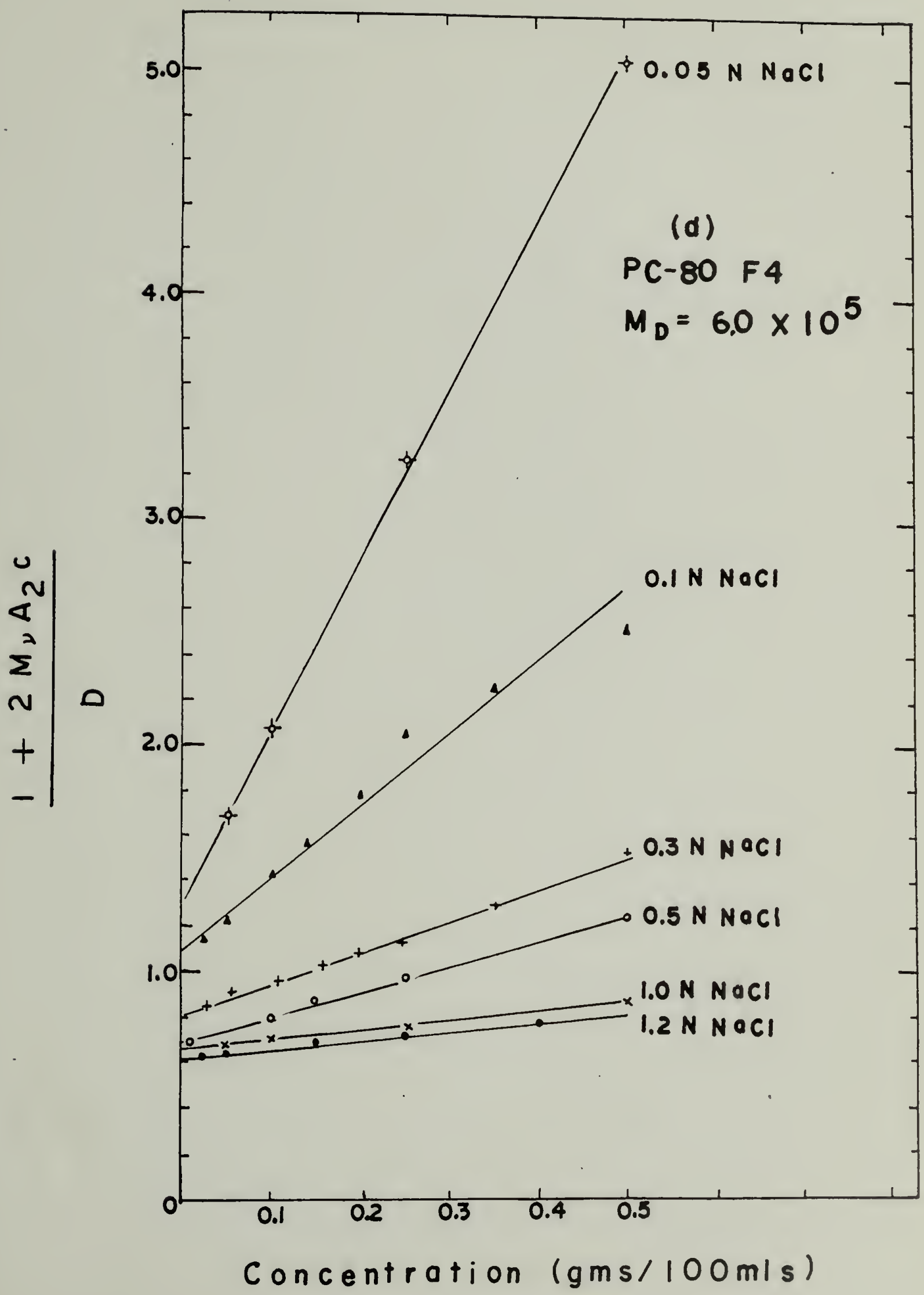
0.05 N NaCl
(d)
PC-80 F4
$M_D = 6.0 \times 10^5$
0.1 N NaCl
0.3 N NaCl
0.5 N NaCl
1.0 N NaCl
1.2 N NaCl
5.0
4.0
3.0
2.0
1.0
0
0.1
0.2
0.3
0.4
0.5
$\frac{D}{1 + 2 M_\nu A_2 c}$
Concentration (gms/100mls)

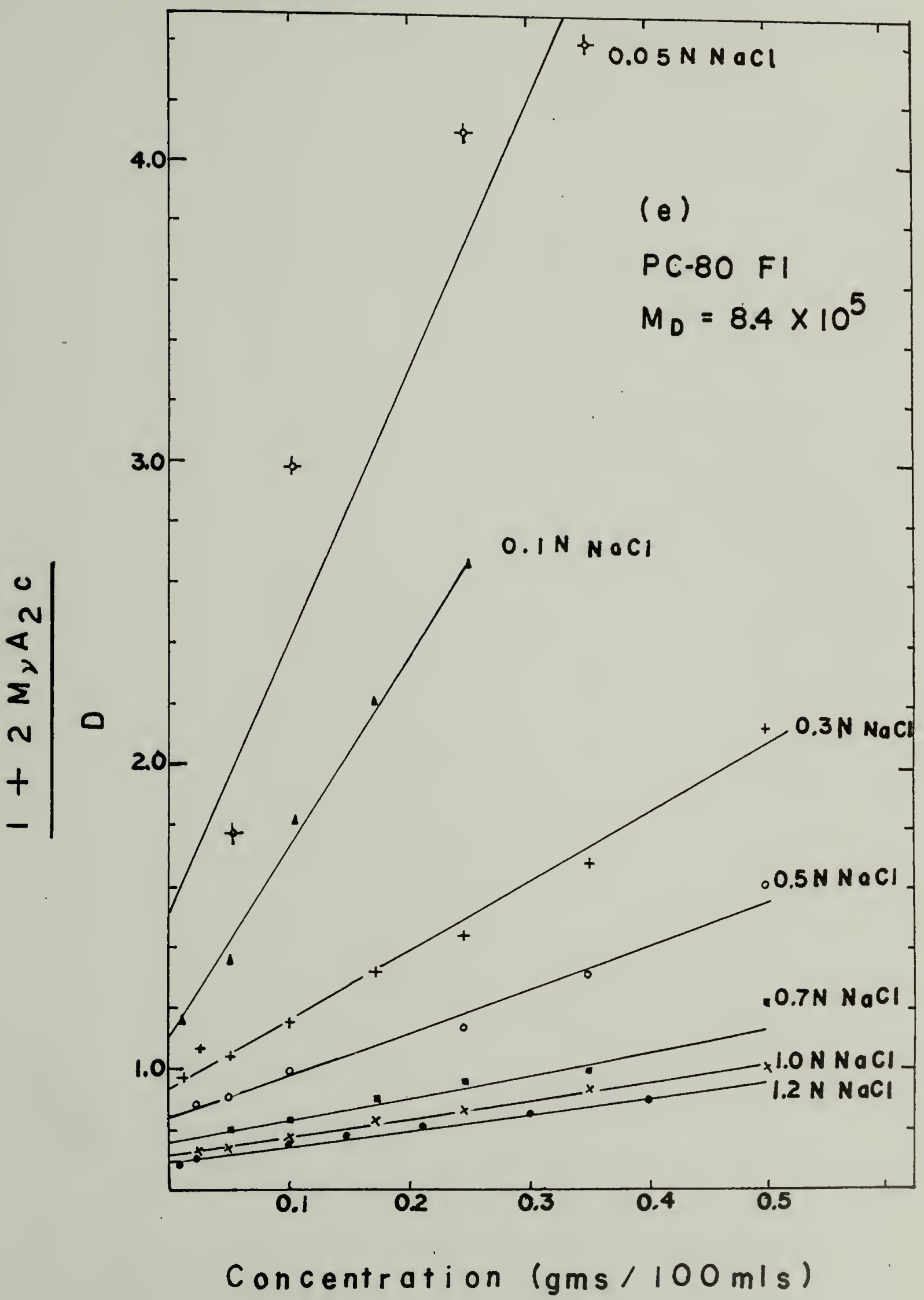
0.05 N NaCl
(e)
PC-80 F1
$M_D = 8.4 \times 10^5$
0.1 N NaCl
0.3N NaCl
0.5 N NaCl
0.7N NaCl
1.0 N NaCl
1.2 N NaCl
4.0
3.0
2.0
1.0
0.1
0.2
0.3
0.4
0.5
$\frac{D}{1 + 2 M_y A_2 c}$
Concentration (gms / 100 mls)

varied with the sample time chosen. In order to make unambiguous comparisons between experiments, diffusion constant measurements must be made as a function of sample time and extrapolated to $\tau = 0$. When this is done, the diffusion constant obtained at $\tau = 0$ is the z average diffusion constant, D_z, and as such is a well defined quantity.

Since the complications arising from the polydispersity of the samples were not realized until most of the data had been obtained, much of the data was accumulated for only two or three sample times. This complicated the analysis since an approximate method had to be developed to obtain the z average diffusion constant. Before discussing this approximate method, the procedure which should have been adopted from the outset will be reviewed so that the errors in the approximations actually used can be estimated.

As discussed in Chapter II, Polydispersity, the method of Brown and Pusey (1) for obtaining the z average diffusion constant consists in fitting the logarithm of the experimental electric field correlation function to a polymonial in τ of appropriate order. In practice Equation (2.39) is used in its linear quadratic, or cubic forms only. The measurements are then made over a range of $\Gamma\tau_{max}$ where $\Gamma\tau_{max}$ is the delay time corresponding to the last channel of the system correlator and the average diffusion constant is obtained as the intercept of a plot of $\bar{\Gamma}\tau_{max}$ versus the effective diffusion constant. The latter is the value of $\bar{\Gamma}$ obtained from a fit of $\ln|g^{(1)}(\tau)|$ to a linear function of τ. In order to obtain the field correlation function from the intensity autocorrelation function, it is necessary to know the value of the correlation function, $G(\infty)$, at $\tau = \infty$. This can be either calculated

from Equation (5.5) or found from a three parameter fit of the intensity autocorrelation function (Equation (6.2)). As the maximum delay time is decreased the result obtained from the three parameter fit increasingly deviates from that obtained when the baseline is calculated from Equation (5.5). At very long delay times, the two results agree within experimental error. For polydisperse samples at very short delay times, it is imperative that the value of $G(\infty)$ be calculated or spuriously high results for the diffusion constant (the errors being at least 100%) will be obtained precisely in the region where the extrapolation for D_z occurs. This method is used by Pusey (1).

In the present study, the values of the diffusion constants were obtained from computer programmed three parameter fits to Equation (6.2) with values of the delay time somewhat arbitrarily chosen so that the correlation functions contained some channels which appeared to have decayed to a baseline value. In addition, a measurement of a shorter delay time was also obtained for comparison. In order to correct these diffusion constant values to obtain the z average diffusion constant, the following procedure was adopted. Samples of F1, FD, F4, F8, and F9 were prepared in 1.2N NaCl and their correlation functions were obtained over a range of sample times from about 20 $\Gamma\tau_{max}$ to about 0.5 $\Gamma\tau_{max}$. D_{LS} was then plotted as a function of $\Gamma\tau_{max}$ as suggested by Brown and Pusey (1). These plots were made with D obtained from both a three parameter least squares fit of the data as well as with D obtained using a two parameter fit and a value of $G(\infty)$ calculated from the total scattered light. The results for one sample are shown in Figure 6.4 for several polymer concentrations where the difference in the values of D

Figure 6.4

Plots of diffusion constants for PC-80 F1 in 1.2N NaCl as a function of $\Gamma\tau_{max}$ for several polymer concentrations. Data points indicated by crosses x were obtained using a three parameter least squares fit whereas data points indicated by dots • were obtained using a two parameter fit and calculated baseline value.

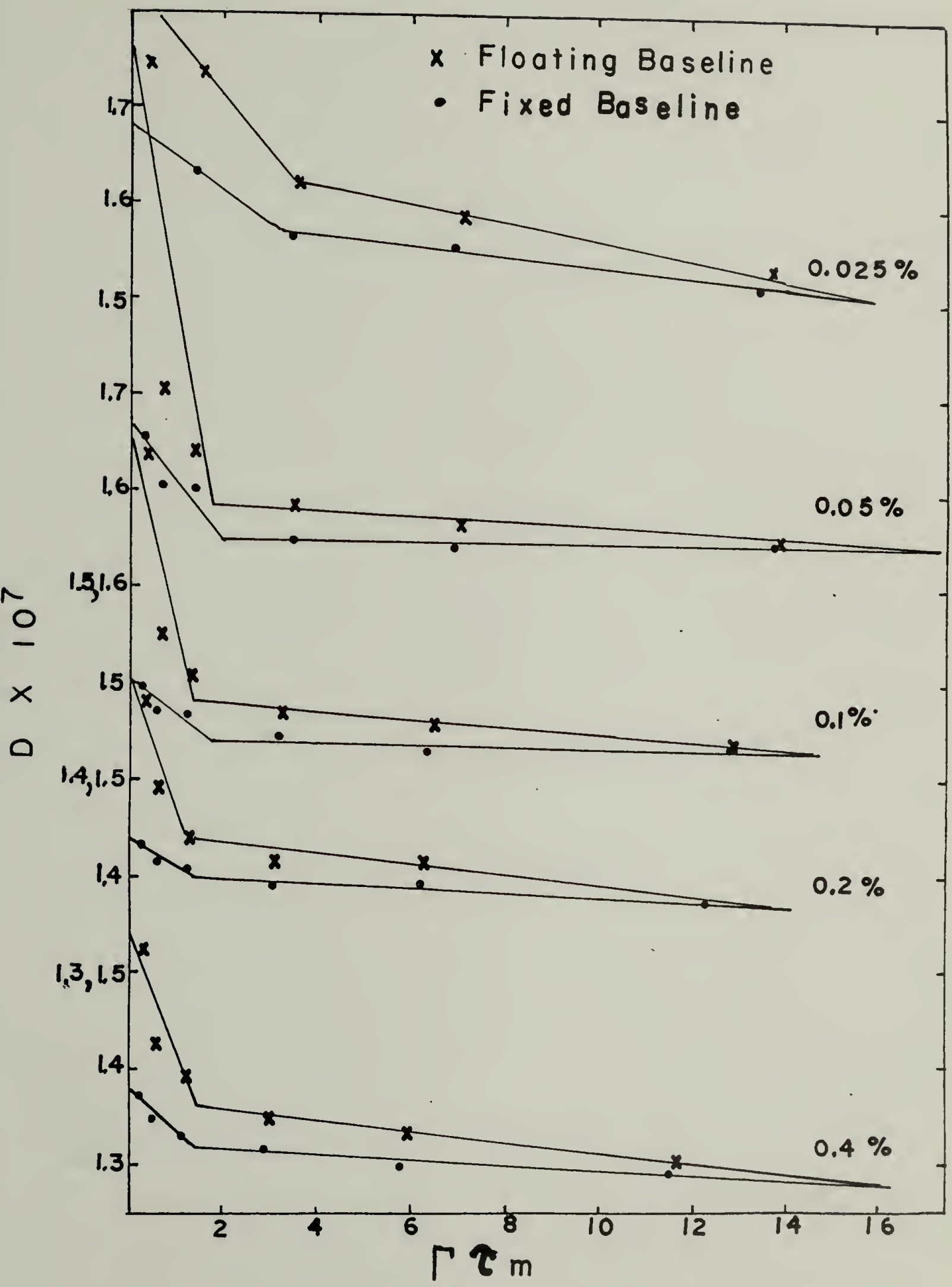
x Floating Baseline
• Fixed Baseline
0.025%
0.05%
0.1%
0.2%
0.4%
1.7
1.6
1.5
1.7
1.6
1.5,1.6
1.5
1.4,1.5
1.4
1.3,1.5
1.4
1.3
2
4
6
8
10
12
14
16
Γ τm
D x 10⁷

obtained from the two methods is apparent. The plots made using a calculated value for $G(\infty)$ indicate that for values of $\Gamma\tau_{max}$ greater than about 5 the value of D is approximately independent of $\Gamma\tau_{max}$. Consequently, it is possible to determine a simple fractional correction to D to obtain D_z provided data have been taken with $\Gamma\tau_{max} > 5$ (which was the case for all the samples studied) and the diffusion constants are obtained using a calculated value for $G(\infty)$.

It was found that ΔD, the fractional increase in the extrapolated diffusion constant, $D_{eff}^{0} = D_z$, over the long time apparent diffusion constant, D_{eff}^{∞}, increased with the degree of polydispersity of the samples. The magnitude of the correction as a function of the polydispersity index is shown for the 1.2N NaCl samples in Figure 6.5. The solid line represents an approximate theory derived by analytically least squares fitting a single exponential to the expression

$$g(\tau) = [\int_0^{\infty} M\omega(M)e^{-D(M)K^2\Gamma}dM]^2.$$

The results of this theory, derived by Ford (2) and given in Appendix 6.1, are

$$\frac{D_{eff}^{0}}{D_{eff}^{\infty}} = \frac{3 - 3[1 - \frac{4}{9}(Y + 1)]^{1/2}}{Y + 1} \qquad (6.3a)$$

where

$$Y = \frac{\Gamma(2 - 2b + h)\Gamma(2 + h)}{\Gamma(2 - b + h)^2}, \qquad (6.3b)$$

Figure 6.5

Percentage increase in diffusion constant as a function of the polydispersity index M_w/M_n for fractions of Na-copoly (ethyl acrylate-acrylic acid) in 1.2N NaCl. The solid line is a theoretical curve from an approximate theory developed by Ford.

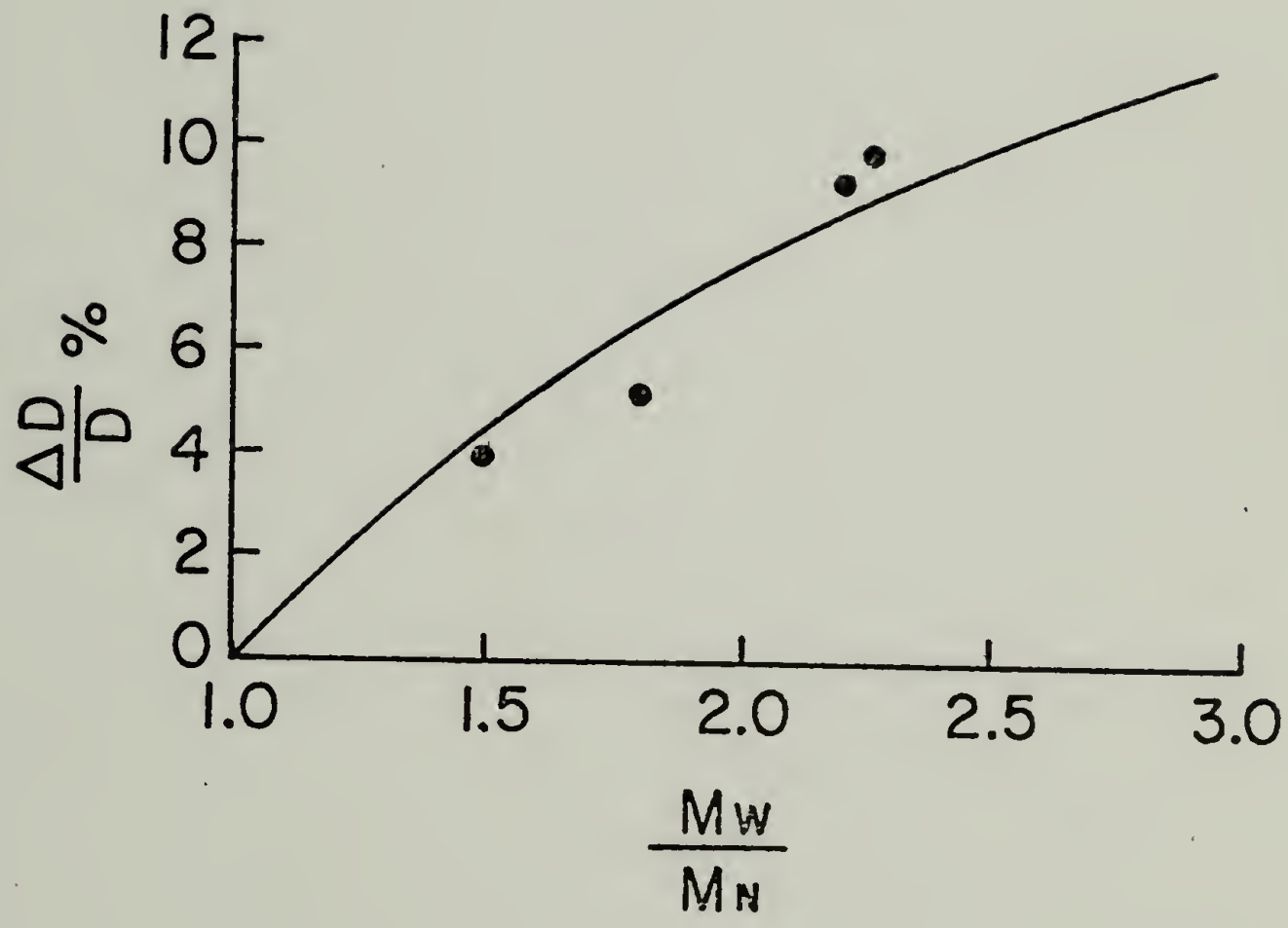
12
10
8
6
4
2
0
$\frac{\Delta D}{D}$ %
1.0
1.5
2.0
2.5
3.0
$\frac{M_W}{M_N}$

D_{eff}^{0} is the extrapolated value of D at $\tau = 0$ giving D_z, D_{eff}^{∞} is the long time value of D obtained at $\tau \to \infty$, h is the width parameter of the Schulz distribution and b the exponent in $D = K_D M^{-b}$, related to the Mark-Houwink-Sakurada exponent a by $3b = a + 1$.

As can be seen the theoretical predictions and the experimental observations are in reasonable agreement for the 1.2N NaCl solutions despite the inaccuracies of the extrapolation procedure. On the present correlator these are mainly due to the number of sample times available, which are limited to intervals spaced in multiples of 1, 2 and 5, and to the increased inaccuracy of the diffusion constant obtained at very short sample times, where both the time required to obtain a reasonable signal and the number of spurious photocounts increases. The estimated error is about 20%.

As indicated previously, this correction is applicable only for data obtained using $G(\infty)$ calculated from Equation (5.5). The bulk of the data, however, was obtained using a three parameter fit of the correlation function. As can be seen from the graphs in which D was obtained in this way (Figure 6.4), the diffusion constant continually decreases with increasing $\Gamma\tau_{max}$ within the range of $\Gamma\tau_{max}$ studied. Thus the fractional increase to be applied when obtaining the z average diffusion constant depends on the value of $\Gamma\tau_{max}$ at which the measurement was originally made. The data taken for all the samples studied was obtained in the range of $\Gamma\tau_{max}$ from about 3 to 12. For a given molecular weight, the diffusion constant decreases with decreasing ionic strength. Thus $\Gamma\tau_{max}$ will be smaller (for a given sample time) for the lower ionic strength solutions and the fractional increase to be applied to obtain

the z average diffusion constant will decrease with decreasing ionic strength. As estimated from the slope of the lines in the region of $\Gamma\tau_{max}$ from 3 to 12, the relative change in ΔD is about 10%. On the other hand, the theoretical expression, Equations (6.3a) and (6.3b), predicts a relative increase in ΔD with increasing ionic strength of between 6% for the molecular weight sample with the lowest polydispersity index to 13% for that with the highest. Thus the two corrections tend to cancel each other and the approximation has been made that correction for the z average diffusion constants for all the ionic strength samples can be adequately obtained by using the experimentally observed fractional increase in the diffusion constant measured for the 1.2N NaCl samples. I believe that this approximation introduces no serious errors in the interpretation of results. Nevertheless, the absolute values of the theoretical correction for the polydispersity can reach 30% for the lowest ionic strength and highest polydispersity sample, so that it would be worthwhile to perform experiments to check the accuracy of the predictions for other than a theta solvent.

It should be noted that in the method developed by Pusey et al., a measure of the width of the molecular weight distribution can be obtained from the second moment about the mean of $G(\Gamma)$ (see Chapter III, Concentration Dependence of Diffusion Constant) which, however, is not directly related to the polydispersity index conventionally used to characterize polydispersity in polymers, except in the limited region of $M_w/M_n \leq 1.1$. In addition, experimental verification has been limited to the case where two monodisperse solutions have been combined and the resulting calculated second moment compared to that experimentally ob-

tained. This is an artificial distribution for polymers as they are conventionally prepared. Thus for the laser light scattering technique to approach the ubiquitous usage of intrinsic viscosity measurements for polymers, the problem of how to deal with the larger polydispersities typically encountered has to be worked out in more detail. Ford's method should be more useful in this regard, since it can be related to M_w/M_n. However, it must be determined whether a relatively simple time insensitive regime exists for non theta systems as well as for systems with much larger polydispersity indices and experiments should be conducted to see whether the polydispersity indices from these systems then agree with those from conventional determinations such as GPC.

In addition to the polydispersity corrections, the diffusion constant measurements made at arbitrary temperatures T (in °C) and in arbitrary solvents, S, were standardized to the conditions of 20°C with water as solvent, in order to compare experiments conducted under different conditions. This is done using the equation

$$D_{20,w} = D\frac{293}{T}\ \frac{\eta(S,T)}{\eta(H_2O,20)} \qquad (6.4)$$

where T is the absolute temperature of the sample, $\eta(S,T)$, is the viscosity of the solvent, and $\eta(H_2O,20)$ is the viscosity of water at 20°C. All the results reported in this thesis give the corrected value of D, but the subscripts will henceforth not be used.

For data obtained in 2-heptanone, in addition to the viscosity correction, it is necessary to use the correct refractive index, n_D, in the equation $D = \Gamma/2K^2$, since $K = (4\pi n_D/\lambda)\sin(\theta/2)$. The value of n_D

Figure 6.6

Plots of P corrected for polydispersity effects as a function of ionic strength for fractions of Na-copoly (ethyl acrylate-acrylic acid).

Top group of data points fitted to $P = q_p P_{APP}$.

Bottom group of data points fitted to $P = P_0(\frac{\alpha_f}{\alpha_s})$.

---- Empirical fit of Meyerhoff $P = P_0(1.31)[1 - 0.33(2a - 1)]$ where a = Mark-Houwink exponent

•••• Theoretical curve calculated from

$$P = \frac{P_0}{3\sqrt{6}}(1 - \varepsilon)(3 - \varepsilon)(6 + 5\varepsilon + \varepsilon^2)^{1/2}, \text{ where } \varepsilon = \frac{2a - 1}{3}$$

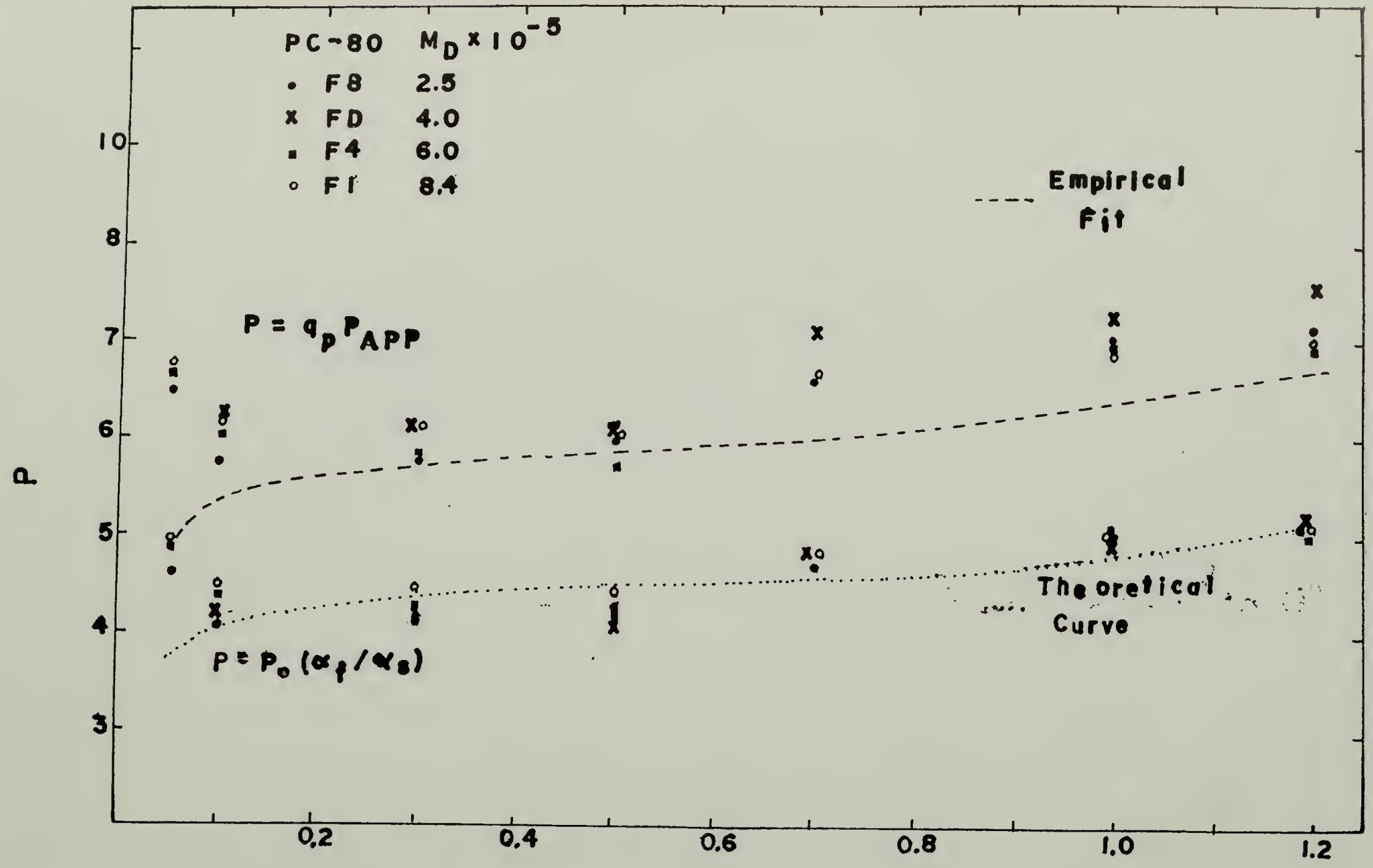
PC-80 $M_D \times 10^{-5}$
• F8 2.5
x FD 4.0
▪ F4 6.0
○ F1 8.4
Empirical Fit
$P = q_p P_{APP}$
Theoretical Curve
$P = P_0 (\alpha_f / \alpha_s)$
q
10
8
7
6
5
4
3
0.2
0.4
0.6
0.8
1.0
1.2
Ionic Strength C_{NaCl} (mol/l)

is 1.406 at 25°C from the Handbook of Chemistry and Physics, in contrast to the value of n_D^{water} of 1.33.

It should also be noted that all diffusion constant measurements were the average of between 5 and 10 separate determinations. For reasonably clean samples, the diffusion constant values did not differ by more than about 5%.

The values of D_{z_o} and k_f^c obtained after all the above corrections were applied are listed in Table 6.1. Values of D_{z_o} can be used in conjunction with the light scattering data of Tan to test the two parameter theory of polymer solutions by evaluating the parameter P in the defining relation

$$P_{APP} = \frac{f}{6^{1/2}} \eta_o \langle s^2 \rangle^{1/2},$$

Equation (3.56b).

The value of P as a function of ionic strength, corrected for polydispersity effects according to Equation (3.128) is plotted in Figure 6.6 along with the theoretical curve of Equation (3.70). The theoretical curve predicts a monotonic decrease in P as the ionic strength decreases. From the relation $R_H = P\langle s^2 \rangle^{1/2}$, this means that the hydrodynamic radius decreases as the ionic strength decreases, or in other words, that there is a non-gaussian expansion of the polymer coil. Also plotted are the values of P obtained from Equation (3.58b), $P = P_o(\alpha_f/\alpha_s)$ and the empirical curve obtained by Meyerhoff (3), Equation (3.74) which was a best fit for existing experimental data on nonionic polymers. Several aspects of these plots are of interest.

TABLE 6.1

Values of D_{z_o} and k_f^c for Na-copoly (ethyl acrylate-acrylic acid) Fractions

	Ionic Strength N (NaCl)	$D_{z_o} \times 10^7$	k_f^c
PC-80 F8			
$M_D = 2.6 \times 10^5$	1.2	2.717	56.7
	1.0	2.657	60.8
	.7	2.599	76.4
	.5	2.3978	112.7
	.3	2.248	137.4
	.1	1.815	278.7
	.05	1.444	420.1
PC-80 FD			
$M_D = 4.0 \times 10^5$	1.2	2.071	29.2
	1.0	2.045	43.8
	.7	1.922	52.6
	.5	1.867	102.1
	.3	1.669	126.2
	.1	1.336	290.8
PC-80 F9			
$M_D = 5.1 \times 10^5$	1.2	1.971	50.6
PC-80 F4			
$M_D = 6.1 \times 10^5$	1.2	1.672	61.0
	1.0	1.606	64.2
	.5	1.474	147.8
	.3	1.299	177.9
	.1	1.008	394.8
	.05	.7998	569.4
PC-80 F1			
$M_D = 8.4 \times 10^5$	1.2	1.470	74.2
	1.0	1.416	80.3
	.7	1.350	120.1
	.5	1.216	179.9
	.3	1.072	237.2
	.1	.8611	501.9
	.05	.6861	601.8

The most obvious observation is that the absolute values of $P_{experimental}$ from the present data as well as the data fitted by Meyerhoff are larger by about 25% than the value predicted theoretically. Differences between values of P predicted theoretically are less than 5%, so that it is impossible to corroborate any particular theoretical value. The larger values of P found experimentally means that the radii of gyration calculated from the hydrodynamic measurements will be smaller by about 25% than that determined by light scattering. The values of P obtained from Equation (3.58b) are normalized to that of P_0 by definition. From this curve as well as that from Equation (3.70), it can be seen that in addition to a difference in absolute magnitude, the change in P with ionic strength differs from that predicted theoretically. Instead of the latter's monotonic decrease, the experimental curves for the polyelectrolyte system studied show an upward trend at low ionic strength. Physically this means that the hydrodynamic radius begins to increase with decreasing ionic strength. The empirical fit of Meyerhoff, which is a fit of nonionic polymer data, shows no upward trend as the solvent becomes better.

Corroboration for this phenomenon can be seen in plots of the Flory constant Φ, Figure 6.7 (where Φ was calculated from Equations (3.58a) and $\Phi = \Phi_{APP} q_{\phi}$). This upward shift can be seen more clearly in Figure 3.3 both for other fractions of Na-copoly (ethyl acrylate-acrylic acid) and for other polyelectrolyte systems. The magnitude of Φ for the former system is seen to be approximately 40% higher than the theoretical value and so as was the case for P indicates a value for the hydrodynamic radius which is 40% larger than expected.

Figure 6.7

Plot of Flory viscosity constant Φ corrected for polydispersity effects as a function of ionic strength for fractions of Na-copoly (ethyl acrylate-acrylic acid).

Top group of data points fitted to $\Phi = q_{\phi}\Phi_{APP}$.

Bottom group of data points fitted to $\Phi = \Phi_0(\frac{\alpha_\eta}{\alpha_s})^3$.

Solid line represents theoretical curve of Tschoegl.

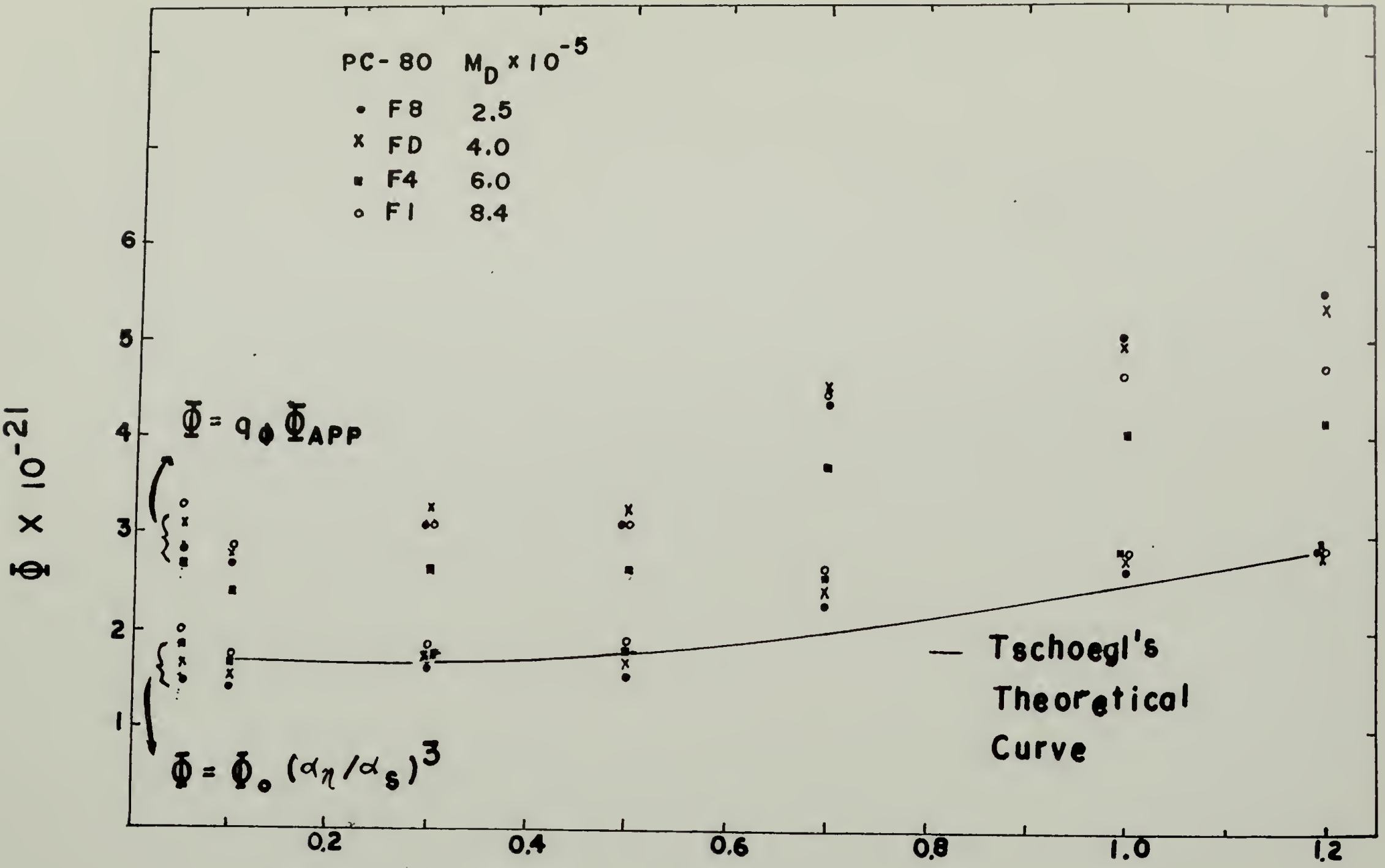
PC-80 $M_D \times 10^{-5}$
• F8 2.5
× FD 4.0
▪ F4 6.0
○ F1 8.4
$\Phi = q_\phi \Phi_{APP}$
$\Phi = \Phi_o (\alpha_\eta / \alpha_s)^3$
— Tschoegl's Theoretical Curve
$\Phi \times 10^{-21}$
1
2
3
4
5
6
0.2
0.4
0.6
0.8
1.0
1.2
Ionic Strength C_{NaCl} (mol/l)

In both the cases of P and Φ the corrections for polydispersity increase their values. Since the values of P_{APP} and Φ_{APP}, i.e., the apparent values of these quantities uncorrected for polydispersity effects, for the polyelectrolyte system were larger than the theoretical values, the polydispersity corrections increase the difference. Since values of P_0 and Φ_0 for the non free draining case are predicted to be lower than Equations (5.11) and (2.87) respectively, the polyelectrolytes studied can be considered non free draining. Further verification for this can be seen from the independence of these parameters on molecular weight.

In Figures 6.8 and 6.9, the values of P_0 and Φ_0 calculated from Equations (3.131) and (3.123) are plotted. These equations correct P_{APP} and Φ_{APP} for both polydispersity and excluded volume. Thus the values of P_0 and Φ_0 obtained in this way should have been independent of ionic strength. However, as can be seen from Figures 6.8 and 6.9, the values of P_0 and Φ_0 are not random but preserve the same dependence on ionic strength as the uncorrected values. Nevertheless the values of P_0 and Φ_0 have been averaged with the result that $P_0 = 6.45$ and $\Phi_0 = 3.99 \times 10^{21}$, giving the approximately 25% and 40% increase respectively over the theoretical ones.

The upshift in Φ and P at low ionic strengths cannot be readily explained. There is evidence that at the lowest ionic strength P increases with increasing molecular weight, indicating that the draining effect might begin to become apparent in very good solvents. However, the draining effect acts in the same manner as the effect of excluded volume--it tends to decrease not increase P or Φ. Thus there seems to

Figure 6.8

Plot of P_0 calculated from $P_0 = P_{APP} q_p(\varepsilon)$ as a function of ionic strength for fractions of Na-copoly (ethyl acrylate-acrylic acid).

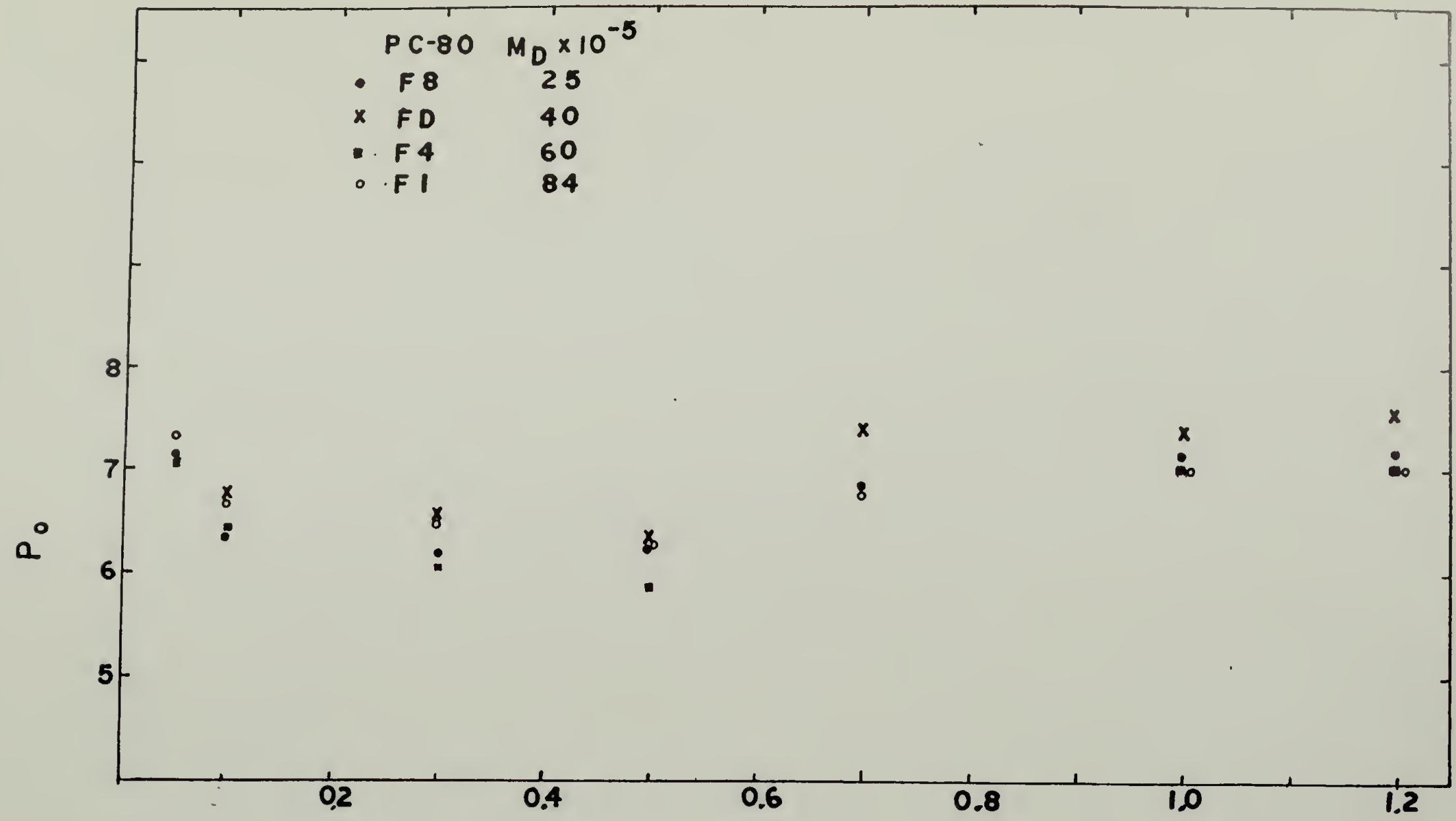
PC-80 $M_D \times 10^{-5}$
• F8 25
x FD 40
▪ F4 60
○ F1 84
8
7
6
5
P_o
0.2
0.4
0.6
0.8
1.0
1.2
Ionic Strength C_{NaCl} (mol / l)

Figure 6.9

Plot of Φ_0 calculated from $\Phi_0 = \Phi_{APP} q_\phi(\varepsilon)$ as a function of ionic strength for fractions of Na-copoly (ethyl acrylate-acrylic acid).

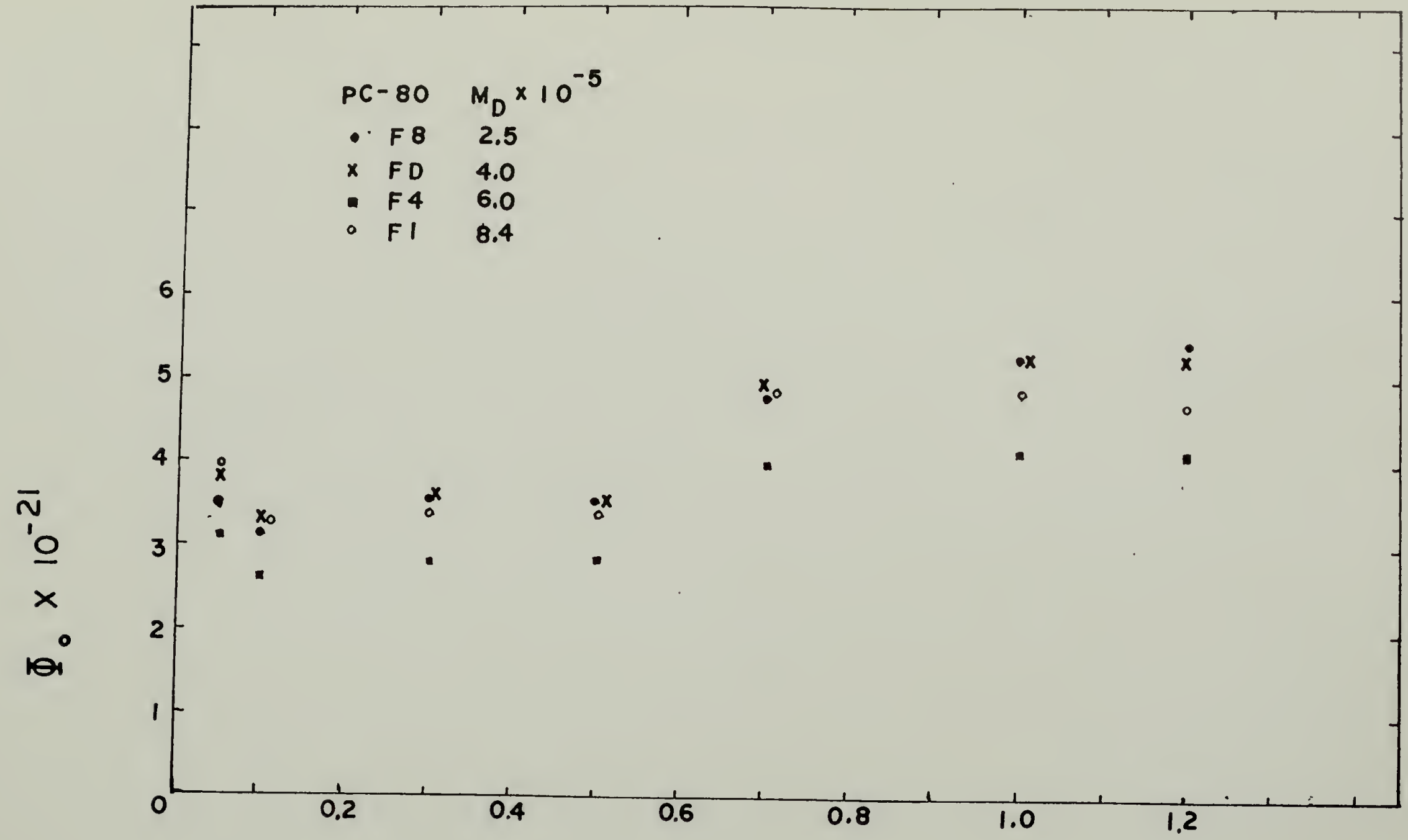
PC-80 $M_D \times 10^{-5}$
• F8 2.5
x FD 4.0
■ F4 6.0
○ F1 8.4
$\Phi_o \times 10^{-21}$
0
1
2
3
4
5
6
0.2
0.4
0.6
0.8
1.0
1.2
Ionic Strength C_{NaCl} (mol/l)

be no apparent physical reason why the hydrodynamic radius should start increasing as the polymer coil expands. As indicated in Figure 3.3, this effect occurs for Φ even in nonionic polymers but to a lesser extent. For the case of P, there was one other reported case of an increase in P with increasing solvent power, which was made by Cowie and Cussler (4). They studied three well fractionated samples of polystyrene in a theta solvent, observing a value of P of 5.71. The results in a better solvent (where b = .58) were P = 5.26 and they noted that this increase was contrary to theoretical predictions. However, it occurs at approximately the same excluded volume as was observed in Na-copoly (ethyl acrylate-acrylic acid).

Another parameter of interest, β, is plotted in Figure 6.10 along with the theoretical values calculated numerically from the theoretical values of P and Φ. In Figure 16.11, β calculated from Equation (3.76) is plotted and in Figure 6.12 are displayed values of β_0 calculated from P_0 and Φ_0. Again, β_0 should be independent of ionic strength and except for the values at 0.1N NaCl and 0.05N NaCl, it is in fact the least dependent on this quantity. The average value of β_0 for all ionic strengths is 2.33, or 16% below the theoretical value, which is smaller than the error found for P_0 and Φ_0 individually. Values of β_0 for nonionic polymers are typically around 2.5, so the present value is only 6.8% below this. The shape of the theoretical curve for β is simply a manifestation of its functional form in terms of P and Φ which predicts an increase in β at small excluded volume (see Equation (3.77)) and a minimum in β as a function of ionic strength. The experimental curves increase with decreasing ionic strength until 0.3N and then de-

Figure 6.10

Plot of β corrected for polydispersity effects as a function of ionic strength for fractions of Na-copoly (ethyl acrylate-acrylic acid).

---- Theoretical curve calculated from theoretical values of P and Φ.

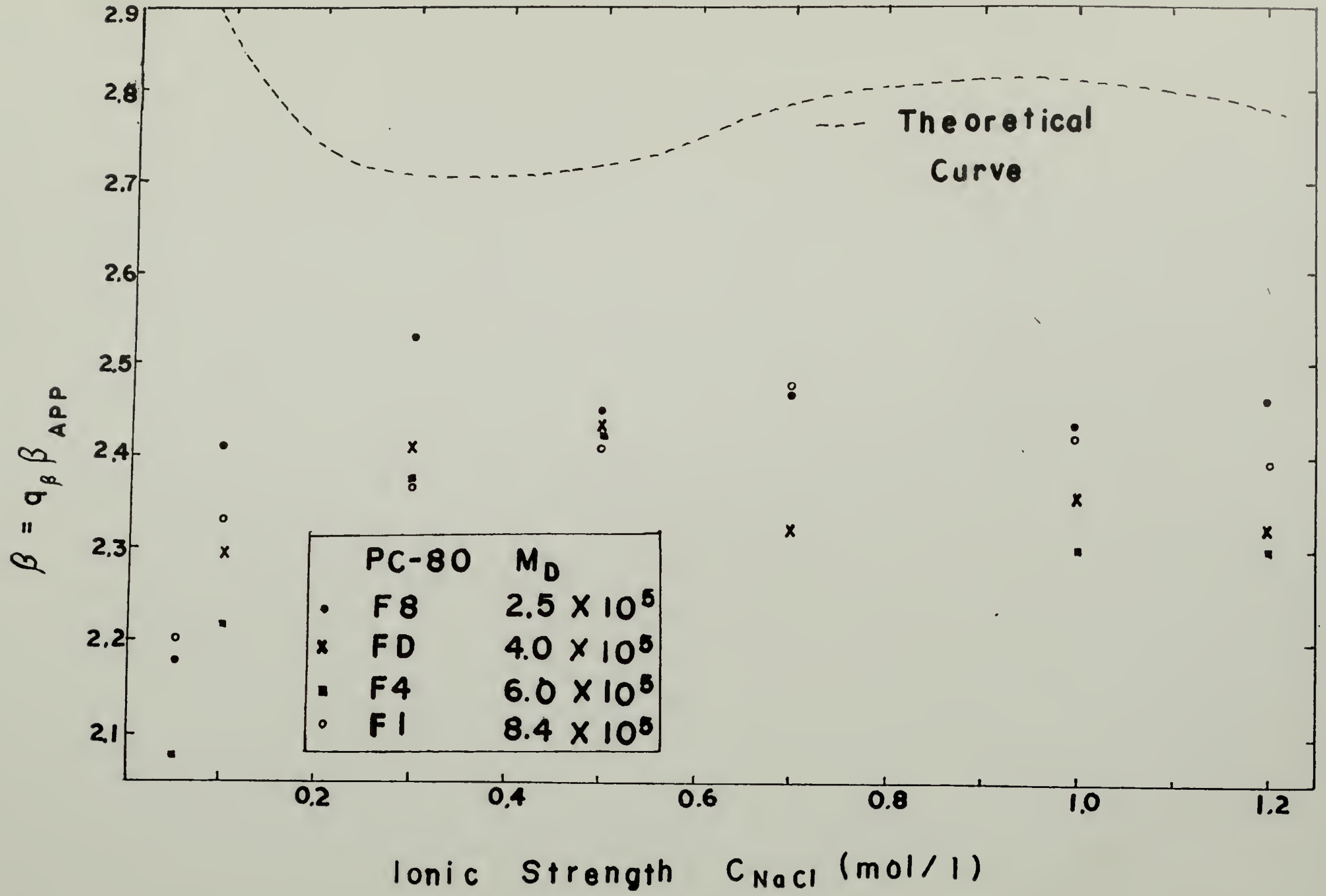
Theoretical Curve
$\beta = q_\beta \beta_{APP}$
2.9
2.8
2.7
2.6
2.5
2.4
2.3
2.2
2.1
0.2
0.4
0.6
0.8
1.0
1.2
PC-80 M_D
F8 2.5×10^5
FD 4.0×10^5
F4 6.0×10^5
F1 8.4×10^5
Ionic Strength C_{NaCl} (mol/l)

Figure 6.11

Plot of β calculated from $\beta = 2.78(\alpha_\eta/\alpha_f)$ as a function of ionic strength for fractions of Na-copoly (ethyl acrylate-acrylic acid).

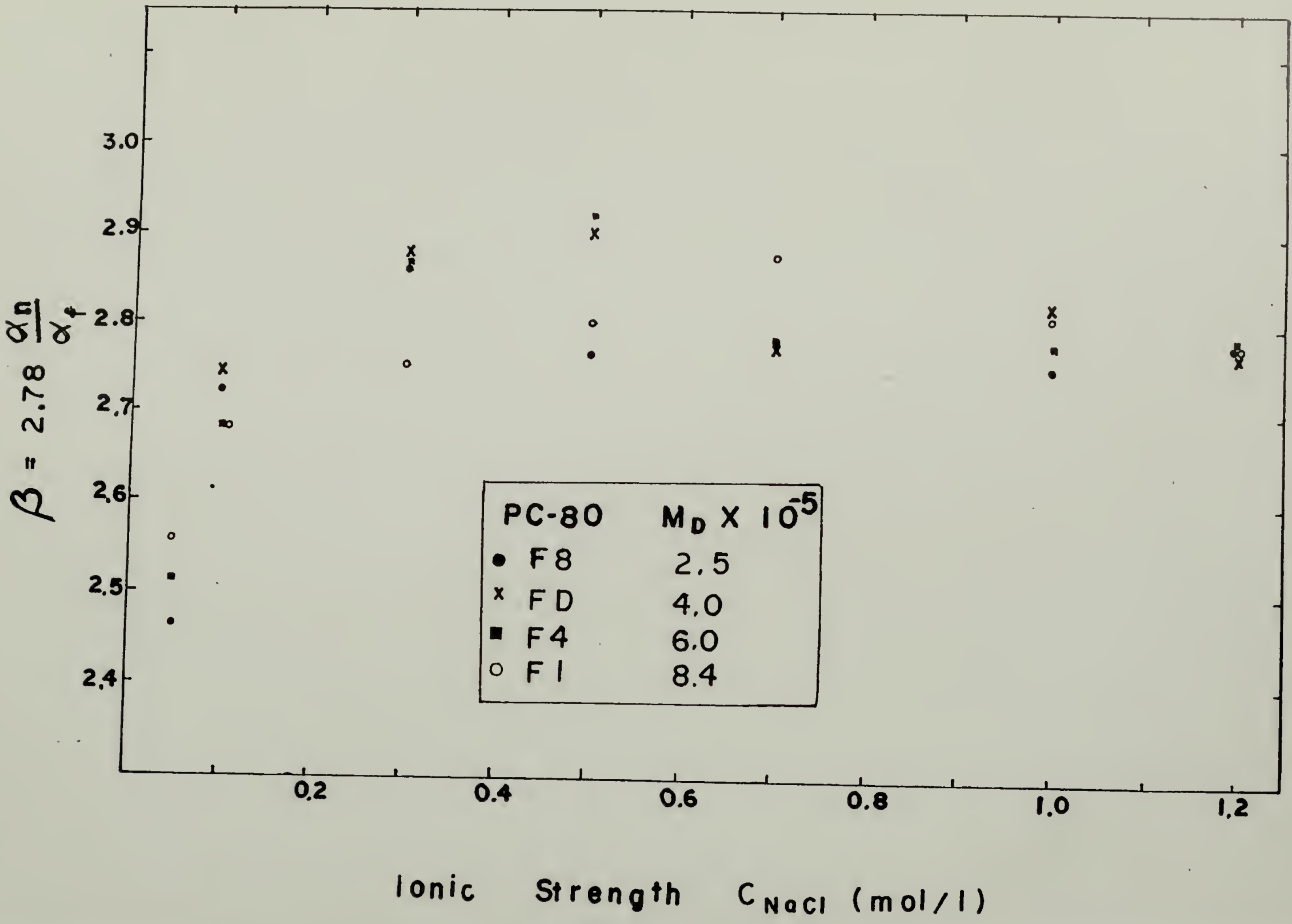
$\beta = 2.78 \frac{\alpha_n}{\alpha_f}$
3.0
2.9
2.8
2.7
2.6
2.5
2.4
0.2
0.4
0.6
0.8
1.0
1.2
PC-80
$M_D \times 10^{-5}$
F8 2.5
FD 4.0
F4 6.0
F1 8.4
Ionic Strength C_{NaCl} (mol/l)

Figure 6.12

Plot of β_0 calculated from $\beta_0 = \Phi_0^{1/3} P_0^{-1}$ as a function of ionic strength for fractions of Na-copoly (ethyl acrylate-acrylic acid).

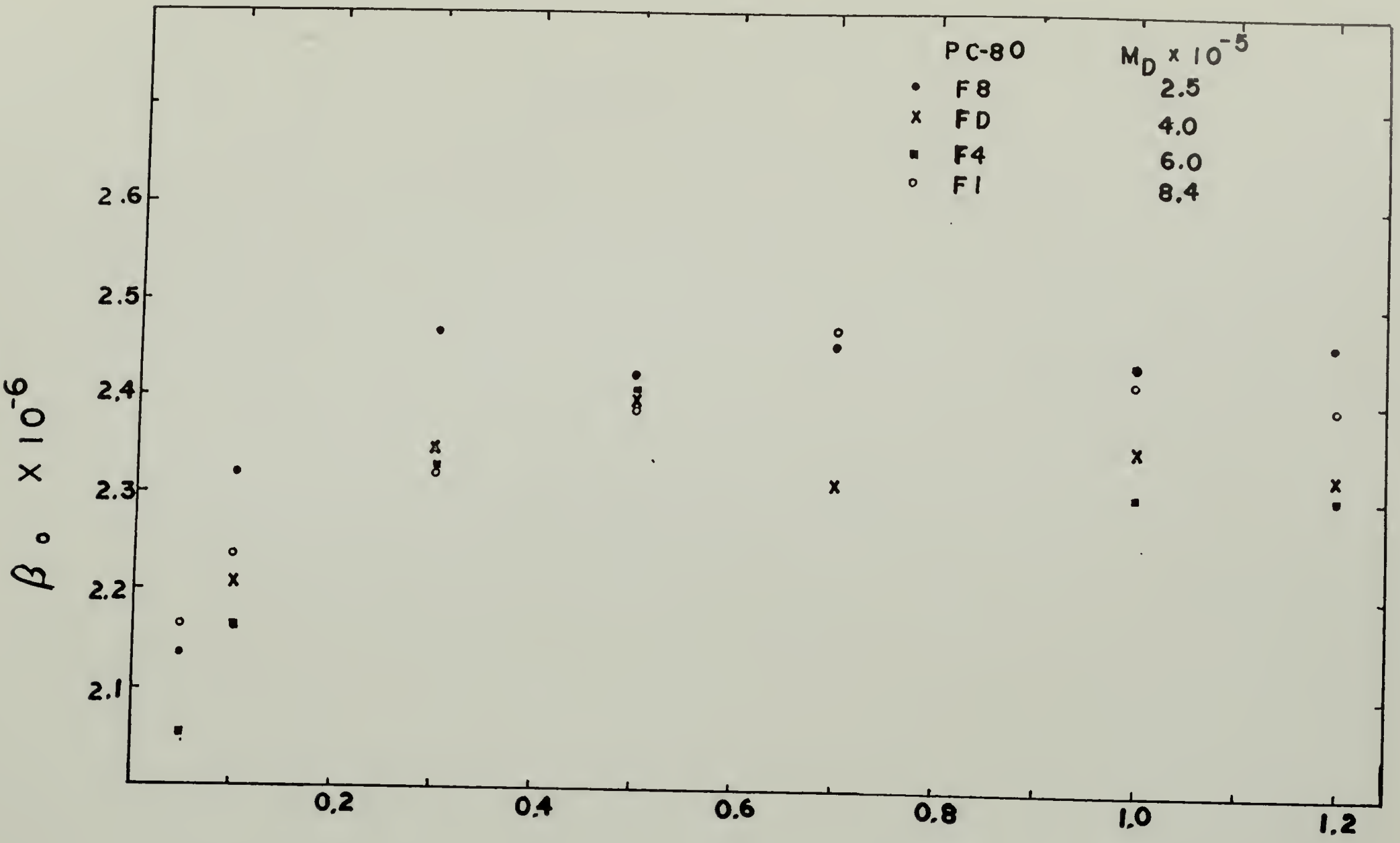
PC-80
$M_D \times 10^{-5}$
F8 2.5
FD 4.0
F4 6.0
F1 8.4
$\beta_0 \times 10^{-6}$
2.6
2.5
2.4
2.3
2.2
2.1
0.2
0.4
0.6
0.8
1.0
1.2
Ionic Strength C_{NaCl} (mol/l)

crease. The latter phenomenon reflects the anomolous behaviors shown in the curves of P and Φ in this low ionic strength region.

In work on the sedimentation of the polyelectrolyte sodium polystyrene sulfonate in the ionic strength range of 0.005N to 0.2N NaCl, Nagasawa and Eguchi (5) observed an increase in β_0 with increasing ionic strength except above .02N, where β_0 decreased. Although most of their data was taken below .2N NaCl, whereas the reverse was true in the present study, it is interesting that the reversal of slope occurs around the same ionic strength for both polyelectrolytes. For Na-copoly (ethyl acrylate-acrylic acid), this is demonstrated in Figure 6.12.

Nagasawa and Eguchi point out that the effect of the ionic atmosphere exists even in the limiting sedimentation coefficient (i.e., that at zero macromolecular concentration or infinite ionic strength) as an interaction between the polyion and simple salt arising from the unequal sedimentation coefficients of polyion and counterion causing a sedimentation potential to be set up which diminishes the sedimentation velocity of the macroion. Thus the latter is not the value which would be obtained for the corresponding un-ionized macromolecule of the same molecular size, conformation and partial specific volume. They reasoned that since β_0 was obtained by elimination of the radius of gyration in the expressions for $[\eta]$ and S (the sedimentation velocity), thus eliminating the effect of ionic atmosphere on the size of the polyion, any change in β_0 with ionic strength would have to be due to the effect of the ionic atmosphere. Using a representation of a polyion coil as a hydrodynamically equivalent sphere having a uniform distribution of fixed charges with a Debye-Hückel ionic atmosphere, they derived

an expression for β_0 for a nondraining polyion as

$$\beta_0(\text{ionic}) = \beta_0(\text{nonionic})[1 - f(K)] \tag{6.5}$$

where K is the Debye-Hückel screening length. Thus, since K increases as the ionic strength decreases, they predicted that β_0 for ionic polymers should decrease with decreasing ionic strength.

As presented in the original paper, the effect of excluded volume on β was neglected and possible changes in β_0 were discussed in terms of the effect of drainage. It was noted that the latter would result in an effect opposite to that caused by an ionic atmosphere. More recent treatments of the two parameter theory, as discussed in Chapter III, have to take into account the effects of excluded volume, especially in the ionic strength range used in their study. Nevertheless, the effects of excluded volume would result in an effect similar to that of drainage and hence opposite to that of ionic atmosphere. It would account for the increase in β with decreasing ionic strength observed in the high ionic strength region, which Nagasawa and Eguchi attribute to the effect of partial drainage and which they also observed for sodium polyacrylate. A closer look at their data indicates the interesting result that below 0.2N salt β_0 clearly decreases with increasing molecular weight. Since β_0 is the ratio of $\Phi_0^{1/3}$ to P_0, both of which depend approximately on molecular weight in the free draining case, β_0 is predicted theoretically to behave as their experimental results do, indicating at least partial free drainage in this ionic strength regime. Above 0.02N salt however, the dependence on molecular weight becomes randomized. In the data on sodium poly (ethyl acrylate-acrylic acid)

it is only the random behavior which is also observed. This would be expected since the copolymer has a lower charge density along the chain and hence would require lower ionic strengths to achieve the same degree of expansion occurring in the sodium poly-sulfonate. Although the low ionic strength regime would have been interesting to study, experimental difficulties precluded performing studies in this region. Since decreasing the ionic strength increases the expansion of the polyion, it becomes impossible to filter the sample through a filter of small enough pore size to also eliminate dust. Unfortunately, no way was found around this problem. Nevertheless, the decrease in β_0 at 0.1N NaCl demonstrated in Figure 6.12 is probably due to the effects of ionic atmosphere as predicted by Equation (6.5).

Values of β_0 reported in the literature for polyions are lower than for nonionic polymers, as was the case with sodium copoly (ethyl acrylate-acrylic acid). However, the effects of polydispersity and excluded volume have not always been taken into account. The latter omission means that β not β_0 has been reported, and the former that the reported values should be increased. In the study of Nagasawa and Eguchi for example, the one sample for which they reported values of both M_w and M_n gave a polydispersity index of 1.53, which would necessitate increases of at least 7% in β_0.

The diffusion constant measurements from Table 6.1 can be used to test the relation $D = K_D M^{-b}$. As shown in Figure 6.13 the data are adequately represented by rectilinear double logarithmic plots for all the solutions, although the scatter becomes worse as the ionic strength is decreased. The plots also appear to deviate from linearity at the

Figure 6.13

Double logarithmic plots of D_{z_o} versus M_D for Na-copoly (ethyl acrylate-acrylic acid) in aqueous salt solutions and 2-heptanone.

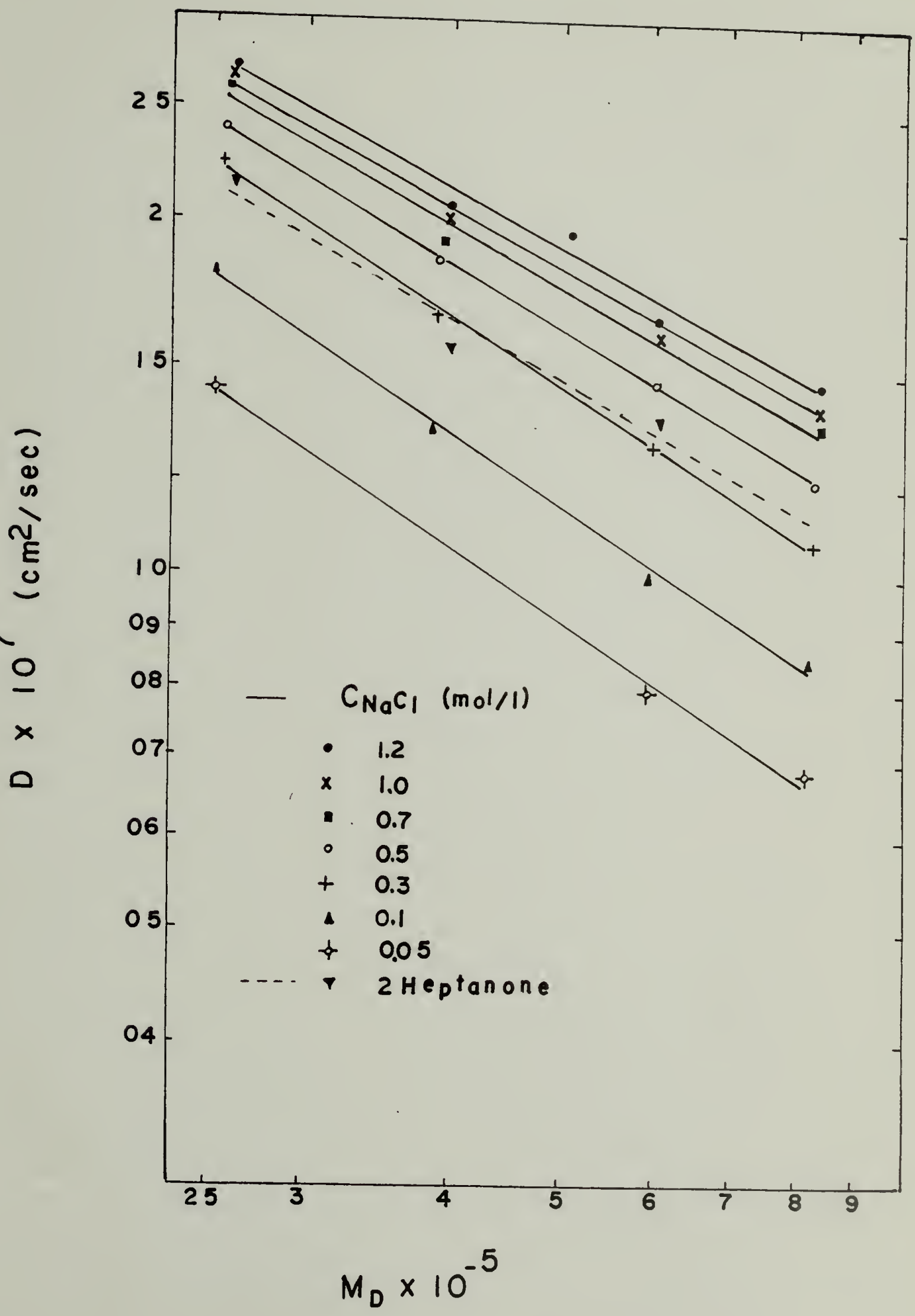
D x 10^7 (cm²/sec)
25
2
15
10
09
08
07
06
05
04
25
3
4
5
6
7
8
9
M_D x 10^-5
C_NaCl (mol/l)
1.2
1.0
0.7
0.5
0.3
0.1
0.05
2 Heptanone

highest molecular weight. Nagasawa and Eguchi (5), studying the polyelectrolyte Na-polystyrene sulfonate using sedimentation equilibrium also observed a curvature at high molecular weights in the corresponding sedimentation plots. In both cases the curvature was not observed in plots of $\ln[\eta]$ vs. $\ln M$. A comparison between values of b determined from the slopes of plots $\ln D_{z_o}$ versus $\ln M_D$ and those calculated from $3b = a + 1$ using values of a from Tan's intrinsic viscosity data of Table 5.3 is summarized in Table 6.2, where the value of the constant K_D is also listed. The agreement between the two methods is reasonable. An estimation of the errors contributing to the uncertainty in b can be obtained from standard error analysis, yielding

$$\frac{db}{b} = -\frac{dM}{M \ln M} + \frac{dD}{D \ln D/K} \cdot \qquad (6.6)$$

The biggest source of error is from uncertainties in the molecular weights as can be seen from Table 5.2. Using an uncertainty of 20% for this quantity and a value of 10% for that in D leads to only a 3% error in b. At the low ionic strengths, the error in D could be 30%, leading to an error in b of 6%. It should also be noted that changes in a are three times the corresponding change in b and so are inherently less sensitive to error. In addition, values of a calculated from $[\eta] = K_\eta M_w^a$ should be obtained using monodisperse molecular weight samples, but for polyelectrolytes these monodisperse samples actually have fairly broad molecular weight distributions with polydispersity indices of at least 1.5.

The derivation of the relation $3b = a + 1$ proceeds from the

TABLE 6.2

Comparison of Values of b Obtained Experimentally from $Dz_o = K_D M_D^{-b}$ and From The Relation $3b' = a+1$

	b (experimental)	b' (= $\frac{a+1}{3}$)	$K_D \times 10^4$
2 Heptanone	.53	.52	1.61
1.2 N NaCl	.51	.50	1.73
1.0 N NaCl	.53	.53	2.17
0.7 N NaCl	.54	.56	2.25
0.5 N NaCl	.57	.56	2.94
0.3 N NaCl	.62	.57	5.06
0.1 N NaCl	.63	.60	4.68
0.05 N NaCl	.64	.64	4.06

combination of Equations (3.56a) and (3.56b) with elimination of the radius of gyration between them. The result is

$$M^{a+1} = \Phi_0 (P_0)^{-3} \left(\frac{\alpha_\eta}{\alpha_f}\right)^3 K_\eta^3 \left(\frac{\eta_0 K_D}{T}\right)^{-3} M^{3b}. \qquad (6.7)$$

Thus the relation 3b = a + 1 is only true provided that α_η/α_f is not a function of M. Since α_η/α_f is a function of z which in turn is proportional to $M^{1/2}$, deviations should occur as the excluded volume parameter increases. Numerical calculations using the theoretical expressions for α_η and α_f at large excluded volume indicates that $(\alpha_\eta/\alpha_f)^3$ changes by 7% until 0.1N NaCl for the present system and jumps to 44% at 0.5N NaCl. Thus the only significant deviation from 3b = a + 1 should occur at the lowest ionic strength. However, experimentally, as can be seen from the variation in β (which is proportional to α_η/α_f) in Figure 6.10, the change in $(\alpha_\eta/\alpha_f)^3$ for the lowest ionic strength is about 25% which is within the experimental uncertainty under these conditions.

Survey of other literature comparisons of the values of b measured experimentally from diffusion measurements (obtained from either conventional diffusion studies or laser Rayleigh scattering) and theoretically from the relation 3b = a + 1 indicate that the agreement is within the presently obtainable accuracy of the diffusion measurements. The one exception is that of King et al. (9) whose values disagreed beyond experimental uncertainty.

Diffusion constant measurements, like the corresponding intrinsic viscosity data, can be used to obtain unperturbed dimensions of polymers. The problem of obtaining unperturbed dimensions from diffu-

sion constant measurements made under non theta conditions has been discussed in the literature (6,7) and the lack of agreement between $\langle S^2 \rangle_0^{1/2}$ obtained from laser light scattering and from conventional methods observed. There are two sources of error which can contribute to this disagreement. One is the previously discussed discrepancy between experimental and theoretical values of P, the multiplicative factor necessary to compare values of $\langle S^2 \rangle_0^{1/2}$ obtained by the two methods, which is observed even under theta conditions. The other is the extrapolation procedure chosen to obtain unperturbed dimensions from measurements made under non theta conditions. In addition to discussing the merits of the extrapolation methods used with diffusion constant data, these methods will be compared to their analogs in intrinsic viscosity studies.

The equivalent of the Stockmayer-Fixman intrinsic viscosity plots used in diffusion constant measurements is Equation (3.80). In Figure 6.14 are plots of $1/(D z_o M_D^{1/2})$ versus $M_D^{1/2}$ for the Na-copoly (ethyl acrylate-acrylic acid) samples under the ionic strength conditions studied. It should be remembered that both Stockmayer-Fixman plots and Equation (3.80) are derived for small excluded volume. Equation (3.83), applicable for large excluded volumes, is plotted in Figure 6.15 for the same data. The solid lines in both figures represent linear least square fits to the data. The fit is better to Equation (3.83) but the intercepts, at least in the ionic strength region greater than 0.1N, are closer together for Equation (3.80). Comparison of Figure 6.14 with the comparable intrinsic viscosity plots of Tan indicate that although there is more scatter to the points when fitted to a straight line for the former, the unperturbed dimensions obtained from the inter-

Figure 6.14

Plots of $(1/D_{z_o}M_D^{1/2})$ versus $M_D^{1/2}$ for the fractionated samples of Na-copoly (ethyl acrylate-acrylic acid) for the designated ionic strengths.

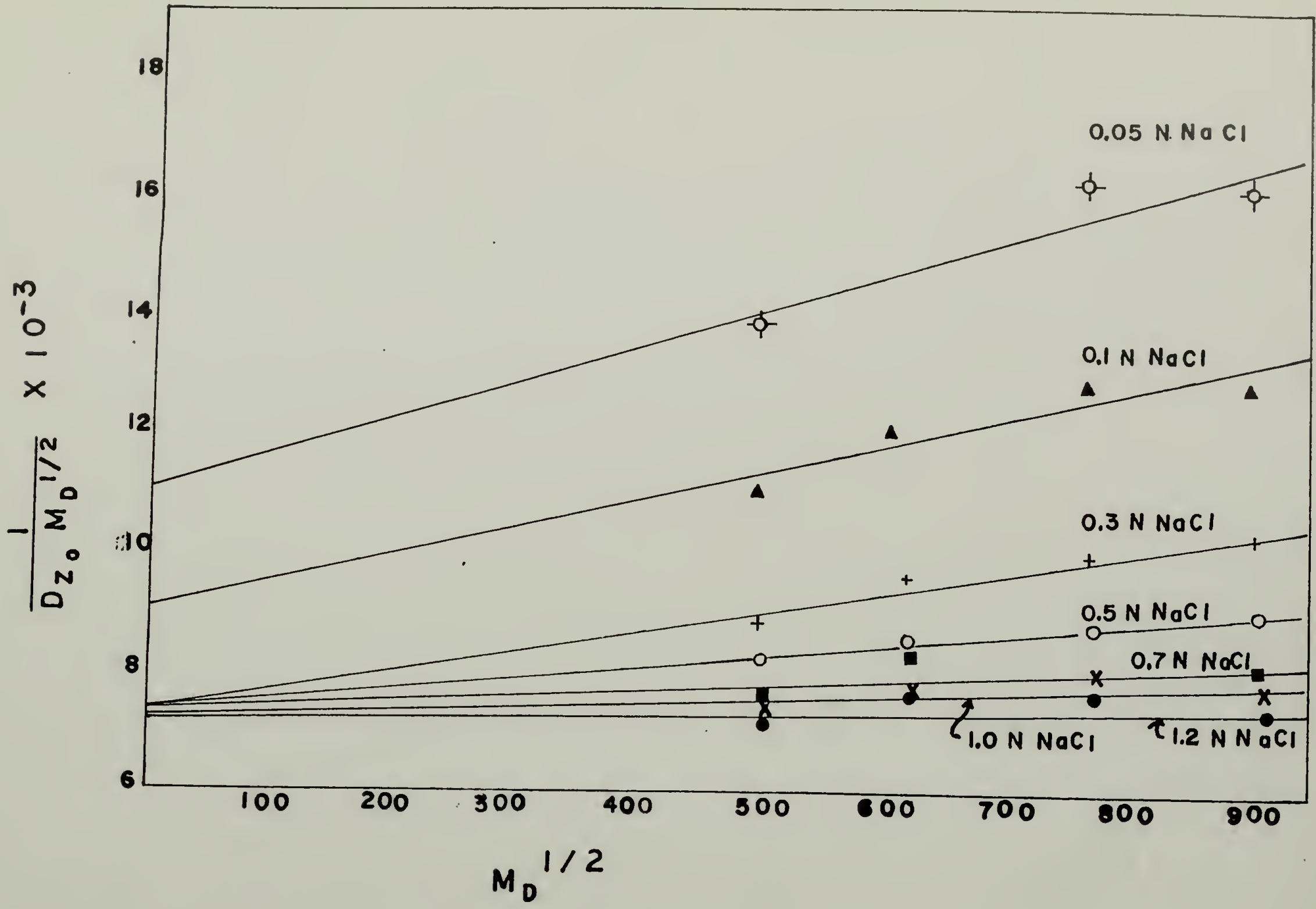
0.05 N Na Cl
0.1 N NaCl
0.3 N NaCl
0.5 N NaCl
0.7 N NaCl
1.0 N NaCl
1.2 N NaCl
18
16
14
12
10
8
6
100
200
300
400
500
600
700
800
900
$\frac{1}{D_{Z_o} M_D^{1/2}} \times 10^{-3}$
$M_D^{1/2}$

Figure 6.15

Plots of $(1/D_{z_o}^2 M_D)$ versus $D_{z_o}^3 M_D^2$ for the fracionated samples of Na-copoly (ethyl acrylate-acrylic acid) in the designated ionic strength solutions.

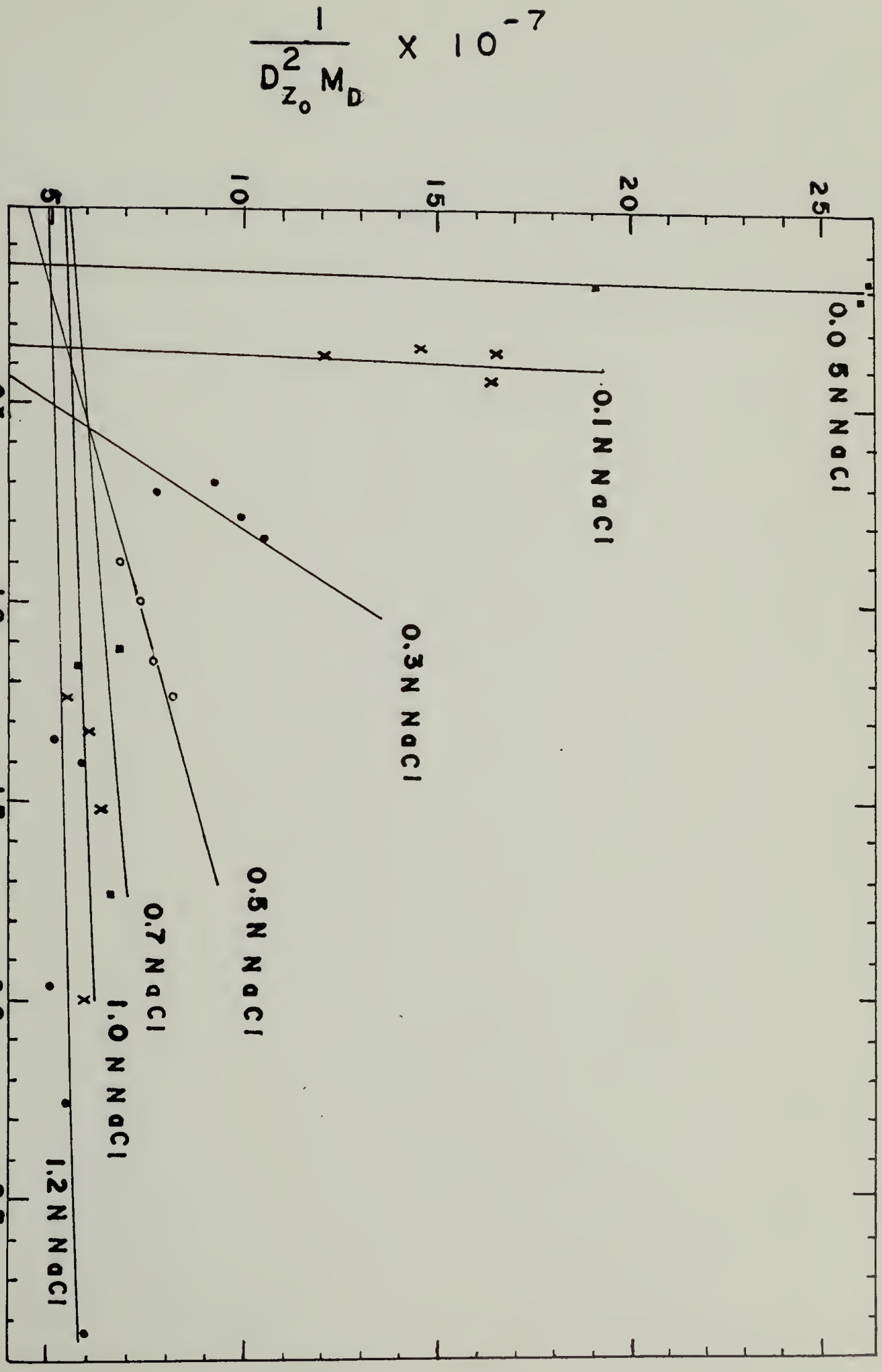
$\frac{1}{D_{z_o}^2 M_D} \times 10^{-7}$
$D_{z_o}^3 M_D^2 \times 10^9$
0.0 5 N NaCl
0.1 N NaCl
0.3 N NaCl
0.5 N NaCl
0.7 N NaCl
1.0 N NaCl
1.2 N NaCl
5
10
15
20
25
0.5
1.0
1.5
2.0
2.5

section of the lines for the ionic strength solutions greater than 0.1N NaCl are as close together as the ones from the intrinsic viscosity plots. Although the latter for this copolymer are all grouped together, it is not uncommon for there to be scatter or grouping of the points of intersection from intrinsic viscosity plots which have been interpreted as real differences in unperturbed dimensions. However, the noninter-section of the 0.1N and 0.05N ionic strength samples here in the diffusion constant plots is probably just due to the uncertainty in their diffu-sion constant measurements. Whereas there is no increased error in intrinsic viscosity measurements as the ionic strength is decreased (provided, as has been the case here, that kinetic energy corrections are negligible), the uncertainty in diffusion constant measurements does increase for reasons discussed earlier.

Over the narrow molecular weight range studied, Equations (3.80) and (3.83) are both well represented by straight lines when smoothed data calculations employing $D = K_D M^{-b}$ are used. However, this relation and Equation (3.83) are basically incompatible except for very large molecular extensions and under theta conditions as mentioned by Ford et al. (6). Over a large molecular weight range, Equations (3.80) and (3.83) become markedly curved, more so for larger volumes of b. In addition, the relation cannot be arbitrarily applied for calculations on low molecular weights before checking that it is in fact valid at these molecular weights.

The results of the present study therefore indicate that the best method of determining unperturbed dimensions is by the use of Equation (3.80), with the disagreement between light scattering and diffu-

sion constant measurements arising because of errors in theoretical estimates of P.

The limited information available from other polymer systems for which diffusion constant studies have been made yields conflicting evidence on this point. Analyzing the data of King et al. (8) on polystyrene in a theta solvent indicates that $P(\langle R\rangle_0^2/M)^{1/2}$ is greater than the value expected from light scattering. McDonnell and Jamieson (7) used Equation (3.80) on low molecular weight polystyrene fractions in a solvent for which b = .549 and similarly observed curvature in their plot. Since Equation (3.80) can contain higher order terms from the series expansion in z from which it was derived, McDonnell and Jamieson fitted their data to a parabola and obtained a value of $P(\langle R\rangle_0^2/M)^{1/2}$ only 12% greater than expected. In the last two cases it is of course impossible to separate out the contributions due to errors in P and extrapolation procedures. What is puzzling about the data is the lack of linearity in the plots, irrespective of the equation used; Ford's data (6), when replotted using Equation (3.80), also exhibits curvature. Over a similar molecular weight range, Stockmayer-Fixman plots of polystyrene in non theta solvents are linear. Since intrinsic viscosity and diffusion are both transport properties of polymers and since the expansion factors α_η and α_f are derived as functions of z (which is proportional to $M^{1/2}$ and B) using the same assumptions and approximations, and in fact are practically equivalent, Equation (3.80) and the Stockmayer-Fixman equation should be linear over approximately the same molecular weight region. Noting that $\alpha_\eta^3 = 1 + 1.06z$ and $\alpha_f = 1 + 0.609z$, it is possible that higher order terms, whose coefficients have not as yet been evalu-

ated, become important sooner for α_f, which would account for the curvature observed on the plots using Equation (3.80). In order to resolve this point, what is needed is a systematic study of α_f as a function of z. The widespread use of the Stockmayer-Fixman plot arises from the fortuitous approximate linearity of α_η^3 with z, over a range of z from 0 to 6. Even for larger z, if α_η^3 is approximately linear over some finite range of z, the result will be an equation formally similar to the Stockmayer-Fixman equation, with different slope and intercept. Due to the lack of accurate reliable diffusion data on polymer solutions the range of linearity between α_f and z is not known.

Plots of α_f versus z and α_η^3 versus z for values of z less than 12 (corresponding to ionic strength solutions greater than 0.1N) for this copolymer are shown in Figure 6.16. Values of z were obtained using light scattering data and Equation (3.102). The values of $\langle S^2 \rangle^{1/2}$ were calculated using the already smoothed data calculations of Table 5.5 which is the cause of the artifice in the "grouping" in the values of z. Nevertheless, both plots are reasonably well represented by straight lines, accounting for the linearity of both the Stockmayer-Fixman and diffusion constant plots. Thus the present data seems to confirm that unperturbed dimensions can be just as well obtained from diffusion constant plots as from Stockmayer-Fixman plots. Extending the studies to nonionic polymers is important at this point to establish the universality of the conclusions.

Perhaps one of the most important parameters obtained from diffusion constant measurements is the correction factor to the friction coefficient, k_f, the values of which for the present system are listed

Figure 6.16

Plots of the expansion factors α_f and α_η^3 as a function of the excluded volume parameter z for fractions of Na-copoly (ethyl acrylate-acrylic acid).

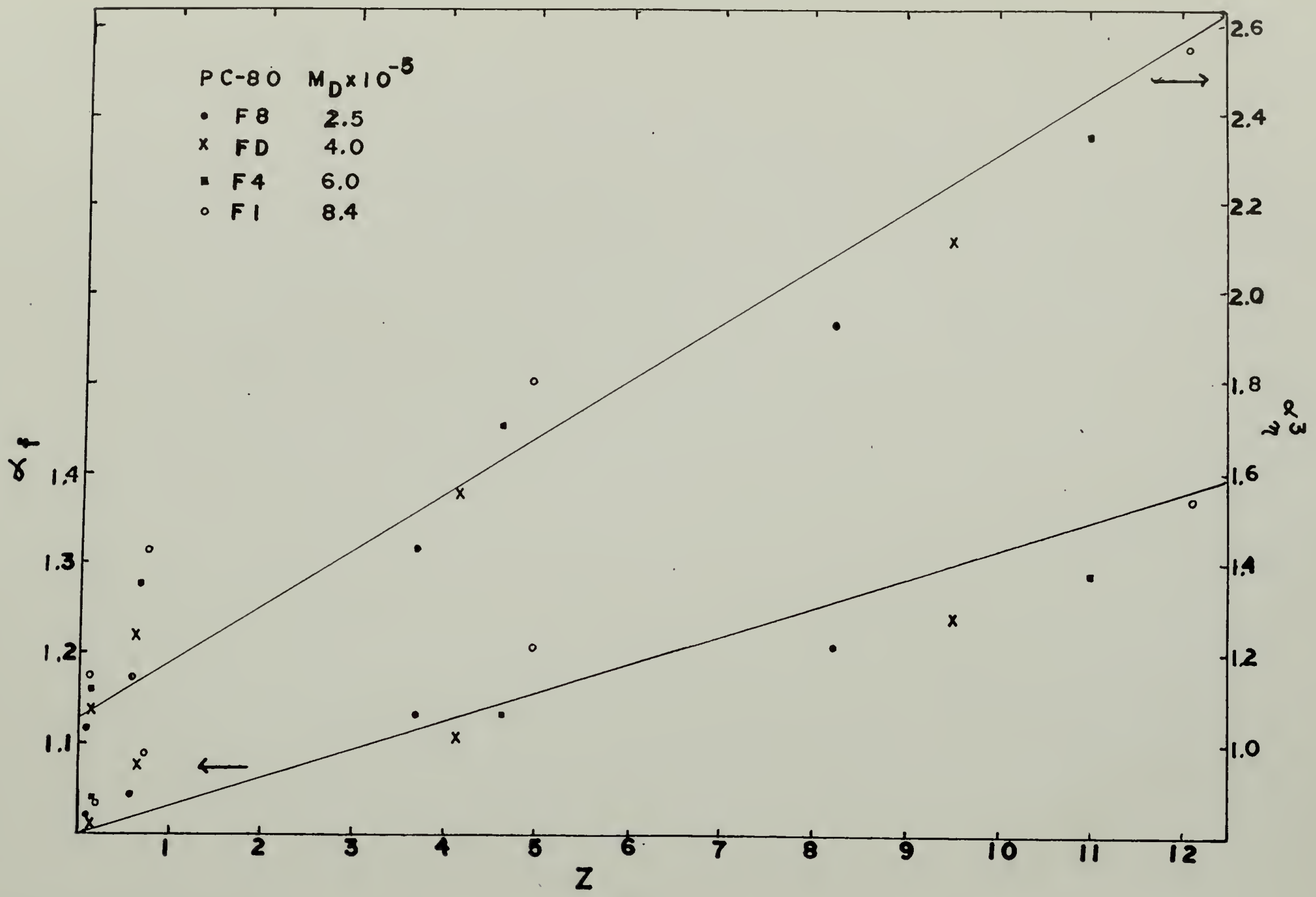
PC-80 $M_D \times 10^{-5}$
• F8 2.5
x FD 4.0
▪ F4 6.0
○ F1 8.4
γ_+
γ_-
Z
1.1
1.2
1.3
1.4
1.0
1.2
1.4
1.6
1.8
2.0
2.2
2.4
2.6
1
2
3
4
5
6
7
8
9
10
11
12

in Table 6.1, and plotted in Figure 6.17. The ease and rapidity with which diffusion constant measurements can now be made makes it possible to obtain values of k_f and make comparisons with the theories which have been advanced to predict them.

Before testing the various theories discussed in Chapter III, Concentration Dependence of Diffusion Constant, it should be pointed out that the values of k_f are very dependent on the second virial coefficients. The values listed in Table 6.1 were obtained using the slopes of D versus concentration plots and A_2 either through $(1 + 2MA_2c)/(1 + k_f^c c)$ or the approximation that this quantity is equal to $[1 + (2MA_2 - k_f)c]$. The uncertainty in A_2 is 10% and the uncertainty in the slope is about 30%, making the uncertainty in k_f^c about 40%.

The theory proposed by Yamakawa, as discussed in Chapter III, Concentration Dependence of Diffusion Constant, is suitable only for small values of excluded volume. It equates k_f^c to the quantity $\lambda(\bar{z})A_2M$. The parameter $\lambda(\bar{z})$ is tabulated for values of $\bar{z} = z/\alpha_s^3$ ranging from 0 to 1.2 with $\lambda(\bar{z})$ decreasing from 1.345 to 1.06. This covers the range of excluded volume estimated by Yamakawa to be suitably small. Using values of z and α_s from Tan's light scattering data, $\bar{z} = 1.2$ corresponds to a value of ionic strength between 0.7N and 0.5N NaCl, indicating that the theory should only be applicable for ionic strengths greater than 0.5N NaCl for the system Na-copoly (ethyl acrylate-acrylic acid). This corresponds to a value of b of about .54. It is important to be aware of this range of applicability. King et al. (9) and McDonnell and Jamieson (7) applied it to systems with values of b of .56 and .55 respectively, which might or might not have been ac-

Figure 6.17

The correction factor to the frictional coefficient k_f^c versus ionic strength for fractions of Na-copoly (ethyl acrylate-acrylic acid).

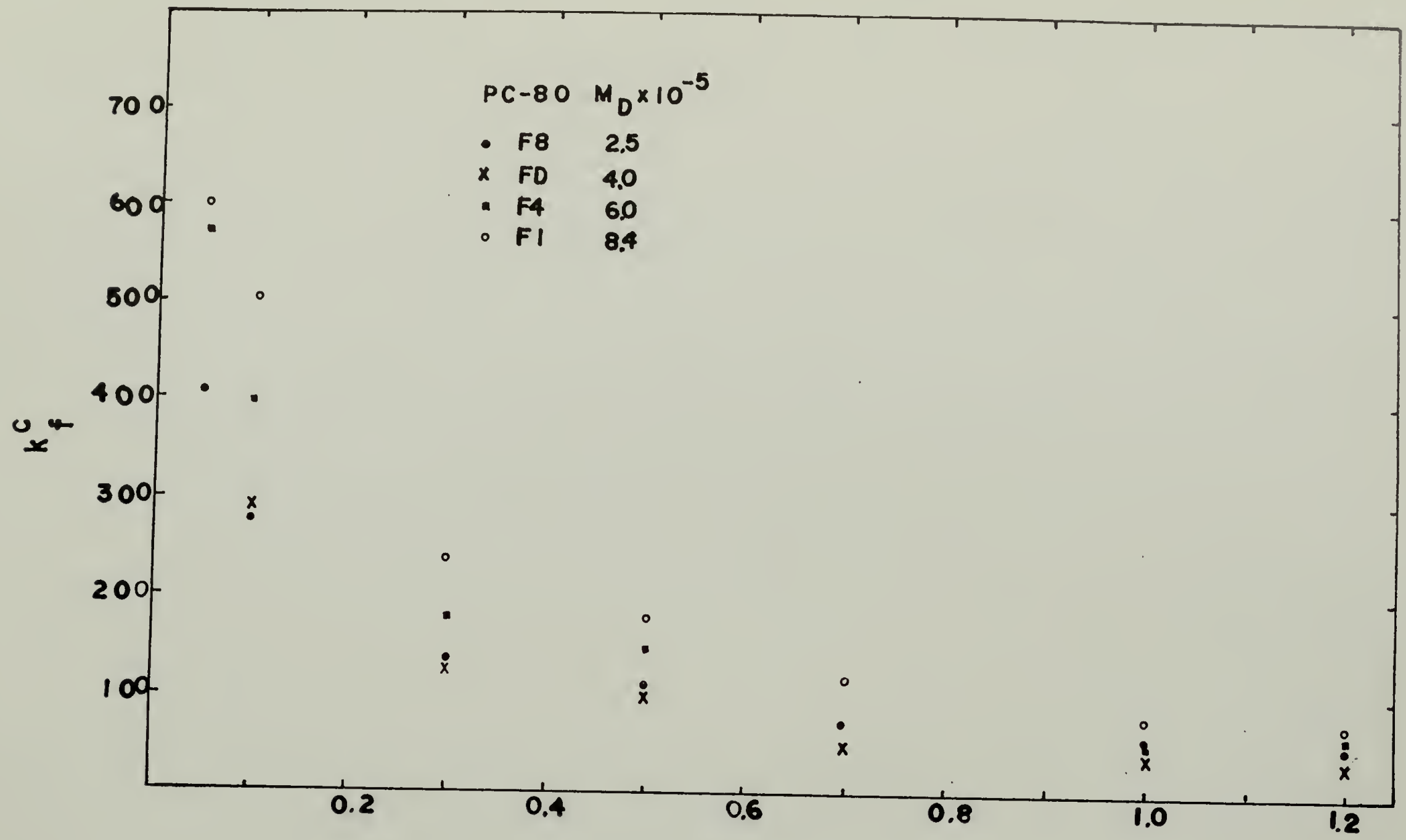
PC-80 $M_D \times 10^{-5}$
• F8 2.5
x FD 4.0
▪ F4 6.0
○ F1 8.4
k_f^c
700
600
500
400
300
200
100
0.2
0.4
0.6
0.8
1.0
1.2
Ionic Strength C_{NaCl} (mol/l)

ceptable.

Table 6.3 is a comparison of experimental values of k_f^c with ones calculated from Equation (3.109). The values predicted theoretically are all too low by at least 100%. In addition, k_f^c determined experimentally in a theta solvent is clearly positive whereas Yamakawa predicts a zero value.

The theory derived by Imai relates k_f^c to the viscosity expansion factor α_η so that $k_f^c = C_0 M_\eta^{1/2} (\alpha_\eta - \alpha_\eta^{-1})$. Here $M_\eta^{1/2}$ is the correct molecular weight average to use and is given by Equation (3.115). Using values of α_η from Tan's viscosity data, experimental values of k_f^c are plotted against $M_\eta^{1/2} (\alpha_\eta - \alpha_\eta^{-1})$ in Figure 6.18. The solid line represents a linear least squares fit of the data, which appears to be reasonably well represented by a straight line. Again, according to Imai, the intercept is predicted to be zero, however, there is clearly a non zero intercept. The value of the slope, C_0, which is related to the unperturbed dimensions is about 16% lower than that of the experimental value of the polystyrene samples used to compare theory and experiment in Imai's paper. Thus, values of k_f^c for the present polyelectrolyte system are the same order of magnitude as those obtained in nonionic polymers.

The theory of Pyun and Fixman predicts a non zero value for k_f^c in a theta solvent and so is in agreement with the results of this study. Comparison of the experimental values with those calculated according to Equation (3.94),

$$k_f^c = k_f^\phi \frac{4\pi R_H^3 N_A}{3M_f}$$

TABLE 6.3

Comparison of Experimental Values of k_f^c with Predictions of Yamakawa, and Pyun and Fixman

	Ionic Strength (N NaCl)	k_f^c (experimental)	$k_f^c = \lambda(\bar{z})A_2M_w$	$k_f^c = \frac{k_f\Phi 4\pi R_H^3 N_A}{3M_f}$
PC-80 F8				
$M_D = 2.5 \times 10^5$	1.2	56.7	0	10.7
	1.0	60.8	8.7	17.0
	.7	76.4	14.8	26.5
	.5	112.7		43.3
	.3	137.4		57.1
	.1	278.7		117.5
	.05	420.1		233.6
PC-80 FD				
$M_D = 4.0 \times 10^5$	1.2	29.2	0	15.8
	1.0	43.8	11.4	24.3
	.7	52.6	19.3	41.0
	.5	102.1		59.7
	.3	126.2		90.2
	.1	290.8		188.8
PC-80 F9				
$M_D = 5.1 \times 10^5$	1.2	50.6	0	14.2
PC-80 F4				
$M_D = 6.0 \times 10^5$	1.2	61.0	0	19.5
	1.0	64.2	14.7	33.3
	.5	147.8		78.6
	.3	177.9		122.0
	.1	394.8		278.4
	.05	569.4		573.8
PC-80 F1				
$M_D = 8.4 \times 10^5$	1.2	74.2	0	20.3
	1.0	80.3	18.2	36.6
	.7	120.1	30.8	59.8
	.5	180.0		99.7
	.3	237.3		156.4
	.1	501.9		321.8
	.05	601.8		642.0

Figure 6.18

Plot of k_f^c versus $M_\eta^{1/2}(\alpha_\eta - \alpha_\eta^{-1})$ for fractions of Na-copoly (ethyl acrylate-acrylic acid) which is predicted to be linear according to theory of Imai.

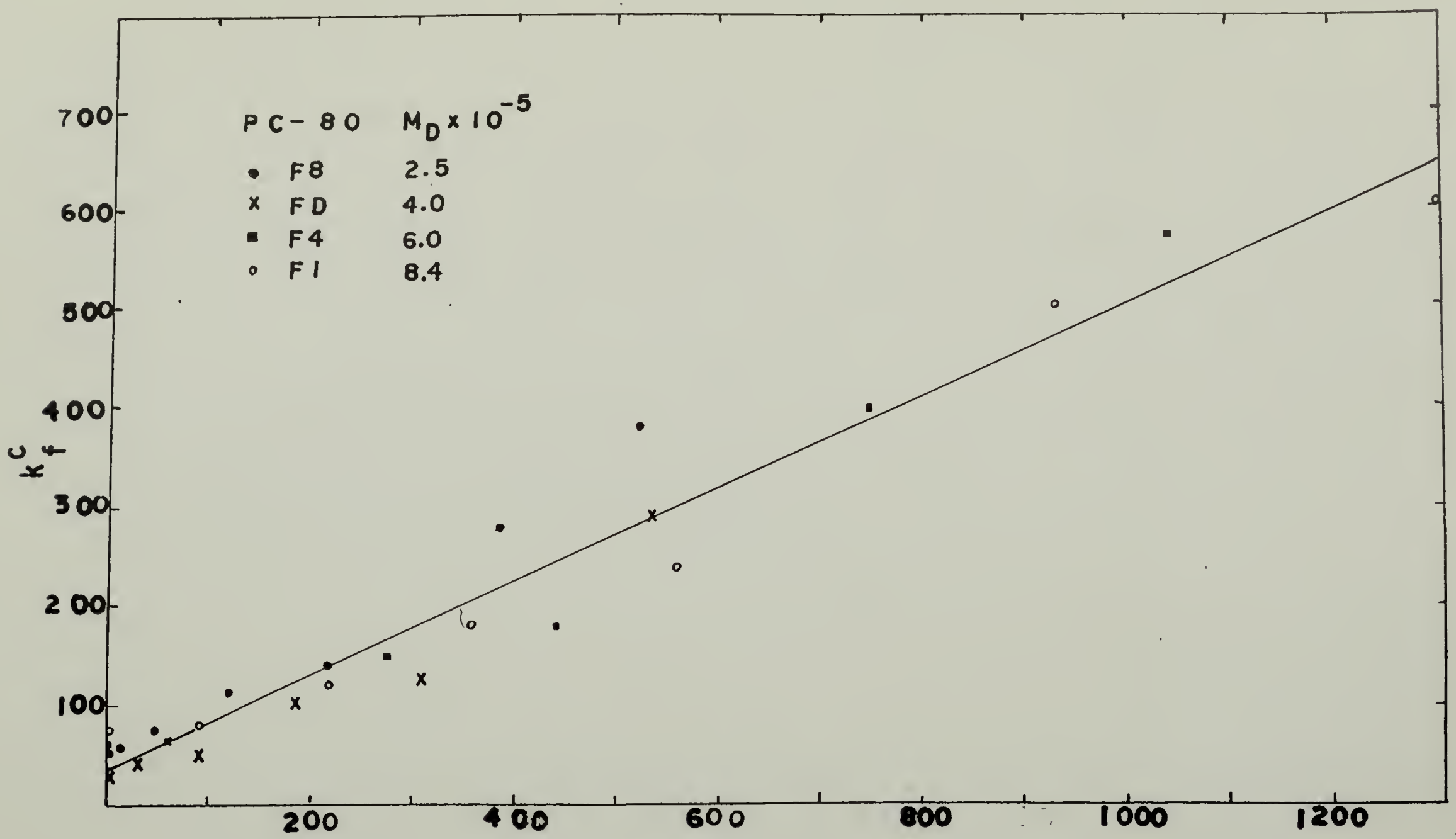
PC-80 $M_D \times 10^{-5}$
• F8 2.5
× FD 4.0
▪ F4 6.0
○ F1 8.4
k_f^c
700
600
500
400
300
200
100
200
400
600
800
1000
1200
$M_\eta^{1/2}(\alpha_\eta - \alpha_\eta^{-1})$

where $k_f^{\phi} = [7.16 - K(A)]$, is complicated by the need to evaluate k_f^{ϕ} and the necessity of using the experimental value of R_H in the calculation. In order to evaluate K(A), Equation (3.95) or Figure 3.1 was used. The quantity A in turn was calculated from a modified form of Equation (3.97),

$$A = 3\pi^{1/2} z \left(\frac{\langle s^2 \rangle_0^{1/2}}{R_H}\right)^3.$$

Here, unperturbed radii of gyration were obtained from Tan's light scattering data and values of z were also calculated from light scattering data using Equation (3.102). Values of R_H used were those obtained experimentally from diffusion data. Table 6.3 lists values of k_f^c obtained this way as well as values obtained experimentally. The calculated values increase with molecular weight at a given ionic strength as well as increasing with ionic strength for a given molecular weight. These trends also apply to the experimental values except those of the lowest molecular weight sample whose values of k_f^c are larger than expected. That the lowest molecular weight sample has abnormally large values of k_f^c can be seen almost by inspection of the raw data of Figure 6.1, where the slopes of the D versus c curves are much steeper than those for the other fractions. To obtain a smaller value of k_f^c would have meant that a larger value of A_2 would have had to been used in the data analysis. However, smoothed data calculations using $A_2 = aM_w^{-\delta}$ were employed in the analysis rather than real data, and as noted by Tan and others, the errors in the light scattering data increase at these low molecular weights. It is interesting to note that McDonnell and Jamie-

son also observed an anomolously high value of k_f^c for their lowest molecular weight sample which they could not explain theoretically and so consigned the observation to experimental error.

Comparing the magnitude of k_f^c obtained experimentally and theoretically, it is seen from Table 6.3 that except in a theta solvent, the errors are on the order of 30-50%, with the experimental values being larger than the ones predicted by Pyun and Fixman. For this polyelectrolyte system at least, these errors lie within the experimental uncertainties of the measurements needed to obtain k_f^c.

Graphically, it is easier to compare theory and experiment by comparing values of k_f^ϕ. As can be seen from Figure 6.19, k_f^ϕ predicted by Pyun and Fixman increases with decreasing ionic strength and levels off below 0.5N NaCl. This is the general trend of the experimental data, except that the data is more erratic and exhibits a decrease at 0.05N NaCl. In addition, it is obvious that the absolute magnitude of k_f^ϕ is larger for the experimental values. Analyzing the data of McDonnell and Jamieson on polystyrene fractions in THF, their experimental values of k_f^ϕ are low by between 20 and 100%. King et al. (9) used incorrect equations to obtain their values of k_f^ϕ so they cannot be used for comparison here.

Another test of the theory of Pyun and Fixman is a plot of $[k_f^c - (k_f^c)_\theta]$ versus $M_\nu A_2$ which according to Equation (3.108) should be linear for small values of $M_\nu A_2$. Figure 6.20 demonstrates that for the Na-copoly (ethyl acrylate-acrylic acid) system studied, the plot is linear for all conditions except the 2 highest molecular weights at 0.05N NaCl. It is interesting to observe that when the calculations for k_f

Figure 6.19

The correction factor to the frictional coefficient, k_f^{ϕ} when polymer concentration expressed as a volume fraction as a function of ionic strength for fractions of Na-copoly (ethyl acrylate-acrylic acid).

---- Theoretical prediction of Pyun and Fixman:

$k_f^{\phi} = [7.16 - K(A)]$

where K(A) found using Figure 3.1 or Equation (3.95).

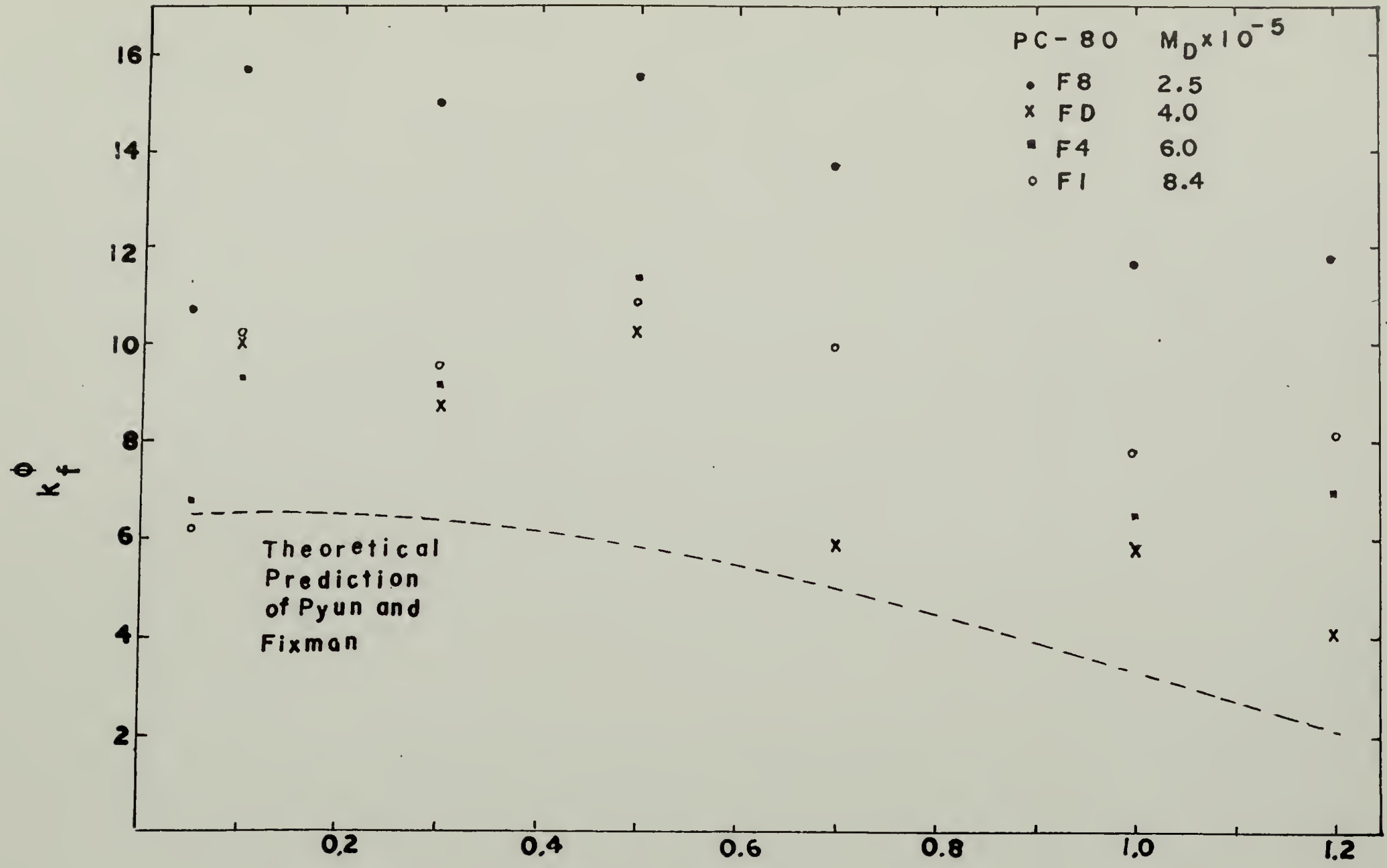
PC-80 $M_D \times 10^{-5}$
• F8 2.5
x FD 4.0
▪ F4 6.0
○ F1 8.4
Theoretical Prediction of Pyun and Fixman
Φ_{Kf}
16
14
12
10
8
6
4
2
0.2
0.4
0.6
0.8
1.0
1.2
Ionic Strength C_{NaCl} (mol/l)

Figure 6.20

Plot of $k_f^c - (k_f^c)_\theta$ versus $M_\nu A_2$ for fractions of Na-copoly (ethyl acrylate-acrylic acid) to test linear relationship predicted by Pyun and Fixman. Here values of k_f^c are those observed experimentally.

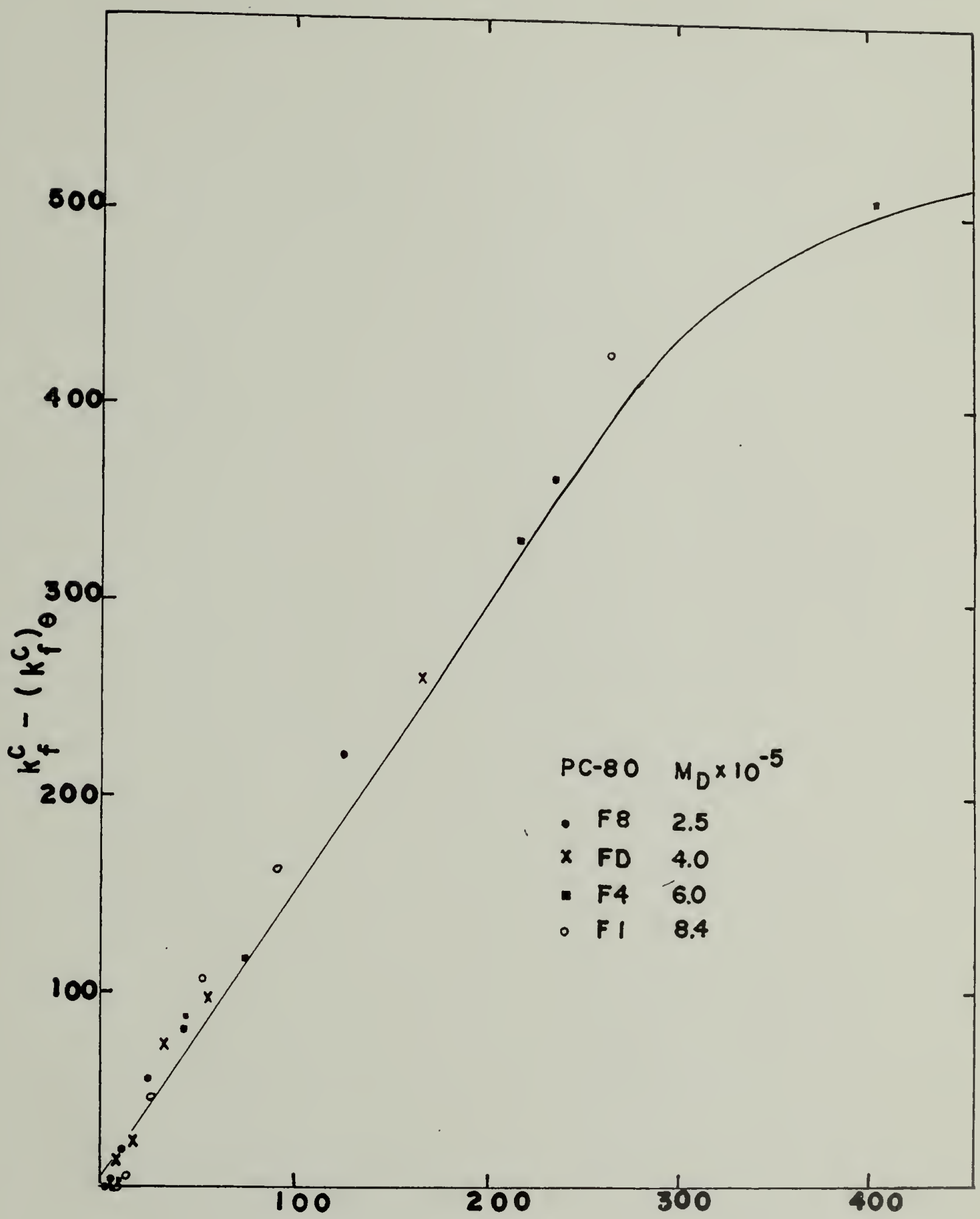
500
400
300
200
100
100
200
300
400
$k_f^c - (k_f^c)_\theta$
PC-80 $M_D \times 10^{-5}$
• F8 2.5
x FD 4.0
▪ F4 6.0
○ F1 8.4

$M_\nu A_2$

are made with data taken only from light scattering data (that is using $R_H = P/\langle S^2\rangle^{1/2}/6^{1/2}\pi$ and theoretical values of P), plots of $k_f^c - (k_f^c)_\theta$ are linear over a much smaller range as can be observed in Figure 6.21.

The theory of Pyun and Fixman also predicts that for a theta solvent a plot of $(k_f^c)_\theta$ versus $M_\eta^{1/2}$ should be linear. Figure 6.22 demonstrates this is so although there is scatter in the points. The solid line is a linear least squares fit of the data. Also in the figure is the same plot using calculated values of k_f^c which has less scatter in the data points and whose least squares fit of the data goes through the origin.

As can be seen from the raw data of Figures 6.1, there is a change in slope of $k_D = 2MA_2 - k_f^c$ as a function of ionic strength and molecular weight. The crossover occurs at lower ionic strengths as the molecular weight is decreased. The lowest molecular weight sample in fact has no crossover point at all. While it is impossible to predict the exact ionic strength at which the crossover occurs for a given molecular weight without knowing a priori the functional form of k_f^c and A_2 it is possible to verify that qualitatively the trend occurs in the right direction. Using the relatively simple expression of Yamakawa that $k_f^c = \lambda(\bar{z})MA_2$, the expression for k_D becomes $K_D = MA_2[2 - \lambda(\bar{z})]$ and k_D goes to zero sooner as $\lambda(\bar{z})$ increases. Now $\lambda(\bar{z})$ is a decreasing function of z and thus a decreasing function of A_2. Since A_2 is for a given ionic strength greater for smaller values of molecular weight, k_D goes to zero sooner for higher molecular weights as is observed.

While the testing of the two parameter theory of polymer solutions using diffusion constant measurements made possible by the recent

Figure 6.21

Plot of $k_f^c - (k_f^c)_\theta$ versus $M_\nu A_2$ for fractions of Na-copoly (ethyl acrylate-acrylic acid). Here values of k_f^c are calculated from data obtained exclusively from conventional light scattering.

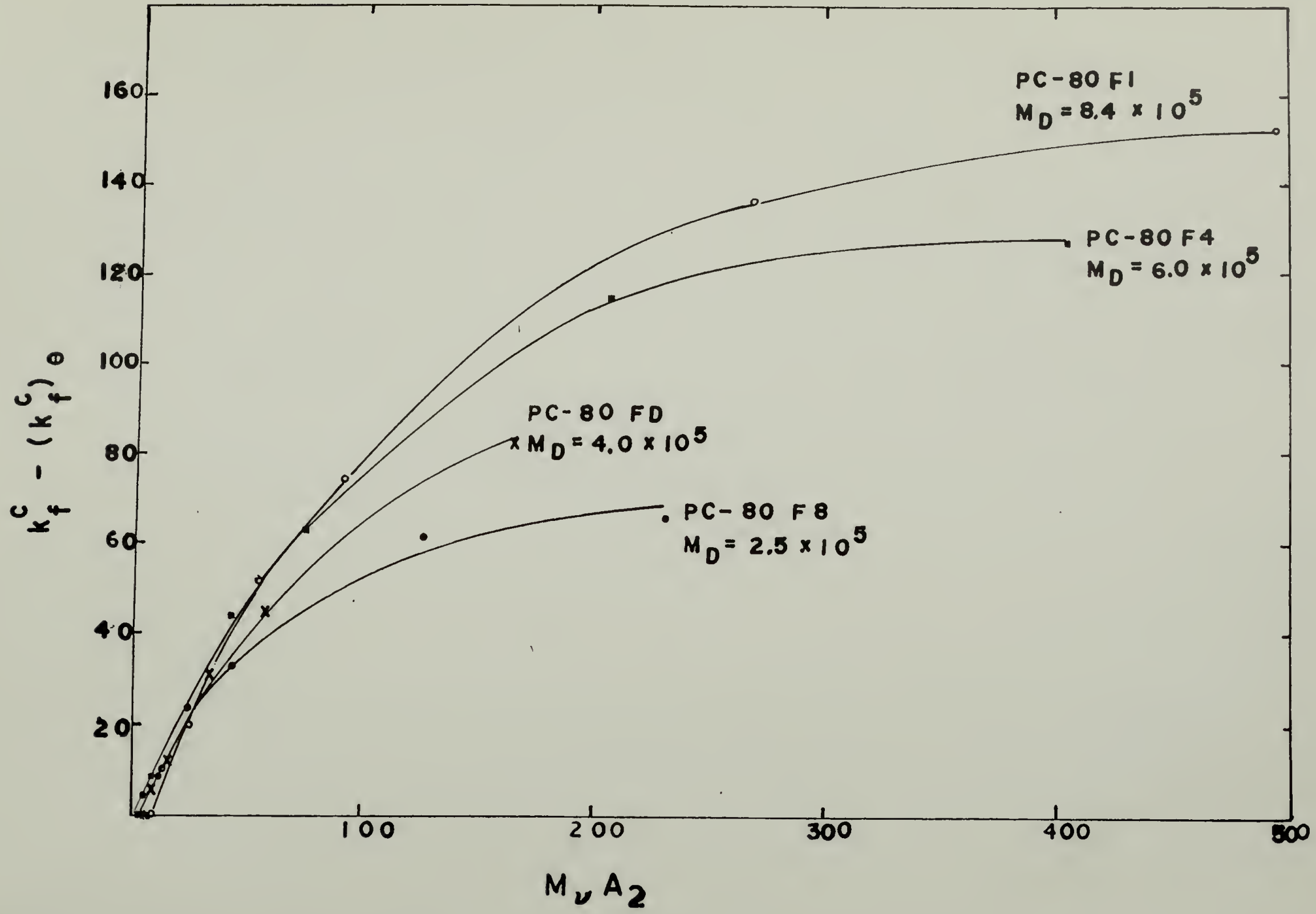
PC-80 F1
$M_D = 8.4 \times 10^5$
PC-80 F4
$M_D = 6.0 \times 10^5$
PC-80 FD
$M_D = 4.0 \times 10^5$
PC-80 F8
$M_D = 2.5 \times 10^5$
$[C/(k_f)_\theta] - 1$
$M_w A_2$
160
140
120
100
80
60
40
20
100
200
300
400
500

Figure 6.22

Correction factor to the frictional coefficient at the theta point, $(k_f^c)_\theta$, plotted versus $M_\eta^{1/2}$ for fractions of Na-copoly (ethyl acrylate-acrylic acid).

- Solid circles are experimental data points.

- Open circles are calculated values of $(k_f^c)_\theta$ from

$$k_f^c = [7.16 - K(A)] \frac{4\pi R_H^3 N_A}{3M_f}$$

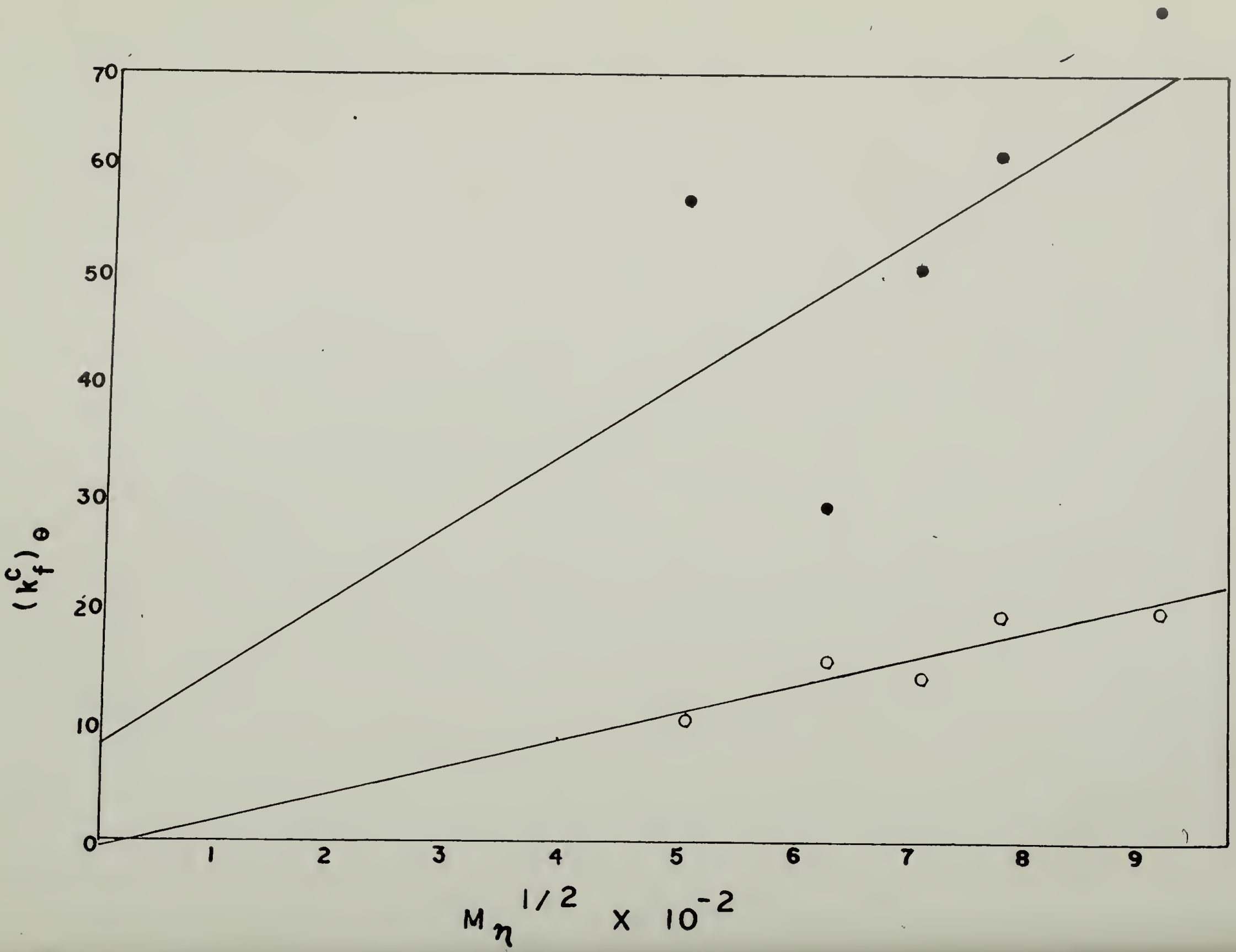
70
60
50
40
30
20
10
0
1
2
3
4
5
6
7
8
9
$(k_f^c)_\theta$
$M_\eta^{1/2} \times 10^{-2}$

accessibility of laser Rayleigh scattering is in itself of interest, the use of the technique to study conformational transitions of polyelectrolytes was the original purpose of the experiment. As was confirmed by Lee et al. (10), the helix coil transition of poly α-benzyl-L-glutamate could be observed as a function of pH by measurements of the diffusion constants. In the present system, Na-copoly (ethyl acrylate-acrylic acid), the presence of hydrophobic side groups as well as charged groups along the chain suggested the possibility of a cooperative transition as a function of ionic strength. Chapter IV, Na-copoly (ethyl acrylate-acrylic acid), reviews the evidence which has been accumulated by other methods supporting this idea.

Figure 6.23 is a plot of the infinite dilution value of the diffusion constant as a function of ionic strength and Figure 6.24 is the hydrodynamic radius as a function of this same quantity. It is not apparent from these plots that a transition takes place. There is a change in slope somewhere between 0.2 and 0.5N NaCl which suggests that there is a change from an extended to a compact random coil as the ionic strength is increased. This is the same type of behavior which was observed using light scattering and intrinsic viscosity, both of which also measure some size parameter of the polymer. However, it should be emphasized that this phenomenon is not a true cooperative transition, where sigmoidal behavior would be expected. It was not possible to obtain conditions such that in the low ionic strength region there was a flattening of the curves D or R_H versus I so that the total curve would be sigmoidal. Aside from this point the analysis of the diffusion constant measurements was hindered by the polydispersity of the samples and

Figure 6.23

Plots of D_{z_o} as a function of ionic strength for fractions of Na-copoly (ethyl acrylate-acrylic acid).

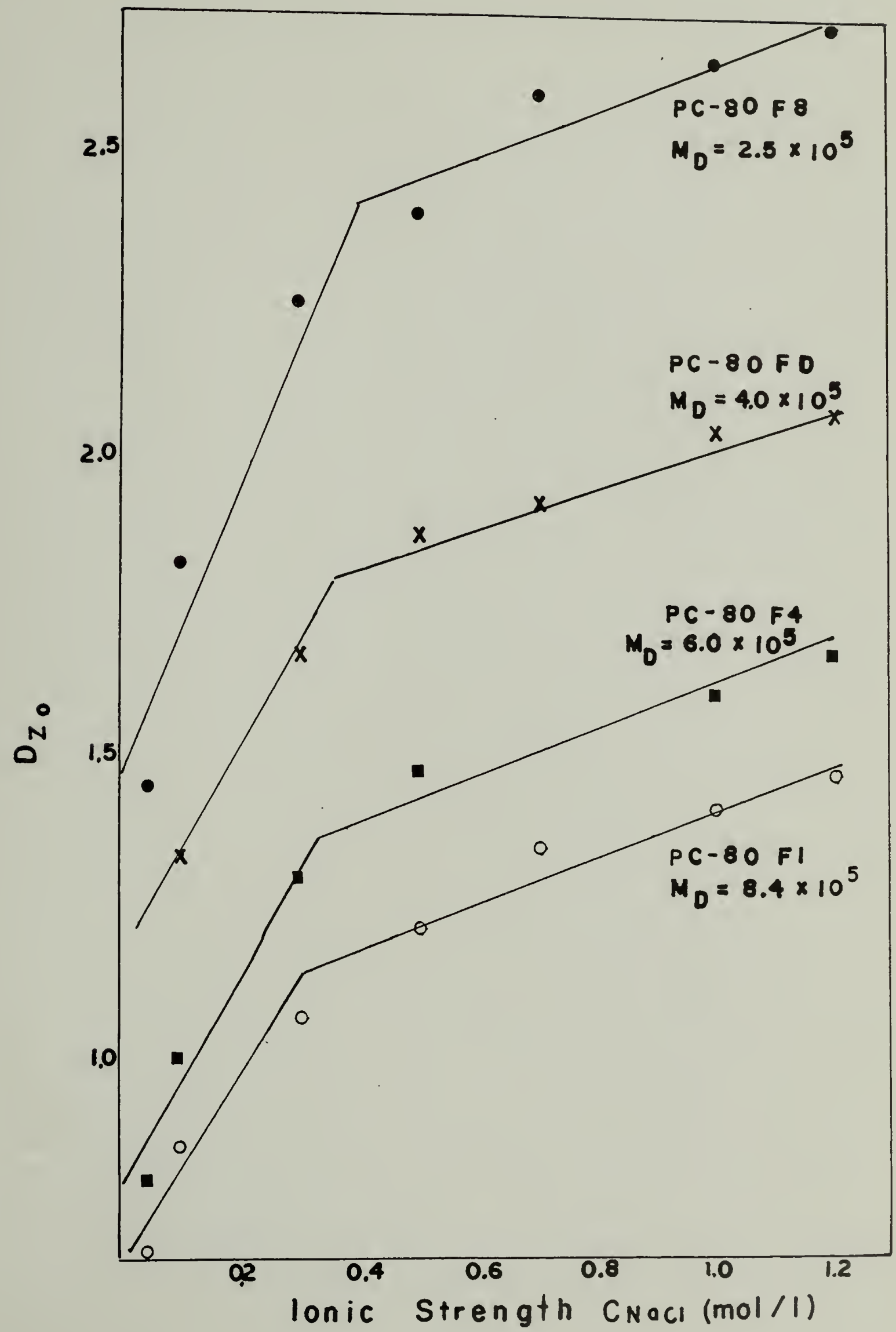
PC-80 F8
$M_D = 2.5 \times 10^5$
PC-80 FD
$M_D = 4.0 \times 10^5$
PC-80 F4
$M_D = 6.0 \times 10^5$
PC-80 F1
$M_D = 8.4 \times 10^5$
D_{Z_0}
2.5
2.0
1.5
1.0
0.2
0.4
0.6
0.8
1.0
1.2
Ionic Strength C_{NaCl} (mol/l)

Figure 6.24

Plots of hydrodynamic radius, R_H, as a function of ionic strength for fractions of Na-copoly (ethyl acrylate-acrylic acid).

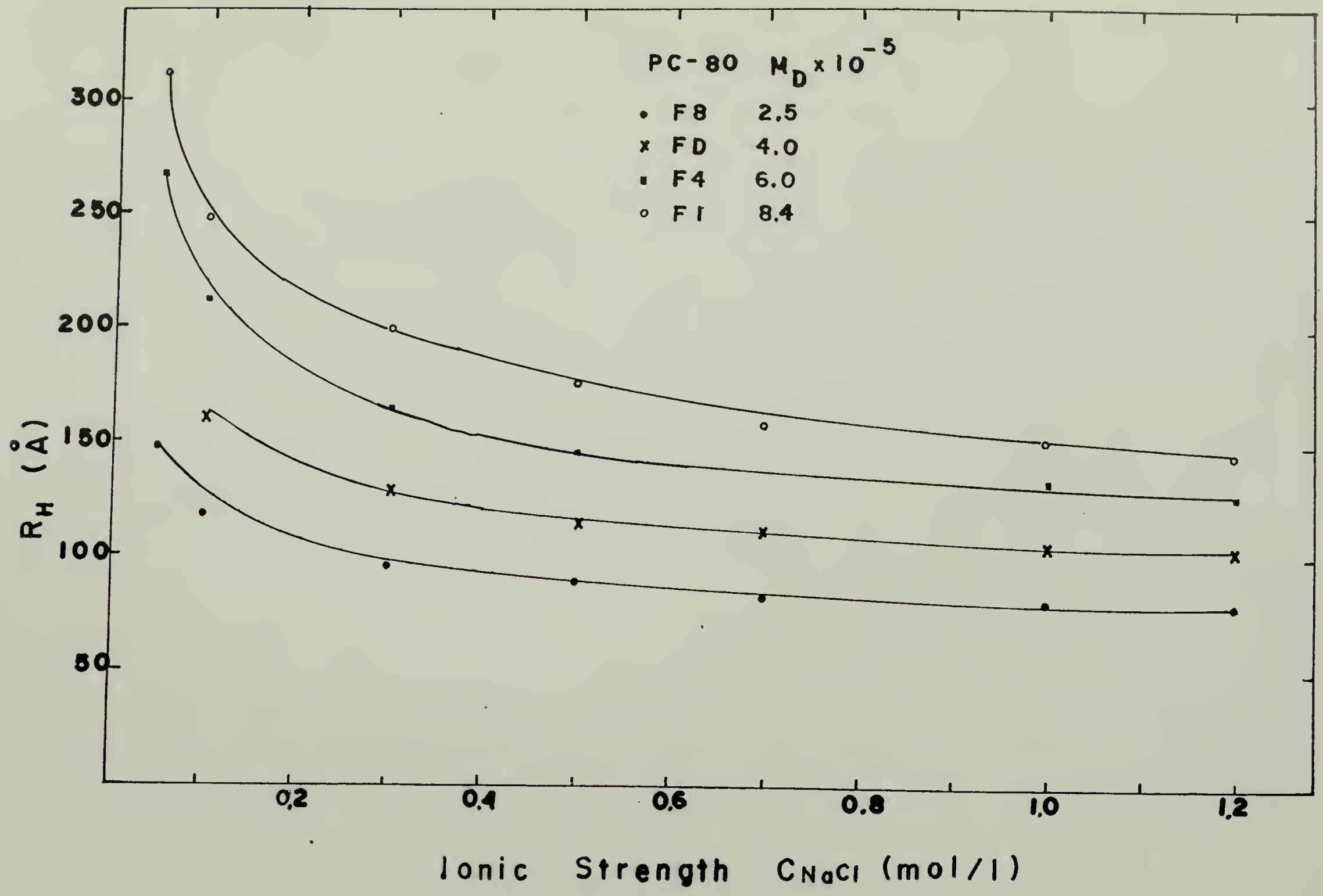
PC-80 $M_D \times 10^{-5}$
• F8 2.5
x FD 4.0
▪ F4 6.0
○ F1 8.4
300
250
200
150
100
50
R_H (Å)
0.2
0.4
0.6
0.8
1.0
1.2
Ionic Strength C_{NaCl} (mol/l)

the approximate method which had to be developed to account for it. In Lee's study as well as most others not directly concerned with polydispersity itself, very monodisperse samples were used. The lack of a sharp change in slope in the D or R_H versus I curves compared to the corresponding ones from light scattering and intrinsic viscosity is probably due to the uncertainty introduced by the not completely satisfactory handling of the polydispersity effects.

Nevertheless, the change in slope becomes more apparent in plots of R_H versus ln I, Figure 6.25, and is especially clear in Figure 6.26, the plot of α_f versus ln z, where ln z is proportional to ln I. Some of Tan's data are also log-log or semi-log plots of the intrinsic viscosity or light scattering data and serve to enhance the change in slope. However there is no theoretical justification of this procedure.

Comparison of the diffusion constants measured in the aqueous theta solvent, 1.2N NaCl and the organic theta solvent, 2-heptanone, indicate that the hydrodynamic radii are larger in the latter than the former by a factor of about 1.3. This is in confirmation of the same phenomenon observed on measurements of the radii of gyration and hydrodynamic radii from the intrinsic viscosity and light scattering data of Tan.

In conclusion, the technique of intensity fluctuation spectroscopy has the potential of being an invaluable tool in the characterization of polymer solutions although the problem of handling polydispersity effects, especially when they are large, has not been adequately resolved. Nevertheless, in the present experiments, despite this difficulty, the diffusion constant measurements could be success-

Figure 6.25

Plots of the hydrodynamic radius, $R_H(\mathring{A})$, versus logarithm of the ionic strength for four fractions of Na-copoly (ethyl acrylate-acrylic acid).

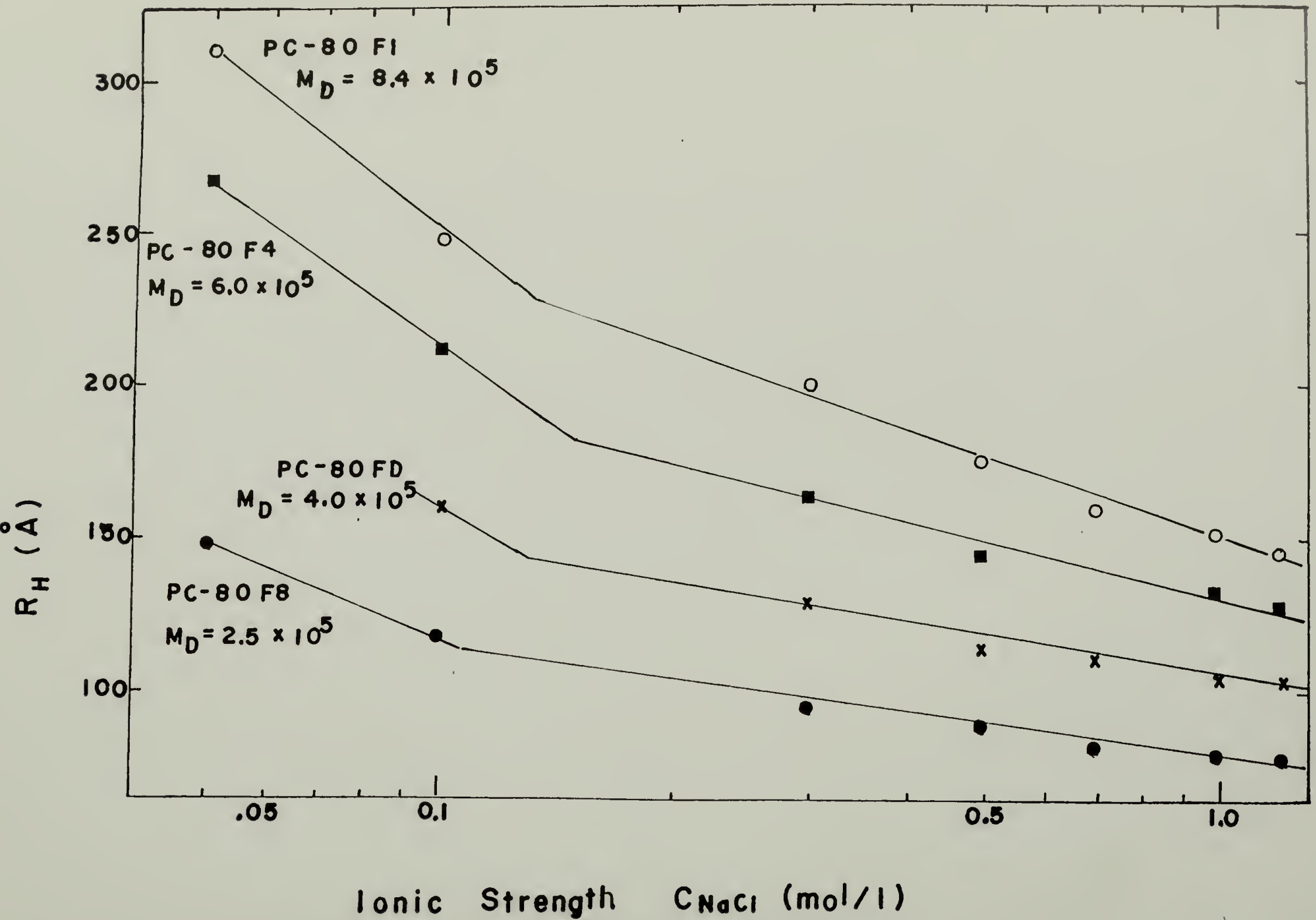
PC-80 F1
$M_D = 8.4 \times 10^5$
PC-80 F4
$M_D = 6.0 \times 10^5$
PC-80 FD
$M_D = 4.0 \times 10^5$
PC-80 F8
$M_D = 2.5 \times 10^5$
300
250
200
150
100
R_H (Å)
.05
0.1
0.5
1.0
Ionic Strength C_{NaCl} (mol/l)

Figure 6.26

The expansion factors α_f and α_η^3 versus $\ln z$ for fractions of Na-copoly (ethyl acrylate-acrylic acid) where $\ln z$ is proportional to $\ln I$. Here z is the excluded volume parameter and I is the ionic strength.

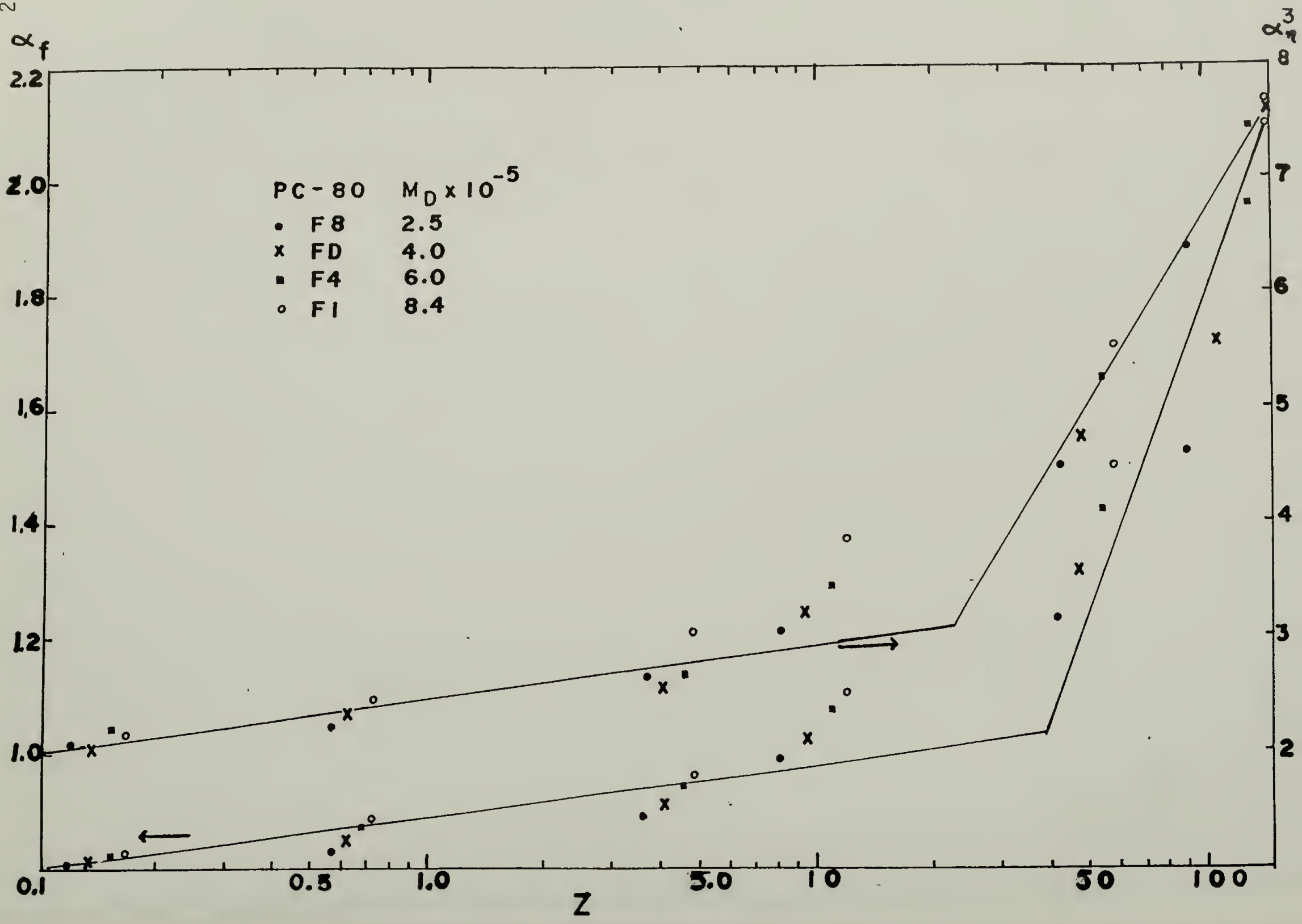
α_f
α_s^3
PC-80 $M_D \times 10^{-5}$
• F8 2.5
x FD 4.0
▪ F4 6.0
○ F1 8.4
2.2
2.0
1.8
1.6
1.4
1.2
1.0
8
7
6
5
4
3
2
0.1
0.5
1.0
5.0
10
50
100
Z

fully analyzed to obtain information on the conformational changes in Na-copoly (ethyl acrylate-acrylic acid), the two parameter theory of polymer solutions and the ionic atmosphere around polyions.

Conclusions

The analysis of the diffusion constant measurements of Na-copoly (ethyl acrylate-acrylic acid) lead to several conclusions on the behavior of the polymer which will be summarized here.

It was found that the polydispersity index of the fractions in a theta solvent could be correlated with the fractional increase in the extrapolated z average diffusion constant over that obtained at very long sample times. The results agreed well with a theory derived by Ford.

The values of b in the relation $D = KM^{-b}$ were obtained experimentally from log-log plots and were found to agree within experimental error with the values calculated from the relation $3b = a + 1$, where the Mark-Houwink exponents used were from Tan's intrinsic viscosity data.

The proportionality factor P_0 relating the radius of gyration obtained from light scattering and the hydrodynamic radius from diffusion measurements was found to be about 25% larger than any theoretical predictions. The experimental values of P did decrease with decreasing ionic strength until the lowest ionic strengths as predicated theoretically, but then there occurred an increase at the lowest ionic strength for which there has not been any theoretical explanation. The values of P observed, except for the lowest ionic strength, did agree with a curve developed as an empirical fit for existing experimental data on

nonionic polymers.

It is believed from the present studies that this discrepancy between theoretical and experimental estimates of P accounts for the lack of agreement noted in the literature for unperturbed dimensions of polymers when the values obtained from diffusion and light scattering measurements are compared. Plots from diffusion constant measurements which are the equivalent of the Stockmayer-Fixman plots for intrinsic viscosity indicate that the unperturbed dimensions of polymers can be obtained by this method, since extrapolations from theta solvents and nontheta solvents intersect.

It was found that the parameter of β agreed better with theoretical values than either P or Φ separately. In addition, the decrease in β_0 with decreasing ionic strength at low ionic strengths could be explained by the effects of the ionic atmosphere on the motion of the macroions.

The correction factors to the frictional coefficient obtained for Na-copoly (ethyl acrylate-acrylic acid) from the concentration dependence of the diffusion constant were found to be in reasonable agreement with the theory of Pyun and Fixman. In addition to predicting a non zero value of k_f^c in a theta solvent as was experimentally observed, the predicted linearity of $[k_f^c - (k_f^c)_\theta]$ versus MA_2 and of $(k_f^c)_\theta$ versus $M^{1/2}$ was also observed.

The data accumulated from the diffusion measurements on the aqueous and nonionic solutions of Na-copoly (ethyl acrylate-acrylic acid) infer strongly the existence of a conformational transition from a compact to an extended random coil. The hydrodynamic radius in the

organic theta solvent 2-heptanone was 1.3 times larger than that in the aqueous theta solvent 1.2N NaCl. The transition was observed as a change in slope of the diffusion constant plotted as a function of ionic strength.

Some of the results summarized above will appear in a paper accepted for publication in the Journal of Colloid and Surface Chemistry. The results reported include the polydispersity effects, the parameter P, the concentration dependence of the diffusion constant and the correction factor to the frictional coefficient, and the parameters b and K_D in the molecular weight dependence of the infinite dilution value of the diffusion constant.

Suggestions for Further Work

In order to use the technique of laser Rayleigh spectroscopy as a general analytic tool for polymers, a more thorough investigation of the effects of polydispersity should be undertaken. Instead of the artificial distributions studied in the literature, it would be preferable to use a combination of well fractionated polymers and polymers of varying degrees of polydispersity in solutions covering a wide range of excluded volume conditions. The range and applicability of the theories developed to take into account polydispersity effects could then be studied.

A further extension of the present work is the study of polyelectrolytes under very low ionic strength conditions and higher concentrations. However, Na-copoly (ethyl acrylate-acrylic acid) would not be suitable for this type of investigation because of its relatively

high polydispersity. Since long range ordering and other electrostatic effects would be expected to show up as deviations from single exponential behavior, other contributions to this nonexponentiality such as polydispersity should be minimized. In addition, Na-copoly (ethyl acrylate-acrylic acid) is both a surfactant and not directly soluble in NaCl solutions. This makes it unsuitable for study in the low ionic strength regime, since it becomes both bubbly and impossible to filter. A polymer directly soluble in salt solution (one with higher charge density along the chain and no nonionic groups) could be refractionated several times in clean water, dried, placed in a cuvette and redissolved in clean water directly in the cuvette. This is the only feasible way to study the low ionic strength regime which is of considerable interest.

Another subject of investigation which is of importance is the determination of α_f as a function of z as well as the applicability of $1/DM$ versus $M^{1/2}$ for nonionic polymers. A simple experiment using well fractionated polystyrene in both theta and non theta solvents would yield the necessary information.

REFERENCES

1. J.C. Brown and P.N. Pusey, J. Chem. Phys., 62, 1136 (1975).

2. N.C. Ford, private communication.

3. G. Meyerhoff, Makromol. Chem., 72, 214 (1964).

4. J.M.G. Cowie and E.L. Cussler, J. Chem. Phys., 46, 4886 (1967).

5. M. Nagasawa and Y. Eguchi, J. Phys. Chem., 71, 880 (1967).

6. N.C. Ford, Jr., F.E. Kmasz and J.E.M. Owen, Disc. Farad. Soc., 49, 228 (1970).

7. M.E. McDonnell and A.M. Jamieson, Macromolecules, to be published.

8. T.A. King, A. Knox, W.J. Lee and J.D.G. McAdam, Polymer, 14, 151 (1973).

9. T.A. King, A. Knox and J.D.G. McAdam, Polymer, 14, 293 (1973).

10. N.C. Ford, Jr. and W. Lee, J. Chem. Phys., 50, 3098 (1969).

APPENDICES

APPENDIX 3.1

The diffusion constant for polydisperse systems is a z average diffusion constant, D_z. The equation for the concentration dependence of the diffusion constant

$$D = D_o [1 + (2MA_2 - k_f{}^c)c] \tag{1}$$

where $$k_f{}^c = \frac{1}{MD_o{}^3} \; k_f{}^\phi \; \frac{4\pi N_A}{3} \; \left(\frac{kT}{6\pi n_o}\right)^3 = \frac{F}{MD_o{}^3} \tag{2}$$

and $$A_2 = aM_W{}^{-\delta} \tag{3}$$

must therefore be averaged on both sides as a z average. Thus,

$$D_z = D_{z_o} + \frac{c\int[2MA_2 - k_f{}^c)M\omega(M)\,dM}{M\omega(M)\,dM} \tag{4}$$

Upon substitution of Equations (2) and (3) into Equation (4), setting

$$D = KM^{-b} \tag{5}$$

and using a Schultz distribution for $\omega(M)$,

$$\omega(M) \sim M^h e^{-\gamma z} \tag{6}$$

Equation (4) becomes

$$D_z = D_{z_o} + \frac{2\,acK\,\Gamma(h + 3 - b - \delta)}{\gamma^{1-b-\delta}\Gamma(h + 2)} - \frac{cF}{K^2} \; \frac{\Gamma(h + 1 + 2b)}{\gamma^{2b-1}\,\Gamma(h + 2)} \tag{7}$$

Now

$$D_{z_o} = \frac{K\int M^{-b} M\omega(M)}{\int M\omega(M)} = \frac{K}{\gamma - b} \frac{\Gamma(h + 2 - b)}{\Gamma(h + 2)} \tag{8}$$

Therefore Equation (7) becomes

$$D_z = D_{z_o} \left[1 + 2M_W A_2 c\left(\frac{1}{h+1}\right)^{-\delta} \frac{\Gamma(h+3-b-\delta)}{\Gamma(h+2-b)} - \frac{cF}{D_{z_o}{}^3 M_W} \frac{\Gamma(h+1+2b)\Gamma(h+2-b)^2}{(h+1)^2\Gamma(h+1)^3}\right] \tag{9}$$

Therefore, since

$$D_z = D_{z_o} \left[1 + 2\left(M_\nu A_2 - \frac{F}{M_f D_{z_o}{}^3}\right) c\right] \tag{10}$$

comparison of terms between Equation (9) and Equation (10) leads to

$$M_\nu = M_W \left(\frac{1}{1+h}\right)^{-\delta} \frac{\Gamma(h + 3 - b - \delta)}{\Gamma(h + 2 - b)} \tag{11}$$

$$M_f = M_W \frac{(h + 1)^2 \Gamma(h + 1)^3}{\Gamma(h+1+2b)\Gamma(h+2-b)^2} \tag{12}$$

Also,

$$k_f{}^\phi = k_f{}^c \frac{3}{4\pi N_A} \frac{M_f}{(R_D)^3} = 3.9656 \times 10^{-1} \frac{k_f{}^c M_f}{[R_D(A^o)]^3}$$

APPENDIX 3.2

Since the diffusion constant and hence the frictional coefficient are z averages, the correct average for the macromolecular radius is a "diffusion average" radius defined as

$$\langle R_H \rangle_D = \frac{\sum N_i M_i^2}{\sum N_i M_i^2 R_{H_i}^{-1}} = \frac{\int M\omega(M)\, dM}{\int M\omega(M) R_H(M)^{-1} dM} \qquad (1)$$

Since the radius obtained from light scattering is a z average, $\langle S^2 \rangle_z^{1/2}$, defined as

$$\langle S^2 \rangle_z^{1/2} = \left[\frac{\sum N_i M_i^2 S_i^2}{\sum N_i M_i^2} \right]^{1/2} = \left[\frac{\int M\omega(M) S^2(M)\, dM}{\int M\omega(M) dM} \right]^{1/2} \qquad (2)$$

the following correction factor must be introduced:

$$f = \frac{P n_o}{q_p} \langle S^2 \rangle_z^{1/2} \qquad (3)$$

where

$$q_p = \frac{\langle S^2 \rangle_z^{1/2}}{\langle R_H \rangle_D} \qquad (4)$$

For a theta solvent $R_H(M) \sim M^{1/2}$; $R_H^{-1}(M) \sim M^{1/2}$
$S(M) \sim M^{1/2}$; $S^2(M) \sim M$ (5)

and for a Schultz distribution $\omega(M) \sim M^h e^{-\gamma M}$

so

$$q_p = \frac{[\int M^{2+h} e^{-\gamma M} dM]^{-1/2} [\int M^{1/2+h} e^{-\gamma M} dM]}{[\int M^{1+h} e^{-\gamma M} dM]^{3/2}} = \frac{\Gamma(h+3)^{1/2} \Gamma(h+3/2)}{\Gamma(h+2)^{3/2}} \tag{6}$$

When the excluded volume effect is included, using

$$R_i^2 \sim M_i^{1+2\varepsilon} \tag{7}$$

then

$$\begin{aligned} R_H(M) &\sim M^{1/2+\varepsilon} \quad ; R_H^{-1}(M) \sim M^{-1/2-\varepsilon} \\ S(M) &\sim M^{1/2+\varepsilon} \quad ; S^2(M) \sim M^{1+2\varepsilon} \end{aligned} \tag{8}$$

and

$$q_p = \frac{[\int M^{2+h+2\varepsilon} e^{-\gamma M} dM]^{1/2} [\int M^{1/2+h-\varepsilon} e^{-\gamma M} dM]}{[\int M^{1+h} e^{-\gamma M} dM]^{3/2}} \tag{9}$$

$$= \frac{\Gamma(3+h+2\varepsilon)^{1/2} \Gamma(3/2+h-\varepsilon)}{\Gamma(h+2)^{3/2}} \tag{10}$$

ε can be related to the exponents a and b in the empirical equations $[\eta] = K_\eta M^a$ and $D = K_D M^{-b}$ by

$$\begin{aligned} a &= .5 + 3\varepsilon \qquad & \varepsilon &= (a - .5)/3 \\ b &= .5 + \varepsilon \qquad & \varepsilon &= b - .5 \end{aligned} \tag{11}$$

Thus

$$q_p = \frac{\Gamma(2 + h + 2b)^{1/2} \Gamma(h + h - b)}{\Gamma(h + 2)^{3/2}} \tag{12a}$$

or

$$q_p = \frac{\Gamma(8/3 + h + 29/3)^{1/2}\Gamma(5/3 + h - 9/3)}{\Gamma(h + 2)^{3/2}} \qquad (12b)$$

APPENDIX 6.1

An approximate theory relating ΔD to the polydispersity index is derived by analytically least squares fitting a single exponential to the expression

$$g(\tau) = [\int_0^\infty M\omega(M)e^{-D(M)K^2\Gamma}dM]^2. \qquad (1)$$

The definitions of the calculated quantities are indicated below:

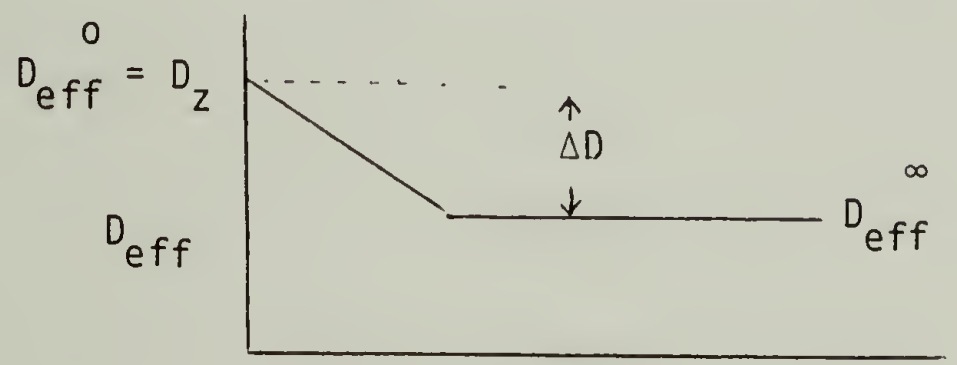

$\Gamma\tau_{max}$

$$D_{eff}^{o} = \frac{\int DM\omega(M)\,dM}{\int M\omega(M)\,dM} \qquad (2)$$

D_{eff}^{∞} is found by minimizing

$$\int[Q^2 - Ae^{-2D_{eff}^{\infty}K^2\tau}]^2\,d\tau \qquad (3)$$

where

$$Q^2 = [\int_0^\infty M\omega(M)e^{-D(M)K^2\tau}dM]^2 \qquad (4)$$

with respect to A and D_{eff}^{∞}, e.g., by setting

$$\frac{d}{dD_{eff}^{\infty}} \int_0^{\infty} [Q^2 - Ae^{-2D_{eff}^{\infty}K^2\tau}]^2 d\tau = 0 \qquad (5)$$

and

$$\frac{d}{dA} \int_0^{\infty} [Q^2 - Ae^{-2D_{eff}^{\infty}K^2\tau}]^2 d\tau = 0 \qquad (6)$$

After differentiation of Equations (5) and (6), combining them results in

$$4D_{eff}^{\infty}K^2 = \frac{\int e^{-2D_{eff}^{\infty}K^2\tau} Q^2 d\tau}{\int \tau e^{-2D_{eff}^{\infty}K^2\tau} Q^2 d\tau} \qquad (7)$$

Assuming a Schultz distribution,

$$\omega(M) = \frac{\gamma^{1+2}}{\Gamma(1+z)} M^z e^{-\gamma M} \qquad (8)$$

and using the relation

$$D(M) = K_D M^{-b} \qquad (9)$$

Equation (7) can be evaluated with the result that

$$1 = \frac{\iint \frac{MM'\omega(M)\omega(M')dMdM'}{1+x}}{\iint \frac{MM'\omega(M)\omega(M')dMdM'}{(1+x)^2}} \qquad (10)$$

where

$$x = \frac{1}{4}\left[\left(\frac{M}{M_{eff}^{\infty}}\right)^{-b} - 1 \right] + \frac{1}{4}\left[\left(\frac{M'}{M_{eff}^{\infty}}\right)^{-b} - 1 \right] \tag{11}$$

After expansion of $1/1+x$ and $1/(1+x)^2$ for small x, Equation (10) becomes

$$\iint MM'\omega(M)\omega(M')(x - \dot{2}x^2)\,dMdM' = 0 \tag{12}$$

or

$$\iint MM'\omega(M)\omega(M') \left\{ \left(\frac{M}{M_{eff}^{\infty}}\right)^{-2b} + 2\left(\frac{MM'}{M_{eff}^{\infty}}\right)^{2} + \left(\frac{M'}{M_{eff}^{\infty}}\right)^{-2b} - 6\left(\frac{M}{M_{eff}^{\infty}}\right)^{-b} \right.$$

$$\left. - 6\left(\frac{M'}{M_{eff}^{\infty}}\right)^{-b} + 8 \right\} dMdM' = 0 \tag{13}$$

Using

$$\int M^n \omega(M)\,dM = \frac{\Gamma(n+z+1)}{\gamma^{n+z+1}} \tag{14}$$

To evaluate the integrals, Equation (9), and the result from Equation (2) that

$$D_{eff}^{\infty} = \frac{K_D}{\gamma^{-b}} \frac{\Gamma(2 - b + z)}{\gamma^{-b}\Gamma(2 + z)} \tag{15}$$

leads to the final result that:

$$\frac{D_{eff}^{o}}{D_{eff}^{\infty}} = \frac{3 \pm 3\left[1 - \frac{4}{9}(Y + 1)\right]^{1/2}}{Y + 1} \tag{16}$$

where

$$Y = \frac{\Gamma(2 - 2b + z)\Gamma(2 + z)}{\Gamma(2 - b + z)^2} \tag{17}$$